Disruption of Monoamine Homeostasis in Models of Neurological and Neuroendocrine Diseases

By

Erika Danielle Dean, M.S.

Doctor of Philosophy

Graduate Division of Biological and Biomedical Science

Molecular Systems Pharmacology

_____

Gary W. Miller, Ph.D.

Advisor

_____

Victor Faundez, M.D., Ph.D.

Committee Member

_____

Randy Hall, Ph.D.

Committee Member

_____

Zixu Mao, Ph.D.

Committee Member

Accepted:

_____

Lisa A. Tedesco, Ph.D.

Dean of the James T. Laney School of Graduate Studies

_____

Date

Disruption of Monoamine Homeostasis in Models of Neurological and Neuroendocrine Diseases

By

Erika Danielle Dean

M.S., University of Tennessee, Knoxville, 2002

Advisor: Gary W. Miller, Ph.D.

An abstract of

A dissertation submitted to the Faculty of the

James T. Laney School of Graduate Studies of Emory University

in partial fulfillment of the requirements for the degree of

Doctor of Philosophy

in Graduate Division of Biological and Biomedical Science

Molecular Systems Pharmacology

2011.

Abstract

Disruption of Monoamine Homeostasis in Models of Neurological and Neuroendocrine Diseases

By Erika Danielle Dean

While glucose intolerance has been associated with Parkinson's disease (PD), a link between PD and diabetes has been demonstrated in epidemiological studies only recently. Additionally, numerous studies have shown that polychlorinated biphenyls (PCBs) increase the risk of developing both PD and diabetes suggesting that common molecular pathways targeted by PCBs may be involved in both diseases. Disruption of dopamine homeostasis is linked to PCBs in PD; however, disruption of dopamine homeostasis with relation to glucose homeostasis is unknown. Since the pancreas is dopaminergic, the effects of PCBs on glucose homeostasis were investigated.

Female mice treated with PCBs gain weight, develop impaired glucose tolerance, and have reduced adiponectin serum levels. PCB-treated female mice have a 36% reduction in pancreatic dopamine levels and increased glucose-sensitive secretion of insulin. PCBs inhibit the vesicular monoamine transporter 2 (VMAT2) that packages dopamine into vesicles in neurons and beta cells at low micromolar concentrations. Unlike PCB-treated females, female mice expressing low levels of VMAT2 (VMAT2 LO) do not develop age-associated changes in glucose homeostasis that wild-type mice develop. VMAT2 LO mice have low fasting glucose and improved glucose tolerance at 24 months of age when wild-type littermates have begun to develop impaired fasting glucose and glucose tolerance. Like PCB-treated female mice, VMAT2 LO female mice have a 70% reduction in pancreatic dopamine levels and secrete more insulin in response to rising blood glucose levels than wild-type mice. Intriguingly, glucose tolerance in male mice treated with PCBs is improved as it is in VMAT2 LO mice. Thus, loss of dopamine is sufficient to affect glucose-stimulated insulin release, but does not promote insulin resistance in mice.

Disruption of Monoamine Homeostasis in Models of Neurological and Neuroendocrine Diseases

By

Erika Danielle Dean

M.S., University of Tennessee, Knoxville, 2002

Advisor: Gary W. Miller, Ph.D.

A dissertation submitted to the Faculty of the

James T. Laney School of Graduate Studies of Emory University

in partial fulfillment of the requirements for the degree of

Doctor of Philosophy

in Graduate Division of Biological and Biomedical Science

Molecular Systems Pharmacology

2011.

For my father and mother, Joe and Shirley Dean: Thank you for your love and support of an

unusually curious child. All that I am is because of you.

CONTENTS

Chapter 1: Introduction and Background

Chapter 5: Summary and Conclusions

Appendix: Vitamin D Depletion Does Not Exacerbate MPTP-Induced Dopamine Neuron Damage in Mice

LIST OF FIGURES

Chapter 1: Introduction and Background

Chapter 2: Polychlorinated Biphenyl Mixtures Reduce Dopamine Levels in the Pancreas and Impair Glucose Tolerance and Insulin Release

Chapter 3: Reduced Vesicular Monoamine Transporter 2 Protein expression Prevents Age-Associated Glucose Intolerance

Chapter 4: The Parkinson Disease Associated Protein α-synuclein Interacts with the Vesicular Monoamine Transporter 2 and Facilitates Packaging of Monoamines

Chapter 5: Summary and Conclusions

Appendix: Vitamin D Depletion Does Not Exacerbate MPTP-Induced Dopamine Neuron Damage in Mice

Chapter 1

Introduction and Background

Introduction

Parkinson's disease is a neurodegenerative disease that affects circuitry in the basal ganglia of the brain controlling voluntary movement. While largely considered a movement disorder with a loss of the dopaminergic nigrostriatal neurons in the brain, extranigral pathology is also present in the disease. This extranigral pathology is believed to give rise to a many of the non-motor symptoms of Parkinson's disease. More recently, alterations in blood glucose management has been appreciated in Parkinson's disease patients. Additionally, patients with diabetes mellitus have an increased risk of developing Parkinson's disease. This suggests that these two diseases may share a common etiology and common molecular pathways of pathogenesis. Among possible shared etiologies is the exposure to polychlorinated biphenyls (PCBs) and resulting dysregulation of dopamine homeostasis.

Monoaminergic Neurotransmission

Neuropsychiatric disorders, including Parkinson's disease, Huntington's disease, Alzheimer's disease, depression, bipolar disorder, autism spectrum disorder, and schizophrenia, result from dysfunction in neurotransmission. More specifically, these disorders all share some dysfunction in monoaminergic signaling. Monoamines, including dopamine, norepinephrine, epinephrine, serotonin (5-HT), melatonin, and histamine, are so named because they share a similar structure consisting of an amine group connected to an aromatic ring by a two-chain carbon. Of these, the major monoaminergic signaling molecules of the central and peripheral nervous systems are comprised of catecholamines (dopamine, norepinephrine, and epinephrine) and tryptamines (5-HT and melatonin).

Catecholamines and tryptamines are synthesized by similar yet distinct mechanisms. All catecholamines are derived from L-tyrosine metabolism while all tryptamines are derived from L-tryptophan metabolism. For catecholamines, L-tyrosine is taken up into the neuron by the large

neutral L-amino acid transporter (LNAAT) where it is converted to L-DOPA by tyrosine hydroxylase (TH) using tetrahydrobiopteran as a cofactor (Figure 1.1) (Eisenhofer et al., 2004a). L-DOPA is then converted to dopamine, by aromatic L-amino acid decarboxylase (AADC). TH and AADC are not only expressed in dopamine-producing cells, but also in norepinephrine and epinephrine producing cells. In noradrenergic cell populations, dopamine is converted into NE by dopamine β hydroxylase (DβH) in synaptic vesicles. Phenylethylnolamine-N-methyltransferase (PNMT) can convert norepinephrine to epinephrine using S-adenosylmethionine as a cofactor (Goldstein, 2010).

For tryptamine synthesis, L-tryptophan is taken up into neurons by LNAAT where it is converted to 5-hydroxytryptophan (5-HTP) by tryptophan hydroxylase (TPH) using tetrahydrobiopteran as a cofactor. 5-HTP is then converted to 5-HT by AADC. 5-HT can be further catabolized by N-acetyltransferase to 5-hydroxyindole and then by 5-hydroxyindole-O-methyltransferase to melatonin.

After monoamines are produced, they are packaged into synaptic vesicles in most neurons by the vesicular monoamine transporter 2 (VMAT2) (Figure 1.2). Monoamines can then be released into the synaptic cleft where they bind to and activate monoamine receptors. This activation can be terminated by downregulation or endocytosis of the receptor. However, an excess of monoamine can be present in the synaptic cleft and must be removed to attenuate signaling by the monoamine. Monoamines can be cleared from the extracellular space by reuptake transport or monoamine catabolism. For example, the dopamine transporter (DAT) transports dopamine from the extracellular space back into the cytosol of the dopamine neuron, and interference with this process is the mechanism by which many psychotropic drugs act (i.e. cocaine). Dopamine is then typically recycled by repackaging into synaptic vesicles by VMAT2 for subsequent release. When not recycled, dopamine may be metabolized by catechol-*O*-methyltransferase (COMT) to 3-methoxytyramine which is then metabolized to homovanillic acid

Figure 1.1: Monoamine Metabolism. TH converts L-tyrosine into L-DOPA. L-DOPA is converted to dopamine by AADC. DβH converts dopamine to norepinephrine which is then converted to epinephrine by PNMT. Dopamine can also be metabolized by COMT to 3-MT and then to HVA by MAO. Alternatively, dopamine can be metabolized to DOPAL by MAO and then to DOPAC ALDH. DOPAC is further metabolized to HVA by COMT.

TPH converts L-tryptophan 5-HTP. 5-HTP is then converted to serotonin by AADC. Serotonin can be metabolized by N-acetyltransferase (NAT) to 5-hydroxyindole and then by 5-hydroxyindole-O-methyltransferase (IOMT) to melatonin.

Dopamine (DA) Metabolism
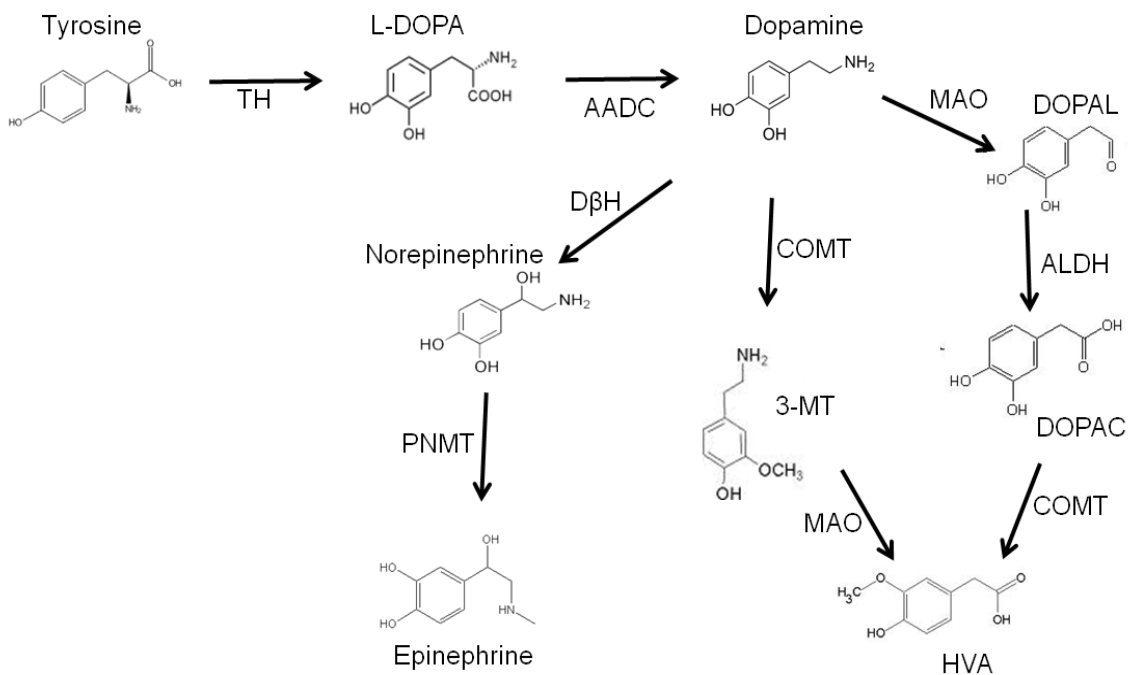
Serotonin (5-HT) Metabolism
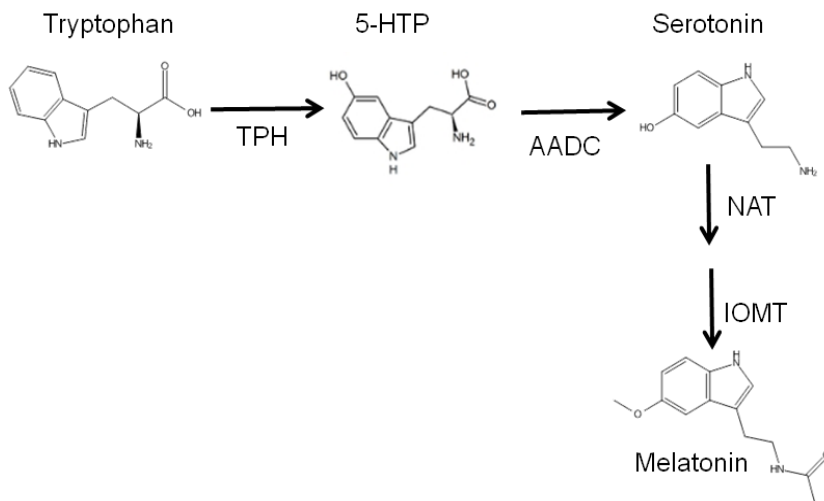
Figure 1.2: Monoamine Homeostasis. Dopamine is synthesized in neurons by the concerted actions of tyrosine hydroxylase and aromatic L-amino acid decarboxylase. Once dopamine is synthesized, it is packaged into synaptic vesicles by the vesicular monoamine transporter 2 (VMAT2) where it is stored until membrane depolarization and subsequent release from docked synaptic vesicles. After release, dopamine can then bind to pre or post-synaptic dopamine receptors. D1 receptors are coupled to Gsα subunits; therefore, activation of these receptors by dopamine promotes the formation of cAMP from ATP. cAMP can then perform as second messenger activating downstream pathways, including changes in gene expression. D2 receptors are coupled to Giα subunits; therefore, activation of these receptors by dopamine inhibits the formation of cAMP from ATP. In order to attenuate dopamine signaling after release, dopamine can be metabolized by enzymes or taken back up into the presynaptic neuron by the dopamine transporter (DAT). Once reuptake occurs, dopamine can either be metabolized by enzymes or repackaged into synaptic vesicles by VMAT2 for later release.
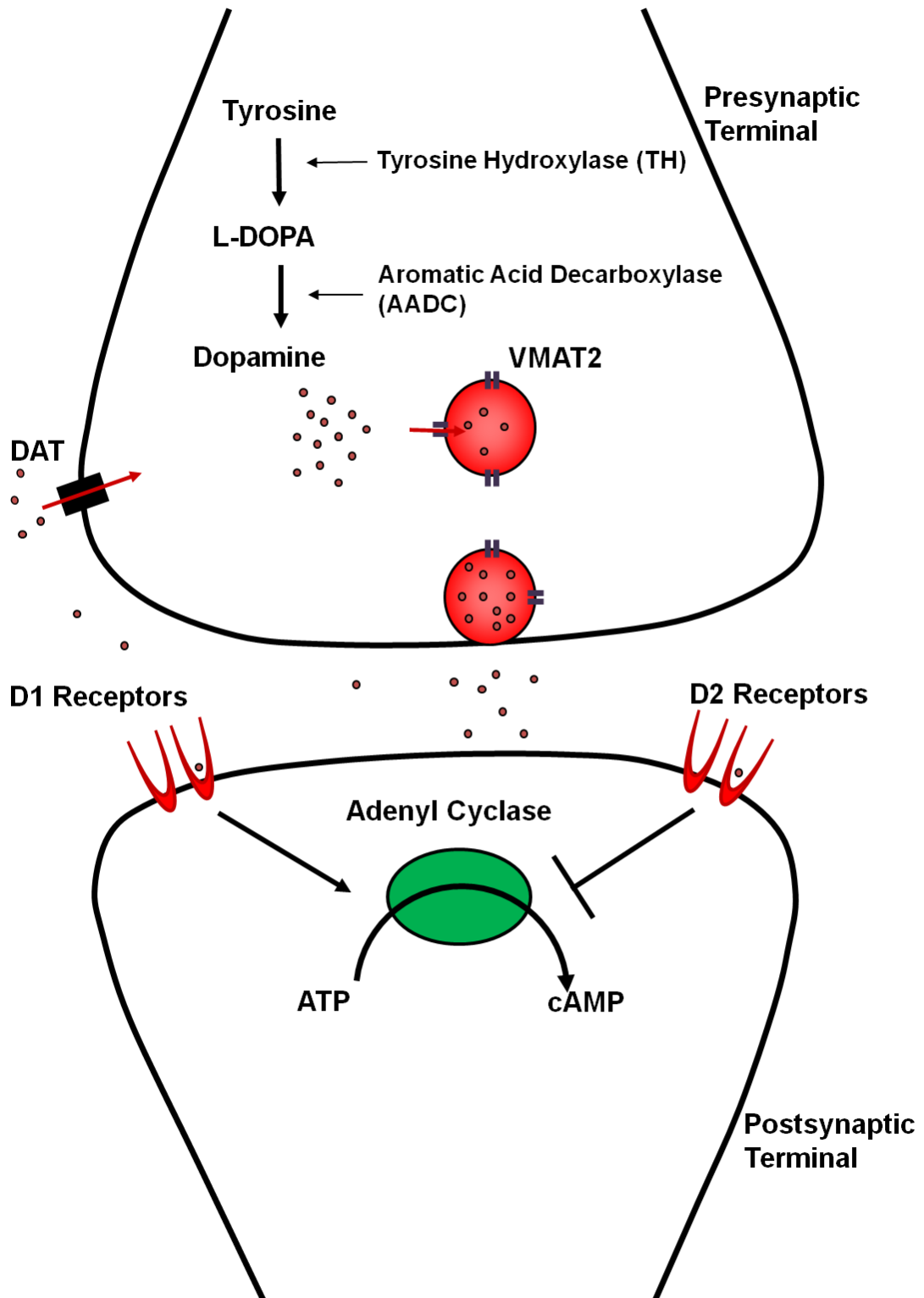
(HVA) by monoamine oxidase (MAO) (Figure 1.1). Alternatively, dopamine may be metabolized by (MAO) to 3,4-dihydroxyphenylacetaldehyde (DOPAL) which is rapidly metabolized by aldehyde dehydrogenase (ALDH) to 3,4- dihydroxyphenylacetaldehyde (DOPAC). Then, DOPAC can be further metabolized by COMT to HVA.

Monoaminergic neurotransmitters function by binding to cellular receptors that then transduce signaling cascades. For dopamine signaling, dopamine binds to G-protein coupled dopamine receptors that are expressed on membranes in multiple tissues throughout the body. There are two classes of dopamine receptors D1-like (D1 and D5) and D2-like (D2, D3, and D4) receptors. D1-like receptors are couple to $G_s\alpha$ proteins and stimulate cAMP production while D2-like receptors are coupled to $G_i\alpha$ proteins and inhibit cAMP production.

Introduction to Parkinson's Disease

Parkinson's disease is the 2nd most common neurodegenerative disorder that is commonly characterized by two pathological hallmarks, loss of dopamine neurons and the presence of protein inclusions called Lewy bodies (Jankovic, 2008). Parkinson's disease is a classically described as a movement disorder characterized by several well-known motor symptoms including tremor, rigidity, bradykinesia, postural instability, and shuffled gait; lesser known motor symptoms include difficulty speaking, excessive salivation, difficulty swallowing, drooling, masked facial expression, micrographia, dystonia, striatal deformities, and stooped posture; however, Parkinson's disease patients also experience a variety of non-motor symptoms. Dementia, cognitive impairment, and loss of executive functions can develop. Psychiatric disturbances such as hallucinations delusions are common late in the disease. Depression and anxiety are often comorbid with Parkinson's disease. Sleep disturbance in Parkinson's disease include excessive daytime sleepiness, restless leg syndrome, and REM sleep behavior disorder. Patients may experience sensory disturbances such as pain, numbness, or tingling; patients will often lose their sense of smell years before the onset of motor symptoms. Also, urinary

dysfunction, sexual dysfunction, constipation, and delayed gastric emptying also are common in this disease.

Parkinson's disease was first formally described by James Parkinson, MD in "An Essay on the Shaking Palsy" in 1819 (Kempster et al., 2007); however, it wasn't until 1960 that striatal dopamine deficiency was first described in Parkinson's disease (Tolosa et al., 1998). Parkinson's disease is pathologically characterized by the loss of dopaminergic neurons in the substantia nigra. This region of the midbrain projects to the striatum in the forebrain and is responsible for the regulation of voluntary movement. Dopamine receptor agonists (apomorphine and bromocriptine), dopamine replacement (i.e. Sinemet®- levodopa/carbidopa combination), and MAO inhibitors (selegiline and rasagiline) are commonly used to treat the motor symptoms of Parkinson's disease, but these are not affective at treating all other symptoms. Surgical techniques and anticholinergic drugs are also used in combination with or in place of dopaminergic drugs. With the numerous extra-motor symptoms associated with Parkinson's disease, it is not surprising that multiple other neuronal nuclei (especially monoaminergic neuronal nuclei) are affected in the disease.

Another clue to the role of dopaminergic neuronal loss in Parkinson's disease resulted from the inadvertent poisoning of a group of heroin addicts in the San Francisco Bay area. Over just a few days, the otherwise healthy addicts became parkinsonian (Langston et al., 1983). They responded to L-DOPA therapy, and it was revealed that they had taken a synthetic opioid contaminated with the compound 1-methyl-4-phenyl-1,2,3,6-tetrahydropyridine (MPTP). The exposure resulted in dramatic loss of TH+ neurons in the substantia nigra pars compacta. Additionally, a chemist at a pharmaceutical company that repeatedly worked with MPTP later developed Parkinson's disease (Langston and Ballard, 1983). He also responded to L-DOPA therapy. These observations suggest that MPTP selectively targets dopamine neurons. This effect has been repeatedly confirmed in animal studies. MPTP is the precursor to the neurotoxin

1-methyl-4-phenylpyridine (MPP+) which is generated by the metabolism of MPTP by MAO_B (glial MAO). The selectivity of MPP+, a mitochondrial complex I inhibitor, is due to its selective transport into dopamine neurons by DAT. MPP+ can also be transported into synaptic vesicles by VMAT2 where it is sequestered (Liu et al., 1992).   Interestingly, both DAT and VMAT2 levels are reduced in the brains of Parkinson's disease patients (Brooks et al., 2003). Overall, these studies suggest that factors involved in regulating dopamine packaging and release may be involved in Parkinson's disease pathology.

The other pathological hallmark of Parkinson's disease is the Lewy body. Lewy bodies are eosinophilic, protein aggregates found throughout the brain stem and cortical regions of Parkinson's disease patients' brains. Brain stem or classical Lewy bodies have a dense core of protein with a halo of protein fibrils surrounding the core, while cortical Lewy bodies are compact dense cores lacking any halo. Lewy neurites are also found in Parkinson's disease and represent swollen dystrophic neuritic processes.   The primary component of Lewy bodies is the Parkinson's disease associated protein α-synuclein (α-syn); however, over 70 other proteins have been demonstrated to be components of Lewy bodies, including several proteins implicated in familial Parkinson's disease, protein clearance, or dopamine homeostasis (ubiquitin, synphilin-1, parkin, DJ-1, LRRK2, PINK1, TH, VMAT2, etc) (Wakabayashi et al., 2007). It is unknown what role Lewy bodies play in Parkinson's disease pathogenesis; however, the fact that more Lewy bodies are typically present in post-mortem analyses of patients in earlier stages of the disease than those with late-stage diseases suggests that Lewy bodies mark neurons destined to die. It is still intensely debated whether Lewy bodies actually cause neuronal death or if they serve some protective purpose by sparing the neuron from aberrantly folded proteins interfering with other cellular processes.

While the major pathological hallmarks of Parkinson's disease have been identified, the underlying causes of the pathology remain poorly understood. Several genes have been identified

as risk factors or responsible for familial forms of Parkinson's disease; however, these appear to only account for a small percentage of Parkinson's disease suggesting that environmental factors play a large role in Parkinson's disease pathogenesis. Although the number of genetic cases is considered to be low, identification of the responsible genes has led to a much deeper understanding of potential pathways involved. Oxidative stress, mitochondrial dysfunction, and aberrant protein clearance are all now believed to be partially responsible for Parkinson's disease pathogenesis (Greenamyre and Hastings, 2004). However, factors affecting neurotransmission are also affected in Parkinson's disease.

Polychlorinated Biphenyls in Parkinson's Disease

While several genetic loci are linked to familial and sporadic Parkinson's disease, numerous epidemiological studies have demonstrated a clear link between environmental exposures and Parkinson's disease. Several toxicants and metals have been identified to be linked, including organochlorines (Hatcher et al., 2008a). While multiple toxicants have been identified, no pure toxicant based model has reliably reproduced all or even most of the symptoms of Parkinson's disease. Unfortunately, neither have pure genetic models. This has led to a great debate in the field as to what exactly "causes" Parkinson's disease. It now seems clear that a complex interaction between genetic susceptibly, dietary factors, and environmental toxicant exposure most likely accounts for the majority of Parkinson's disease cases. Despite the lack of a single unifying cause, studying these multiple genetic and environmental factors has led to the discovery of several common biochemical pathways affected by these triggers, including mitochondrial respiration, oxidative stress, and dopamine /monoamine homeostasis.

Among these factors, organochlorines stand out as a disease modifier because so many different organochlorines have been associated with Parkinson's disease (Corrigan et al., 2000; Elbaz et al., 2009; Fleming et al., 1994; Richardson et al., 2009; Weisskopf et al., 2010). One large class of organochlorines associated with Parkinson's disease is the polychlorinated

biphenyls (PCBs). Post-mortem analyses show that PCBs are elevated in the caudate nucleus of Parkinson's disease patients (Corrigan et al., 1998). Recent unpublished data from our laboratory has confirmed this link between PCB exposure and Parkinson's disease. Several individual PCB congeners and the class as a whole are detected at higher concentrations in the brains of Parkinson's disease patients versus age-matched controls by postmortem analyses, but only in women. (unpublished observations). This is most striking because the incidence of Parkinson's disease is higher in men (Wooten et al., 2004).

PCBs are a large class of organochlorines characterized by the presence of a double-ring structure that can be substituted at a combination of sites around the bi-ring backbone by chlorine atoms to make up different individual compounds called congeners (Figure 1.3). There are 209 different PCB congeners named PCB 1 through PCB 209 with an increasing amount of chlorine substitution corresponding to the increased numerical value of each congener (Mills et al., 2007). PCBs were largely marketed in the US by Monsanto Company under the trade name Aroclor until their ban in 1979, but were also widely produced and used throughout the world. PCBs as a class have been shown to disrupt or activate several different biochemical pathways; however, each PCB congener appears to act upon only a subset of these pathways. The ability to affect only a subset of pathways is largely due to structural differences within the class and the varying degree of chlorination.

Some PCB congeners have a planar or dioxin-like structure, and these congeners typically have high affinity for the aryl hydrocarbon receptor (AhR). Traditionally, PCB toxicity has been largely attributed to the dioxin-like congeners. This is because PCB binding of AhR has been shown to activate transcription of genes related to the xenobiotic response, which has been strongly linked to carcinogenesis and other forms of toxicity (Bemis et al., 2005; Pocar et al., 2006). However, evidence exists of AhR-independent activation of gene transcription (Kietz and Fischer, 2003). Another demonstrated mechanism of PCB effects is via estrogen receptor (ER),

Figure 1.3: Structure of PCB. The general structure of a PCB includes biphenyl rings with ortho (2, 2', 6, or 6'), meta (3, 3', 5, or 5'), and/or para (4, 4') chlorine substitutions. Individual congeners are named PCB 0- PCB 209 with increasing degrees of chlorination corresponding to increasing congener number (Examples- PCB 0 or biphenyl is not chlorinated where as PCB 209 or decachlorobiphenyl is fully substituted.)
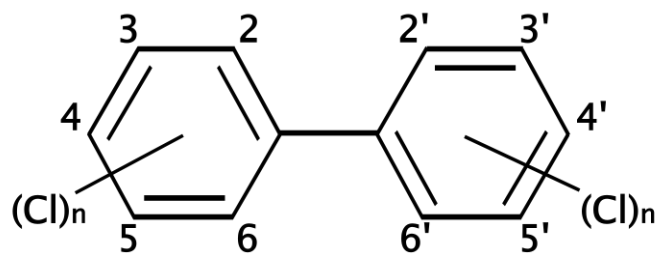
but affinity for each ER subtype and associated cofactors is also affected differentially by congener structure (Wu et al., 2008). In addition to transcriptional changes, ortho-substituted (non-dioxin-like) PCBs have been shown to affect Ca^{2+} signaling pathways via Ca^{2+} channels activation and to compete with thyroxine for transthyretin binding thus affecting thyroid hormone signaling (Chauhan et al., 2000; Fonnum and Mariussen, 2009).

Polychlorinated Biphenyls in Diabetes Mellitus

With a variety of mechanisms of action, PCBs are able to exert their effects in multiple cell types and tissues. Not surprisingly, PCBs are associated with multiple diseases. In addition to evidence linking PCB exposure to Parkinson's disease, PCB exposure is also linked by epidemiological studies to cancer (Hoque et al., 1998) . However, perhaps the strongest link between PCB exposure and disease is PCB exposure and diabetes mellitus. Diabetes mellitus is narrowly defined as a chronic disease state of hyperglycemia (fasting blood glucose >125mg/dl). The cause of this imbalance in blood glucose is largely the effect of impaired signaling of the hormone insulin. Normally, insulin is released in response to elevated blood glucose levels. Then, insulin interacts with cells throughout the body to signal that blood glucose concentrations are excessive and production of glucose (gluconeogenesis) needs to halt and glucose must be taken up into cells to provide fuel (ATP). When an individual has diabetes, this process is impaired. Release of insulin in response to elevated glucose can fail for any number of reasons, including impaired production of insulin or impaired recognition of glucose levels. Often time beta cells die in the course of the disease leading to a reduced insulin pool available for release. Alternatively, insulin may be released, but insulin receptors fail to transduce the appropriate response, a condition called insulin resistance.

There are 3 types of diabetes. The most common form is type II diabetes. This form is characterized by insulin resistance where beta cells do not produce enough insulin to respond properly to rising blood glucose levels and is often associated with obesity and sedentary

lifestyle. Patients typically present with symptoms in adulthood which is why this form is formerly referred to as adult-onset diabetes; however, childhood type II diabetes is becoming increasingly common as childhood obesity rates skyrocket. Type I diabetes is an autoimmune form of diabetes where beta cells are immunogenic and little or no insulin is produced causing patients to be dependent on insulin replacement therapy. The disease onset is most common in childhood which is why type I diabetes is formerly referred to as juvenile diabetes; however in type I, symptoms can also present in adulthood. This late onset is sometimes referred to as type 1.5 diabetes or latent autoimmune diabetes of adults (LADA). The third form of diabetes is gestational diabetes, which affects women during pregnancy. During gestation, increased metabolic demands on the mother to provide nutrition for the developing fetus challenge the endocrine system. Normally, beta cell mass expansion occurs to facilitate better insulin response and sensitivity. If the body fails to respond properly, the result can be intermittent diabetes during the second and third trimesters. While this form typically resolves after birth, women with gestational diabetes are at a much higher risk for developing type II diabetes later in life.

Currently, diabetes affects approximately 1 in 10 individuals in the US (Prevention, 2011). The most recent projections predict that a child born in the US in the year 2000 will have a greater than 30% chance of developing either type I or type II diabetes with the vast majority developing type II (Narayan et al., 2003). Incidence rates for type II diabetes are rapidly rising worldwide, causing many scientists to investigate both new therapies for and potential causes of diabetes mellitus.

Several risks factors for Type II diabetes have been identified, including age, body mass, family history, a history of gestational diabetes, heart disease, sedentary lifestyle, polycystic ovary syndrome, and race. Symptoms are often undetected until many years after disease onset. While dietary factors such as a high fat diet are commonly associated with type II diabetes, other factors are also currently under scrutiny.

Over the last decade, epidemiologists have investigated more deeply the complex link between obesity, diet, and environmental toxicant exposure. A multitude of environmental toxicants have been associated with increased incidence of disease. Typically these toxicants are lipophilic in nature and accumulate in body fat (Pelletier et al., 2003). Organochlorines are believed to accumulate in body fat in both lean and obese persons; however, lean persons appear to clear these toxicants from the body more readily than obese individuals shortening the duration of exposure (Wolff and Anderson, 1999). Exposure to these compounds as measured by blood concentrations are now commonly regarded as a risk factor for diabetes and may in part explain the relationship between obesity and diabetes.

Indeed, numerous epidemiological studies over the last decade support a link between organochlorines and diabetes. Most have found strong positive associations. Multiple studies have shown associations with dioxins, PCBs, dichloro-diphenyl-dichloroethylene (DDE), β-hexachlorocyclohexane, and heptachlor (Everett et al., 2011; Patel et al., 2010). Since both dioxins and PCBs are structurally similar, these chemicals are often grouped together in studies. However as mentioned previously, these compounds can exert their effects through sometimes different mechanisms.

Unfortunately, relatively poor mechanistic data exist to support a role for PCBs and other organochlorines in the pathogenesis of diabetes mellitus. Furthermore, metrics such as glucose tolerance and insulin sensitivity in animals chronically exposed to PCBs and other organochlorines to replicate a human exposure either have not been measured or do not support such an association and went unpublished. Fasting glucose measures in rats chronically exposed to PCB mixtures indicate that PCBs reduce blood glucose levels (Narbonne et al., 1978a; Narbonne et al., 1978b). This seems counterintuitive at first that PCBs could then play a role in diabetes mellitus since hyperglycemia is the primary symptom of the disease; however, increased insulin secretion can result in hypoglycemia. This suggests that PCBs may regulate insulin

secretion. While this affect has not been tested in animals or in isolated islets, experiments performed in a rat insulinoma cancer cell line exposed to PCB congeners demonstrate that ortho-substituted PCB congeners, but not dioxin-like PCB congeners can increase glucose-stimulated insulin release in low micromolar concentrations (Fischer et al., 1996; Fischer et al., 1999). Therefore, PCBs may be linked to diabetes mellitus because they promote hyperinsulinemia, an early symptom of Type II DM where the pancreas secretes too much insulin typically because of underlying insulin resistance.

A recent study has examined the effect of PCB 77 (a dioxin-like PCB congener) on adipocyte function. PCB 77 promotes body fat deposition in WT mice, but not AhR knockout mice (Arsenescu et al., 2008). Additionally, differentiation of adipocytes increased in response to low concentration of PCB 77, but high concentrations are inhibitory. Therefore, excessive concentrations may simply be toxic to the cells masking their true effects at more physiologically relevant exposures.

Is There a Link Between Parkinson's Disease and Diabetes Mellitus?

Since epidemiological studies link PCBs to both Parkinson's disease and diabetes, naturally the question has been asked- "is there a link between Parkinson's disease and diabetes (Sandyk, 1993)?" There is a growing body of evidence that supports an association between diabetes mellitus and Parkinson's disease. One very large prospective study of over 50,000 Finnish people finds that a history of type II diabetes increases risk for Parkinson's disease in men and women when adjusted for confounders {Hazard ratio 1.83 (95% CI 1.21-2.76)} (Hu et al., 2007); however, surveillance bias may have influenced the findings. Additionally, a prospective cohort study of 22,050 US male physicians (the Physicians Health Study) finds that diabetes history increases the risk of Parkinson's disease {Relative risk 1.34 (95% CI 1.02-1.80)} after adjustment for confounders (Driver et al., 2008). This risk is highest in persons with a normal body mass index, indicating that obesity is not necessarily driving the diabetes phenotype.

However, one very large prospective study combining the Nurses' Health Study (121,046 women) and the Health Professionals Follow-up Study (50,833 men) cohorts finds no association between diabetes and Parkinson's disease (Simon et al., 2007). A small case-control study in a Japanese cohort found a reduced risk of Parkinson's disease in diabetic patients (Miyake et al., 2010). Another study finds a lower incidence of diabetes among Parkinson's disease patients, but only among patients receiving L-DOPA treatment (Becker et al., 2008). This may be related to the known effects of dopamine and dopamine agonists on glucose homeostasis. Most recently, being diabetic increases an individual's risk of having Parkinson's disease by 35% in a Danish cohort {Odds Ratio 1.36 (95% CI 1.08-1.71)}. Also in this cohort, the use of any antidiabetic medication results in a 35% increase in the risk of developing Parkinson's disease {Odds Ratio (1.35 (1.10-1.65)}. This effect is strongest in women {Odds Ratio 2.92 (1.34-6.36)} and with the development of early-onset Parkinson's disease {Odds Ratio 3.07 (1.65-5.70)}. Therefore, epidemiological studies are beginning to support the hypothesis that Parkinson's disease and diabetes mellitus may be linked by a common pathological mechanism.

Perhaps the most intriguing associations are the common genetic polymorphisms associated with both Parkinson's disease and diabetes mellitus. The overlapping genetic loci on Chromosome 10 containing the gene for insulin degrading enzyme is associated with diabetes mellitus, Alzheimer's disease, and Parkinson's disease in independent mapping studies (Blomqvist et al., 2004; Kwak et al., 2008; Rudovich et al., 2009; Vepsalainen et al., 2007). Since insulin is a known neuroprotective agent, dysregulation of insulin peptide turnover may make neurons vulnerable to neuronal death. Also, the PARK2 locus encoding the gene parkin is associated not only with autosomal recessive juvenile Parkinson's disease, but also type II diabetes mellitus (Wongseree et al., 2009). Since parkin is also involved in protein catabolism, aberrant protein clearance may be a common mechanism in both neurodegenerative diseases and diabetes mellitus. Indeed, Parkinson's disease, Alzheimer's disease, and diabetes mellitus all have both an amyloid aggregation component and degenerative component to their disease

pathology. These genetic associations suggest that common molecular pathways may be associated with these diseases.

In rodent studies, diabetic rats do not respond to the stimulatory effects of amphetamine suggesting that dopamine circuits are impaired in these animals (Sandyk, 1993). Developmentally-exposed PCB mice also fail to respond to the behavioral effects of amphetamine (Chou et al., 1979; Sable et al., 2009; Sable et al., 2010). Furthermore, rats fed a high fast diet to induce insulin resistance are more susceptible to dopamine neuron death from the dopaminergic neurotoxin 6-hydroxydopamine, and lesioned animals develop greater striatal insulin resistance (Morris et al., 2010; Morris et al., 2008). These data suggest that underlying insulin resistance can influence dopamine neuron vulnerability to toxic insult and dopamine lesions can influence insulin resistance at least at the lesion site itself.

Insulin Resistance and Hyperinsulinemia Hypothesis in Neurodegeneration

Insulin is known to have a protective effect on neurons suggesting that hyperinsulinemia may be neuroprotective. However, peripheral hyperinsulinemia and insulin resistance have been shown in several model systems to drive decreased uptake of insulin by the blood brain barrier that results in lower brain levels of insulin (Neumann et al., 2008). Therefore, peripheral hyperinsulinemia may predispose neurons for death. Much of our knowledge of the role of peripheral hyperinsulinemia and insulin resistance in neurodegenerative disease has evolved from work in the Alzheimer's disease field. Alzheimer's disease is the most common neurodegenerative disorder characterized initially by mild memory impairment that progresses to a more prominent loss of cognitive and executive function (Pimplikar et al., 2010). Alzheimer's disease has been referred to as type III diabetes mellitus because of its high comorbidity with diabetes mellitus (Han and Li, 2010; Steen et al., 2005). Alzheimer's disease is also highly comorbid with Parkinson's disease (Boller et al., 1980; Brown et al., 1998; Heintz and Zoghbi, 1997; Riederer et al., 2011; Sabbagh et al., 2009). Peripheral hyperinsulinemia and insulin resistance have been linked to poor memory which is responsive to intranasal treatment with

insulin (Benedict et al., 2004; Stockhorst et al., 2004; Watson and Craft, 2003). Intranasal insulin provides a direct means for the insulin to reach the brain independently of the blood brain barrier via direct uptake from the olfactory epithelium. Intranasal insulin treatment can thereby bypass the peripheral system and potentially restore brain insulin levels and is now in trials for aiding memory function in Alzheimer's disease patients (Benedict et al., 2007; Reger et al., 2008). Additionally, insulin drives the exocytosis of Aβ peptide (found in amyloid plaques of Alzheimer's disease patients' brains) from within neurons and regulates expression of the protease insulin degrading enzyme` that aids Aβ clearance (Messier and Teutenberg, 2005). Therefore, decreased brain insulin levels have been proposed to participate in the intraneuronal accumulation of Aβ peptide in Alzheimer's disease. Alterations in brain levels of insulin and the effects of insulin therapy in other models of neurodegeneration are unknown.

VMAT2 as a Critical Regulator of Monoaminergic Signaling

One protein that has attracted much attention for its role in neurodegeneration is VMAT2. The VMATs are major players in the regulation of monoaminergic homeostasis. They are composed of a single gene family in the mammalian solute carrier superfamily with two genes that encode two different transporter proteins. The SLC18A1 gene encodes the vesicular monoamine transporter 1 (VMAT1) protein, while the SLC18A2 gene encodes the vesicular monoamine transporter 2 (VMAT2) protein. Both proteins play a critical role in the packaging of monoamines into vesicles for subsequent release. VMAT2 is a member of the toxin extruding exporter (TEXAN) superfamily of proteins (Yelin and Schuldiner, 1995). This ancient class of proteins is present in both prokaryotes and eukaryotes. VMAT2 is a 12 transmembrane domain containing 45-75kDa phosphoglycoprotein that is essential for packaging monoamines into synaptic vesicles for release at synaptic terminals (Liu and Edwards, 1997) (Figure 1.4). VMAT2 overexpression increases quantal size of dopamine release from cultured neurons and PC12 cells (Pothos et al., 2000). Cytosolic pH is 7.4 while intravesicular pH is 5.6, and VMAT2 activity is

Figure 1.4: Vesicular Monoamine Transporter 2 Topography. VMAT2 is a 12 transmembrane domain integral membrane protein. It is oriented in the vesicular membrane with the N-terminus and C-terminus forming cytoplasmic tails. There is large intravesicular loop (Loop 1) containing several sites of N-linked glycosylation. The typical 3 bands of VMAT2 observed by Western analyses represent fully glycosylated VMAT2 (75 kDa), partially glycosylated (55 kDa), and unglycosylated (45 kDa) forms of VMAT2 (Cruz-Muros et al., 2007).

VMAT2

Vesicle Lumen

Cytoplasm

NH2

COOH
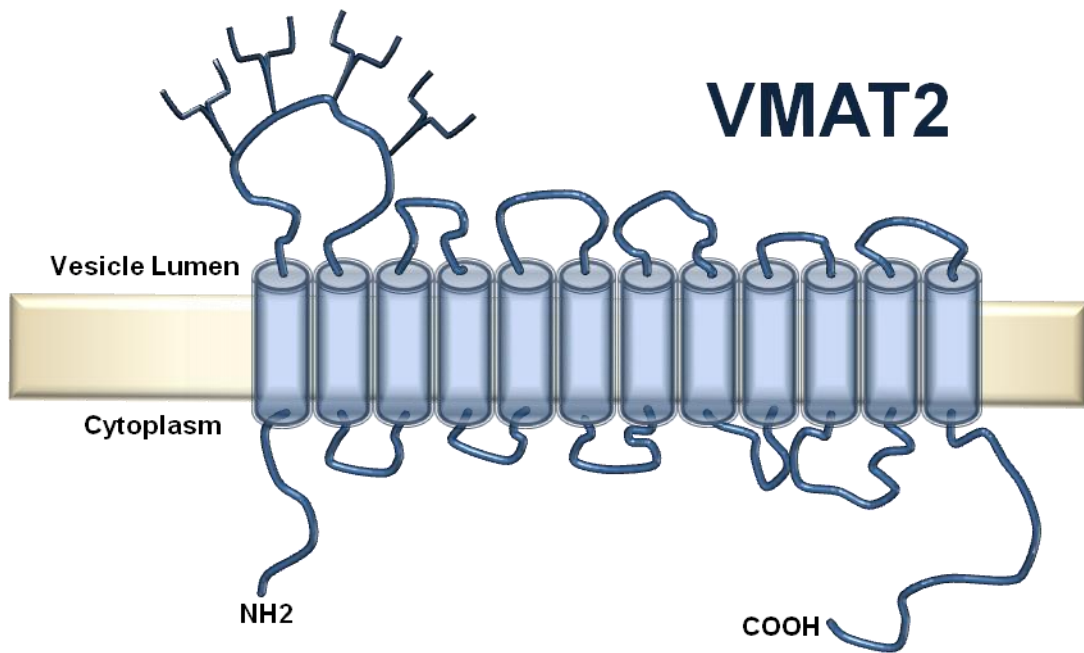
tightly linked to its proton antiporter activity (Figure 1.5). Bafilomycin A, a vesicular H+-ATPase inhibitor, indirectly inhibits VMAT2 activity. Thus, the vesicular H^+-ATPase is indirectly responsible for VMAT activity via the proton gradient it establishes (Toll and Howard, 1978; Toll et al., 1977). For every monoamine VMAT2 transports across the vesicular membrane, it also expels two H+ from the vesicle. As intravesicular pH moves toward a more neutral pH, VMAT2 loses its ability to transport monoamines. Therefore, other known cellular factors can influence VMAT2 activity.

VMAT2 in Aging and Neurodegenerative Disease

Positron emission transmission studies reveals that Parkinson's disease patients have markedly reduced VMAT2 levels in the brain (Frey et al., 2001). VMAT2 mRNA is dramatically reduced in the brains and in the platelets of Parkinson's disease patients (Harrington et al., 1996; Sala et al., 2010). Immunohistochemical studies demonstrate that Parkinson's disease patients also lose VMAT2 protein expression during the course of the disease (Miller et al., 1999b). Due to the ability of dopamine and NE to become oxidized in the cytosol, timely packaging of these monoamines into synaptic vesicles by VMAT2 may play a critical role in the survival of neurons. When the activity of VMAT2 is lost, impaired sequestration of monoamines from the cytosol may result in oxidation of monoamines potentially affecting the overall oxidation state of the neuron. Indeed, persons with allelic haplotypes of VMAT2 that increase the promoter activity of the gene have lower incidence of Parkinson's disease, indicating that higher expression of VMAT2 may be protective against Parkinson's disease in part because of better storage of monoamines (Glatt et al., 2006). Therefore, VMAT2 might be a target for dysregulation of monoamine homeostasis and subsequent neurodegeneration in Parkinson's disease.

Understanding how the brain changes with age and the regulation of such processes are paramount for the study of Parkinson's disease since age is the single greatest risk factor for the

Figure 1.5: Vesicular Packaging of Monoamines. VMAT2 facilitates packaging of monoamines by utilizing its proton antiporter activity and the proton gradient established by vesicular H+-ATPase (V-ATPase). In Step 1, V-ATPase uses ATP to drive the proton pump causing vesicular pH to drop acidifying the vesicle. This action can be blocked using bafilomycin. In Step 2, VMAT2 transport one monoamine across the vesicular membrane into the vesicular lumen while simultaneously transporting two protons across the vesicular membrane in the cytosolic space. This action is sensitive to several chemicals, including tetrabenazine, reserpine, lobeline, and ketanserin. Chloride channels transport Cl⁻ anions into the vesicle lumen to depolarize the vesicular membrane and protect the packaged monoamines from repulsive forces.
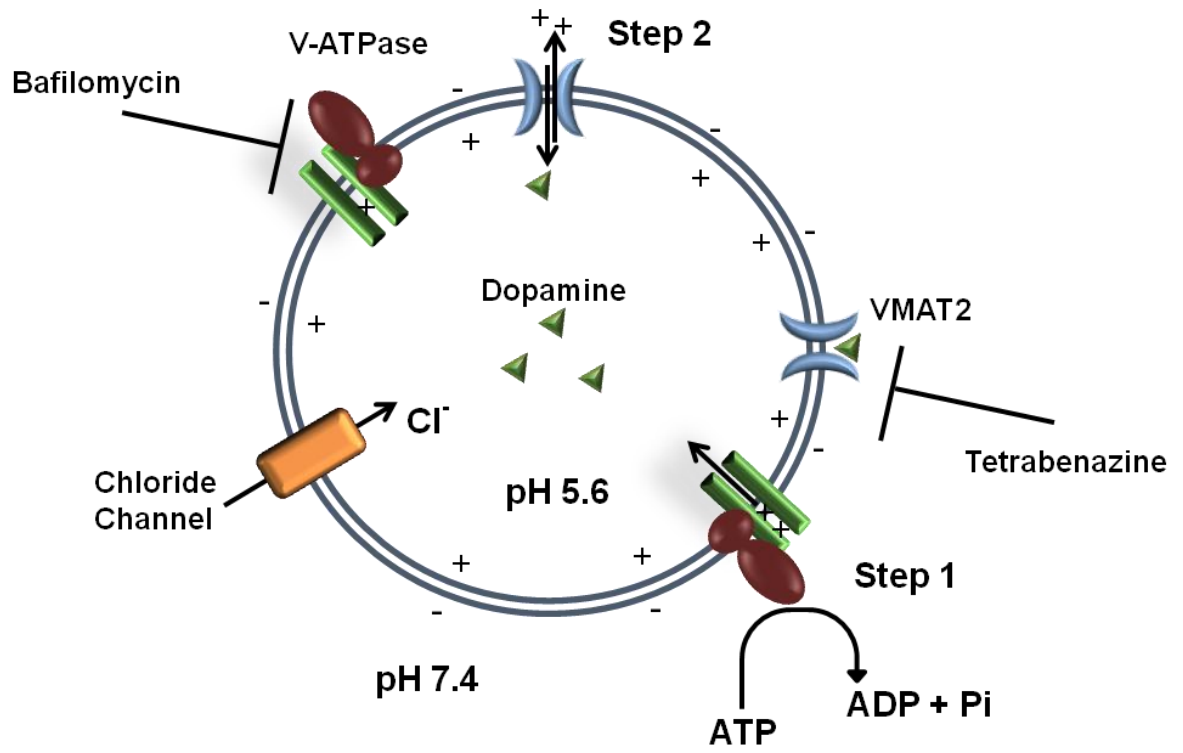
disease. In humans and rodents, VMAT2 expression levels do not appear to change with aging (Harrington et al., 1996). While in rats changes in VMAT2 subcellular localization and glycosylation are a normal part of aging, it is unclear whether this could result in changes in function. Since Parkinson's disease patients lose VMAT2 during the disease, understanding the role VMAT2 in monoamine homeostasis has become a topic of intense investigation.

Effect of VMAT2 Inhibition

Pharmacological studies with VMAT2 non-selective and selective inhibitors and various genetic studies of VMAT2 knockout mice illuminate the critical role of VMAT2 in disease pathology. Reserpine is a non-selective irreversible inhibitor of VMAT2 as it also inhibits VMAT1. Reserpine competitively labels monoaminergic vesicles of both the mammalian striatum and adrenal chromaffin granules (Giachetti et al., 1974; Near and Mahler, 1983). While reserpine has been used as anti-hypertensive agent, it is rarely prescribed as an antihypertensive today due to several unwanted side effects. Most notably a subset of patients treated for hypertension in the 1960s developed a depressed affect over time. (Freis, 1954; Freis and Ari, 1954). This delirious effect of reserpine treatment helped to form the basis of the monoamine hypothesis of depression stating that depletion of serotonin, dopamine, and norepinephrine are responsible for the pathophysiological changes that occur in depression. Animal studies reveal that reserpine treatment dramatically reduces monoamine levels in monoaminergic nuclei and striatal dopamine terminals (Liu and Edwards, 1997). Thus, the effect of VMAT2 inhibition as it relates to disease has been appreciated long before VMAT2 was identified and cloned as a factor protecting against MPP+ toxicity and the molecular target of reserpine action (Chen et al., 2005; Liu et al., 1992).

Tetrabenazine (TBZ) is another VMAT2 inhibitor that has been used to study the role of VMAT2 in cellular systems that is a reversible and binds at a site distinct from reserpine (Guay,

2010) (Figure 1.4). TBZ binding is stereoselective where (-) stereoisomers have low micromolar affinity for VMAT2 while (+) stereoisomers have very low nanomolar affinities (Kilbourn et al., 1995; Yao et al., 2011). TBZ treatment rapidly depletes monoamines from monoaminergic nuclei. TBZ is used clinically to treat chorea symptoms in Huntington's disease. It is presumed that TBZ exerts its therapeutic effect by depleting striatal dopamine; however, TBZ also has effects outside of the central nervous system (Pearson and Reynolds, 1988). A negative side effect of TBZ is that it promotes orthostatic hypotension by impairing sympathetic neuron signaling (Huang et al., 1976; Poon et al., 2010). TBZ administration, like reserpine, also results in a depressant effect in rodents (Adler, 1964). Interestingly, acute administration of TBZ has been recently shown to improve glucose tolerance and glucose-stimulated insulin release in a rat model of glucose intolerance and TBZ-like ligands have been used to approximate beta cell mass in models and patients of Type I diabetes (Ichise and Harris, 2010; Raffo et al., 2008). This suggests that VMAT2 may place an important role in the regulation of islet physiology.

Other inhibitors include ketanserin and lobeline both of which bind to the TBZ site; however, these both have potent off-target effects at 5-HT receptors and nicotinic acetylcholine receptors, respectively. Therefore, these are rarely used to approximate VMAT2 function or expression. Amphetamine and methamphetamine also inhibit VMAT2 the micromolar range but also have effects on plasma membrane transporters.

Genetic Mouse Models of VMAT2 Inhibition

Several laboratories have generated knockout mice to investigate VMAT2 function. These studies have shown that compete or partial of loss VMAT2 protein expression decreases monoamine levels in target tissues, increases susceptibility to various neurotoxins, and results in a variety of alterations in behavior and responses to psychoactive drugs (Alvarez et al., 2002; Fon et al., 1997; Fumagalli et al., 1999; Gainetdinov et al., 1998; Hall et al., 2003; Larsen et al., 2002;

Savelieva et al., 2006; Takahashi et al., 1997; Travis et al., 2000; Wang et al., 1997). However, VMAT2 knockout mice die only a few days after birth making characterization of long-term loss of VMAT2 impossible in these mice.

One laboratory attempting to generate VMAT2 knockout mice discovered a fortuitous recombination event occurred in one transgenic line that allowed small amounts of VMAT2 transcript to be produced. Expressing only 5-7% of normal striatal VMAT2 protein levels, these mice (called VMAT2 LO mice) exhibit progressive nigrostriatal degeneration similar to that seen in human Parkinson's disease (e.g. progressive loss of DAT and TH in the striatum, progressive loss of TH+ nigral neurons, and increased α-syn accumulation) and have evidence of increased oxidative stress (Caudle et al., 2007). VMAT2 LO mice are hypokinetic and display increased susceptibility to dopaminergic neurotoxins (Caudle et al., 2007; Colebrooke et al., 2007; Colebrooke et al., 2006; Guillot et al., 2008a; Mooslehner et al., 2001). In addition to dopaminergic effects, these mice also display loss of 5-HT and norepinephrine, age-dependent loss of noradrenergic neurons in the locus coeruleus, and non-motor behaviors that are responsive to adrenergic and serotoninergic drugs (Taylor et al., 2009). Together these data show that maintenance of proper VMAT2 activity is critical for the overall health of dopaminergic and other monoaminergic neurons.

Regulation of VMAT2 Protein Function

Several studies have been conducted to determine how VMAT2 is regulated. Several domains in the C-terminus of VMAT2 appear to be critical for the proper trafficking of VMAT2 to synaptic vesicles and for the retention of VMAT2 on endocytic vesicles. These include studies that show the mechanism by which phosphorylation of VMAT2 or other unidentified signaling partners by casein kinase II and PKA target VMAT2 to different populations of synaptic vesicles or large dense core vesicles. More recently, the molecular chaperone Hsc70 was identified as

regulator of VMAT2 activity through an interaction with the 3rd cytoplasmic loop of VMAT2 (Requena et al., 2009). Hsc70 cofractionated with VMAT2 in a synaptic vesicle fraction and coexpression of Hsc70 or the related Hsp70 protein dose-dependently inhibits VMAT2 activity. Additionally, VMAT2 has recently been shown to interact with TH and AADC at synaptic vesicles (Cartier et al., 2010). This discovery has important implications for synaptic biology because dopamine synthesis and packaging into synaptic vesicles appears to be tightly orchestrated possibly due to the oxidation potential of dopamine.

Additionally, intravesicular monoamine regulates monoamine loading into synaptic vesicles through a G protein-dependent mechanism (Holtje et al., 2000). $G_{o2}\alpha$ and $G_{q}\alpha$ inhibit vesicular uptake of monoamines (VMAT2 activity), but only in monoamine-preloaded vesicles and through a first luminal loop interaction with VMAT2 (Brunk et al., 2006). Moreover, this effect is independent of heptahelical G-protein coupled receptors. This novel mechanism for G protein regulation of VMAT2 activity suggests that quantal storage of monoamines and not simply exocytic release is an important point of regulation for neurotransmission. Additionally, Ca^{2+} activator proteins of secretion (CAPS) 1 and 2 increase vesicular uptake of monoamines (VMAT2 activity) (Brunk et al., 2009). Identification of new VMAT2 binding partners may shed light on this complex regulation and aid in our understanding of the potential neurotoxic effects of dopamine.

PCBs as Environmental Targets of VMAT2

PCB mixtures are also neurotoxic (Mariussen et al., 2002; Shain et al., 1991). In dopamine neurons, acute and subchronic exposure to PCB mixtures can result in reduced striatal DAT and/or VMAT2 expression of animals (Caudle et al., 2006; Richardson and Miller, 2004). Losses of nigral or striatal dopamine and dopamine metabolites have also been reported (Chu et al., 1995; Chu et al., 1996; Lyng and Seegal, 2008; Richardson and Miller, 2004; Seegal et al., 1986; Seegal et al., 1990; Seegal et al., 1991; Seegal et al., 2002). These changes in dopamine

may be explained at least in part by decreases in packaging (and reuptake) of dopamine (Bemis and Seegal, 2004; Seegal et al., 2002). Some PCB congeners inhibit vesicular packaging of dopamine in the low micromolar concentrations; however, it is uncertain whether this effect is due to inhibition of VMAT2 (Mariussen et al., 1999; Mariussen et al., 2001). Moreover, ortho-substituted PCBs are better inhibitors of vesicular uptake than dioxin-like PCBs. Given that VMAT2 loss in mice has been shown to result in monoaminergic neuronal loss over time, chronic inhibition of VMAT2 by PCBs may be one mechanism linking exposure to the neurodegeneration seen in Parkinson's disease. While current evidence does not exist to support such a claim, it is an intriguing hypothesis that should be further tested.

Monoaminergic signaling in the regulation of glucose homeostasis

While PCBs are associated with both Parkinson's disease and diabetes, no studies have tried to elucidate any common mechanisms associated with both diseases. While monoaminergic dysfunction is the most commonly recognized pathological criteria for Parkinson's disease, it is unclear whether monoaminergic dysfunction plays any role in diabetes mellitus. However, much evidence exists supporting the role of monoamines in regulating normal pancreatic physiology related to insulin release. Also, drugs targeting monoaminergic signaling are increasingly used as therapies for the treatment of diabetes mellitus.

Mechanism of Glucose-stimulated Insulin Release in Beta Cells of the Pancreatic Islets

Pancreatic islets are endocrine cells of multiple cell types organized into groups throughout the exocrine pancreas (Figure 1.6). Beta cells are believed to have evolved in vertebrates from a primitive group of insulin-secreting neurons. In fruit flies, there are insulin-secreting cells in the brain that are homologous to the islet beta cells of vertebrates (Wang et al., 2007). New evidence suggests that these cells in fruit flies originate from the neuroectoderm that is homologous to the precursor of pituitary and hypothalamic cells. In vertebrates, pancreas

Figure 1.6: Pancreatic Islet Organization. The pancreatic islet is the compact collection of cells comprising the endocrine pancreas. Islets account for approximately 1-2% of total pancreas mass. Within islets several different cell types are present distinguished by the secretagogue produced and released by the cell. Beta cells make up the bulk of islet mass (approximately 65-80% of total islet cells). These cells secrete insulin and the amyloid protein amylin (shown as red cells). Alpha cells are the second most common cell type in the islet (15-20%). These cells secrete glucagon (shown as green cells). Delta cells are the third most common cell type (3-10%). These cells secrete somatostatin (shown as blue cells). The fourth cell type is the PP cell (3-5%). These cells secrete pancreatic polypeptide (shown as orange cell). The fifth cell type is epsilon cell (<1%). These cells are very uncommon and secrete gherlin (not shown). In addition to these cell types, innervation received from the sympathetic pancreatic ganglion (shown in purple) which contains VMAT2 and secretes norepinephrine is present as well as parasympathetic innervations (not shown).

Sympathetic Nerve Fibers

δ

Delta Cell
(Somatostatin-Producing)

Alpha Cell
(Glucagon-Producing)

α

PP

β

Beta Cell
(Insulin &
Amylin-Producing)

Pancreatic Polypeptide Cell
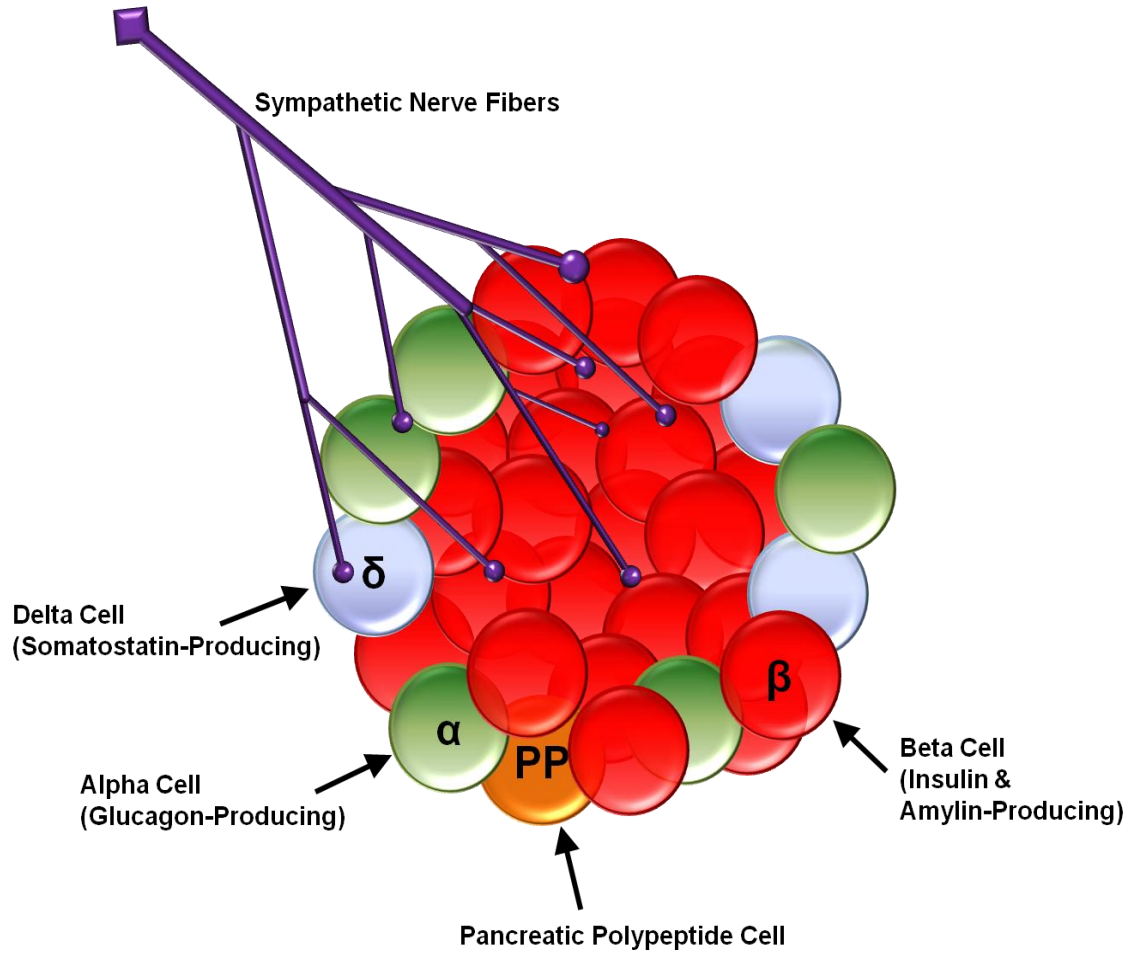
forms from a different embryonic tissue than flies. Involution of the endoderm from the developing digestive tract forms the pancreas in higher organisms. However, this indicates that a common ancestor to both flies and vertebrates displayed similar insulin-driven endocrine function. Despite the divergence in mammalian pancreatic and brain tissue origins, expression of neuronal proteins in pancreatic islets is common and knockout studies of islet proteins often result in concomitant loss of expression in the brain (Song et al., 2010). Indeed, pancreatic islets in general and beta cells in particular have long been recognized as monoaminergic in nature (Burr et al., 1974; Cegrell, 1968; Gagliardino et al., 1970; Iturriza et al., 1970; Jaim-Etcheverry and Zieher, 1968; Lebovitz and Feldman, 1973; Lundquist, 1971; Tjalve, 1971; Wilson et al., 1974).

When blood glucose levels rise typically after a meal, the body must clear excess glucose from the blood (Figure 1.7). Glucose is transported into the beta cell by glucose transporter 2 (GLUT2). Once inside the cell, glucose is catabolized through glycolysis. This leads to an increase in ATP production by mitochondria. As ATP/ADP ratios increase, the ATP –dependent K^+ channel is blocked preventing K^+ efflux and depolarizing the beta cell membrane. Depolarization stimulates Ca^{2+} channels to open promoting exocytosis of docked secretory granules at the plasma membrane. Insulin is released from secretory granules and enters the blood circulation to act on insulin–sensitive tissues. Insulin acts on the liver to promote glucose uptake and inhibit gluconeogenesis and on muscle tissues to promote glucose uptake. Approximately one third of post-prandial blood glucose is removed from the blood this way (Moore et al., 2003). Therefore, glucose is the most potent driver of insulin release from the pancreas. However, a variety neurotransmitters and neuropeptides have been shown to modulate these processes, including monoamines.

Monoamine Regulation of Insulin Release and Glucose Metabolism

Beta cells appear to utilize a mechanism similar to neurons to synthesize and package dopamine. Beta cells express TH, AADC, and MAO_A to synthesize and metabolize dopamine while also

Figure 1.7: Monoamine Regulation of Glucose-Stimulated Insulin Release. Beta cells express many enzymes involved in dopamine synthesis including TH and AADC. After dopamine is synthesized, it is packaged into secretory vesicles contain insulin via VMAT2. The beta cell releases insulin in response to glucose stimulus. In step 1, glucose is transported into the beta cell by glucose transporter 2 (GLUT-2). In Step 2, glucose undergoes glycolysis raising intracellular ATP levels. In Step 3, ATP/ADP cellular ratios increase inhibiting K^+ efflux via the ATP-dependent K^+ channel. This causes the beta cell to depolarize. In Step 4, upon depolarization voltage-dependent Ca^{2+} channels open allowing Ca^{2+} influx into the cytosol of the beta cell. In Step 5, Ca^{2+} influx results in plasma membrane-vesicle fusion leading to exocytosis of insulin and copackaged dopamine. In Step 6, released dopamine can bind dopamine autoreceptors located on the beta cell membrane. This leads to feedback inhibition of insulin release under glucose stimulation. Additionally, sympathetic neurons synthesize and release dopamine and norepinephrine in response to a need for more circulating glucose to fuel the metabolic demands of the organism. Dopamine and norepinephrine released from these neurons can also activate dopamine and adrenergic receptors on beta cells inhibiting further insulin secretion.
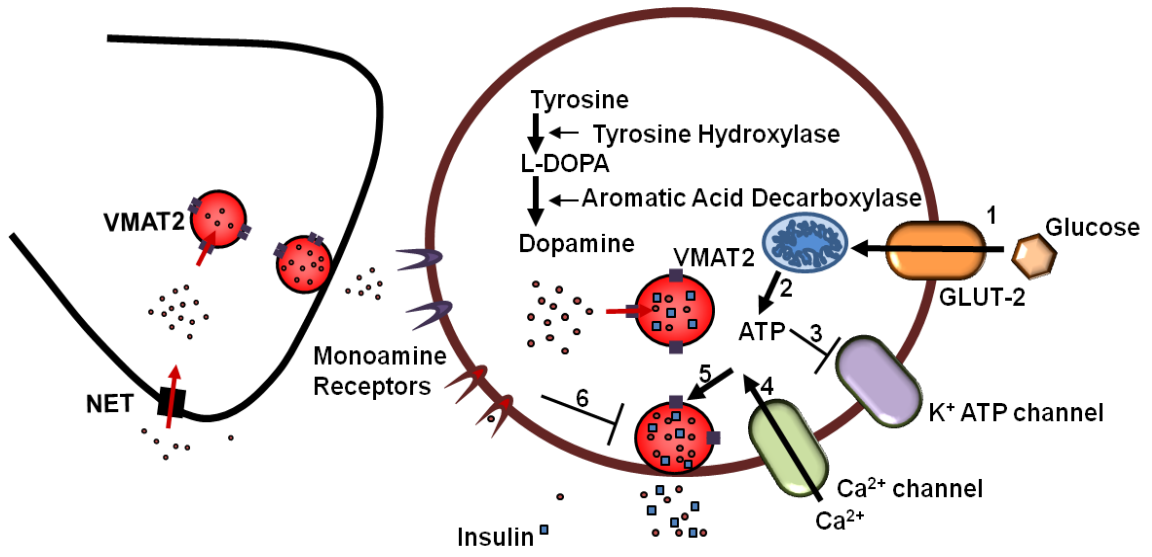
expressing VMAT2 and α-syn in insulin-containing secretory vesicles (Billett, 2004; Geng et al., 2010). Some evidence suggests that norepinephrine may also be present in beta cells as DβH is expressed in some insulin-containing secretory vesicles (Takayanagi and Watanabe, 1996; Watanabe and Nagatsu, 1991). Beta cells also express both D1 and D2 receptors and α_{2a} adrenergic receptors. VMAT2 is also highly expressed in the sympathetic neurons innervating the pancreas, and previous studies in rats treated with the beta cell-selective toxin streptozocin have shown a dramatic reduction in VMAT2-positive sympathetic fibers innervating islets and loss of total islet VMAT2 expression while the innervation to the exocrine pancreas is spared. This suggests that islet innervations are lost upon the death of beta cells (Mei et al., 2002).

Dopamine Regulation of Insulin Release and Glucose Metabolism

It has been proposed that dopamine acts on nearby beta cells to attenuate insulin secretion. Several studies have been done to characterize the effects of dopamine and dopamine receptor agonists and antagonists on glucose-stimulated insulin release. Most notably the D2 receptor agonist bromocriptine has been approved for the treatment of diabetes. D2 receptors are expressed on beta cells, colocalized at insulin containing secretory granules, and inhibit glucose-stimulated insulin release when activated; however, complete genetic ablation of D2 receptors results in impaired glucose-stimulated insulin release and glucose intolerance (Garcia-Tornadu et al., 2010; Rubi et al., 2005). Therefore, chronic loss of D2 receptor signaling is not necessarily beneficial. In addition, catecholamines as a whole (dopamine, norepinephrine, and epinephrine) have long been known to directly inhibit glucose-stimulated insulin release (Feldman et al., 1971; Quickel et al., 1971). Therefore, the sum effects of dopamine are extremely complicated and may be related to a combination of direct effects on the pancreas and indirect effects on the central nervous system, opposing D1 and D2 receptor effects, or may be temporal in nature.

Indeed, L-DOPA treatment in Parkinson's disease patients promotes hyperglycemia and hypoinsulinemia early in treatment; however, these side effects can be blocked with carbidopa (peripheral AADC inhibitor) suggesting that peripherally-sourced dopamine, not centrally-sourced dopamine is responsible for this effect. Chronic administration of L-DOPA/carbidopa in rats does lead to obesity, hyperglycemia, and slight hyperinsulinemia though. Thus, chronically elevated central dopamine most likely promotes blood glucose dysregulation through regulation of feeding.

Norepinephrine Regulation of Insulin Release and Glucose Metabolism

Previous studies have shown that activation of the sympathetic pathway in the pancreas blocks release of insulin and stimulates release of glucagon causing blood glucose levels to rise (Ahren and Taborsky, 1988; Dunning et al., 1988; Kurose et al., 1990; Kurose et al., 1992). This latter physiological response is important to combat exercise-induced hypoglycemia (Tuttle et al., 1988). These data implicate the monoaminergic neurotransmitter norepinephrine as playing an important role in islet physiology. α_{2a} adrenergic receptors expressed on beta cells play a critical role regulating insulin secretion. α_{2a} adrenergic receptor knockout mice have a 30% reduction in fasting glucose levels than WT littermates and a near significant increase in fasting insulin levels, indicating that adrenergic action plays an important role in normal glucose metabolism (Savontaus et al., 2008). Activation of adrenergic receptors blocks insulin release, and polymorphisms in the α_{2a} adrenergic receptor gene locus resulting in overexpression were recently identified as a susceptibility gene for diabetes in both humans and a rat model (Nakaki et al., 1980; Rosengren et al., 2010). Interestingly, one report suggests that the beneficial effects of bromocriptine therapy for diabetes are actually mediated through α_{2a} receptors (de Leeuw van Weenen et al., 2010). Thus, further investigation is required to dissect the contribution of each monoamine system to VMAT2's role in the regulation of glucose homeostasis and islet physiology.

Serotonin Regulation of Insulin Release and Beta Cell Mass

5-HT has also been shown to regulate insulin release under certain physiological conditions. Recently, the role of 5-HT in the regulation of beta cell mass expansion during pregnancy has been demonstrated (Kim et al., 2010; Schraenen et al., 2010). 5-HT is expressed at extremely low levels in islets under normal conditions. However, during mid-gestation prolactin and placental lactogen levels rise in order to prepare the mother for the demands of caring for her offspring. During this time, the metabolic demands on the mother are sharply increased and beta cell mass expands in response to increase insulin responses during the remainder of gestation. TPH expression increases dramatically in response to prolactin leading to increased 5-HT production (Schraenen et al., 2010). 5-HT$_{2B}$ receptor activation then leads to beta cell proliferation. Just prior to birth, 5-HT$_{2B}$ levels return to pre-pregnancy levels and expression of 5-HT$_{1D}$ increases returning beta cell mass to pre-pregnancy size (Kim et al., 2010). These data highlight the role of 5-HT in regulation of pregnancy energy balance and suggest a mechanism describing the known link between depression and gestational diabetes. Some studies suggest that 5-HT has a greater role in islet physiology, but these were not typically done in whole animal studies. Basal pancreatic 5-HT levels appear simply too low to have physiological consequences (Schraenen et al., 2010).

Potential Role of VMAT2 in Glucose Homeostasis and Beta Cell Imaging

Since dopamine and adrenergic receptors blockers affect insulin secretion, VMAT2 may also have a role in insulin secretion. A recent study showed that acute administration of TBZ markedly reduced pancreatic dopamine levels, improved glucose tolerance, and increased glucose-stimulated insulin release in the streptozocin-induced rat model of diabetes (Raffo et al., 2008). This suggests that TBZ may be a useful drug for the treatment of diabetes and the glucose

intolerance observed in Huntington's patients (Andreassen et al., 2002; Hunt and Morton, 2005; Josefsen et al., 2008).

More recently, the monoaminergic nature of the endocrine pancreas system suggests that monoaminergic proteins may be excellent markers of islet and beta cell mass (Ichise and Harris, 2010). VMAT2 is the leading monoaminergic biomarker because several reports indicate that VMAT2 is selectively expressed in beta cells and nerve terminals innervating the pancreas. Additionally, TBZ PET ligands are being developed to approximate beta cell mass in models of diabetes (Leung, 2004a; Leung, 2004b). *In vivo* imaging of beta cell mass by non-invasive PET imaging would be an extraordinarily useful tool for physicians treating diabetic patients. While TBZ ligands are lead compounds for this, much controversy exists as to the usefulness of TBZ ligands to approximate true beta cell mass. While one group shows a loss of beta cell mass by PET imaging using the TBZ ligand [11C]dihydrotetrabenazine ([11C]DTBZ), other groups have shown that [11C]DTBZ binding occurs throughout the exocrine and endocrine pancreas (Eriksson et al., 2010; Fagerholm et al., 2010; Freeby et al., 2008; Kilbourn, 2010; Kung et al., 2008a; Kung et al., 2008b; Lin et al., 2010; Simpson et al., 2006; Souza et al., 2006). While TBZ is believed to be a specific inhibitor of VMAT2, it is unclear whether VMAT2 targeted ligands such as TBZ truly represent total VMAT2, whether VMAT2 region and cell type expression data in the pancreas is inaccurate, or whether VMAT2-nonspecific binding of TBZ is present in the pancreas. Regardless, (18)F-labeled TBZ derivatives and other TBZ ligands have been shown to be an extremely useful tools in approximating the integrity of monoaminergic cell bodies and synapses in Parkinson's disease (Frey et al., 2001).

α-Synuclein in the Beta Cell and Neuron

Recently, other proteins associated neurodegeneration have been implicated in the regulation insulin secretion. α-Syn is expressed on insulin-containing secretory vesicles in beta

cells, and loss of α-syn expression results in increased glucose-stimulated insulin release in isolated mouse islets (Geng et al., 2010). It is conceivable that α-syn in the islet may be a previously unappreciated target of dysregulation in Parkinson's disease. Since α-syn is known regulator of monoamine homeostasis and monoamines affect insulin release in multiple models, α-syn regulation of monoamine homeostasis may be the mechanism by which α-syn exerts its effects in glucose-stimulated insulin release. Understanding the mechanisms of α-syn regulation of monoamine homeostasis is necessary to fully appreciate any potential link.

Originally reported to be a nuclear protein, subsequent studies have shown that α-syn primarily exists at synaptic terminals (Schulz-Schaeffer, 2010). α-syn typically exists as a monomer or dimer (Nakajo et al., 1993). Structural studies show that as a monomer α-syn exists in either an a α-helical or random coil confirmation (Jo et al., 2004). *In vitro* studies have shown that changes in α-syn structure resulting in increased α-helical formation increases α-syn ability to bind to artificial membranes (Chandra et al., 2003; Davidson et al., 1998; Eliezer et al., 2001; Jo et al., 2000). However, upon adoption of a β-sheet confirmation, α-syn begins to form insoluble aggregates (Volles and Lansbury, 2003). Oxidation of α-syn is necessary to form dimers through dityrosine interactions and promotes subsequent aggregation (Krishnan et al., 2003). Parkinson's disease-associated mutant α-syn appears to be more susceptible to this modification. Early on in aggregation, α-syn transiently forms soluble oligomers or protofibrils that are thought to be toxic to cells and lose toxicity as they further oligomerize into larger fibrils possibly because of subsequent compartmentalization into Lewy bodies (Wood et al., 1999). Phosphorylation and proteolytic cleavage also affects α-syn solubility and toxicity (Mishizen-Eberz et al., 2003). α-syn protofibril formation may be an early feature of Parkinson's disease pathology that initiates events leading to neuronal cell death. In mice, nigral α-syn levels peak after birth and steadily decline with age (Mak et al., 2009).

Cell culture studies have also shown that dopamine is necessary for α-syn-induced cell toxicity (Bisaglia et al., 2010a; Hasegawa et al., 2006). Both oxidized dopamine and oxidized NE inhibit formation of the less toxic α-syn fibril by stabilizing the more toxic protofibril form of α-syn leading to alterations in protein clearance (Bisaglia et al., 2007; Conway et al., 2001; Martinez-Vicente et al., 2008; Norris et al., 2005). Interestingly, an estimated 90% of aggregated α-syn protein is located at the presynaptic terminal (Schulz-Schaeffer, 2010). Also, it has been postulated that these protofibrils can form pores that permeate vesicle causing dopamine leakage (Volles and Lansbury 2002). Thus, decreased VMAT2 activity may actually exacerbate the toxicity of α-syn overexpression (Lotharius et al., 2002). In VMAT2 LO mice, α-syn accumulation increases as the mice age; however, no direct evidence exists that α-syn is aggregating in this model (Caudle et al., 2007). Consistent with this interpretation, decreases in VMAT2 expression during Parkinson's disease progression are observed in human PET studies (Bohnen et al., 2006; Frey et al., 1996). This suggests that as Parkinson's disease progresses, neurons may become even more susceptible to insult from misplaced monoamines.

α-Synuclein Regulation of Monoamine Homeostasis

α-Syn shares high structural homology to the 14-3-3 family of chaperone proteins that increase TH activity, and several studies have suggested a chaperone-like role for α-syn (Burre et al., 2010; Chua and Tang, 2006; Xu et al., 2002). α-Syn interacts with both TH and AADC, decreasing the activity of both enzymes (Perez et al., 2002; Tehranian et al., 2006). Lentivirally-overexpression of A53T mutant α-syn in MESC2.10 dopaminergic cells results in decreased dopamine uptake and release (Lotharius et al., 2002). This supports data showing that α-syn interacts with DAT (Lee et al., 2001; Wersinger et al., 2003b); however, conflicting reports exist as to what functional effects on DAT activity result from this interaction. Indeed, these data have led to the study of α-syn effects on proteins involved in the regulation of the norepinephrine and serotonin transporters (Wersinger et al., 2006a; Wersinger et al., 2006b).

Additionally, overexpression of WT, A53T, or A30P α-syn increases cytosolic dopamine levels and impairs vesicular pH in PC12 cells (Mosharov et al., 2006). This demonstrates that overexpression of α-syn protein impairs vesicular storage of dopamine by either compromising membrane integrity resulting in proton and/or dopamine leakage, inhibiting dopamine vesicular transport by direct inhibition of VMAT2 or indirect impairment of vesicular pH gradient, or some combination of these mechanisms. Indeed, one report suggests that α-syn directly interacts with VMAT2 and overexpression inhibits VMAT2 activity (Guo et al., 2008). Other experiments suggest that α-syn overexpression impairs endocytosis of synaptic vesicle resulting in decreased dopamine release (Nemani et al., 2010). Perhaps overexpression of wild-type α-syn or expression of mutant α-syn increases α-syn's ability to aggregate into protofibrils, greatly decreasing the amount of soluble α-syn and leading to α-syn loss-of-function and mishandling of dopamine (Perez and Hastings, 2004). In support of this hypothesis, flies overexpressing A30P α-syn have selective dopaminergic degeneration that was similar to that of overexpression of TH. Additionally, overexpression of VMAT2 or decreasing dopamine production can both rescue this α-syn induced damage (Park 2007).

Several transgenic and knockout mouse models affecting neuronal α-syn expression have been created to study the role α-syn plays in dopamine neuron function. While alterations in the vesicular pool size have been shown in α-syn transgenic mice, changes in dopamine levels have also been observed (Chesselet, 2008; Yavich et al., 2005). This suggests that α-syn plays some role in regulating dopamine homeostasis. However, nigral cell loss is not observed in any of these transgenic models suggesting that α-syn ablation or overexpression in neurons is insufficient to cause nigral cell death. Interestingly, in rat virally-transduced models where α-syn overexpression is driven in both neurons and glia, dopamine neuronal death does occur suggesting that overexpression of α-syn may be necessary in both glia and neurons to promote

neuronal death or species differences affect vulnerability to α-syn-induced neuronal death(Dawson et al., 2010).

Introduction to Specific Aims

Central Hypothesis- PCBs have been linked to both Parkinson's disease and diabetes in epidemiological studies. While PCBs are known to act via a variety of mechanisms to exert their toxic effects, dysregulation of dopamine is strongly linked the neurotoxic effects of PCBs. The mechanisms by which PCBs may promote diabetes mellitus are not well understood. Dopamine and other dopaminergic drugs are known to act directly on islets in the pancreas to affect glucose homeostasis and insulin release in humans and animal models of diabetes mellitus. Therefore, dopamine homeostasis may be a target of PCBs in the pancreas. Since drugs that target VMAT2 can decrease dopamine levels in the pancreas and affect insulin release, VMAT2 may be the mechanism by which PCBs disrupt glucose homeostasis. *I predict that both PCB exposure and genetic deficiency in VMAT2 expression will alter dopamine levels in the pancreas leading to impaired glucose homeostasis in mice.*

Rationale

Epidemiological studies suggest that having diabetes increases the risk of developing Parkinson's disease. Interestingly, exposure to PCBs is strongly linked to both diabetes mellitus and Parkinson's disease. This suggests that a common pathophysiological mechanism may exist in both diseases. PCBs are known to disrupt dopamine homeostasis in the striatum of exposed animals. Therefore, the mechanism of action of PCBs in Parkinson's disease may be events leading to dopamine dysfunction. While the link between PCB exposure and diabetes has been well documented by human epidemiological studies, the potential mechanisms by which this may occur are not understood.

I suggest that PCBs act by a common mechanism to promote both Parkinson's disease and diabetes mellitus (Figure 1.8). I propose that PCBs will promote monoaminergic dysfunction in both the brain and pancreas. I believe that PCBs will be able to do this via VMAT2 inhibition resulting in reduced dopamine levels. In addition to the known effects in Parkinson's disease, this loss of dopamine will also alter glucose homeostasis. Demonstration of this effect will greatly support the proposed link between Parkinson's disease and diabetes mellitus.

Much evidence exists to suggest a link between these diseases, including a large body of basic research that indicates potential common mechanisms, one of those being the common control of monoamines in the physiological functions affected by both diseases (Arneric et al., 1984; Caudle et al., 2006; Corrigan et al., 1998; Corrigan et al., 2000; Everett et al., 2011; Hampshire et al., 1978; Jetton et al., 2001; Liang et al., 1998; Raffo et al., 2008; Richardson and Miller, 2004; Sandyk, 1993). Currently, there is little evidence as to causality relationship between PCBs and diabetes or PCBs and Parkinson's disease. This is largely due to poor animal data supporting such a link. Since I estimate that VMAT2 inhibition in the pancreas results in alterations in glucose tolerance and insulin release and that PCBs may inhibit VMAT2, I chose to use the VMAT2 LO model and Aroclor 1254: Aroclor 1260 (PCB) models as tools to investigate the role of pure genetically-induced VMAT2 inhibition on glucose homeostasis versus a "dirty", more environmentally-relevant toxicant model of VMAT2 inhibition on glucose homeostasis (Figure 1.9 and Figure 1.10). It is the hope that comparing the outcomes of these two experiments will shed light on the relative contribution of monoaminergic dysfunction in PCB exposure as it relates to glucose homeostasis.

VMAT2 plays a critical role in the health of monoaminergic neurons in the brain. Mice with very low levels of VMAT2 expression have near complete loss of monoamine levels in various brain regions and progressive nigrostriatal dopaminergic and locus coeruleus noradrenergic degeneration. This loss leads to a variety of behavior abnormalities consistent with

Figure 1.8: Proposed Model of the Interaction Between Parkinson's Disease and Diabetes Mellitus. In this model, PCBs affect monoaminergic function via VMAT2 inhibition. This leads to Parkinson's disease and diabetes mellitus.
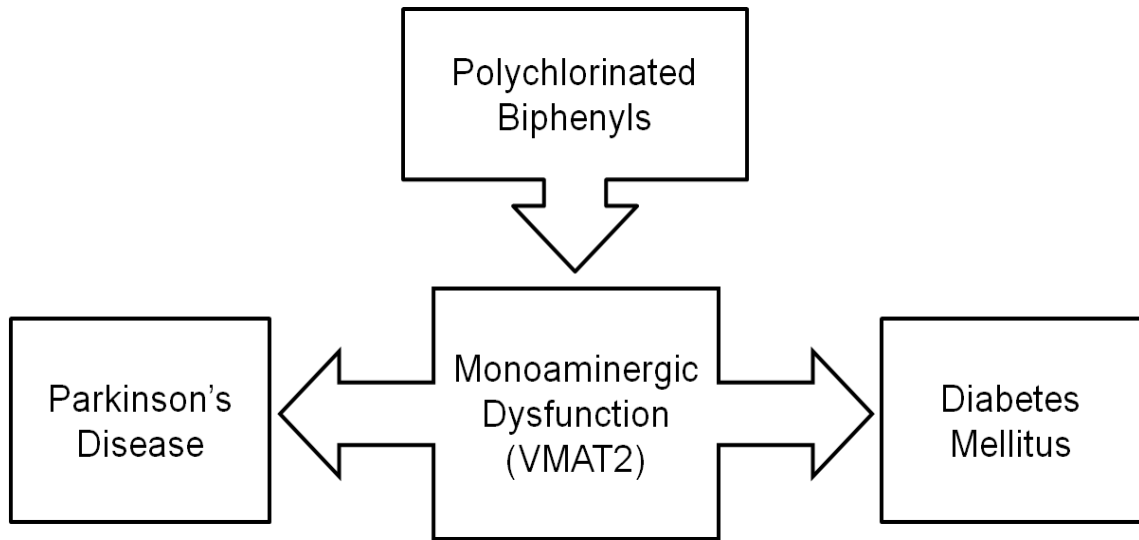
Figure 1.9: Proposed Effect of PCB-mediated VMAT2 Inhibition on Glucose-Stimulated Insulin Release. Many studies have shown that dopamine and norepinephrine directly suppress glucose-stimulated insulin release by action on dopamine and adrenergic receptors located on beta cells. Since beta cells corelease dopamine with insulin upon glucose stimulation, local action of dopamine on dopamine receptors can act as feedback inhibition of insulin release. Additionally, sympathetic activation results in norepinephrine release from sympathetic nerves innervating the pancreas. Since insulin action inhibits gluconeogenesis in the liver and promotes lower blood glucose levels, sympathetic activation inhibits glucose-stimulated insulin release to promote circulating glucose levels to provide the necessary fuel for the "fight or flight" response. Thus, activation of adrenergic receptors on beta cells suppresses glucose-stimulated insulin release. PCBs have been shown to inhibit VMAT2 in isolated vesicles and to reduce dopamine levels in dopaminergic regions of the brain. Therefore, we hypothesize that PCB-treated mice will have reduced dopamine levels in the pancreas. This loss of dopamine will result in impaired feedback inhibition leading to increased glucose-stimulated insulin release.
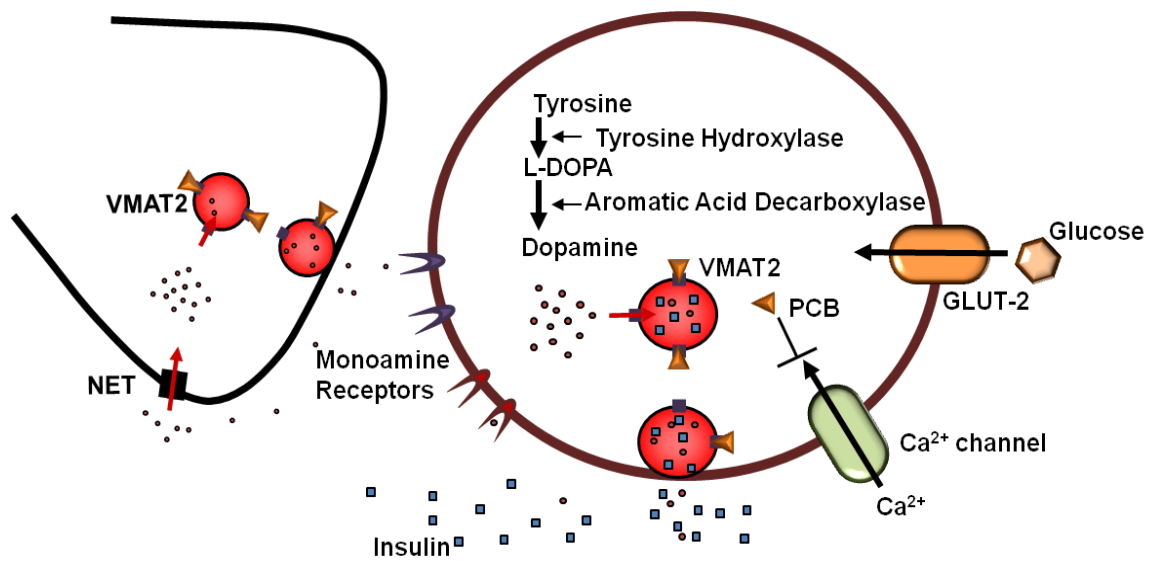
Figure 1.10: Proposed Effect of VMAT2 Inhibition on Glucose-Stimulated Insulin Release.
Previous studies have shown that dopamine and norepinephrine can affect glucose-stimulated insulin release in beta cells. Dopamine and norepinephrine directly suppress glucose-stimulated insulin release by action on dopamine and adrenergic receptors located on beta cells. Since beta cells corelease dopamine with insulin upon stimulation, local action of dopamine on dopamine receptors can act as feedback inhibition of insulin release. Additionally, sympathetic activation results in norepinephrine release from sympathetic nerves innervating the pancreas. Since insulin action inhibits gluconeogenesis in the liver and promotes lower blood glucose levels, sympathetic activation inhibits glucose-stimulated insulin release to promote circulating glucose levels to provide the necessary fuel for the "fight or flight" response. Thus, activation of adrenergic receptors on beta cells suppresses glucose-stimulated insulin release. When VMAT2 expression is loss in other tissues, monoamine levels are dramatically reduced. Therefore, we hypothesize that VMAT2 LO mice will have reduced dopamine and norepinephrine levels in the pancreas. This loss of dopamine and norepinephrine will result in impaired feedback inhibition leading to increased glucose-stimulated insulin release.
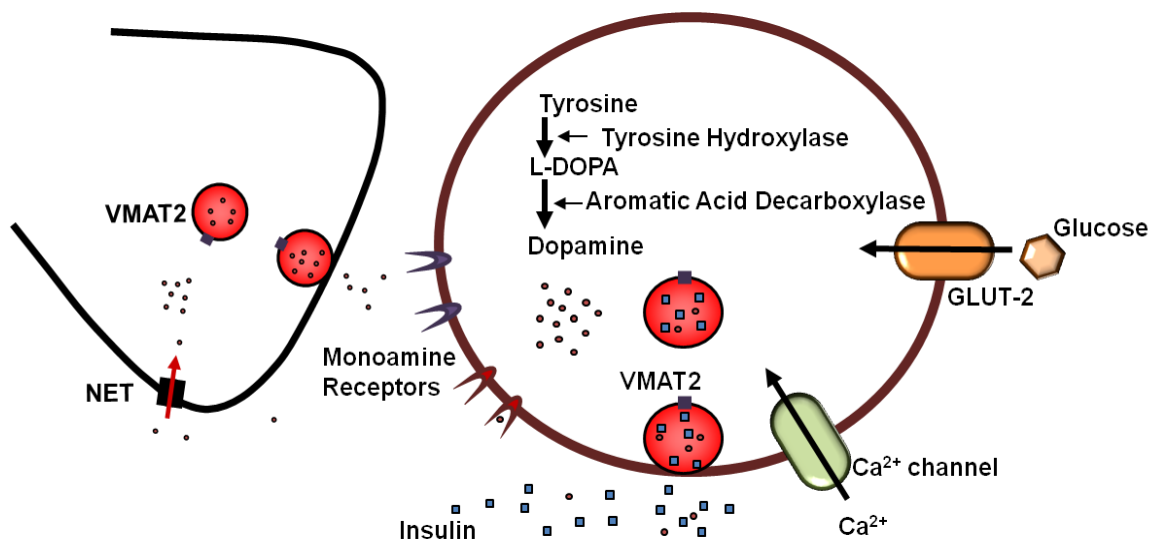
the loss of monoaminergic signaling in the brain. However, VMAT2 is not solely expressed in the brain. Therefore, loss of VMAT2 expression in the peripheral nervous system and in non-neuronal tissues may have other effects on the body. This is of great interest since VMAT2 expression is loss in the brains of Parkinson's disease patients, but also other monoaminergic nuclei outside of the brain are affected particularly sympathetic tracts innervating a multitude of tissues throughout the body. Alterations in sympathetic innervation to the heart and other components of the circulatory system result in autonomic dysfunction such as orthostatic hypotension. Additionally, glucose intolerance and diabetes are often reported in patients with Parkinson's disease (Barbeau et al., 1961; Boyd et al., 1971; Lipman et al., 1974). This suggests that Parkinson's disease pathology may involve other hormonally active tissues that affect blood glucose homeostasis. Additionally, bromocriptine is approved to treat both Parkinson's disease and diabetes, suggesting that loss of dopamine signaling may be common to both diseases and thus dopamine replacement is therapeutic in both diseases. Since VMAT2 expression has been shown in islet cells of the pancreas and is expressed in sympathetic neurons innervating the pancreas, we propose that loss of VMAT2 expression in the pancreas will alter blood glucose homeostasis in the VMAT2 hypomorph mouse (Figure 1.10).

While several lines of evidence show the role of α-syn in vesicular storage when highly overexpressed, these experiments appear to only represent α-syn effects under pathological conditions. It is unknown what role, if any, α-syn plays in the storage of dopamine under normal expression conditions. Studies of TH expression and phosphorylation under pathological conditions, indicate that α-syn may exert opposing roles on TH activity under low and high (pathological) expression conditions (Alerte et al., 2008). While α-syn has been shown to downregulate TH activity by blocking phosphorylation of TH Ser 40 in cell cultures, under virally-transduced α-syn overexpression *in vivo* TH is hyperphosphorylated and thus most likely overactive. Again, α-syn appears to increase DAT activity by increasing cytoplasmic clustering

of DAT protein, while α-syn also decreases DAT activity via a microtubule-dependent trafficking mechanism (Lee et al., 2001; Moszczynska et al., 2007; Wersinger and Sidhu, 2003; Wersinger and Sidhu, 2005). This suggests that α-syn expression level or other factors may be critical determinants of the effects that α-syn exerts. Since previous studies with TH have suggested that α-syn has dramatically different effects under pathological and non-pathological conditions, the simplest explanation for the discrepancy seen with respect to DAT and α-syn is that these experiments are done under different levels of α-syn expression. To this end, determining the role of α-syn on dopamine vesicular packaging is critical to discriminate the role of α-syn in normal physiological conditions and under pathophysiological conditions.

While there is evidence supporting an *in vivo* interaction between α-syn and VMAT2, data demonstrating a direct effect on VMAT2 activity is unfortunately weak. No experiments relating dopamine vesicular storage and α-syn have been done in the presence of VMAT2 inhibitors. This makes dissecting the relative contribution of VMAT2-specific effects from VMAT2 non-specific effects on vesicular storage or leakage difficult. Therefore to approximate α-syn effects under normal non-pathological conditions, we will determine TBZ-sensitive VMAT2 activity under low α-syn expression levels. We will also determine dose-response effects of α-syn on TBZ-sensitive vesicular dopamine uptake to determine if like DAT and TH α-syn effects vesicular dopamine storage differently under different conditions. We will confirm and map the sites of interaction between α-syn and VMAT2 and confirm these interactions *in vivo*. Completion of these experiments will fill a critical gap in the field by expanding our understanding of the role of α-syn in vesicular storage of dopamine under non-pathological conditions.

Specific Aim 1: *Subchronic exposure to PCBs leads to hyperinsulinemia and impaired glucose tolerance in mice.*

Specific Aim 2: *Genetic ablation of VMAT2 leads to improved fasting glucose, glucose tolerance, and insulin release in mice.*

Specific Aim 3: *α-syn protein regulates VMAT2 activity*

Chapter 2

Polychlorinated Biphenyl Mixtures Reduce

Dopamine Levels in the Pancreas and Impair

Glucose Tolerance and Insulin Release

Abstract

Exposure to polychlorinated biphenyls (PCBs) is associated with increased risk of diabetes; however, poor experimental evidence exists supporting this link. We gave mice Aroclor 1254:Aroclor 1260 mixtures daily for 28 days to determine the effect of PCB exposure on both the pancreatic dopaminergic system and glucose homeostasis. Interestingly, female mice show a consistent impairment (18% and 30% increase over treatment period) of glucose tolerance versus vehicle-treated controls; however, PCB-treated male mice show improved glucose tolerance at 14 days versus vehicle-treated controls. Additionally, PCB-treated female mice showed a trend towards increased weight gain than controls over the study, increased glucose-stimulated insulin release, and had significantly reduced (22%) serum adiponectin levels, a strong indicator of insulin resistance. Previous studies show that PCBs can affect dopamine levels in the brain and inhibit the vesicular packaging of dopamine. Pancreatic dopamine levels were reduced by over 35% in PCB-treated female and male mice. These data strongly support a role for PCBs in the development of diabetes and suggest that alterations in catecholamine signaling in the pancreas may play a role. Sexual dimorphic responses in glucose homeostasis to PCBs may be due to estrogenic effects and suggest future studies should include analyses in females.

Introduction

Diabetes mellitus is a metabolic disorder characterized by loss of insulin signaling and glucose homeostasis. The diabetes epidemic has reached enormous rates domestically with 8.3% of the US population affected by diabetes mellitus while approximately 1 in 3 individuals over the age of 20 are estimated to be prediabetic in 2010 (Prevention, 2011). Over a lifetime a male or female child born in the year 2000 in the US has a 32.8% or 38.5% risk of developing diabetes mellitus, respectively (Narayan et al., 2003). Nearly 90% of those individuals will develop Type II diabetes mellitus. While genetics may play some role, several environmental factors are believed to be responsible for this risk, including obesity and toxicant exposure.

Several epidemiological reports suggest a strong link between exposure to organochlorines and Type II diabetes mellitus (Everett et al., 2011). Among the highest correlation are the polychlorinated biphenyls (PCB) (Patel et al., 2010). PCBs are ubiquitous environmental contaminants; while marketed under a variety commercial names, the Aroclor mixtures manufactured by Monsanto make up the majority of use in the US. The Aroclor mixtures were comprised of a broad assortment of individual PCB congeners with varying degrees of chlorination and were used in a variety of industrial applications including hydraulic and lubricant fluids, insulators for electrical transformers, paints, adhesives, and pesticide extenders (Fishbein, 1974) (Figure 1.3). Thermostability, resistance to biological and environmental degradation, and lipophilicity have led most countries to ban the use of PCBs. Still, PCBs persist in the environment and bioaccumulate up the food chain. Despite the US's ban on domestic production in 1979, PCBs can be found in the low 0.1 to high 100 ppb lipid-adjusted serum concentrations in humans (Prevention, 2009). While several studies in animals have shown a loose association between PCBs and the underlying mechanisms involved in diabetes pathophysiology, studies have failed to reliably show a causal link between PCB

exposure and DM. Since PCB exposure in humans is associated with diabetes mellitus, we predicted that PCB-exposed mice develop alterations in their glucose homeostasis.

PCBs exposure has also been associated with an increased risk of cancer, depressed immune function, and reproductive impairment possibly for their ability to disrupt cellular processes by aryl hydrocarbon receptor (AhR) and estradiol β receptor (ER) signaling mechanisms. Further, PCBs promote neurotoxic effects particularly those in dopamine-producing neurons. In addition to others' studies in nonhuman primates, rats, and cell culture, previous studies from our lab have shown that exposure to PCB mixtures causes a reduction in the markers of dopamine neurons in the brains of mice (Caudle et al., 2006; Richardson and Miller, 2004). Acute administration of Aroclor 1260 (single dose 500mg/kg) results in a marked reduction in striatal dopamine and dopamine metabolites. Additionally, striatal dopamine transporter (DAT) and vesicular monoamine transporter 2 (VMAT2) protein levels are reduced. These data support the inverse association between PCB serum levels and DAT levels observed in the female members of a cohort of former capacitor factory workers (Seegal et al., 2010). Various ortho-substituted PCB congeners and PCB mixtures inhibit either plasmalemmal or vesicular dopamine uptake or both at low micromolar concentrations; however, coplanar or dioxin-like PCBs fail to inhibit and appear to act primarily though AhR or ER signaling (Bemis and Seegal, 2004; Mariussen and Fonnum, 2001; Mariussen et al., 1999; Mariussen et al., 2001). Expression of DAT and VMAT2 represent a key level of regulation of dopamine signaling and protect dopamine neurons from the toxic effect of dopamine autooxidation. Reduced vesicular storage of dopamine in mice results in dramatic reduction of striatal dopamine levels and progressive nigrostriatal neuronal death (Caudle et al., 2007). It has been suggested that PCB-induced toxicity to dopamine neurons is initiated through inhibition of VMAT2 leading to increased cytosolic dopamine that can quickly oxidize (Fonnum and Mariussen, 2009). Together these data support a strong link between PCB exposure and alterations in dopamine homeostasis. We

hypothesize that mice exposed to PCBs develop glucose intolerance. We also hypothesize that PCBs are inhibitors of VMAT2 activity thus PCB exposed mice might have reduced dopamine levels in the brain and pancreas.

Materials and Methods

Chemicals and Antibodies

Aroclor 1254 and 1260 were purchased from Accustandard (New Haven, CT). Individual vials were resuspended in acetone and added to corn oil for oral gavage dosing. Acetone was allowed to evaporate in a chemical safety hood overnight before use. Both nitrile and latex gloves were worn at all times when handling PCB mixtures. All animal cages and bedding were treated as biohazardous waste. All other chemicals were purchased from Sigma Aldrich (St. Louis, MO.)

Animals

All animal procedures were conducted in accordance with the National Institutes of Health *Guide for Care and Use of Laboratory Animals* and were approved by Emory University Institutional Animal Care and Use Committee for these specific experiments. Mice were maintained on a 12 hour light: 12 hour dark cycle and were given food and water *ad libitum*. 8 week old male and female C57Bl/6J mice were purchased from Jackson Laboratories (Jackson, ME) and individually housed.

PCB Dosing

C57Bl/6J mice were allowed to acclimate for 4-5 days before dosing. On day one, all mice were weighed and randomly assigned to either the control group or treatment (PCB) group. It was confirmed that there was no statistical difference between groups. Each mouse was orally gavaged with ~30 µl of corn oil or 50mg/kg of a 1:1 ratio of Aroclor 1254:1260 in corn oil once

daily for 28 days. Mice were weighed weekly to monitor any change in body mass. Glucose tolerance tests were performed on either days 14 and 15 or 29 and 30. On day 31, mice were sacrificed either by live decapitation for tissue collections with trunk blood collected for post-sacrifice serum analyses or anesthetized by isofluorane and transcardially perfused with PBS followed by 4% paraformaldehyde in PBS (PFA).

Glucose Tolerance Tests

Glucose tolerance tests were performed as described previously (Chapter 2). Mice were fasted by cage change and removal for 5-8 hours but given water *ad libitum*. To determine fasting glucose levels, each mouse was nicked with razor; a drop of blood was collected on an Accuchek® Comfort Curve Testing Strip and read on an Accuchek® Advantage® Glucometer. Immediately following, each mouse was given an intraperitoneal injection of 2g/kg sterile-filtered glucose in PBS. A drop of blood was collected at 15, 30, 45, 60, 90, and 120 minutes for glucose measurement. Measurements were plotted as blood glucose (mg/dL) versus time (minutes). Area under the curve (AUC) of glucose tolerance was also calculated by the linear trapezoidal method for each mouse and reported in relative units.

Glucose-stimulated insulin release

Mice were fasted by cage change and removal for 5-8 hours but given water *ad libitum*. To determine GSIR, each mouse was nicked with a razor; approximately 50-75 µl of blood was collected in a heparinized hematocrit tube. Blood was then transferred to a BD Microtainer SST tube (BD Bioscience) and placed on ice. Immediately following, each mouse was given an intraperitoneal injection of 3g/kg sterile-filtered glucose in PBS. Blood was collected as before at 2.5 minutes and immediately centrifuged for 10 minutes at 10,000 x g. Blood plasma was removed and stored at -80°C until assayed. Insulin levels were measured by mouse/rat Insulin

ELISA assay (Linco Research Inc., St Charles, MO) according to manufacturer's protocol. All values are reported as ng/ml of insulin.

Immunohistochemistry and Hematoxylin and Eosin Staining

Tissues were processed similarly as described previously (Chapter 2). Whole pancreas, whole brain, median lobe of the liver, right ovary, and the biceps femoris of the right hind leg were removed and stored overnight at 4°C in 4% PFA. The tissues were transferred 24 hours later to 30% sucrose in PBS and stored at 4°C to allow tissues to drop. Tissues were then processed for paraffin embedding. Eight micron-thick, paraffin-embedded sections were stained with hematoxylin-eosin (H&E). For immunohistochemistry in the pancreas, eight micron thick sections were subjected to antigen retrieval by microwave method in 100 mM Sodium citrate buffer pH 6.0 for 10 minutes each, twice. Following block in 10% Normal Goat Serum (Gibco), slides were incubated with a guinea pig anti-insulin antibody (1:2000; Abcam), rabbit anti- mouse VMAT2 antibody (1:250; Miller Lab) overnight at 4°C and then incubated in Alexa Fluor 488-conjugated minimally crass reactive goat anti-rabbit secondary antibody and Alexa Fluor 594-conjugated minimally cross reactive goat anti-guinea pig secondary antibody (both Invitrogen, Carlsbad, CA) for 1 hour at room temperature. Visualization was performed using a Zeiss Epifluorescent Microscope.

Determination of Serum Cholesterol, Triglycerides, and Adiponectin Levels

Trunk blood recovered with a SST tube at sacrifice was immediately centrifuged for 10 minutes at 10,000 x g. Blood serum was removed and stored at -80°C until assayed. Serum cholesterol (total, HDL, and VLDL/LDL) and triglyceride levels were determined by colorimetric assay kits per manufacturer's protocol (Biovision, Mountain View, CA). Serum adiponectin was determined by the mouse adiponectin ELISA kit per manufacturer's protocol (Alpco Diagnostics, Salem, NH).

VMAT2 Uptake in Isolated Mouse Brain Vesicles

VMAT2 uptake was performed as previously reported (Caudle et al., 2007; Hatcher et al., 2008b). Briefly, mice were sacrificed by decapitation and whole brains removed. Brains were homogenized in ice-cold buffer (4 mM HEPES, 0.32 M sucrose, pH 7.4) Homogenates were centrifuged at 1000 x g for 10 min, and the resulting supernatant was centrifuged at 20,000 x g for 20 min. The resulting pellet was resuspended in 1.6 ml of 0.32 M sucrose before being transferred to a glass/Teflon homogenizer containing 6.4 ml of water and subjected to 10 up-and-down strokes by hand. All contents of the homogenizer were then poured into a tube containing 1 ml each of 250 mM HEPES and 1 M potassium tartrate and inverted to mix. The mixture was then centrifuged at 20,000 x g for 20 min, and the resulting supernatant was placed in an ultracentrifuge tube and spun at 120,000 x g for 2 h. Vesicles were resuspended in 1.8 ml of buffer (100 mM potassium tartrate, 25 mM HEPES, 0.1 mM EDTA, 0.05 mM EGTA, 1.7 mM ascorbate, pH 7.4). Uptake assays used 300 µl of vesicle stock solution for each PCB concentration, with 0.1 µM dopamine with a 2% ^{3}H- dopamine tracer in 2mM Mg^{2+}-ATP with and without 10 M tetrabenazine to determine specific uptake. Samples were incubated for 10 min with 0.1 nM to 0.1 mM concentrations of individual PCB congeners or mixtures at 30°C followed by the addition of ^{3}H- dopamine and further incubation for 5 min at 30°C. The assay was terminated by addition of 5 ml of ice-cold assay buffer before filtration through 0.5% Polyethylenimine-soaked Whatman GF/F filters (Brandel, Gaithersburg, MD). Filters were then placed in scintillation fluid and counted using a Beckman LS6500 (Beckman Instruments, Fullerton, CA). IC$_{50}$ values were calculated by nonlinear regression using GraphPad Prism 4.0 software (San Diego, CA).

HPLC Analyses of Dopamine levels

HPLC analyses were performed as described previously (Chapter 2). An Agilent 1100 Series Capillary HPLC system coupled with an ESA Coulochem III electrochemical detector was used for separation and quantification of dopamine. Briefly, the pancreas of each mouse was weighed and homogenized using a sucrose media (0.25 M sucrose, 10 mM Tris base, 0.5 mM EDTA) at 10% w/v. A 100 µL aliquot was taken and proteins were precipitated by addition of 5 µL perchloric acid. Samples were then spun at 10,000 x g for 3 min to pellet precipitated proteins. 10 µL of each sample solution was injected and separated using a Thermo Scientific C18 Aquasil column (2.1 x 150 mm, 100 Å). Mobile phase consisted of 50 mM citric acid, 1.8 mM sodium heptane sulfonate, 0.2% trifluoroacetic acid (v/v), pH 3.0 (A) and acetonitrile (B). Gradient conditions were as follows: 3% B at 0 min, 3% B at 8 min, 18% B at 19 min, 3% B at 20 min and 3 % B at 35 min using a flow rate of 250 µL/min. dopamine was detected using electrodes set at potentials of -150 and +300 mV. Retention time for dopamine was 12.7 minutes. A calibration curve was generated using a dopamine standard and utilized to convert peak area to concentration units.

Statistical Analyses

Values are represented as means ± SEM. All statistical analyses were performed using Graph Pad Prism 5.0 unless otherwise noted. Student t-tests were performed for initial two group comparisons with significant values reported as $p < 0.05$. Two-way ANOVA analyses were performed on all multi-group comparisons with Bonferroni post-hoc tests to determine significant interactions. Significant values are reported as $p < 0.05$.

Results

PCB Exposure Impairs Glucose Tolerance and Increases Body Mass in Females

Changes in body mass were observed in female mice over the course of the study. There were no difference between control and PCB-treated groups when the treatment protocol began

(Figure 2.1A). Interestingly, while both control and PCB-treated female mice gained weight over the study, female mice showed a greater trend in increased body mass over the study (approximately 5% more weight gain when compared to control). Weight gain in general is expected in 8 week old mice; however, the rate at which PCB-treated female mice gained was double that of control females (Control females rate of growth = 0.44 ± 0.07 g/week; PCB females rate of growth = 0.82 ± 0.12 g/week; $F_{(1,16)}= 7.31$; $p=0.008$) (Figure 2.1C). By day 14, a nearly significant increase in body mass is seen in treated females (14 days Control females fed body mass- 18.6 ± 0.36 g; PCB females fed body mass- 19.8 ± 0.53 g; $p= 0.087$; 14 days Control females fasting body mass- 17.1 ± 0.28 g; PCB females fasting body mass- 18.1 ± 0.39 g; $p= 0.052$). This increase continues to statistical significance by day 21 (21 days Control females body mass- 19.3 ± 0.25 g; PCB females body mass- 20.2 ± 0.38 g; *, $p<0.05$) (Figure 2.1B). Additionally, fasting body mass at 28 days of treatment is increased over controls (28 days Control females fasting body mass- 18.5 ± 0.21 g; PCB females fasting body mass- 19.3 ± 0.25 g *, $p<0.03$).

To assess the physiological effect of PCB treatment on glucose homeostasis, we first measured fasting glucose and then glucose tolerance in the PCB-treated female mice following an intraperitoneal injection of glucose. In females, PCB treatment for 14 days resulted in *impaired* glucose tolerance over control treated mice (Figure 2.3A). Repeated measure, two-way ANOVA analyses revealed a significant main effect for treatment, $F_{(1,9)}=9.56$, $p=0.0129$, a significant effect of time, $F_{(6,54)}=103.26$, $p<0.0001$, and a insignificant interaction for time at all values of treatment, $F_{(6,54)}=1.59$, $p=0.1667$. By day 28 of treatment, PCB treated female mice continued to display impaired glucose tolerance (Figure 2.3B). PCB-treated females display a 16% increase in AUC at 14 days and a 30% increase in AUC at 28 days over control female AUC levels (14 days Control females AUC- 3333 ± 499; PCB females AUC- 3878 ± 282; 28 days Control females AUC- 3270 ± 307; PCB females AUC- 4255 ± 627) (Figure 2.3C).

PCB Exposure Improves Glucose Tolerance and Decreases Body Mass in Males

By day 21, PCB-treated male mice begin to show a small trend towards loss of body mass (5%) and are no longer gaining weight as quickly as the control animals (21 days Control males body mass- 26.6 ± 0.54 g; PCB males body mass- 25.3 ± 0.37 g; *, p<0.05) (Figure 2.2A and B). Similar effects on body mass loss in males and body mass gain in females are observed in older mice under the same treatment conditions (data not shown).

In males, PCB treatment for 14 days resulted in *improved* glucose tolerance over control treated mice (Figure 2.4A). Repeated measure, two-way ANOVA analyses revealed a significant main effect for PCB treatment in males, $F(1,8)=8.05$, $p=0.0219$, a significant effect of time, $F(6,48)=350.21$, $p<0.0001$, and a significant interaction for time at all values of treatment, $F(6,48)=9.19$, $p<0.0001$. PCB-treated males had a lower AUC than control males (14 days Control males AUC- 5990 ± 265; PCB males AUC- 5798 ± 224) (Figure 2.4A and C). At 28 days, there was surprisingly no difference in males between groups (28 days Control males AUC- 3132 ± 172; PCB males AUC- 3249 ± 273) (Figure 2.4B and C).

No differences were observed in fasting glucose levels in female or male mice. Similar trends in blood glucose tolerance and body mass were found in retired breeder females (increased body mass/impaired GTT) and males (decreased body mass/improved GTT) although the dosing paradigm was too aggressive for the retired breeder males (data not shown). Treatment was stopped for retired breeders on day 24 after 3 mice died in a 24 hour period. Therefore, direct comparisons between those two groups are impossible to make.

PCB Exposure Increases GSIR and Reduces Serum Adiponectin Levels in Females

Since female mice appear to have early changes consistent with impaired glucose tolerance, we investigated whether these mice also display other pathology related to DM. We first measured basal insulin levels. At day 14, PCB-treated female mice have a modest decrease

in fasting insulin levels when compared to control female mice (14 days Control females fasting insulin- 0.272 ± 0.048 ng/ml; PCB-treated females fasting insulin - 0.202 ± 0.060 ng/ml) (Figure 2.5A). By day 28, PCB female mice have a significant decrease in fasting insulin levels (28 days Control females fasting insulin- 0.229 ± 0.036 ng/ml; PCB females fasting insulin - 0.118 ± 0.010 ng/ml; *, $p<0.05$) (Figure 2.5B). No difference in fasting insulin levels was observed in control mice over the study.

We then measured insulin levels in PCB-treated female mice in response to a 3g/kg glucose stimulation. At day 14, there is no difference in the fed insulin levels when compared to control female mice (14 days Control females fed insulin- 0.30 ± 0.05 ng/ml; PCB females fed insulin - 0.36 ± 0.11 ng/ml) (Figure 2.5C). By day 28, fed insulin levels have doubled in PCB treated female mice (28 days Control females fed insulin- 0.29 ± 0.03 ng/ml; PCB females fed insulin - 0.64 ± 0.20 ng/ml; $p=0.096$) (Figure 2.5D). No difference in fed insulin levels was observed in control mice over the study. Thus, PCB-treated female mice showed a dramatic 317% and a significant 516% increase in circulating insulin levels upon glucose stimulation as compared to the 139% and 148% increase in control females at 14 days and 28 days, respectively (Figure 2.5E and 2.5F).

Since PCB-treated female mice display evidence of dysregulation of insulin release, we wanted to determine whether there were any functional consequences of these changes. Insulin has been shown to regulate adiponectin expression and secretion from adipocytes (Hajri et al., 2011; Mohlig et al., 2002). Additionally, serum adiponectin levels are reduced in obese and diabetic humans (Kadowaki et al., 2006). Therefore, we measured serum adiponectin levels in PCB-treated female mice. PCB-treated female mice had a significant 22% reduction in serum total adiponectin levels compared to control female mice (28 days Control females total adiponectin- 31350 ± 1550 ng/ml; PCB females total adiponectin - 25500 ± 1470 ng/ml; *, $p<0.05$) (Figure 2.6).

PCB Exposure Increased Serum Cholesterol Levels, but not Triglycerides in Females

Previous studies in humans suggest a link between changes in cardiovascular factors such as serum triglycerides and cholesterol levels and PCB exposure (Everett et al., 2011). Animal data support this link (Lind et al., 2004). We measured HDL, combined VLDL/LDL, total cholesterol, and triglyceride levels in control and PCB-treated female mice. Total cholesterol serum was increased by greater than two-fold (Control females Total Cholesterol- 0.35 ± 0.02 mg/ml; PCB females Total Cholesterol- 0.83 ± 0.06 mg/ml; $p<0.001$) (Figure 2.7A). Serum VLDL/LDL levels were increased by four-fold (Control females VLDL/LDL- 0.06 ± 0.01 mg/ml; PCB females VLDL/LDL- 0.24 ± 0.05 mg/ml; $p<0.001$) (Figure 2.7B). We found that serum HDL levels generally doubled in PCB-treated females (Control females HDL- 0.29 ± 0.01 mg/ml; PCB females HDL- 0.59 ± 0.03 mg/ml; $p<0.001$) (Figure 4.7C). Interestingly, serum triglyceride levels remained unaffected in PCB-treated females (Control females triglycerides- 0.40 ± 0.03 mM; PCB females triglycerides- 0.48 ± 0.10 mM) (Figure 2.7D).

Various PCB Congeners and Mixtures Inhibit VMAT2 Activity

We saw significant physiological changes in blood glucose homeostasis and other related factors in PCB-treated mice. Previous studies in our lab have suggested that PCBs can affect monoaminergic systems in the brain, especially VMAT2 (Caudle et al., 2006; Richardson and Miller, 2004). Since PCB treatment has been shown to affect dopamine levels in the brain, we determined the effect of PCB treatment on pancreatic dopamine.

Previous studies suggested that one mechanism of PCB action is to impair dopamine packaging. Therefore, we wanted to determine if individual PCB congeners and PCB mixtures do inhibit VMAT2 activity by determining the IC_{50} value for TBZ-sensitive VMAT2 inhibition in isolated brain vesicles. Uptake experiments confirmed that PCB mixtures inhibit VMAT2 activity with Aroclor 1260 mixture alone being the best VMAT2 inhibitor ($IC_{50} = 1.0$ µM) (Table

2.1). Aroclor 1254 has a similar but slightly higher IC_{50} value of 5.2 μM. When Aroclor 1254 and Aroclor 1260 are combined, the VMAT2 IC_{50} value is 6.1 μM. These data confirm that Aroclor mixtures of PCBs inhibit vesicular transport of dopamine in micromolar concentrations. These data demonstrate that this occurs through TBZ-sensitive VMAT2 inhibition.

Next, we evaluated the ability of individual congeners to inhibit VMAT2 activity. We selected several ortho-substituted congeners based both upon previous studies by our lab and others indicating relevant congeners found in human samples and congeners most highly found in mice exposed to Aroclor 1254:Aroclor 1260 mixtures (Caudle et al., 2006). PCB 95 showed the lowest IC_{50} of all congeners tested at 1.7 μM. PCB 138, PCB 153, PCB 170, and PCB 180 have all been found at high levels in human serum and brain samples and in the brains of Aroclor 1254: Aroclor 1260 treated mice. Each inhibited VMAT2 activity at very low micromolar concentration (Table 2.1). Interestingly, the coplanar PCB congener PCB 118 inhibits VMAT2 but at a much higher concentration than the ortho-substituted congeners (PCB 118 VMAT2 IC_{50} = 42.5 μM.)

PCB Exposure Alters Dopamine Levels in the Brain and Pancreas

VMAT2 is a key regulator of monoaminergic signaling as loss or inhibition results in rapid reduction of monoamine levels in the target tissue. Having confirmed that individual PCB congeners and mixtures inhibit VMAT2 activity, we next wanted to determine whether PCB exposure in mice could affect monoamine levels in VMAT2-rich tissues. We chose the 1:1 ratio of Aroclor 1254: Aroclor 1260 mixtures via oral gavage since exposure to this mixture in mice represents relevant environmental PCB exposure to humans living in the US during the last fifty years. Exposure to Aroclor mixtures have been shown to reduce dopamine and dopamine metabolite levels in striatum of animals (Seegal et al., 1986; Seegal et al., 1991); however, the effects of PCB exposure on pancreatic dopamine levels are unknown. We confirmed that PCB

treatment in male mice reduces striatal and cortical dopamine and dopamine metabolite levels. PCB treatment reduced striatal dopamine, DOPAC, and HVA levels in mice by 22%, 32%, and 18%, respectively. PCB treatment also reduced cortical dopamine, DOPAC, and HVA levels in mice by 28%, 24%, and 24%, respectively (data not shown).

Next, we investigated the effect of PCB exposure on pancreatic dopamine levels. Since PCBs inhibit VMAT2 activity and reduce catecholamine levels in the brain, we predicted that they would also target VMAT2 activity in the pancreas. PCB treatment reduced pancreatic dopamine, levels by 36% and 38% in female and male mice, respectively (Figure 2.8). Therefore, PCB-treatment affects dopamine levels in the pancreas regardless of gender.

Discussion

Exposure to persistent organic pollutants has been strongly linked to insulin resistance, diabetes mellitus, hypertension, and metabolic syndrome in humans (Everett et al., 2011). A recent study in rats showed a high fat-diet supplemented with crude Atlantic salmon oil resulted in increased insulin resistance compared to rats fed a high fat-diet supplemented with refined Atlantic salmon oil or high fat diet alone (Ruzzin et al., 2010). This suggests that persistent organic pollutants associated with high fat dietary sources help to contribute to insulin resistance. The crude salmon oil used was confirmed to be enriched in among other things the PCB congeners that comprise the Aroclor mixtures that we used in the present study.

We chose to use a mixture of Aroclor 1254:1260 because these two mixtures were commonly manufactured and used in various applications in the US and their congener profiles reproduce similar patterns in mice as those found in human serum and tissue. Previously, we have shown that exposure to these PCB mixtures decrease VMAT2 and DAT levels in mice, while others have shown that exposure to these mixtures decrease dopamine levels in the brain (Caudle et al., 2006; Richardson and Miller, 2004; Seegal et al., 1986; Seegal et al., 1991). We

have confirmed that these mixtures inhibit VMAT2 (Table 2.1) and now demonstrate for the first time that PCB exposure alters pancreatic dopamine levels (Figure 2.8). These results show that PCB-treated females have impaired fasting insulin and increased fed insulin levels (Figure 2.5). Consistent with our findings, *in vitro* studies demonstrate that PCBs increase glucose-stimulated insulin release in the rat insulinomas RINm5F cell line (Fischer et al., 1999; Fischer et al., 1998). These effects are rapid, blocked by Ca^{2+} channel blockers, and only seen with mixtures or ortho-substituted PCB congeners. Interestingly, concentrations of PCB 153 that we show to inhibit VMAT2 activity have been shown to increase glucose-stimulated insulin release in RINm5F cells, while the dioxin-like congener PCB 77 failed to increase glucose-stimulated insulin release (Fischer et al., 1996). Together, this suggests that dioxin-like congeners do not directly increase insulin release and that the ability of PCBs to promote insulin release may be independent of their AhR effects and possibly driven by reduced dopamine signaling. It is undetermined whether RINm5F cells are dopaminergic and/or express VMAT2. However, the potential for VMAT2 inhibition in insulin secreting cells remains an unappreciated potential mechanism for the effect of PCBs on glucose-stimulated insulin release (Figure 1.10). One study characterizing these cells showed that a fraction expressed the closely related vesicular monoamine transporter 1 and serotonin (Bargsten, 2004). Future studies aimed at the direct effect of PCB congener and mixtures on glucose-stimulated insulin release in isolated islets and insulinomas cell lines may help to dissect apart the contribution of each potential mechanism.

The increase in weight gain observed in the PCB-treated female mice in our study is a stark contrast to the weight loss seen in the PCB-treated males (Figure 2.1 and 2.3). Studies report that high concentration PCB treatment causes a wasting syndrome in rodents, and in fact, male mice were more susceptible to wasting-like syndrome under our experimental conditions (Figure 2.3 and 2.4). Perhaps females are more resistant to these effects due to metabolic differences, hormonal differences, and/or differences in adiposity, whereby females are able to

sequester more PCBs in fat tissue. Still, we saw dramatic hepatomegaly in both PCB-treated males and females (data not shown). Therefore, the increase in body mass observed in females may only be due to the increase in liver wet weight. Further studies are necessary to understand the role of PCBs in adiposity; however, WT mice treated with the single coplanar congener PCB 77 have shown an increase in adiposity that was not observed in their AhR knockout littermates (Arsenescu et al., 2008). This suggests that PCBs do cause adiposity through an AhR-dependent mechanism. It is unknown whether non-coplanar PCB congeners can elicit similar effects though another mechanism.

Adiponectin is a critical regulator of energy homeostasis acting via adiponectin receptors to affect glucose uptake in muscle fiber and the liver and reduce gluconeogenesis in the liver. Its expression and release is regulated by insulin (Mohlig et al., 2002). Serum adiponectin levels are decreased in Type II diabetes mellitus patients and it is considered "among the strongest and most consistent biochemical predictors of type 2 diabetes" (Li et al., 2009). Additionally, adiponectin levels are reduced in rodent models of obesity and insulin resistance (Hu et al., 1996; Yamauchi et al., 2001). We hypothesized that since GSIR was increased in PCB-treated mice that adiponectin levels might also be affected. Human studies have shown a link between elevated serum levels of the ortho-substituted congener PCB 153 with reduced serum adiponectin levels in obese women (Mullerova et al., 2008). The authors suggest that PCB 153 and other persistent organic pollutants are associated with DM because they may regulate serum adiponectin levels. To our knowledge, our results are the first demonstration that PCB exposures can directly affect circulating adiponectin levels (Figure 2.6).

Despite the mounting evidence linking PCB exposure to diabetes mellitus and the other pathologies falling under the umbrella diagnosis of metabolic syndrome in humans, animal data supporting this link has been tenuous. More so, the underlying mechanism(s) of such an interaction remain elusive. As a mixture of compounds having different physiochemical

properties that affect each congener's metabolism and mechanism of action, the term *PCB exposure* represents a very broad definition related to a sequence of potential molecular events that can persist for decades due to intrinsic half lives of 10-15 years for several congeners (Ritter et al., 2011). Modeling such exposures in animals is not only difficult, but costly. As such, laboratory studies rely on acute to subchronic exposures to high dosages of PCBs. Unfortunately, these paradigms do not accurately reflect actual human exposures, and more chronic studies on the long term effects of PCBs are necessary to fully understand their effects on the human body. While we did not develop a PCB model of diabetes mellitus, the data presented here suggest that PCBs modulate physiological processes related to diabetes mellitus. Thus, subchronic oral exposure in females to moderate doses of PCB mixtures may provide a useful and, more-importantly, environmentally-relevant, alternative model to genetic models of metabolic syndrome for studying the early effects of PCBs on metabolic function, which might represent a unique opportunity to identify interventions that reduce or prevent the progression towards disease.

Conclusions

PCB exposure has been linked to a variety of illness in human, notably metabolic syndrome and diabetes mellitus. Here, we provide evidence that PCBs alter physiological process core to the development of these pathologies. Of particular note are the potentially novel role for PCB disruption of pancreatic dopamine in the pathology of metabolic disease and the unique susceptibility of female mice to the effects of PCBs. This difference underscores the necessity to perform toxicological studies in both genders particularly when known pathological mechanisms suggest that gender-related hormonal pathways may be involved.

Table 2.1: VMAT2 IC$_{50}$ Values of Various PCB Congeners and Commercial Mixtures. Vesicular tetrabenazine-sensitive dopamine transport was measured in isolated mouse brain vesicles.

PCB Congener or Mixture	IC$_{50}$
Aroclor 1254	*5.2 µM*
Aroclor 1260	*1.0 µM*
Aroclor 1254/1260 Mixture	*6.1 µM*
PCB 95	*1.7 µM*
PCB 118 (Mono-ortho)	*42.5 µM*
PCB 138	*3.6 µM*
PCB 153	*5.3 µM*
PCB 170	*6.0 µM*
PCB 180	*9.1 µM*

Figure 2.1: PCB Exposure Promotes Increased Body Mass Over Time in Female Mice. A) Increased body mass gain over study in PCB-treated females when compared to control females. B) PCB-treated females have a significantly greater body mass at 21 days treatment when compared to control females (Control females 21 days body mass= 19.3 ± 0.25 g; PCB females 21 days body mass = 20.2 ± 0.38 g; *, $p<0.05$) . C) Growth rates in Control and PCB-treated female mice. (Control females rate of growth = 0.44 ± 0.07 g/week; PCB females rate of growth = 0.82 ± 0.12 g/week; $F(1,16)= 7.31$; $p=0.008$).

A
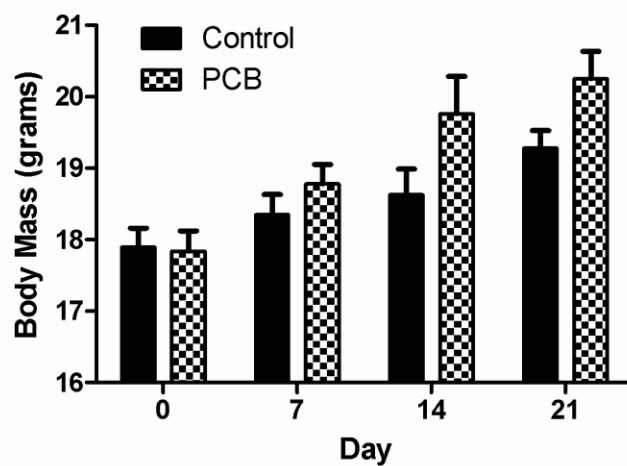
B
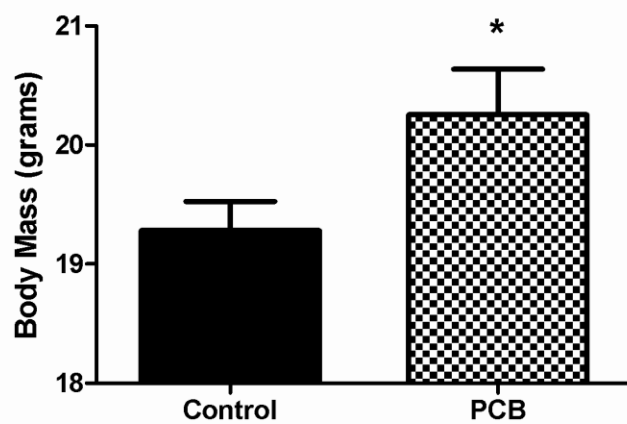
C
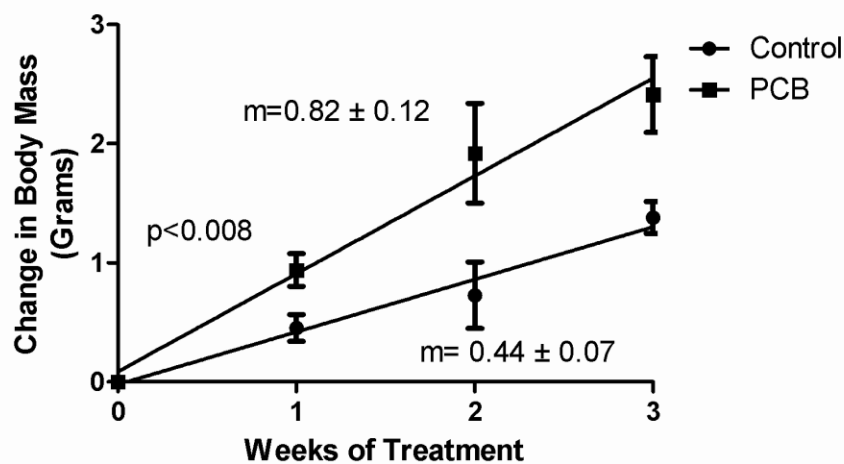
Figure 2.2: PCB Exposure Impairs Glucose Tolerance in Female Mice. A) Glucose tolerance in females at 14 days of treatment. B) Glucose tolerance in females at 28 days of treatment. C) PCB exposed females display a 16% increase in AUC at 14 days and a 30% increase in AUC at 28 days over control female AUC levels.
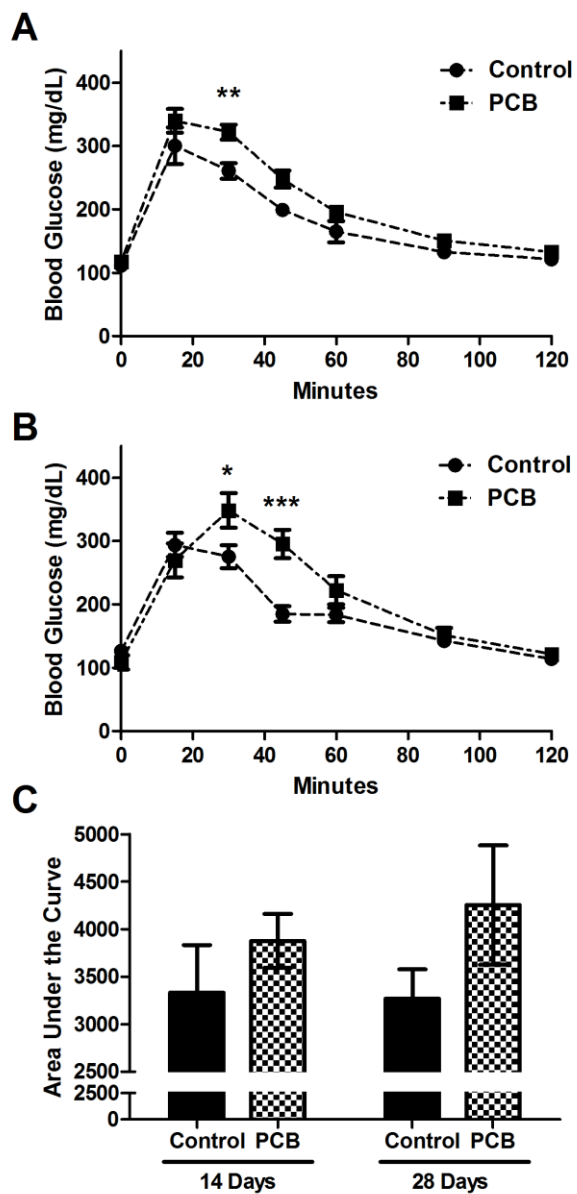
Figure 2.3: PCB exposure promotes wasting and loss of body mass over time in male mice.

A) Decreased body mass over study in PCB-treated males when compared to control males. B) PCB-treated males have a significantly smaller mean body mass at 21 days treatment when compared to control males.
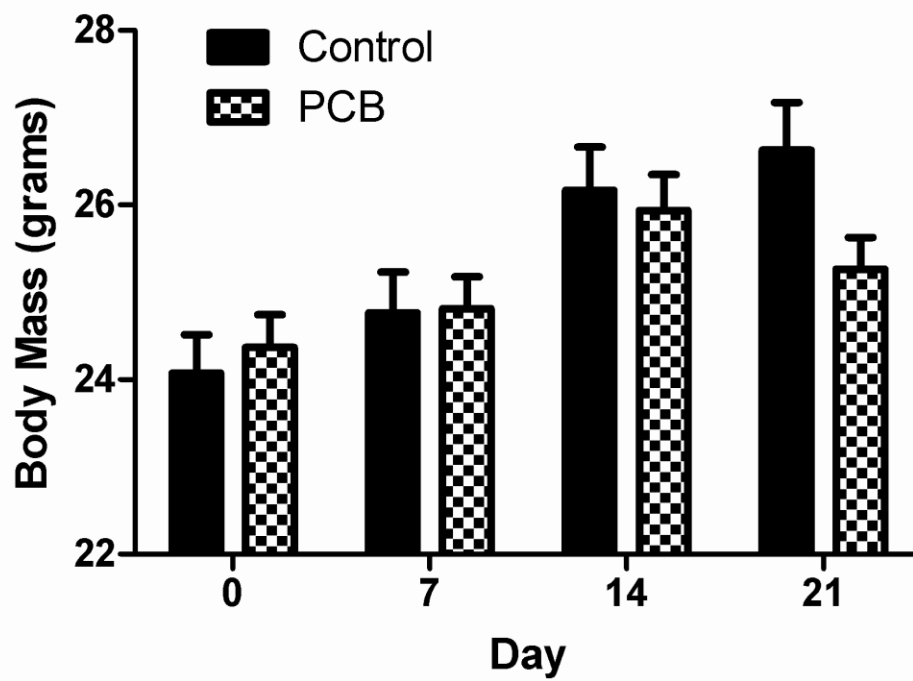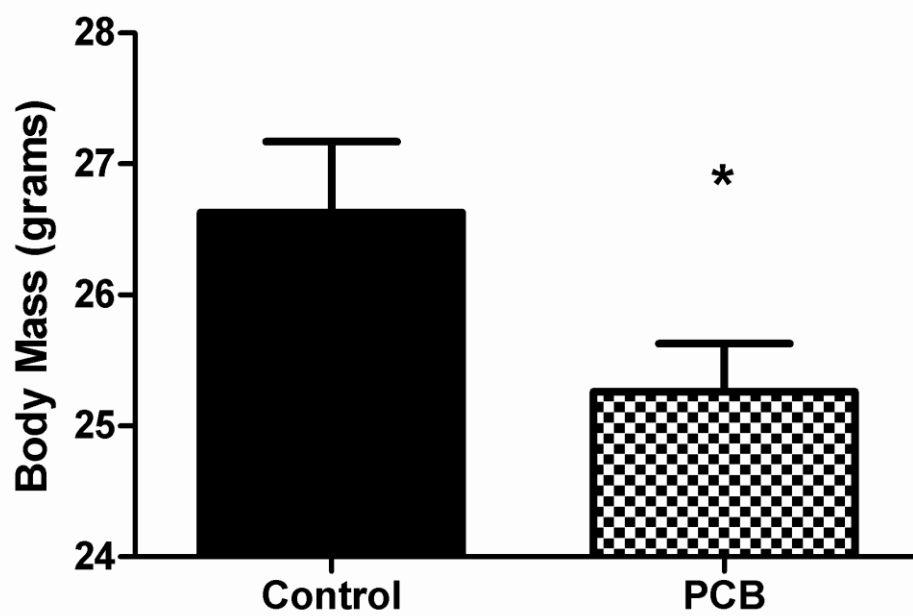
Figure 2.4: PCB Exposure Does Not Impair Glucose Tolerance in Male Mice. A) Glucose tolerance in males at 14 days of treatment. PCB-treated male mice have a faster clearance in blood glucose in response to glucose challenge. B) Glucose tolerance in males at 28 days of treatment. C) PCB-treated males do not have significant change in AUC at 14 days or at 28 days over control male AUC levels.
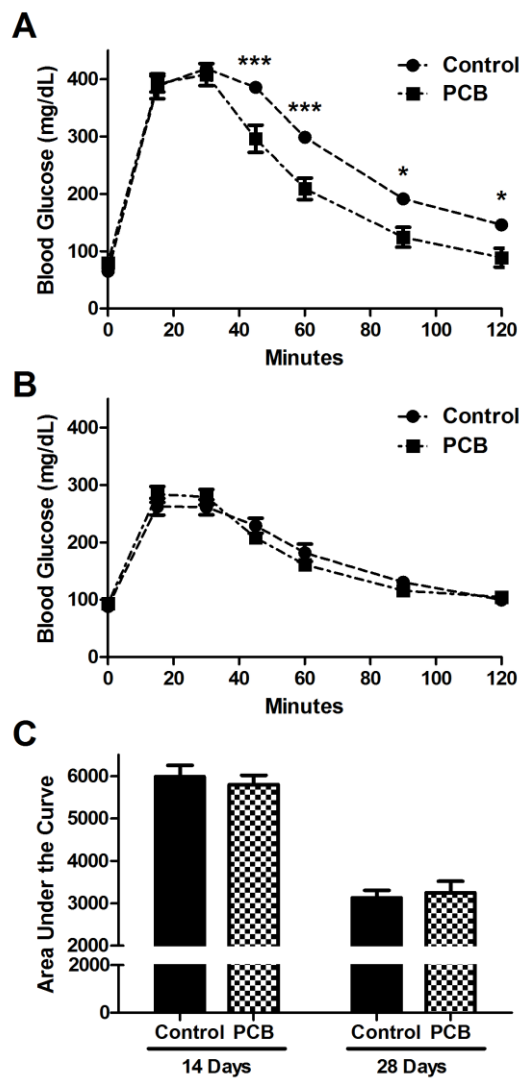
Figure 2.5: PCB Exposure Increases Glucose-Stimulated Insulin Release in Female Mice. A) Fasting levels of insulin at 14 days treatment. B) Fasting levels of insulin at 28 days treatment. C) Fed levels of insulin at 14 days treatment. D) Fed levels of insulin at 28 days treatment. E) Percent increase of fed insulin levels over fasting levels at 14 days treatment. F) Percent increase of fed insulin levels over fasting levels at 28 days treatment.
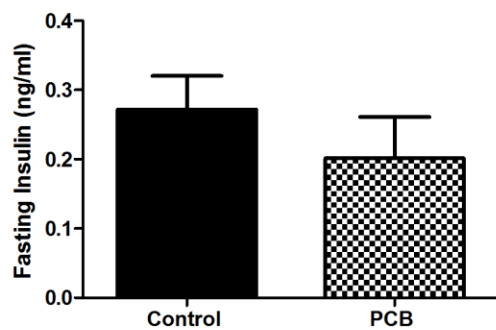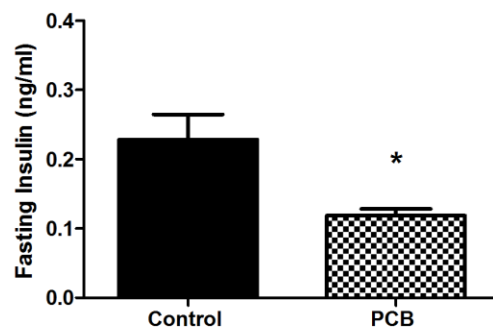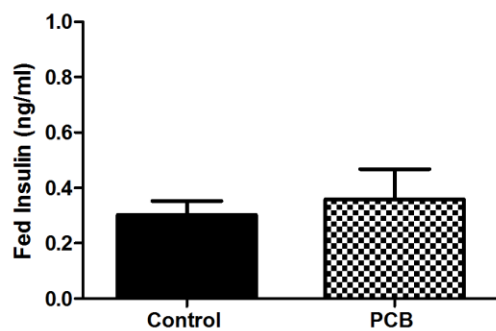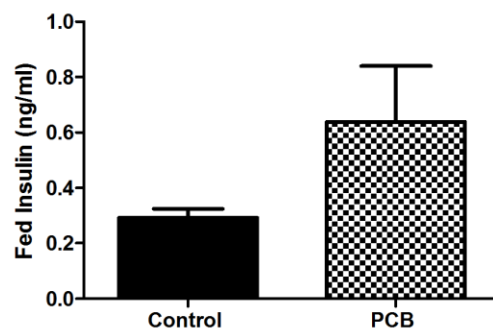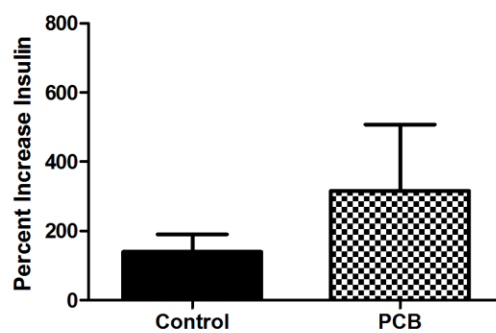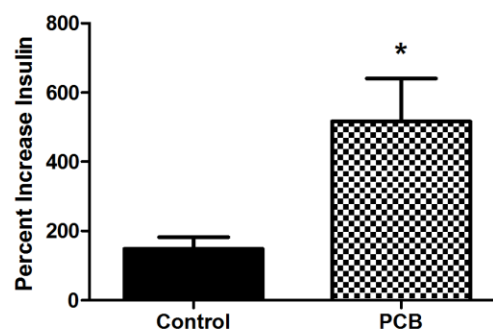
Figure 2.6: PCB Exposure Decreases Serum Adiponectin Levels in Female Mice. Serum adiponectin levels are reduced in PCB-treated mice by 22% when compared to control mice (28 days Control females total adiponectin- 31350 ± 1550 ng/ml; PCB females total adiponectin - 25500 ± 1470 ng/ml; *, $p<0.05$).
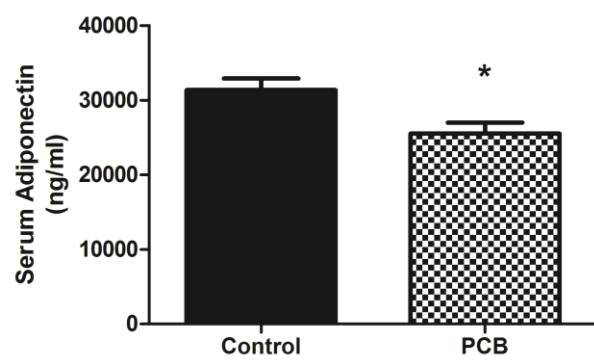
Figure 2.7: PCB Exposure Increases Serum Cholesterol Levels, but Not Triglycerides in Female Mice. PCB-treated females have a 237% increase in serum total cholesterol levels(A), a 400% increase in VLDL/LDL cholesterol levels (B), a 203% increase in HDL cholesterol levels(C), and no change in serum triglyceride level (D) when compared to control mice.
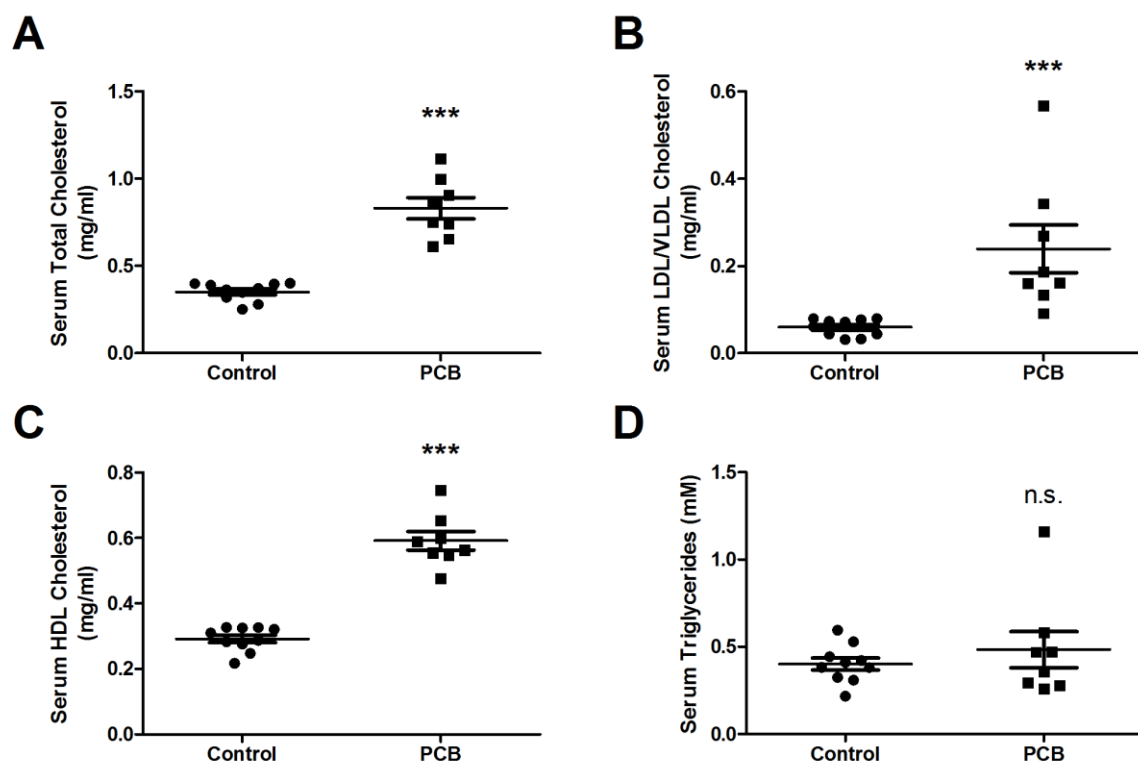
Figure 2.8: PCB exposure decreases dopamine levels in the pancreas.   HPLC analyses were performed on pancreas tissues from mice exposed to 50 mg/kg of Aroclor 1254:1260 mixture daily for 28 days. dopamine levels in the pancreas are reduced by 36% in PCB-treated female mice (Control female pancreas dopamine level- 18.6 ± 1.5 nmol/mg of protein; PCB-treated female pancreas dopamine level- 11.9 ± 0.9 mol/mg of protein; n=7-8, **, p<0.003) and 38% in PCB-treated male mice (Control male pancreas dopamine level- 14.1 ± 3.0 nmol/mg of protein; PCB-treated male pancreas dopamine level- 8.76 ± 1.3 mol/mg of protein; n=5-7, p=0.10).
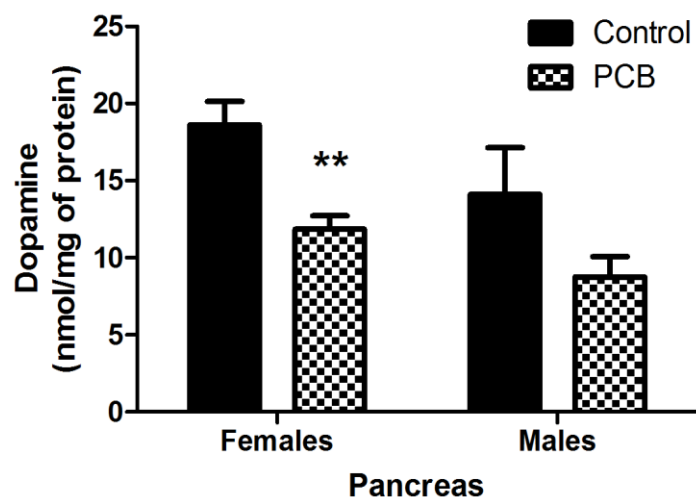
Chapter 3

Reduced Vesicular Monoamine Transporter 2 Protein expression Prevents Age-Associated Glucose Intolerance

Abstract

With incidence rates of diabetes on the rise, new therapies for the management of the disease are needed. Recently, it has been reported that acute treatment with the selective vesicular monoamine transporter 2 (VMAT2) inhibitor tetrabenazine can improve fasting glucose, glucose tolerance, and glucose-stimulated insulin secretion. Much is known about the long term effects of VMAT2 inhibition on brain function, while the effects of long-term inhibition as related to pancreatic function are unknown. Using mice engineered to express very low VMAT2 protein levels (VMAT2 LO), we determine the effects of long-term inhibition of VMAT2 on blood glucose homeostasis. We show that VMAT2 LO mice have decreased norepinephrine, dopamine, and dopamine metabolite levels in the pancreas. Although fasting glucose levels in young VMAT2 LO mice appear normal, aged VMAT2 LO mice do not develop the age-associated increase in fasting glucose levels seen in WT littermates (24 months old VMAT2 WT mice fasting blood glucose – 126.0 ± 10.1 mg/dL; 24 months old VMAT2 LO mice fasting blood glucose – 87.0 ± 5.3 mg/dL). Additionally, aged VMAT2 LO mice have improved glucose tolerance and glucose-stimulated insulin release. These data suggest that long-term VMAT2 inhibition has therapeutic potential for the management of glucose homeostasis; however, expectations should be tempered with the knowledge that long-term inhibition of VMAT2 in the brain can have serious deleterious side effects, including depression and possibly monoaminergic neuronal cell loss. The data highlight the role of VMAT2 and catecholamines in the regulation of blood glucose homeostasis and insulin release.

Introduction

Diabetes mellitus is an endocrine disorder that currently affects approximately 10% of all adults in the US. The estimated risk of developing DM over a lifetime for an individual born in the year 2000 in the US is 32.8% for males and 38.5% for females (Narayan et al., 2003). Since diabetes mellitus also modifies an individual's risk for a variety of diseases, including atherosclerosis, coronary heart disease, kidney disease, stroke, neuropathy, and dementia, treating DM may be critical to manage the development of other associated illnesses (Bielefeldt and Reis, 1989; Grundy et al., 1999; Maser et al., 1989; Vokonas and Kannel, 1996). Therefore, diabetes mellitus poses a significant public health issue both now and in the future.

Diabetes mellitus is characterized by a loss of function of insulin, resulting in the inability to maintain blood glucose levels at proper levels (Sandoval et al., 2009). This can occur by a variety of mechanisms, including insulin resistance in target tissues, loss of beta cell mass in the pancreas, impaired secretion of insulin from beta cells, and loss of circulating insulin from the blood. Understanding islet physiology with respect to how insulin is made and secreted is one key to the discovery of new drug targets and better therapies for the treatment of diabetes. Recently, monoaminergic neurotransmitter receptors and transporters have been identified as in important new drug targets because of their action in islet physiology (Sandoval et al., 2009). The pancreas with associated ducts and vessels contain large amounts of monoamines (Yi et al., 2004). Like neurons, the beta cells of the endocrine pancreas both secrete and respond to monoamines. While adrenergic inputs come from the pancreatic ganglion, dopamine is synthesized and cosecreted with insulin in response to glucose stimulation (Ahren et al., 1981; Ericson et al., 1977; Ichise and Harris, 2010; Yi et al., 2004). Dopamine and norepinephrine both inhibit glucose-stimulated insulin release from beta cells *in vitro* and *in vivo* while both dopamine and dopamine receptor agonists increase insulin release when administered systemically (Borelli and Gagliardino, 2001; Jetton et al., 2001; Lundquist et al., 1991; Zern et al., 1980). Indeed, the

FDA recently approved bromocriptine, a D2 dopamine receptor agonist, to treat diabetes because it modestly decreases A_1C hemoglobin and blood glucose levels (Gaziano et al., 2010). Additional evidence shows that blockade or loss of α_{2a} adrenergic receptor increases insulin secretion and improves fasting glucose levels in mice (Nakadate et al., 1980; Savontaus et al., 2008). Together these data show a definitive role for monoamines in the regulation of islet and nervous system physiology and subsequent management of blood glucose levels.

One major common factor between most monoaminergic neurons and beta cells is the expression of the vesicular monoamine transporter 2 (VMAT2). This protein is critical for packaging monoamines into vesicles for release. When VMAT2 activity is lost, monoamine levels decrease in target tissues. Although largely considered a neuronal protein, several reports have shown that VMAT2 is highly expressed in the pancreas (Anlauf et al., 2003). Recent data show that the VMAT2 selective inhibitor tetrabenazine (TBZ) when given acutely can help improve serum blood glucose levels in slightly insulin resistant rats by increasing insulin release in response to glucose stimulus (Raffo et al., 2008). This suggests that VMAT2 may be a useful drug target for the treatment of diabetes; however, the long term effects of VMAT2 inhibition on glucose homeostasis are unknown.

To investigate the effects of long term inhibition of VMAT2 on blood glucose levels, we utilized the VMAT2 hypomorph mouse (VMAT2 LO). This mouse model expresses only 5-7% of normal VMAT2 levels in the brain and has dramatically reduced monoamine levels in the forebrain and other brain regions (Caudle et al., 2007). Therefore, we hypothesized that VMAT2 levels would be reduced in the pancreas as well leading to reduced monoamine levels in the pancreas. We utilize this model to investigate the effects of chronic VMAT2 inhibition on blood glucose management.

Materials and Methods

Animals

All animal procedures were conducted in accordance with the National Institutes of Health *Guide for Care and Use of Laboratory Animals* and were approved by Emory University Institutional Animal Care and Use Committee for these specific experiments. Mice were maintained on a 12 hour light: 12 hour dark cycle with standard rodent chow and were given food and water *ad libitum* unless otherwise noted. VMAT2 mice were generated as described previously (Mooslehner et al., 2001). Briefly, these mice were created by a fortuitous recombination event during an attempt to make VMAT2 knockout mice. These mice have an intact open reading frame without a frame shift that results in markedly reduced mRNA expression. While complete VMAT2 knockout is lethal within several days of birth, VMAT2 LO mice survive well into adulthood, including up to 36 months of age under our laboratory conditions. While the transgene was introduced into 129/Ola CGR 8.8 embryonic stem cells, the ES cells were injected into C57Bl/6 blastocysts. Of the resulting pups, chimeric males were crossed to C57Bl/6 females followed by several generations of backcrossing to C57Bl/6 mice. VMAT2 transgenic mice were group housed, were bred by VMAT2 heterozygote/ α-syn wildtype x VMAT2 heterozygote/ α-syn wildtype mating, and were genotyped as previously described (Caudle et al., 2007). Our colony was also genotyped to remove all traces of a spontaneous null mutation in the α-synuclein (α-syn) gene that was present in the original C57Bl/6 founder strain as α-syn knockout mice have recently been reported to have alterations in glucose-stimulated insulin release (Geng et al., 2010). Mice were sacrificed by either live decapitation for tissue collections or anesthetized by isofluorane and transcardially perfused with phosphate buffered saline (PBS) followed by 4% paraformaldehyde (Fisher Scientific) in PBS (PFA) for fixed tissue collections.

Histochemistry and Hematoxylin and Eosin Staining

Whole pancreata were removed from perfused mice and stored overnight at 4°C in 4% PFA. The tissues were transferred 24 hours later to 30% sucrose in PBS and stored at 4°C to allow tissues to drop. The tissues were then processed for paraffin embedding. Eight-micron thick paraffin-embedded sections were stained with hematoxylin-eosin (H&E). For immunohistochemistry, eight micron thick sections were subjected to antigen retrieval by microwave method in 100 mM Sodium citrate buffer pH 6.0 for 2 minutes each, twice. After block in 10% Normal Goat Serum (Gibco), slides incubated with a guinea pig anti-insulin antibody (1:2000; Abcam) overnight at 4°C and then incubated in Alexa Fluor 594-conjugated minimally cross reactive goat anti-guinea pig secondary antibody (Invitrogen, Carlsbad, CA) for 1 hour at room temperature. Visualization was performed using a Zeiss Epifluorescent Microscope.

^{3}H-Dihydrotetrabenezine Binding Assay

^{3}H-Dihydrotetrabenazine (^{3}H-DTBZ- American Radiolabeled Chemicals; St. Louis, MO) binding was performed on fresh pancreata fractions. Whole pancreata were harvested in 0.32 M sucrose with 1X protease inhibitor cocktail (Sigma) and homogenized using a glass/Teflon homogenizer with 10 up and down stokes at 1000 rpm. Homogenates were centrifuged at 1000x g at 4°C for 10 minutes. The resulting post-nuclear fraction (supernatant) was reserved and used for binding assays. The supernatants were kept on ice and 25 µl of sample was added to 175 µl of VMAT2 uptake buffer (2mM ATP-Mg^{2+}, 1.7mM Ascorbate, 25mM HEPES, 100mM Potassium tartrate, 0.1mM EDTA, 0.05mM EGTA, pH 7.4). Then either a 20 µM final concentration of cold TBZ (25 µl of 200µM TBZ) for nonspecific binding or 25 µl of buffer for total binding was added followed immediately by the addition of 2 nM ^{3}H-DTBZ (25 µl of 20 nM ^{3}H-DTBZ). The reaction was incubated at 37°C for 2 minutes. Cold uptake buffer (2-3ml) was added to attenuate each reaction and samples were harvested on a Brandel Cell Harvester with Whatman GF/F Filter Paper (Brandel, Inc., Gaithersburg,

MD) presaturated with 0.5% Polyethylenimine. Dried membranes were added to SafeScint Econo1 Scintillation fluid (Fisher Scientific) and bound activity was measured on a LS6500 Beckman Scintillation Counter. Specific ^{3}H-DTBZ binding was determined by subtracting total ^{3}H-DTBZ binding from cold TBZ-sensitive binding and normalized to the total protein per sample as determined by BCA protein assay according to manufacturer's protocol (Pierce).

HPLC Analyses of Norepinephrine, Dopamine, and Dopamine Metabolite Levels

An Agilent 1100 Series Capillary HPLC system coupled with an ESA Coulochem III electrochemical detector was used for separation and quantification of norepinephrine, dopamine, 3,4-dihydroxyphenylacetic acid (DOPAC) and homovanillic acid (HVA). Briefly, the pancreas of each mouse was weighed and homogenized using a sucrose media (0.25 M sucrose, 10 mM Tris base, 0.5 mM EDTA) at 10% w/v. A 100 µL aliquot was taken and proteins were precipitated by addition of 5 µL perchloric acid. Samples were then spun at 10,000 x *g* for 3 minutes to pellet precipitated proteins. 10 µL of each sample solution was injected and separated using a Thermo Scientific C18 Aquasil column (2.1 x 150 mm, 100 Å). Mobile phase consisted of 50 mM citric acid, 1.8 mM sodium heptane sulfonate, 0.2% trifluoroacetic acid (v/v),pH 3.0 (A) and acetonitrile (B). Gradient conditions were as follows: 3% B at 0 min, 3% B at 8 min, 18% B at 19 min, 3% B at 20 min and 3 % B at 35 min using a flow rate of 250 µL/min. Norepinephrine, dopamine, DOPAC, and HVA were detected using electrodes set at potentials of -150 and +300 mV. Retention times for norepinephrine, dopamine, DOPAC, and HVA were 5.5, 12.7, 11.3, and 21.6 minutes, respectively. Calibration curves were generated using standards (i.e., dopamine and HVA) and utilized to convert peak area to concentration units.

Fasting Glucose Measurements

Mice were fasted by cage change 8-12 hours but given water *ad libitum*. To determine fasting glucose levels, each mouse was nicked with razor; a drop of blood was collected on an

Accuchek® Comfort Curve Testing Strip and read on an Accuchek® Advantage® Glucometer that was checked for accuracy against a standard curve before each experiment.

Glucose Tolerance Tests

Mice (n=5) were fasted by cage change for 5-8 hours but given water *ad libitum*. For glucose tolerance tests, each mouse was nicked with razor; a drop of blood was collected on an Accuchek® Comfort Curve Testing Strip and read on an Accuchek® Advantage® Glucometer that was checked for accuracy against a standard curve before each experiment. Then, each mouse was given an intraperitoneal injection of 2g/kg sterile-filtered glucose in PBS immediately following fasting glucose measures (time = 0 minutes). A drop of blood was collected at 15, 30, 45, 60, 90, and 120 minutes after injection for glucose measurement. Measurements were plotted as blood glucose (mg/dL) versus time (minutes). Area under the curve (AUC) of glucose tolerance was also calculated by the linear trapezoidal method for each of mouse and reported in relative units.

Glucose-Stimulated Insulin Release

Mice were fasted by cage change and removal for 5-8 hours but given water *ad libitum*. To determine glucose-stimulated insulin release, each mouse was nicked with a razor; approximately 50-75 µl of blood was collected in a heparinized hematocrit tube. The blood was then transferred to a BD Microtainer SST tube (BD Bioscience) and placed on ice. Immediately following, each mouse was given an intraperitoneal injection of 3g/kg sterile-filtered glucose in PBS. Blood was collected as before at 2.5 minutes and was immediately centrifuged for 10 minutes at 10,000 x g. Blood plasma was removed and stored at -80°C until assayed. Insulin levels were measured by mouse/rat Insulin ELISA assay (Linco Research Inc., St Charles, MO) according to manufacturer's protocol. All values are reported as ng/ml of insulin.

Statistical Analyses

Values are represented as means ± SEM. All statistical analyses were performed using Graph Pad Prism 5.0. Student t-tests were performed for all two group comparisons with significant values reported as p<0.05. One-way ANOVA analyses or two-way AVOVA analyses were performed on all multi-group comparisons with Newman Keuls or Bonferroni post-hoc tests to determine significant interactions, respectively. Significant values are reported as p<0.05.

Results

VMAT2 LO Mice Have Reduced VMAT2 Levels in the Pancreas

Since any difference between VMAT2 WT and LO mice could be due to embryonic changes and result in structural differences in pancreata between the two, we first confirmed that VMAT2 LO mice have similar islet morphology and no gross differences between pancreata as their WT littermates (Figure 3.1). Both VMAT2 WT and LO mice had large and small islets with no differences between total numbers or morphology of islets. Next, we confirmed that VMAT2 levels are reduced in the pancreas of VMAT2 LO mice. To do this, we developed an antibody against the C-terminus of mouse VMAT2. Immunohistochemical staining revealed faint VMAT2 staining throughout that exocrine pancreas and strong islet staining in VMAT2 WT mouse sections (Figure 3.2A). VMAT2 LO mice had markedly reduced VMAT2 staining in pancreatic islets and surrounding exocrine tissues (Figure 3.2D). We also examined insulin distribution and staining within islets from both VMAT2 WT and LO mice. There were no differences between genotypes for insulin staining (Figure 3.2B and E). Merged images revealed that VMAT2 is present in all or nearly all insulin and non-insulin reactive cells of the pancreatic islets in VMAT2 WT mouse sections (Figure 3.2C and G). However, VMAT2 expression is largely absent in VMAT2 LO mouse islets with only faint merged staining in the perinuclear puncta of insulin secretory granules (Figure 3.2F and H).

To further confirm VMAT2 expression in the pancreas, we also performed binding studies on crude lysates of VMAT2 WT and LO mouse pancreas. TBZ is a selective VMAT2 antagonist, and several studies have measured VMAT2 levels in humans and rodents *in vivo* using TBZ-derived PET ligands in an effort to estimate beta cell mass (Eriksson et al., 2010; Goland et al., 2009; Inabnet et al., 2010; Kung et al., 2008a; Kung et al., 2008b; Lin et al., 2010; Simpson et al., 2006; Souza et al., 2006; Tsao et al., 2010). VMAT2 LO mice express only 5-7% of VMAT2 protein in the brain (Caudle et al., 2007). While it is predicted that VMAT2 levels would be reduced in all VMAT2-expressing tissues, VMAT2 expression in the pancreas of VMAT2 LO mice is unknown. We determined loss of VMAT2 expression in VMAT2 LO mice using ^{3}H-DTBZ binding in pancreatic lysates. VMAT2 LO mice have a non-significant 36% reduction in ^{3}H-DTBZ binding in the pancreas (Figure 3.2I). VMAT2 WT mice displayed 21.4 ± 7.47 pmol/min/mg of protein ^{3}H-DTBZ binding in the pancreas versus 13.7 ± 1.99 pmol/min/mg of protein ^{3}H-DTBZ binding in VMAT2 LO mice.

VMAT2 LO Mice Have Reduced Monoamine Levels in the Pancreas

Since even acute loss of VMAT2 activity results in a rapid reduction in dopamine levels in the pancreas (Raffo et al., 2008), we determined the effects of chronic inhibition of VMAT2 on monoamine levels in the pancreas. Previous studies have shown that dopamine and NE levels are significantly reduced in the brains of VMAT2 LO mice when compared to their WT littermates (Caudle et al., 2007; Taylor et al., 2009). Likewise, VMAT2 LO mice have a (70%) loss of dopamine in the pancreas (VMAT2 WT mice pancreas dopamine – 23.09 ± 9.66 pmol/mg of protein; VMAT2 LO mice pancreas dopamine – 6.259 ± 3.22 pmol/mg of protein) (Figure 3.3A). The dopamine metabolites DOPAC and HVA are also reduced by 80% and 65% loss, respectively (VMAT2 WT mice pancreas DOPAC – 29.89 ± 11.5 pmol/mg of protein; VMAT2 LO mice pancreas DOPAC – 6.084 ± 2.56 pmol/mg of protein; VMAT2 WT mice pancreas HVA – 103.5 ± 31.1 pmol/mg of protein; VMAT2 LO mice pancreas HVA – 32.31 ± 14.7 pmol/mg of

protein). (Figure 3.3B and C) We also see a (40%) reduction in pancreatic norepinephrine levels (VMAT2 WT mice pancreas norepinephrine – 0.305 ± 0.09 pmol/mg of protein; VMAT2 LO mice pancreas norepinephrine – 0.158 ± 0.02 pmol/mg of protein) (Figure 3.3D).

Aged VMAT2 LO Mice Have Improved Fasting Blood Glucose Levels

Since loss of VMAT2 results in a dramatic reduction in pancreatic monoamines, we investigated the physiological effects that this loss has on mice as they age. Interestingly, previous studies have shown that both C57Bl/6J and 129/SvJ mice have impaired glucose tolerance and signs of insulin resistance when compared to other strains (Berglund et al., 2008; Champy et al., 2008). Our mouse colony was created in 129/SvJ ES cells and has been backcrossed onto a C57Bl/6J background. Therefore, we suspected that our animals may develop signs of insulin resistance as they reached middle-age.

We measured fasting glucose levels in VMAT2 WT and LO mice of different ages. While there are no differences between VMAT2 WT and LO mice in earlier adulthood (3 months VMAT2 WT mice fasting blood glucose – 63.5 ± 3.2 mg/dL; VMAT2 LO mice fasting blood glucose – 65.5 ± 4.9 mg/dL; 6 months VMAT2 WT mice fasting blood glucose – 79.0 ± 1.8 mg/dL; VMAT2 LO mice fasting blood glucose – 84.0 ± 5.7 mg/dL), aged VMAT2 LO mice do not develop the impaired fasting glucose levels seen in VMAT2 WT animals (15 months VMAT2 WT mice fasting blood glucose – 108.0 ± 5.4 mg/dL; VMAT2 LO mice fasting blood glucose – 81.0 ± 3.4 mg/dL, ***, p<0.001; 24 months VMAT2 WT mice fasting blood glucose – 126.0 ± 10.1 mg/dL; VMAT2 LO mice fasting blood glucose – 87.0 ± 5.3 mg/dL, ***, p<0.001) (Figure 3.4). Fasting glucose levels of VMAT2 heterozygote (VMAT2 HET) mice are similar to that of VMAT2 WT mice (15 months VMAT2 HET blood glucose level - 119.4 ± 4.70 mg/dL). There are no differences in body mass between genotypes in middle-age mice (15 months VMAT2 WT

mice body mass – 28.8 ± 0.9 g; VMAT2 LO mice body mass – 27.1 ± 1.1 g; 24 months VMAT2 WT mice body mass – 28.9 ± 1.1 g; VMAT2 LO mice body mass – 26.4 ± 1.0 g).

Aged VMAT2 LO Mice Have Improved Glucose Tolerance

Since aging VMAT2 LO mice display improved fasting glucose when compared to their WT littermates, we determined the effect of VMAT2 genetic ablation on glucose tolerance. VMAT2 LO mice display improved glucose tolerance when compared to WT littermates (Figure 3.5A). AUC measures are significantly lower in VMAT2 LO mice (Figure 3.5B) indicating that they are much less likely to develop insulin resistance as they age (VMAT2 WT mice AUC – 2516 ± 195.7; VMAT2 LO mice AUC - 1658 ± 287.6; $p < 0.05$).

Aged VMAT2 LO Mice Have Improved Glucose-Stimulated Insulin Release

With improved fasting glucose and glucose tolerance, we proposed that VMAT2 LO mice may respond better to a glucose challenge by secreting more insulin. At baseline fasting levels, VMAT2 LO mice had slightly higher serum insulin levels than their WT littermates (VMAT2 WT mice fasting serum insulin levels – 0.27 ± 0.03 ng/ml; VMAT2 LO mice fasting serum insulin levels – 0.30 ± 0.06 ng/ml)(Figure 3.6). Upon glucose challenge, VMAT2 LO had higher serum insulin levels than their WT littermates (VMAT2 WT mice fed serum insulin levels – 0.41 ± 0.05 ng/ml; VMAT2 LO mice fed serum insulin levels – 0.64 ± 0.20 ng/ml).

Discussion

Pharmacological Implications of VMAT2 inhibition for the Treatment of Diabetes

While previous studies investigating the role of VMAT2 in regulating glucose homeostasis have shown that acute inhibition is beneficial, the effects of chronic inhibition of VMAT2 on glucose homeostasis and any resulting potential for long term therapeutic benefit have remained unclear (Raffo et al., 2008). We found that as our colony aged fasting glucose

levels increased in VMAT2 WT mice; however, VMAT2 LO mice continued to display low fasting glucose levels regardless of age (Figure 3.4). Additionally, VMAT2 LO mice displayed markedly better glucose tolerance than their WT littermates (Figure 3.5). These data suggest that chronic inhibition of VMAT2 may be beneficial for maintaining lower blood glucose levels and preventing the development of insulin resistance. However, there are several issues related to this model that could confound interpretation of these results. The VMAT2 LO mice have a genetic deficiency in VMAT2 protein levels that presumably persists from embryonic stages throughout adulthood. Therefore, the early loss of VMAT2 protein during development may have altered islet physiology from birth. This does not appear to be the case as there is no difference in fasting glucose levels between WT, HET, or LO mice until much later in adulthood (after 6 months of age). Rather, VMAT2 LO mice display consistent management of glucose homeostasis at any age measured. Additional studies are necessary to understand any role of VMAT2 in early islet development. Though VMAT2 does not appear to be expressed in alpha islets cells, they do receive sympathetic innervation. This study has not investigated the role that VMAT2 plays in the regulation of glucagon secretion. Future studies aimed at determining whether VMAT2 plays any role in the control of other pancreatic cell types as it does in beta cell function are critical for fully understanding VMAT2 function in pancreatic physiology.

VMAT2 Loss of function and Impact on Insulin Secretion

Loss of VMAT2 expression also resulted in greater insulin release in response to glucose stimulation (Figure 3.6). This is consistent with the increase in glucose-stimulated insulin release seen under acute administration of TBZ (Raffo et al., 2008). These data suggest that VMAT2 plays a role in regulating the secretion of insulin. Interestingly, as VMAT2 is a marker of beta cells, some insulinomas (cancers of beta cell origin) have been shown to lose VMAT2 expression while other non-insulin secreting pancreatic endocrine tumors retained expression of VMAT2 (Anlauf et al., 2003). This suggests that VMAT2 expression may also be directly related to

certain pancreatic cancer phenotypes. A potential mechanism by which VMAT2 expression and activity may regulate insulin secretion is via the role that VMAT2 plays in regulating vesicular pH. VMAT2 is a proton antiporter where vesicular transport of monoamines occurs by proton-amine exchange (Figure 1.4). Therefore, VMAT2 activity leads to the alkalinization of vesicles and the subsequent inhibition of acid-dependent prohormone convertases (Blackmore et al., 2001). Inhibition of VMAT2 by reserpine has been shown to increase the cleavage of chromogranin A, proenkephalin, and progastrin (Eiden et al., 1984; Voronina et al., 1997; Wolkersdorfer et al., 1996). Therefore, VMAT2 inhibition in the islet may have a similar effect on insulin secretion by increasing proinsulin cleavage and the available pool of insulin peptide for release.

Monoaminergic Transmission in Islet Physiology

The activation of the sympathetic pathway in the pancreas blocks release of insulin and stimulates release of glucagon causing blood glucose levels to rise (Kurose et al., 1990). This latter physiological response implicates the monoaminergic neurotransmitter norepinephrine as playing an important role islet physiology and evolved as an important mechanism to combat exercise-induced hypoglycemia (Tuttle et al., 1988). Additionally, α_{2a} adrenergic receptors expressed on beta cells play a critical role regulating insulin secretion. α_{2a} adrenergic receptor knockout mice have a 30% reduction in fasting glucose levels than WT littermates and a near significant increase in fasting insulin levels, indicating that adrenergic action plays an important role in normal glucose metabolism (Peterhoff et al., 2003; Savontaus et al., 2008). Activation of α_{2a} adrenergic receptors blocks insulin release and the α_{2a} adrenergic receptor gene locus was recently identified as a susceptibility gene for Type II DM in both humans and a rat model (Rosengren et al., 2010). It has also been proposed that dopamine acts on nearby beta cells to attenuate insulin secretion (Ichise and Harris, 2010). Interestingly, one study has shown that bromocriptine (a dopamine receptor agonist) does not exert its pharmacological benefits though

dopamine D2 receptors rather acting as an agonist directly on α_{2a} adrenergic receptors to inhibit glucose-stimulated insulin release (de Leeuw van Weenen et al., 2010). This seems counterintuitive to the evidence supporting that loss of monoaminergic signaling results in improved insulin secretion. Thus, further investigation is required to dissect the contribution of each monoamine system and to VMAT2's role in the regulation of glucose homeostasis and islet physiology.

VMAT2 as a Marker of Beta Cell Mass Integrity

VMAT2 expression and thus TBZ-derived ligands are commonly used as a measure of striatal dopamine terminal integrity in Parkinson's disease and distinctly mark other areas of the brain known for high expression of monoamines (Frey et al., 1996; Vander Borght et al., 1995). More recently, TBZ-derived PET ligands have been used to estimate beta cell integrity in models of diabetes mellitus (Eriksson et al., 2010; Goland et al., 2009; Inabnet et al., 2010; Kung et al., 2008b; Souza et al., 2006); however, conflicting reports exist over the reliability of TBZ ligands to indicate beta cell mass (Fagerholm et al., 2010; Tsao et al., 2010). This is due to possible VMAT2-nonspecific binding of TBZ to the pancreas. In our DTBZ radioligand binding experiment in VMAT2 WT and LO mice, we only saw a 36% reduction in pancreatic binding in VMAT2 LO mice as compared to their WT littermates (Figure 3.2C). This is in contrast to the 95% reduction in VMAT2 protein observed in the striatum of these mice (Caudle et al., 2007). The closely related protein vesicular monoamine transporter 1 (VMAT1) is also expressed in the enterochromaffin cells of the endocrine pancreas (Anlauf et al., 2003). While previous studies have shown that TBZ has 10,000 fold higher affinity for VMAT2 protein versus VMAT1(Erickson et al., 1996; Finn and Edwards, 1997), the absence of VMAT1 protein from the striatum may underlie the more predictable loss in ^{11}C-DTBZ binding in the brains of Parkinson's disease patients(Peter et al., 1995). Additionally, the ligand used in our study is a mixture of (+)alpha- and (-)alpha-DTBZ stereoisomers. Previous studies have shown that large

amounts of nonspecific binding in the pancreas of rats were largely due to the (-)alpha-stereoisomer (Kilbourn, 2010). Two published report suggests that TBZ can actually act as a D2 receptor antagonist because of its ability to block spiperone binding with a K_i of 5μM; however, spiperone is now known to have high affinity for several 5-HT receptors (Login et al., 1982; Login et al., 1983). Newer unpublished data from a company developing novel VMAT2 antagonists suggest that the (-)alpha-stereoisomer has much stronger affinity for the D2 receptor of 192 nM than previously acknowledged (Neurocrine communication). These data suggest that (-)alpha- stereoisomer has the same affinity for D2 receptors as it does for VMAT2 (K_i= 200 nM) while the (+)alpha- stereoisomer has very high affinity for VMAT2 (K_i= 0.97 nM), but negligible affinity for D2 receptors (K_i> 10 μM). Our experiments are performed with 2 nM ^{3}H-DHTBZ. Therefore, we are possibly detecting small amounts of nonspecific binding to D2 receptors under our experimental conditions which are highly expressed in the pancreas (Rubi et al., 2005). Another unknown protein having high affinity for TBZ may also be expressed at high levels in the pancreas. Additionally, species differences in VMAT2 expression may be responsible as the conflicting data were generated from rodents, whereas weak islet-specific TBZ binding was observed in human pancreas sections (Fagerholm et al., 2010; Tsao et al., 2010).

The expression of VMAT2 has also born some controversy. One study reports that VMAT2 transcript is strongly expressed in rat islets (Veluthakal and Harris, 2010). Other studies have shown that VMAT2 protein is expressed in sympathetic nerves innervating the pancreas, in islets, and in some cells lining pancreatic ducts (De Giorgio et al., 1996; Mei et al., 2002). We show that VMAT2 is expressed in both exocrine and endocrine tissues of mice, where both insulin and non-insulin islet cells are stain positive for VMAT2 as measured by immunocytochemistry (Figure 3.2). Previous reports in human tissue have suggested that VMAT2 expression is limited to insulin-reactive and PP-reactive cells in the pancreatic islet and the small amounts of sympathetic nerve fibers throughout the pancreas (Anlauf et al., 2003;

Saisho et al., 2008). As with imaging and binding, it may be that the differences in VMAT2 expression in exocrine and endocrine tissues are due to species difference. However, it is important to note that our clinical chemistry experiments were done in the absence of TBZ and in mice with genetically-deleted VMAT2 protein showing a clear relationship between VMAT2 function and glucose homeostasis.

Conclusions

As we show here, loss of VMAT2 prevents mice from developing age-associated impaired glucose tolerance. These data suggest an exciting new role for VMAT2 in the regulation of islet physiology and hold promise for the development of novel therapeutics targeting VMAT2 for the treatment of diabetes mellitus. Recently, TBZ has been approved for the treatment of chorea in Huntington's disease in the U.S. (Wimalasena, 2010). A patent has already been filed to use TBZ for the treatment of diabetes mellitus and a new VMAT2 inhibitor has already entered a 2nd study in Phase I clinical trials for the treatment of tardive dyskinesia. While TBZ and reserpine (another VMAT2 inhibitor) have been used for decades for their antihypertensive and antipsychotic properties, they are rarely used anymore. The deleterious side effects associated with their use (e.g., parkinsonism, akathisia, depression, suicidality, sedation, and neuroleptic malignant syndrome) has proven them too high of a risk for use when other safer alternatives exist (Guay, 2010). Depression reported in patients upon chronic use of reserpine for the treatment of hypertension helped to build the monoamine hypothesis of depression (Freis, 1954). A newer generation of VMAT2-selective inhibitors that do not cross the blood brain barrier or that have better pharmacokinetics profiles may be therapeutically valuable for the treatment of diabetes mellitus.

Figure 3.1: VMAT2 LO Mice Have Normal Islet Morphology. A) H&E staining of pancreatic islet from VMAT2 WT (left panel) and LO mice (right panel). VMAT2 LO mice have comparable islet size shape and number.
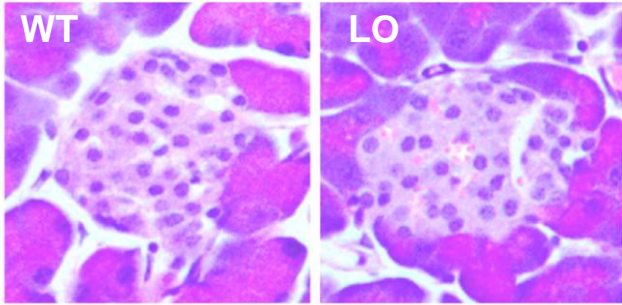
Figure 3.2: VMAT2 LO Mice Have Reduced VMAT2 Levels in the Pancreas. B) Insulin immunohistochemistry of pancreatic islet from VMAT2 WT (left panel) and LO mice (right panel). Insulin is shown in red. I) Tetrabenazine binding in pancreatic lysates from VMAT2 WT and LO mice to determine relative VMAT2 levels. VMAT2 LO mice have a 36% reduction in TBZ binding compared to WT animals. VMAT2 WT mice displayed 21.4 ± 7.47 pmol/min/mg of protein ^{3}H-DTBZ binding in the pancreas versus 13.7 ± 1.99 pmol/min/mg of protein ^{3}H-DTBZ binding in VMAT2 LO mice.
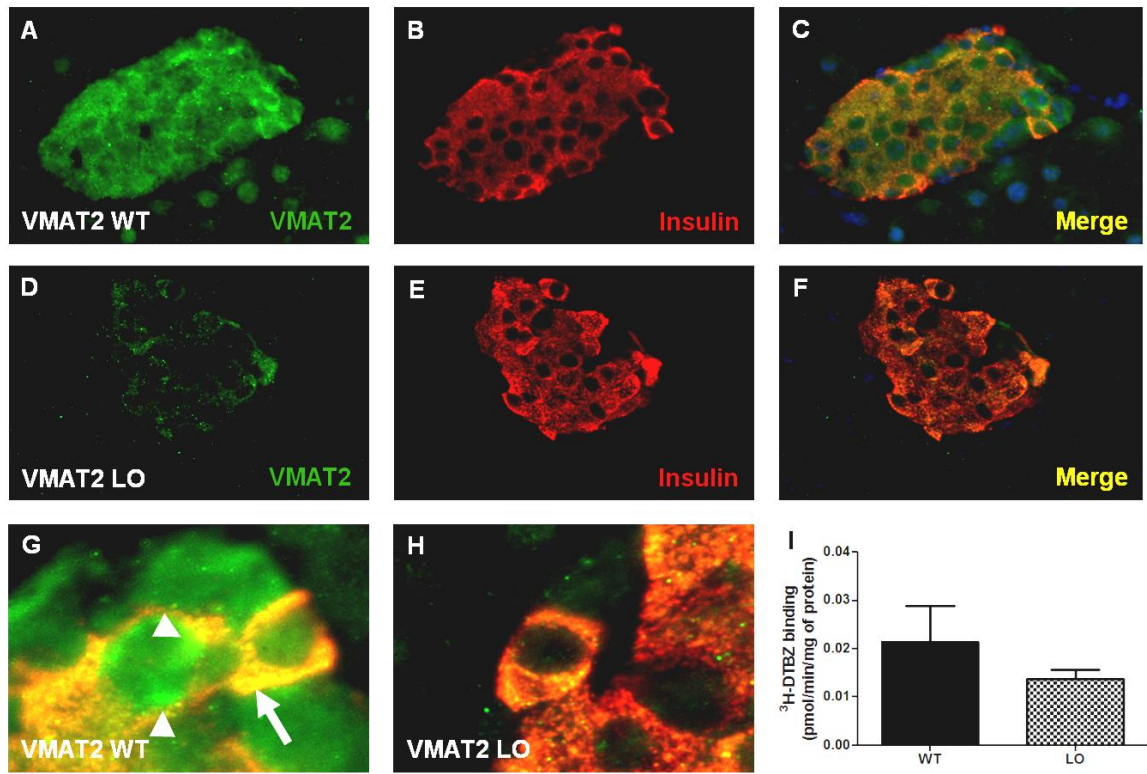
Figure 3.3: VMAT2 LO Mice Have Reduced Monoamine Levels in the Pancreas. Pancreas monoamine levels in aged VMAT2 WT and LO mice were measured by HPLC. A) Dopamine levels in the pancreas were reduced by 70% in VMAT2 LO mice. (VMAT2 WT mice pancreas dopamine – 23.09 ± 9.66 pmol/mg of protein; VMAT2 LO mice pancreas dopamine – 6.259 ± 3.22 pmol/mg of protein). B) 3,4-dihydroxyphenylacetic acid (DOPAC) levels in the pancreas were reduced by 80% in VMAT2 LO mice. (VMAT2 WT mice pancreas DOPAC – 29.89 ± 11.5 pmol/mg of protein; VMAT2 LO mice pancreas DOPAC – 6.084 ± 2.56 pmol/mg of protein; *, p<0.05). C) Homovanillic acid (HVA) levels in the pancreas were reduced by 40% in VMAT2 LO mice. (VMAT2 WT mice pancreas HVA – 103.5 ± 31.1 pmol/mg of protein; VMAT2 LO mice pancreas HVA – 32.31 ± 14.7 pmol/mg of protein). D) Norepinephrine levels in the pancreas were reduced by 40% in VMAT2 LO mice. (VMAT2 WT mice pancreas norepinephrine – 0.305 ± 0.09 pmol/mg of protein; VMAT2 LO mice pancreas norepinephrine – 0.158 ± 0.02 pmol/mg of protein).
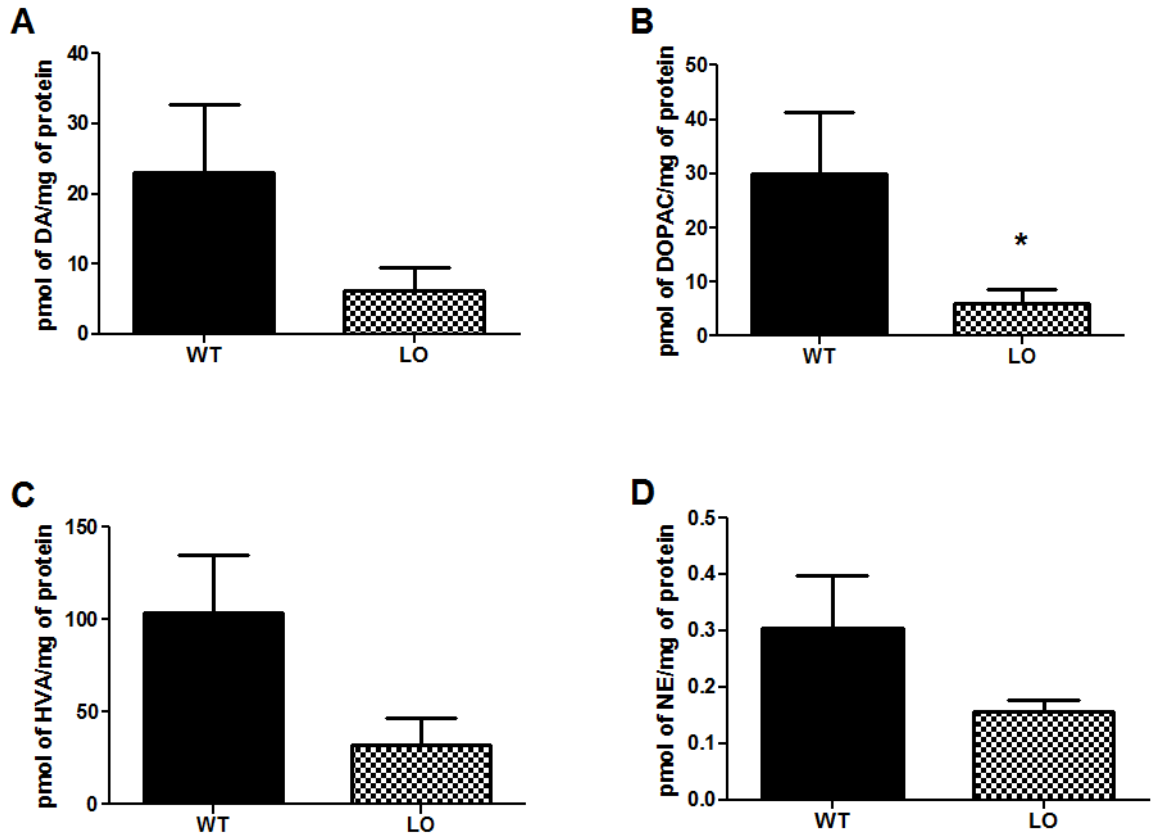
Figure 3.4: VMAT2 LO Mice Show Improved Fasting Glucose Levels as They Age. No statistical differences between VMAT2 WT and LO mice were observed in earlier adulthood (3 months VMAT2 WT mice fasting blood glucose – 63.5 ± 3.2 mg/dL; VMAT2 LO mice fasting blood glucose – 65.5 ± 4.9 mg/dL; 6 months VMAT2 WT mice fasting blood glucose – 79.0 ± 1.8 mg/dL; VMAT2 LO mice fasting blood glucose – 84.0 ± 5.7 mg/dL). Aged VMAT2 LO mice do not develop the impaired fasting glucose levels seen in VMAT2 WT animals (15 months VMAT2 WT mice fasting blood glucose – 108.0 ± 5.4 mg/dL; VMAT2 LO mice fasting blood glucose – 81.0 ± 3.4 mg/dL; 24 months VMAT2 WT mice fasting blood glucose – 126.0 ± 10.1 mg/dL; VMAT2 LO mice fasting blood glucose – 87.0 ± 5.3 mg/dL; n= 5-21; ***, p<0.0001) Statistical differences shown are within age group differences (n=8-18).
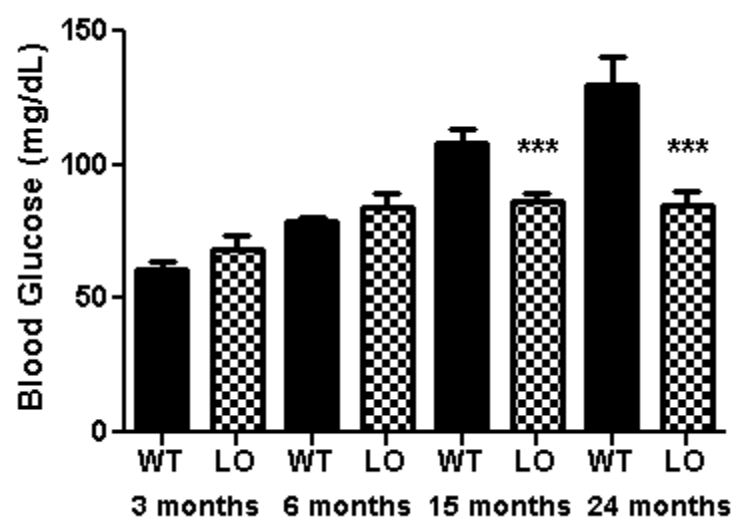
Figure 3.5: VMAT2 LO Mice Do Not Develop Impaired Glucose Tolerance as They Age.

Glucose tolerance was measured in aging VMAT2 transgenic mice. **A)** A plot of blood glucose

measures over time to determine the mice's ability to respond to glucose challenge. VMAT2 WT

mice show elevated blood glucose levels compared to VMAT2 LO mice (n=5; **, $p<0.01$). **B)**

Area Under the Curve (AUC) measurements in VMAT2 WT and LO mice at 15 months of age

were determined using the linear trapezoidal method. VMAT2 WT mice show increased AUCs

compared to VMAT2 LO mice (VMAT2 WT mice AUC – 2516 ± 195.7; VMAT2 LO mice AUC

- 1658 ± 287.6; *, $p<0.05$).
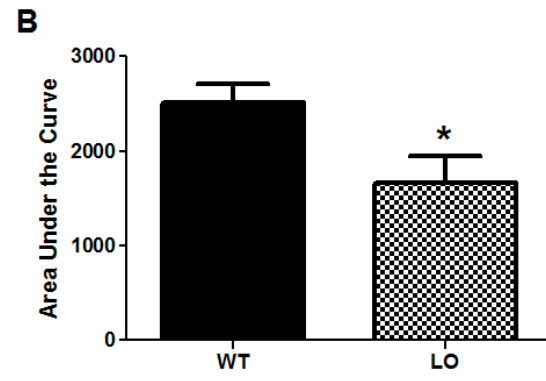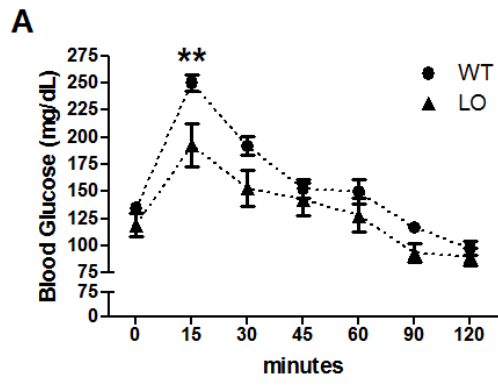
Figure 3.6: VMAT2 LO Mice Have Higher Glucose-Stimulated Insulin Release as Compared to Their WT Littermates. GSIR was measured in aging VMAT2 transgenic mice. Baseline fasting levels in VMAT2 LO mice are slightly higher serum insulin levels than their WT littermates (VMAT2 WT mice fasting serum insulin levels – 0.27 ± 0.03 ng/ml; VMAT2 LO mice fasting serum insulin levels – 0.30 ± 0.06 ng/ml; n=5). Fed serum insulin levels are nearing significantly higher in VMAT2 LO than their WT littermates (VMAT2 WT mice fed serum insulin levels – 0.41 ± 0.05 ng/ml; VMAT2 LO mice fed serum insulin levels – 0.64 ± 0.20 ng/ml).
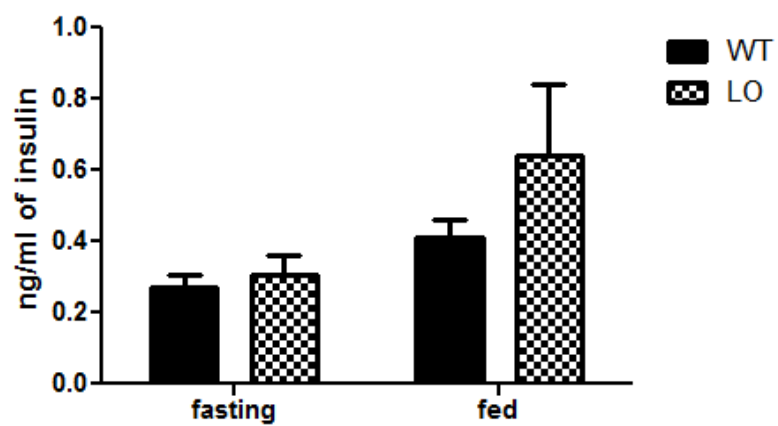
Chapter 4

The Parkinson Disease Associated Protein α-Synuclein Interacts with the Vesicular Monoamine Transporter 2 and Facilitates Packaging of Monoamines

Abstract

α-Synuclein (α-syn), the first protein identified to be associated with familial Parkinson's disease is a major component of Lewy body protein inclusions in Parkinson's disease patient brains. Although α-syn is expressed throughout the brain, monoaminergic neurons are preferentially affected in Parkinson's disease suggesting a unique interaction exists between α-syn and the monoaminergic system. The vesicular monoamine transporter 2 (VMAT2) transports cytosolic monoamines, including dopamine and norepinephrine into synaptic vesicles for sequestration and subsequent release at synaptic terminals. Genetic ablation of VMAT2 in mice results in a substantial loss of dopamine and NE followed by an age-dependent loss of dopamine and norepinephrine neurons with presentation of motor and non-motor symptoms similar to those seen in Parkinson's disease. Thus, factors responsible for maintaining normal VMAT2 activity may be necessary to protect monoaminergic neurons from cell death. We hypothesized that VMAT2 may be a target of α-syn. α-Syn colocalizes with VMAT2 in human substantia nigra, mouse primary nigral neurons, and transiently-transfected monoaminergic SHSY5Y cells. Interestingly, both expression of WT and A53T mutant α-syn increase tetrabenazine-sensitive packaging of dopamine over control by 48% and 47%, respectively. α-Syn expression increases VMAT2 transport of dopamine velocity (Control V_{MAX}- 37.36 ± 3.5 pmol/mg/min; WT α-syn V_{MAX}- 55.17 ± 3.0 pmol/mg/min; A53T α-syn V_{MAX}- 54.85 ± 6.1 pmol/mg/min); however, α-syn has no effect on dopamine affinity for VMAT2 (Control K_M- 4.016 ± 1.2 μM dopamine; WT α-syn K_M- 3.558 ± 0.6 μM dopamine; A53T α-syn K_M- 3.025 ± 1.2 μM dopamine.) Finally, yeast two-hybrid data suggest that α-syn interacts with the C-terminus of VMAT2. These data indicate that one function of α-syn may be to maintain proper storage of dopamine and norepinephrine via VMAT2.

Introduction

Mutations, triplications, and promoter haplotypes in α-syn show an association in genetic studies with Parkinson's disease (Kruger et al., 1998; Kruger et al., 1999; Munoz et al., 1997; Polymeropoulos et al., 1997; Zarranz et al., 2004). α-Syn is enriched in Lewy bodies and dystrophic neurites, both pathological hallmarks of Parkinson's disease and is present in many monoaminergic loci of the brain (Braak et al., 2001; Mochizuki et al., 2002; Spillantini et al., 1998). Though the link between Parkinson's disease and α-syn is strong, the function of α-syn in the neuron remains poorly characterized. While missense mutations in α-syn are known, it is also unclear whether a loss of function or a perhaps a toxic gain of function, as suggested by gene triplication studies, or both contribute to α-syn's role in Parkinson's disease pathogenesis.

One potential mechanism for α-syn's role in Parkinson's disease pathogenesis relates to α-syn formation of toxic aggregates. Studies have shown that these aggregates are stabilized in their most toxic form by oxidized dopamine and norepinephrine (Mazzulli et al., 2007; Mazzulli et al., 2006). Due to the potential for dopamine and norepinephrine to become oxidized in the cytosol, timely packaging of these monoamines into synaptic vesicles by VMAT2 may play a critical role in the survival of neurons. Persons with allelic haplotypes of VMAT2 that increase the promoter activity of the gene have lower incidence of Parkinson's disease, indicating that high levels of expression of VMAT2 may be protective against Parkinson's disease (Glatt et al., 2006). When the activity of VMAT2 is lost, impaired sequestration of monoamines from the cytosol may result in oxidation of monoamines potentially affecting the overall oxidation state of the neuron. VMAT2 mRNA is dramatically reduced in the brains and in the platelets of Parkinson's disease patients (Harrington et al., 1996; Sala et al., 2010). Additionally, VMAT2 protein expression is reduced in the striatum of Parkinson's disease patients (Miller et al., 1999b). Therefore, VMAT2 might be a target for dysregulation of monoamine homeostasis and subsequent neurodegeneration. In support of this hypothesis, mice that express only 5-7% of

normal VMAT2 levels exhibit progressive nigrostriatal and locus coeruleus degeneration similar to that seen in human Parkinson's disease and have evidence of increased oxidative stress and display motor and non-motor symptoms of Parkinson's disease (Caudle et al., 2007; Taylor et al., 2009). Together these data show that maintenance of proper VMAT2 activity is critical for the overall health of dopaminergic neurons.

Previous studies have shown that α-syn is present in the neuron as a soluble cytosolic protein and can transiently associate with synaptic vesicles (Maroteaux et al., 1988). While most investigation of α-syn centers on pathophysiological effects, it remains unclear the exact *normal* physiological function of α-syn. Several transgenic and knockout animal models have been created to study the role α-syn plays. While alterations in the vesicular pool size have been shown in α-syn transgenic mice, changes in dopamine levels in have also been observed, suggesting that α-syn plays some role in regulating dopamine homeostasis (Chesselet, 2008; Perez and Hastings, 2004). α-Syn shares high structural homology to the 14-3-3 family of chaperone proteins that increase TH activity (Xu et al., 2002). α-syn interacts with both TH and AADC decreasing the activity of both enzymes (Perez et al., 2002; Tehranian et al., 2006). Lentivirally-overexpression of A53T mutant α-syn in MESC2.10 dopaminergic cells results in decreased dopamine uptake and release (Lotharius et al., 2002). This supports data showing that α-syn interacts with DAT (Lee et al., 2001; Wersinger et al., 2003b); however, conflicting reports exist as to what functional effects on DAT activity result from this interaction. Indeed, these data have led to the study of α-syn effects on proteins involved in the regulation of the norepinephrine and serotonin transporters (Wersinger et al., 2006a; Wersinger et al., 2006b).

While several factors can influence dopamine levels in the neuron, we and others have previously shown that loss of VMAT2 expression in mice results in a loss of striatal dopamine and dopamine signaling (Caudle et al., 2007; Colebrooke et al., 2006; Fon et al., 1997; Mooslehner et al., 2001; Patel et al., 2003; Takahashi et al., 1997; Wang et al., 1997). Due to

VMAT2's role in maintaining proper storage of dopamine and thus regulating dopamine levels, we wanted to determine if α-syn plays any role for regulating VMAT2. Previous studies report that α-syn interacts with VMAT2 via GST-pull down assay (Guo 2008). Also, a decrease in total dopamine accumulation was observed in cells stably-expressing high levels of α-syn compared to control cells that corresponded to a decrease in VMAT2 expression. To expand the observation that α-syn may affect VMAT2 function, we performed a set of more rigorous experiments to look at VMAT2 expression and activity in the presence of α-syn. We also sought to determine whether mutant (A53T) α-syn could also affect VMAT2 activity.

Materials and Methods

Antibodies

Antibodies used include, rabbit anti-VMAT2 polyclonal antibody 1:250 dilution (Chemicon International Catalog # AB1767, Temecula, CA), mouse anti-α-synuclein 1:500 dilution (BD Bioscience Catalog # 610786, San Jose, CA), mouse anti-tyrosine hydroxylase (TH) 1:500 dilution (Chemicon), rabbit anti-TH 1:500 dilution (Chemicon), Alexa Fluor 488-conjugated Goat Anti-Rabbit IgG (Molecular Probes, Eugene, OR), Cy3-conjugated AffiniPure Goat Anti-Mouse IgG (Jackson Immunoresearch, West Grove, PA) HRP-conjugated Goat Anti-Rabbit antibody 1:5000 dilution (Jackson Immunoresearch, West Grove, PA), HRP-conjugated Goat Anti-Mouse antibody 1:10000 (Jackson Immunoresearch, West Grove, PA), and normal rabbit IgG (Santa Cruz).

Additionally, during the course of these experiments, the VMAT2 Chemicon antibody AB1767 was discontinued. We produced of a rabbit polyclonal antibody against the C-terminus of human VMAT2 using the peptide $^{NH2-}$CTQNNIQSYPIGEDEESESD^{-COOH} (Covance). Post-immunization sera were cleaned over a Protein A column per manufacturer's protocol (Pierce)

prior to use. A final antibody concentration of 15 µg/ml was used for all staining experiments in human brain slices. Antigen preabsorption was performed to ensure antibody specificity.

Immunohistochemistry

Paraffin-embedded 8 µm slices of human midbrain (generous gift of Dr. W. Michael Caudle, Emory University) were deparaffinized in xylene and rehydrated in successive washes with decreasing concentrations of ethanol. Antigen retrieval was performed using the microwave method with 10mM Sodium citrate pH 6.0. Slides were blocked using 10% Normal Goat Serum, 1% BSA, 1% Triton X-100 in 1X PBS. Primary incubations were also performed in 10% Normal Goat Serum, 1% BSA, 1% Triton X-100 in 1X PBS in a humidified chamber overnight at 4°C. Secondary incubations were performed in 1% Normal Goat Serum, 1% BSA, 1% Triton X-100 in 1X PBS in a humidified chamber for one hour at room temperature. Autofluorescence was blocked by postsecondary incubation in 3% Sudan Black prior to coverslipping with Vectashield Mounting media containing DAPI nuclear stain (Vector Laboratories).

Fluorescence microscopy on human midbrain slices were performed using a Zeiss Axio Imager.D2M Microscope.   Image capture was done using Microlucida software (MBF). Colocalization analyses were performed on either RGB or grayscaled images using FIJI Image Analysis software with both the Colocalization Threshold (Costes et al., 2004) and JACoP (Bolte and Cordelieres, 2006) Java Plugins. Pearson Coefficients of Colocalization were calculated for each image pair. A Regions of Interest (ROI) of n=5 individual neurons were used to calculate the overall average Pearson Coefficient. A Pearson Coefficient >0.05 was considered to be colocalization.   ROIs defined outside of neuronal cell bodies displayed no colocalization (data not shown).

Plasmids

hVMAT2/pcDNA3.1-Zeo, hASYNWT/pcB, and hASYNA53T/pcB were generous gifts of A. Levey (Emory University, Atlanta, GA). Each hASYN/pcB was digested with SalI and XhoI and subcloned into XhoI digested pcDNA3.1+Zeo (Invitrogen). Presence and orientation of the insert was confirmed by restriction digestion and sequencing. The resulting vectors were called hASYN-WT/pcDNA3.1+Zeo or hASYN-A53T/pcDNA3.1+Zeo. Empty pcDNA3.1+Zeo vector was used as control vector.

Cell Culture and Transfections

SHSY5Y cells (ATCC, Manassas, VA) were maintained in 50:50 F-12/Dulbecco's Modified Eagle Media with 4.5g/L Glucose and 2mM L-glutamine (DMEM) (Lonza Walkersville, Inc., Walkersville, MD) containing 10% Fetal Bovine Serum (Atlanta Biological, Atlanta, GA) and 1U/mL Penicillin/Streptomycin (Lonza Walkersville Inc., Walkersville, MD). Undifferentiated SHSY5Y cells were grown to 80% confluency on 10-cm culture plates or poly-D-lysine coated coverslips in 6-well plates. Cells were then transfected in Optimem Minimal Serum media (Invitrogen, Carlsbad, CA) with a 1:1 ratio of Lipofectamine 2000 (Invitrogen, Carlsbad, CA) to plasmid DNA. After 8 hours, 2X culture media without Pen/Strep were added and cells were maintained for an additional 40 hours before harvesting. Cells were transfected with 8µg of VMAT2 vector and either 4µg of empty pcDNA3.1+Zeo vector, WT, A30P, or A53T □-syn vector. Cells were cultured at 37°C, 5% CO_2, and 80% humidity.

Mouse postnatal primary cultured nigral neuron-glia co-cultures were generated as described in detail previously (Guillot et al., 2008a), with slight modifications. Briefly, brains from postnatal days 0–6 (P0–6) C57/Bl6J mice (Jackson Labs) were removed and placed in dissociation media containing 90 mM sodium sulfate, 30 mM potassium sulfate, 0.25 mM calcium chloride, 5.8 mM magnesium chloride, 10 mM glucose, 1 mM HEPES, pH 7.4. Under a dissecting microscope, a 0.8–1.0 mm coronal section of the mesencephalon was made using a

scalpel, and the regions containing substantia nigra were isolated. The substantia nigra was dissected, placed in fresh dissociation media, minced into small pieces. The substantia nigra was digested in dissociation media containing papain and DNase (Worthington Biochemical, Freehold, NJ, USA) and incubated at 37°C (2 times for 30 minutes). The tissue was rinsed twice with dissociation media, and once with plating media containing 1 mg/mL bovine serum albumin, 1 mg/mL ovalbumin, 20 mM glucose, 10 mM HEPES, 0.5 mL concentrated media additives dissolved in basal medium Eagle. The substantia nigra pieces were then triturated and the cell suspension was layered over plating media with 100 mg/mL bovine serum albumin and 100 mg/mL ovomucoid albumin. The cell suspension was then centrifuged for 8 minutes at 1400 g. The supernatant was removed, and the pellet was resuspended in PM with 2% rat serum. Cells were counted using Trypan Blue, and plated at 350 000 cells/cm^2 in Lab-Tek four-well Permanox chamber slides that were previously coated with 20 μg/mL laminin and 200 μg/mL poly-D-lysine (Collaborative Biomedical Products, Bedford, MA, USA) at 1 : 1 (vol:vol). Cells were maintained in an incubator at 37°C, 5% CO_2, and fed with plating media containing 2% rat serum. At 24 h post-plating, the cultures were fed with complete feeding media (containing 0.6 mM glutamax, 12 mM glucose, 100 mg/ml transferrin, 60 μM sodium selenite, 2 mM putrescine, 25 mg/mL insulin, 0.02 mL concentrated media additives, and 2% rat serum). The cultures were allowed to rest for 7 days before use.

Immunocytochemistry

Cells were washed in 1X PBS without Mg^{2+} or Ca^{2+} and fixed in 4% paraformaldehyde for 10 minutes. Cells were then permeablized in 0.1% Triton X-100 in PBS for 10 minutes and blocked in 1% BSA (Fisher) in PBS for 1 hour at room temperature. Primary antibodies in 1% BSA/PBS were added and incubated overnight at 4°C. Fluor-conjugated secondary antibodies in 1% BSA/PBS were added and incubated for 2 hours at room temperature in the dark. Coverslips were briefly incubated with Hoechst stain (Sigma) prior to mounting on glass slides with

Vectashield mounting medium (Vector Laboratories) and storage at 4°C in the dark until imaged. All confocal fluorescence microscopy was performed using the Zeiss LSM confocal microscope system. Images are displayed as raw images.

Cell Harvesting for Western Analyses, Uptake, and Binding Assays

Cells were washed and then harvested in 1X PBS without Mg^{2+} or Ca^{2+}. Cells were pelleted at 1000 x g for 2 minutes. Cell pellets were resuspended in 0.32 M sucrose, 5 mM HEPES, pH 7.4 with 1X Protease Inhibitor cocktail (Sigma). Cells were then sonicated at 4°C for 30 seconds and centrifuged at 8000 x g for 8 minutes 4°C. The supernatant was removed and stored at 20°C until use.

Vesicular [^{3}H] Dopamine Uptake Assays

This assay is adapted from the Edwards method of vesicular uptake assay(Merickel and Edwards, 1995). Cell lysates were thawed on ice and 25 µl of lysates (350-450 µg of protein) was added to either 200 µl of VMAT2 uptake buffer (2mM ATP-Mg^{2+}, 1.7mM Ascorbate, 25mM HEPES, 100mM Potassium tartrate, 0.1mM EDTA, 0.05mM EGTA, pH 7.4) or 175µl of uptake buffer plus 25 µl of 200 µM tetrabenazine (TBZ) in uptake buffer to yield a final concentration of 20 µM TBZ. Samples were incubated in a 30°C water bath for 10 minutes to allow TBZ to bind. Then, 25µl of dopamine with a 6% [^{3}H] dopamine (Perkin Elmer Boston, MA) tracer was added to each reaction and incubated for 5 minutes. Final dopamine concentrations ranged from 0.01-30 µM. Cold uptake buffer (2-3ml) was added to attenuate each reaction and samples were harvested on a Brandel Cell Harvester with Whatman GF/F Filter Paper (Brandel, Inc., Gaithersburg, MD) presaturated with 0.5% Polyethylenimine. Dried membranes were added to SafeScint Econo1 Scintillation fluid (Fisher Scientific) and bound activity was measured on a LS6500 Beckman Scintillation Counter. Specific dopamine uptake was determined by subtracting total uptake from TBZ-sensitive uptake and normalized to the total protein per well as

determined by BCA protein assay according to manufacturers protocol (Pierce). Velocity was reported as pmol/mg/min and expressed as raw values. Kinetic parameters (V_{MAX} and K_M) were determined using nonlinear regression with GraphPad Prism 5.0 software (San Diego, CA). Linear regression was also performed; however, these parameters were not used to calculate V_{MAX} and K_M.

[3]H-Dihydrotetrabenezine Binding Assay

[3]H-Dihydrotetrabenezine (^{3}H-DTBZ) binding was performed on cell lysates as described for the vesicular dopamine uptake above with the following modifications. Cell lysates were thawed on ice and added to VMAT2 uptake buffer. Then a 20 µM final concentration of cold TBZ was added followed immediately by the addition of 2 nM ^{3}H-DTBZ. The reaction was incubated at 37°C for 2 minutes. The reaction was immediately attenuated with cold uptake buffer and harvested as described above. Specific ^{3}H-DTBZ binding was determined by subtracting total ^{3}H-DTBZ binding from cold TBZ-sensitive binding and normalized to the total protein per sample as determined by BCA protein assay according to manufacturers protocol.

Western Analysis

Western analyses were performed similarly as described previously(Richardson et al., 2006). Briefly, lysates in 1X SDS loading dye were electrophoresed on either 10% Bis-Tris (for VMAT2) or 4-20% Tris-Glycine (for α-syn) NuPAGE gels (Invitrogen) and transferred to a 0.2µm pore size polyvinylidene difluoride membrane (Invitrogen) or nitrocellulose membrane (Invitrogen), respectively. Membranes were blocked in 8% nonfat dry milk in Tris-buffered saline (135 mM NaCl, 2.5 mM KCl, 50 mM Tris, and 0.1% Tween 20, pH 7.4) for 1 hour at room temperature. Primary antibodies were added to 0.8% nonfat dry milk in Tris-buffered saline and membranes were incubated overnight at 4°C. Secondary antibodies were added in Tris-buffered saline and membranes were incubated 1-2 hours at room temperature. Antibody detection was

measured by chemiluminescence (SuperSignal West Dura Extended Duration Substrate- Pierce) and imaged using an Alpha Innotech Fluorchem Imaging system. Densitometry analysis was performed using the accompanying software suite.

Statistics

In addition to nonlinear regression, statistical analyses were performed using one–way ANOVA on GraphPad Prism 4.0 Software. Tukey post-hoc tests were performed. All significant measures were reported as $P<0.05$.

Results

α-Syn Colocalizes with VMAT2 in Neuronal Cell Bodies and Vesicular Structures

In order to determine the effect of α-syn on VMAT2, we first sought to confirm that both proteins are present in the same cellular compartments. We performed immunohistochemistry on human midbrain slices. We found that both VMAT2 and α-syn largely localized to punctuate perinuclear structures in nigral neurons (Figure 4.1A and 4.1B, respectively). α-Syn and VMAT2 staining was most closely associated with neurons baring very large nuclei (Figure 1C) consistent with the known characteristics of the large dopaminergic neurons of the SNpC. The staining for both of α-syn and VMAT2 demonstrated dramatic colocalization (Figure 4.1D, yellow staining). All VMAT2-positive neurons observed coexpressed α-syn while nearly all α-syn neurons coexpressed VMAT2. All VMAT2 nigral neurons observed were TH positive (data not shown). Finally, quantative analyses of image pixels demonstrate strong colocalization between VMAT2 and α-syn with Pearson Coefficients ranging from 0.7 - 0.93 (Figure 4.1F). These data strongly show that α-syn and VMAT2 colocalize in dopaminergic neurons of the SNpC.

Endogenous expression of α-syn and VMAT2 was also examined in fixed primary cultured nigral neurons from mice by confocal microscopy. Both α-syn and VMAT2 showed

strong expression in nigral neurons. α-Syn colocalized with VMAT2 in the perinuclear compartment and a few punctate structures along the axonal projections similarly as seen in cells (Figure 4.2A). We also looked at TH staining in the nigral neurons. VMAT2 showed considerable overlap in localization with TH indicating that they also reside in a similar subcellular compartment (Figure 4.2B). Additionally, TH and α-syn colocalize in both the perinuclear compartment and in punctate structures along the axonal projections (Figure 4.2C). Furthermore, TH has been shown to localize preferentially to the cytoplasmic/perinuclear compartment of the neuron further supporting that VMAT2 and α-syn also are colocalizing in the cytoplasmic/perinuclear compartment.

Next, we wanted to confirm that VMAT2 and α-syn are located within the same cellular compartments *in vivo*. To do this, we performed subcellular fractionation on mouse striatal samples. Both VMAT2 and α-syn are expressed in crude striatal lysates (S1) (Figure 4.3). Additionally, further fractionation confirmed that both proteins could be found in the vesicular fraction (P4), while α-syn is also highly expressed in the cytosolic fraction (S4).

To determine whether this interaction could be studied *in vitro*, we first confirmed that α-syn colocalized with VMAT2 in transfected dopaminergic cells. As reported previously by other groups, α-syn protein expression was undetectable in untransfected, undifferentiated SHSY5Y cells (Figure 4.4) (Mazzulli et al., 2006). When transiently expressed, both wild-type and A53T mutant forms of α-syn displayed colocalized distribution of expression with VMAT2 and α-syn in a perinuclear compartment and in a few small punctate structures present in the short neuritic processes consistent with a vesicular structure.

α-Syn Expression Increases VMAT2 Activity in Cotransfected Cell Lysates.

To test the effect of coexpression of α-syn with VMAT2 on VMAT2 activity, we performed vesicular ^{3}H- dopamine storage assays on cell lysates. Expression of wild-type or

A53T mutant α-syn increased TBZ-sensitive VMAT2 activity by 48% and 47%, respectively over control transfected cells with an increase in V_{MAX} (Control V_{MAX}- 37.36 ± 3.5 pmol/mg/min; WT α-syn V_{MAX}- 55.17 ± 3.0 pmol/mg/min; A53T α-syn V_{MAX}- 54.85 ± 6.1 pmol/mg/min) (Figure 5A). No effect on dopamine affinity was observed (Control K_M- 4.016 ± 1.2 μM dopamine; WT α-syn K_M- 3.558 ± 0.6 μM dopamine; A53T α-syn K_M- 3.025 ± 1.2 μM dopamine.) A Lineweaver-Burk plot displays a minimal change in substrate affinity with a dramatic change in the velocity of VMAT2 uptake (Figure 4.5B).

A simple explanation for an increase in V_{MAX} is an increase in protein expression. Therefore, we determined the effect of α-syn on VMAT2 protein expression. First, we performed ^{3}H-DTBZ binding. DTBZ is a selective, noncompetitive antagonist of VMAT2. ^{3}H-DTBZ binding confirmed no changes in VMAT2 levels between control and α-syn transfected cells (Figure 4.6A). Next, we performed Western blots on VMAT2 cell lysates from α-syn transfected cells. Western analyses confirm no differences in VMAT2 total protein levels between control and α-syn transfected cells (Figure 4.6B and C). Additionally, there was no difference between the three different glycosylation states (75, 55, and 45 kDa bands of VMAT2 protein) in each group (densitometric data not shown).

α-Syn Interacts with the C-Terminus of hVMAT2

Since a functional interaction of these two proteins may occur via a physical interaction, we sought to determine if α-syn physically binds VMAT2. First, we attempted to demonstrate a direct interaction by using coimmunoprecipitation experiments from cellular lysates of cotransfected cells. Despite troubleshooting many factors including salt and detergent concentrations, epitope tagging, and crosslinking, we were unable to reliably demonstrate a direct link though coimmunoprecipitation. Therefore, we attempted a broader technique. We screened a human cDNA library to determine proteins interacting with human VMAT2. Upon screening,

α-syn was identified as a VMAT2 interacting protein (Figure 4.7A,B). This interaction was confirmed by reselection. Specifically, α-syn interacts with the 480-515 C-terminal fragment of VMAT2.

Discussion

Previous experiments *in vivo* or *in vitro* have not directly tested the effects of α-syn on VMAT2 transport. Several studies have investigated the role of α-syn in the release of dopamine and norepinephrine (Abeliovich et al., 2000; Yavich et al., 2006; Yavich et al., 2004; Yavich et al., 2005). These studies used electrophysiology techniques to measure release directly then make inference from these data about dopamine and norepinephrine packaging. Our experiments directly measure TBZ-sensitive dopamine uptake. Therefore, the observed dopamine uptake can be directly attributed to VMAT2 activity. VMAT2 is a proton antiporter meaning that for every molecule of monoamine transported across the membrane two protons are passed across the membrane in the opposite direction. Thus, other factors independent of VMAT2 itself can influence dopamine uptake, including cellular ATP levels that drive vesicular ATPase production of protons and subsequent affects on vesicle pH. We perform our VMAT2 assays on cellular lysates that are supplemented with physiological concentrations of ATP prior to uptake. This insures that ATP concentrations are not substrate limiting. Therefore, any changes in dopamine uptake under our experimental conditions are most likely due to changes in either VMAT2 protein expression or transporter function (i.e., substrate recognition or velocity with which substrate is transported across the vesicle membrane.) We did not observe a change VMAT2 protein expression or K_M with 5 minutes of uptake (Table 4.1). Our conclusion is that α-syn most likely affects the ability of VMAT2 to transport dopamine. We show here both a functional and physical interaction between VMAT2 and α-syn. These data support the hypothesis that α-syn plays a critical role in maintaining dopamine homeostasis. Other studies have shown A53T α-syn to achieve protofibrils more aggressively and to be more cytotoxic than

WT (Conway et al., 2000; Lehmensiek et al., 2002); however, it is interesting to note that the mutant A53T α-syn behaved similarly to WT α-syn in our experiment.

Surprisingly, our findings directly conflict with the observations by Guo et al. In their study, they found that stable expression of WT α-syn decreases dopamine uptake while decreasing VMAT2 protein expression. Despite both sets of experiments being performed in SHSY5Y cells, there are several methodological difference that may explain the differences observed in results. First, we measured TBZ-sensitive uptake. As TBZ is VMAT2 selective inhibitor, this is a more reliable measure of VMAT2 activity. Therefore, we are able to determine dopamine accumulation due solely to VMAT2 binding or transport and exclude any nonspecific radioactive counts that could result from ^{3}H- dopamine binding to various dopamine receptors including DAT. Secondly, we performed our experiments under transient transfection conditions. We were unable to detect VMAT2 protein in our laboratory stock of untransfected SHSY5Y cells by ICC (Figure 4.4), Western analysis, or by TBZ-sensitive ^{3}H- dopamine uptake using our method (data not shown). Previous reports by Guo et al. did not transiently express VMAT2, but rather relied on endogenous expression of VMAT2. We were unable to do this due to undetectable VMAT2 expression in SHSY5Y in our laboratory stock. Third, along the lines of differences in VMAT2 expression, there is a vast temporal difference between these experiments. We performed our uptake experiments with 5 minutes incubation rather than 45 minutes. This is because our VMAT2 expression is sufficient to reliably determine uptake in a short period of time. Fourth, we performed our assay in cellular extracts from transfected cells similar to experiments performed in isolated synaptic vesicles. We are confident that our experiments produced kinetic values within published parameters for VMAT2 activity (V_{MAX} ~30-40 pmol/mg/min and K_M ~1-4 μM dopamine.) Guo et al. used detergent permeablization methods to bypass the need to transport dopamine into the cell for packaging; however, both methods are commonly used to reliably measure VMAT2 activity. Finally, we transiently expressed low

levels of α-syn in our expression system. Guo et al. used stably-transfected α-syn expressing SHSY5Y before performing dopamine uptake experiments. Myriad studies have shown that overexpression of α-syn eventually leads to the generation of α-syn aggregates. α-Syn oligomers form protofibril pores or disrupt membrane bilayers that cause leakage of synaptic vesicles (van Rooijen et al., 2010a; van Rooijen et al., 2010b; Volles and Lansbury, 2002; Volles et al., 2001). If such structures formed in cells the result may be a loss of dopamine packaging. Therefore, we feel that our experiments better represent α-syn effects on dopamine transport under non-pathological conditions and that α-syn dosage may be responsible for the observed difference between studies. There was no evidence of aggregation by α-syn staining (Figure 4.4) nor by thioflavin-S staining (data not shown) nor any evidence of overt cell toxicity in our experiments.

Conclusions

Taken together these data support a role for α-syn in the regulation of VMAT2 activity. These findings build upon the enormous mounting evidence that α-syn is a critical regulator of presynaptic functions, most notably vesicular functions and dopamine homeostasis(Perez and Hastings, 2004). We have also expanded the understanding of VMAT2, a critical player in the health of monoaminergic synapses and Parkinson's disease.

Table 4.1: Analyses of VMAT2 Kinetic Parameters. V_{MAX} and K_M values for control, WT α-syn and A53T α-syn transfected cells.

	Control	WT α-syn	A53T α-syn
V_{MAX} (pmol/mg/min)	37.36 ± 3.5	55.17 ± 3.0	54.85 ± 6.1
K_M (μM dopamine)	4.016 ± 1.2	3.558 ± 0.6	3.025 ± 1.2

Figure 4.1: **Colocalization of VMAT2 and α-Syn in Human Substantia Nigra Pars Compacta (SNpC) Neurons.** A) Epifluorescent microscopy of large VMAT2 positive neurons in the SNpC. Green indicates VMAT2 expression. Note inset with arrowheads showing smaller punctuate staining. B) Red indicates α-syn expression. C) Blue indicates the presence of nuclei. Note the large nuclei demonstrating the typical large neurons characteristic of dopaminergic neurons in the SNpC. D) Overlay of VMAT2, α-syn, and nuclear staining. E) Overlay of VMAT2 and α-syn colocalization. White indicates colocalization where each pixel met a minimum threshold. Red and green indicate α-syn and VMAT2, respectively that does not colocalize. F) Graphical representation of colocalization data. The slope of the white line indicates colocalization. Pearson coefficient for this image is R=0.9223. Representative data are shown.
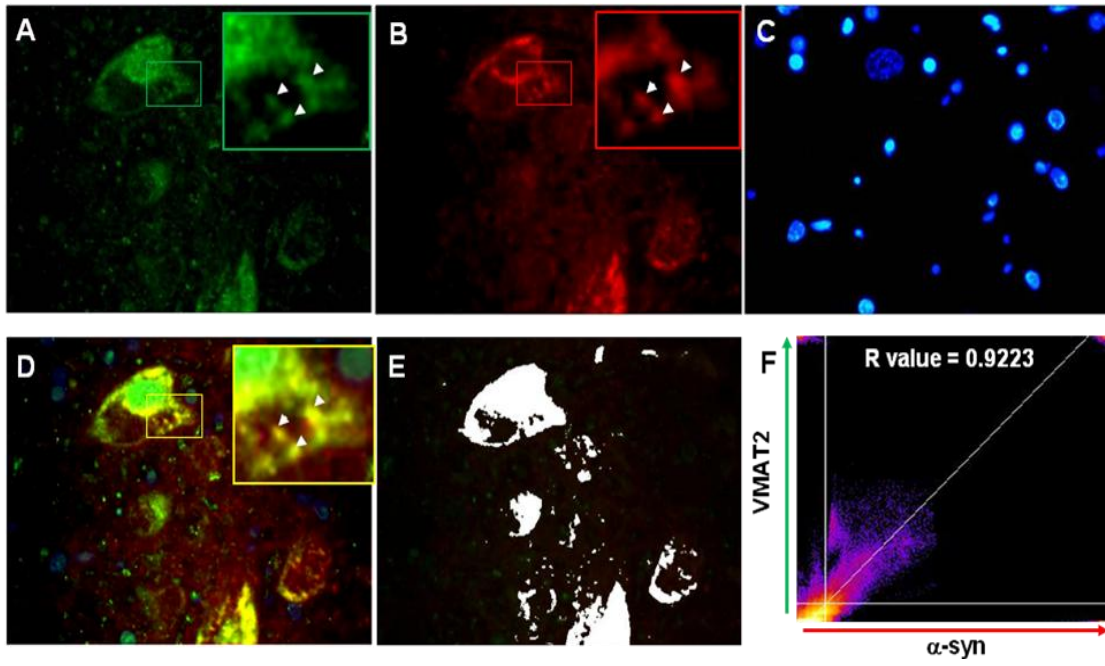
Figure 4.2: Expression of Dopaminergic Neuronal Markers in Mouse Primary Cultured Neuron. A) Native expression of VMAT2 and α-syn in mouse primary nigral neuronal cells observed by immunofluorescence. Confocal microscopy images of VMAT2 and α-syn stained primary nigral neurons. Large white arrows indicate neuronal cell body. Small white arrows indicate areas of punctate colocalization. All VMAT2-positive cells observed were also TH-positive. B) Native expression of VMAT2 and TH in mouse primary nigral neuronal cells observed by immunofluorescence. C) Native expression of TH and α-syn in mouse primary nigral neuronal cells observed by immunofluorescence.
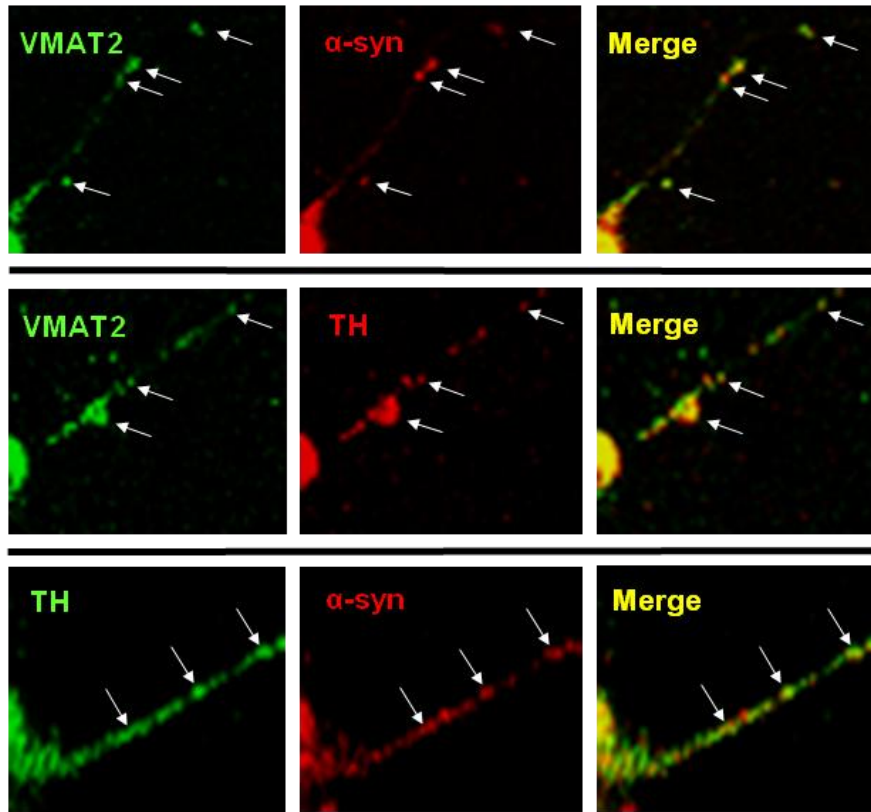
Figure 4.3: VMAT2 and α-Syn Expression from Subcellular Fractionation of Mouse Striatum. A) Diagram of fractionation protocol. The S1 (lysate) fraction, P2 (synaptosome) fraction, S3 (soluble post-synaptosomal) fraction, and P4 (vesicle) fraction are enriched in VMAT2 protein expression. Small amounts of VMAT2 are still associated with the P3 (synaptosomal membrane fraction) and most likely represent docked vesicles. α-syn is found in all fractions, but is enriched in the S3, P4 (vesicle), and S4 (cytosol) fractions. B) Western blot showing coexpression of VMAT2 and α-syn in the vesicular compartment.

A

Homogenize Brain Tissue

1000 x g

S1 (lysate)   P1 (debris)

20000 x g

S2   **P2 (synaptosomes)**

Homogenize with
osmotic shock
20000 x g

S3   P3 (synaptosomal
membranes)

120000 x g

S4   **P4 (vesicles)**
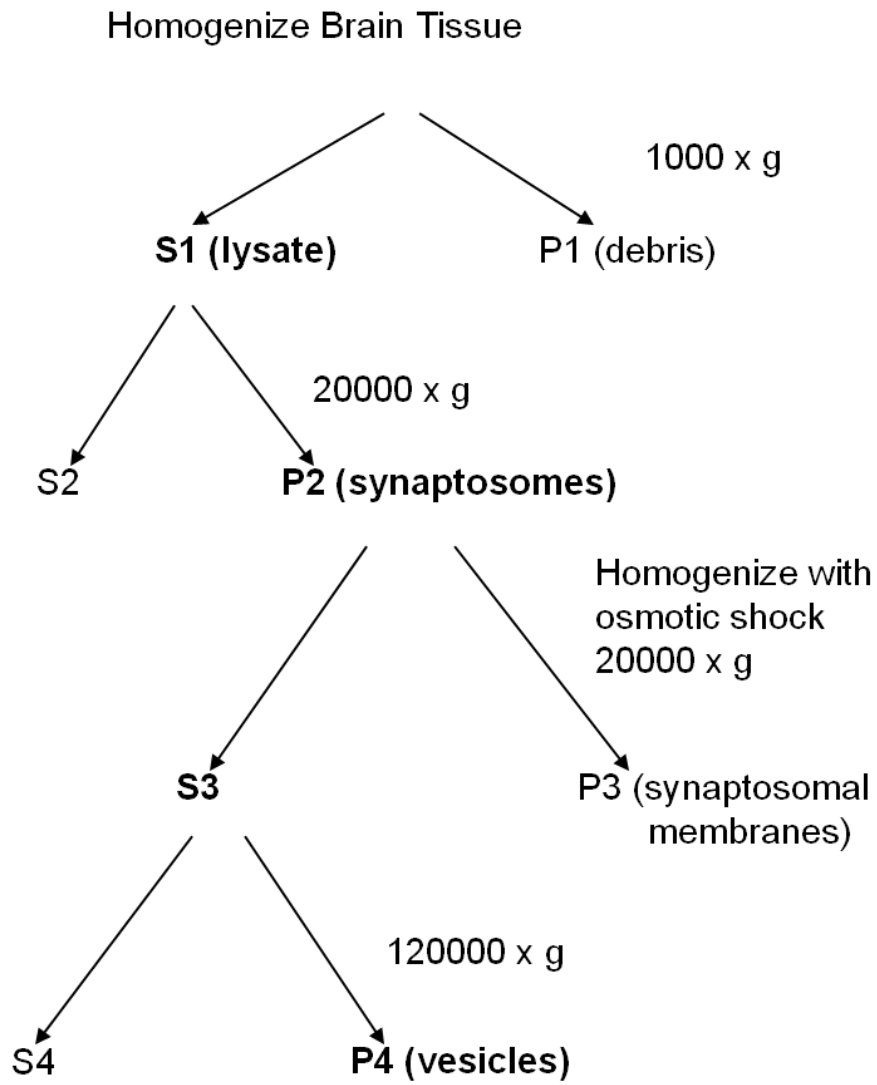
B
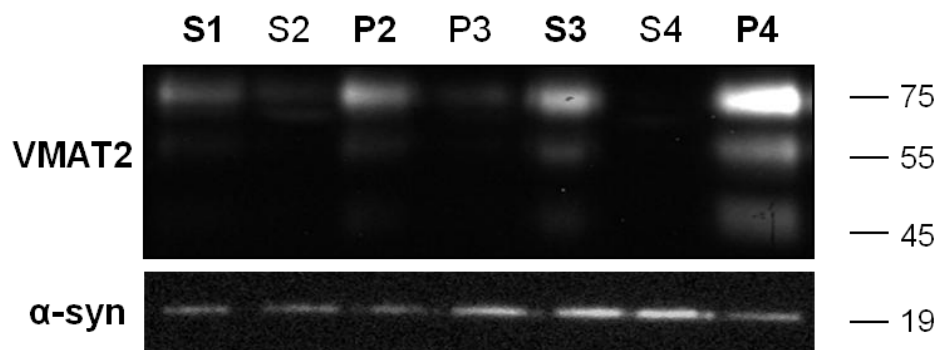
Figure 4.4: Confocal Microscopy Images of α-Syn and VMAT2 in Cultured SHSY5Y Cells.
Expression of VMAT2 and WT or A53T α-syn in cotransfected cells. Green represents VMAT2 immunofluorescence. Red represents α-syn immunofluorescence. Blue represents Hoechst staining of nuclei. Yellow represents merged VMAT2 and α-syn immunofluorescence. Note the presence of punctuate colocalization throughout the cytosol.
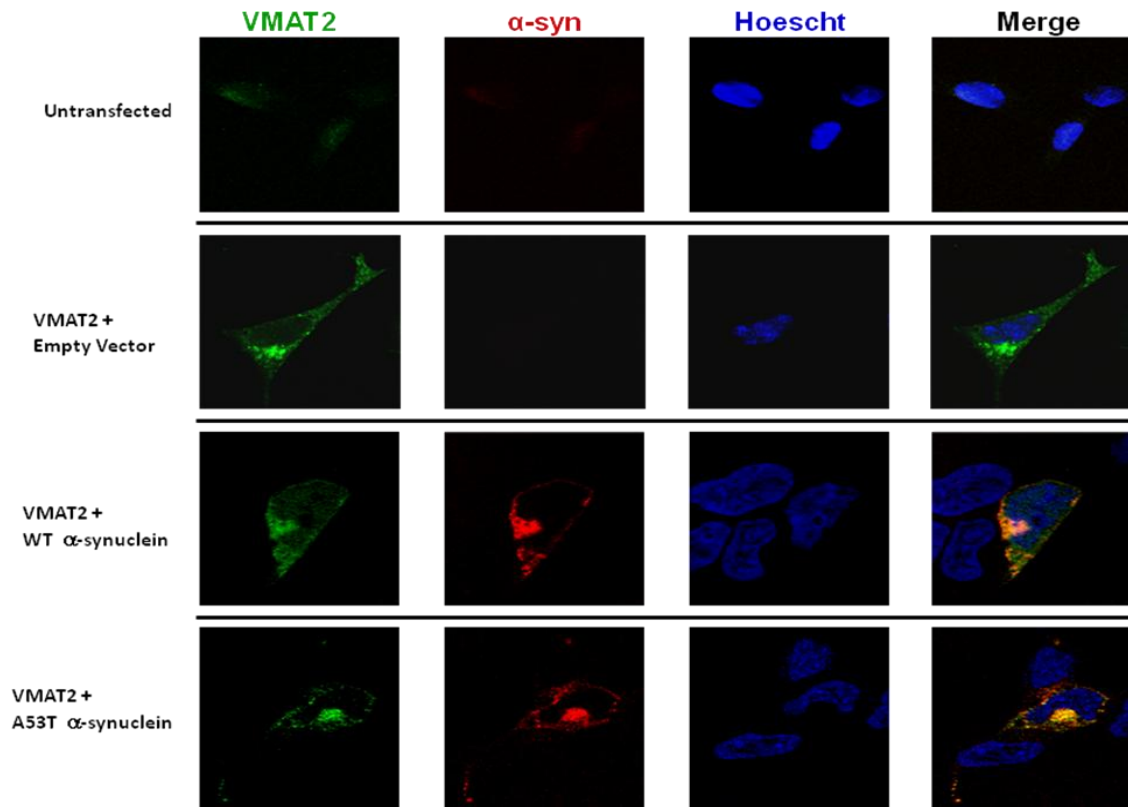
Figure 4.5: **Effect of α-Syn Expression on Dopamine Uptake in Immortalized Dopaminergic Cells.** TBZ-sensitive ^{3}H- dopamine uptake in lysates of VMAT2 and α-syn expressing SHSY5Y cells. A) Kinetic profile of α-syn effects on VMAT2 transport activity. B) Lineweaver-Burk Plot of α-syn effects on VMAT2 transport activity. Data points represent actual values plotted in linear regression; however, slope lines were determined using data from nonlinear regression. C) Eadie-Hofstee Plot of α-syn effects on VMAT2 transport activity. Note the differences in transport velocity between α-syn expressing lysates and control lysate, but little change in K_M (nearly parallel slopes between experimental groups). D) Hanes-Wolff Plot of α-syn effects on VMAT2 transport activity. Note the differences in slope between α-syn expressing lysates and control lysate reflecting the increase in V_{MAX} in α-syn expressing lysates.
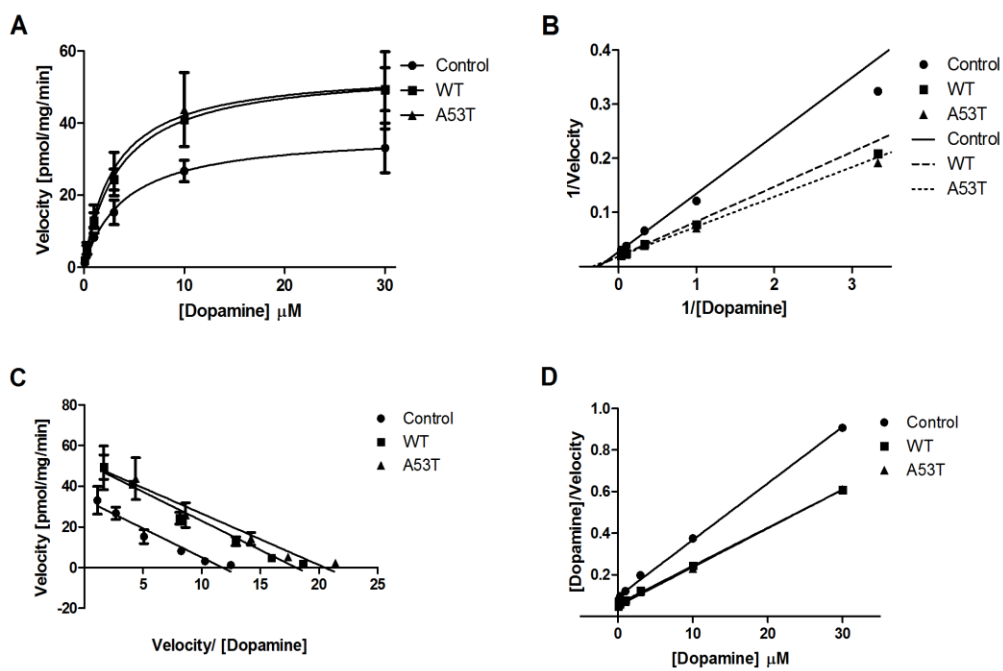
Figure 4.6: Effect of α-Syn on VMAT2 Expression. A) ^{3}H-DTBZ binding in VMAT2 and α-syn coexpressing cell lysates. B) Western blot of VMAT2 expression in α-syn coexpressing SHSY5Y cells. C) Densitometric analyses of VMAT2 expression in α-syn coexpressing SHSY5Y cells. Data are expressed in relative units.
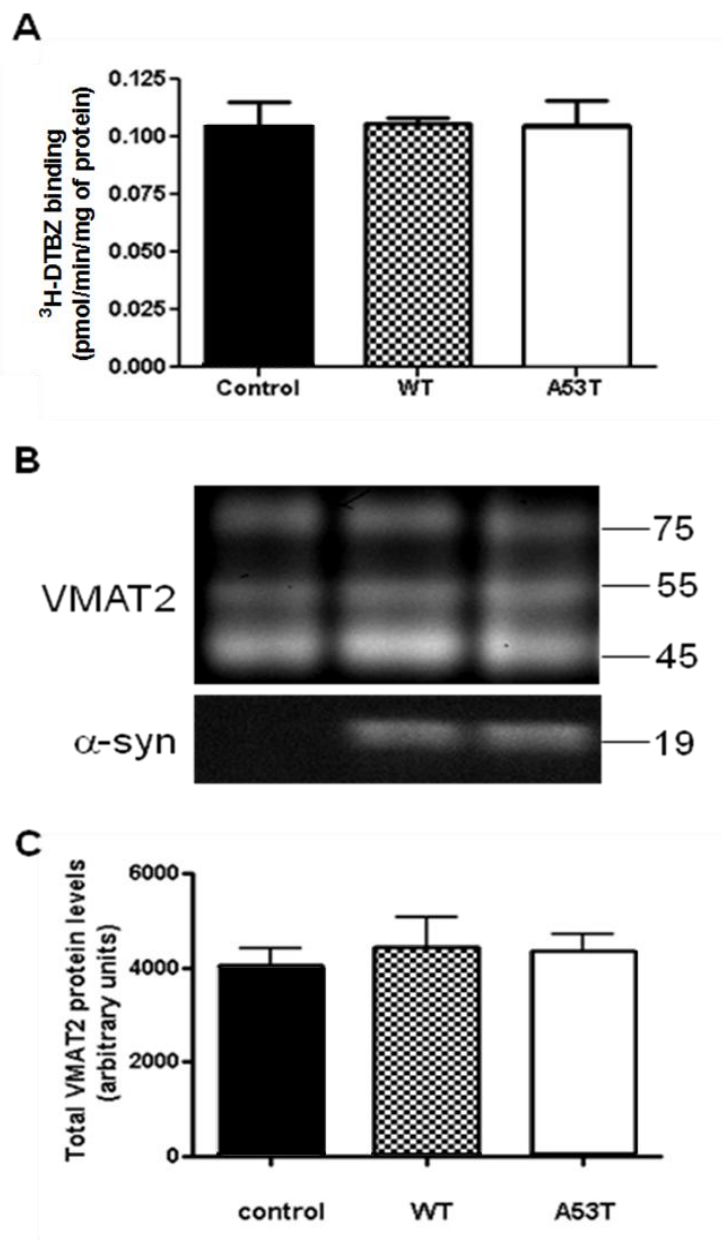
Figure 4.7: VMAT2 Interacts with α-Syn. A) For yeast two-hybrid experiments, sequence of the 480-515 C-terminus of VMAT2 used as bait. B) Yeast two-hybrid experiments reveal a physical interaction between VMAT2 and α-syn. Briefly, yeast were transformed with bait constructs fused to the GAL4 DNA binding domain and prey constructs fused to the GAL4 DNA activation domain. Transformants were allowed to grow for 5-7 days at 30ºC on either control media (L⁻W⁻) or test media (L⁻W⁻A⁻).

A   [480]MA**I**LMDHNCPIKTKMYTQNNIQSYPIGEDEESESD[515]

B

BAIT	PREY	L-W-	L-W-A-
pAS2.1-VMAT2C (480-515)	pGAD10	+	-
pAS2.1-VMAT2C	pGAD10- α-syn	+	+

Chapter 5

Summary and Conclusions

Summary and Discussion

PCBs Impair Glucose Homeostasis and Promote Dyslipidemia in Female Mice

We show that PCB treatment markedly reduces pancreatic dopamine levels in both males and females while VMAT2 expression is unaffected. However, females appear to have a unique susceptibility to obesogenic and metabolic effects of PCB. PCB-treated females gained weight twice as quickly as control animals. Glucose tolerance was also slightly impaired in PCB-treated females while fasting and fed insulin levels were also affected. In contrast, PCB-treated male mice lost body mass and showed improved glucose tolerance when compared to control mice. These sexually dimorphic differences may be the result of differences in hormonal responses as they relate to PCBs. PCBs are known endocrine disruptor able to effect signaling and downstream gene expression through estrogen and androgen receptors. Therefore, while some mechanisms common to both males and females may yield similar phenotypes as is the case with pancreatic dopamine levels, gender-dependent mechanisms may explain the variability in responses seen in glucose tolerance and weight gain. Indeed, one report shows that a positive, linear relationship exists between serum PCB levels and diabetes incidence in women (Vasiliu et al., 2006). However, the vast majority of human studies do not detect any gender differences only showing positive associations between PCB serum levels and diabetes/metabolic disorder/glucose intolerance. Thus, the differences between genders reported here may not translate to a human population. Also, male rats fed high fat diets supplemented with crude salmon oil containing mixtures of multiple different classes of persistent organic pollutants including PCBs developed exacerbated insulin resistance compared to high fat diet alone or high fat diet with refined salmon oil with no persistent organic pollutants (Ruzzin et al., 2010). Therefore, in some models of environmental toxicant exposure, males are susceptible to the effects of these chemicals. Differences in response to PCBs by males and females in this study may simply be a dosage-effect due to gender differences in metabolism and adiposity related to

the local PCB concentration in target tissues (Pelletier et al., 2003). It is important to note though that all of the experiments reported here are performed on mice exposed to standard rodent chow, not high fat rodent chow. Thus, we provide for the first time evidence that PCBs alone are sufficient to drive impairment of glucose homeostasis. Perhaps, combination of high fat diet and exposure is necessary to drive pathology in male rodents. High fat diet combined with PCB treatment in both males and females would be interesting for future studies to investigate this potential interaction further.

Together these data suggest that PCBs may be influencing blood glucose homeostasis by multiple mechanisms, including monoaminergic dysfunction in the pancreas. Other studies have also addressed mechanisms of PCB-induced alterations in glucose homeostasis or obesity. Most notably, male mice treated with the dioxin-like PCB 77 showed increases in body mass, body fat, adipocyte area, and serum cholesterols and changes in liver gene expression, but these effects were diminished in AhR knockout mice (Arsenescu et al., 2008; Arzuaga et al., 2009). However, no evidence of glucose intolerance or alter insulin secretion has been provided. It is unclear whether PCB-77 could affect those systems *in vivo*; however, *in vitro* studies suggest that PCB-77 cannot affect glucose-stimulated insulin release (Fischer et al., 1996). Aroclor 1254:1260 treatment in AhR knockout female mice may help to dissect the contribution of AhR-dependent mechanisms of action, if any, on PCB-induced alterations on glucose homeostasis.

It is important to note though that humans are exposed to mixtures of these individual congeners and other chemicals. Epidemiological data indicate that PCB exposure can drive multiple disease pathologies related to diabetes and cardiovascular disease, including obesity, glucose intolerance, hyperinsulinemia, hypertension, and dyslipidemia. Mechanistic data clearly show that individual congeners affect one or more pathways and this is largely determined by the structural confirmation and the degree of chlorination of the congener (Figure 1.3). Epidemiological data show a correlation between insulin levels and PCB exposure. Indeed, our

data suggests that PCBs affect both fasting and fed levels of insulin and glucose tolerance where this may be associated with the observed concomitant change in dopamine levels in the pancreas (Figure 2.1 and 2.5). This newly implicates pancreatic dopamine homeostasis as potential site of dysregulation from PCB exposure. Perhaps PCB mixtures work in concert together with individual congeners affecting multiple discrete pathways. With multiple pathways affected the net effect could increase risk of disease.

Additionally, PCBs inhibit TBZ-sensitive VMAT2 activity (Table 2.1). Inhibition among individual congeners is greatest in non-dioxin like congeners. Therefore, inhibition of VMAT2 is a likely pathophysiological mechanism of PCB toxicity. Further, other chlorinated compounds have been shown to inhibit VMAT2 activity, including heptachlor epoxide and DDE (metabolites of heptachlor and DDT pesticides, respectively) (Hatcher et al., 2008b; Miller et al., 1999a). The effect of these chlorinated compounds on VMAT2 activity raises concerns as to the ability of other chlorinated compounds found in the environment to also affect VMAT2 activity. The endogenous iodinated thyroid hormones thyronamines also inhibit VMAT2 activity (Snead et al., 2007). Indeed, inhibition of VMAT2 by endogenous compounds may be a normal part of neurophysiology. However, unregulated inhibition by environmentally-persistent halogenated compounds represents a great public health concern. Therefore, other halogenated compounds in the environment should be screened for their ability to affect VMAT2 activity.

Reduced Storage of Monoamines Improves Glucose Tolerance and Fasting Glucose in Aging Mice

We show that VMAT2 LO mice have reduced VMAT2 expression in the pancreas and reduced dopamine and norepinephrine levels in the pancreas (Figures 3.2 and 3.4). VMAT2 is expressed in both the exocrine and endocrine pancreas where both insulin-containing and non-insulin cells express VMAT2 in the islet (Figure 3.3). Although both VMAT2 WT and LO mice

have normal fasting glucose levels during early adulthood, VMAT2 WT mice begin to show signs of glucose intolerance by 12 months of age (Figure 3.5 and 3.6). VMAT2 LO mice do not show these alterations even at 24 months of age. Additionally, GSIR is increased in VMAT2 LO mice (Figure 1.8 and 3.7). Therefore, loss of VMAT2 prevents the development of age-associated impairment of glucose homeostasis. These effects are consistent with the acute effects of TBZ treatment in streptozocin-induced diabetic rats (Raffo et al., 2008).

α-Synuclein Increases VMAT2-Mediated Transport of Dopamine

Here, evidence is presented showing that α-syn expressed in dopamine neurons of the human SNpC colocalizes to areas within these neurons expressing both TH and VMAT2 (Figure 4.1). Our data from cultured nigral neurons show colocalization between TH and α-syn supporting reports that TH and α-syn interact *in vivo* and *in vitro* (Figure 4.3). Recently, TH has also been shown to coimmunoprecipitate with VMAT2 from cultured PC12 cells and rat brain lysates. Our immunohistochemical data from both brain and cultured neurons support the model that TH is found at synaptic vesicles where loading of dopamine can occur in α-syn-regulated fashion.

TBZ-sensitive dopamine uptake is directly measured in our experiment demonstrating that α-syn increases VMAT2-specific uptake of dopamine. ATP is supplemented at physiological conditions during uptake in our experiment. Therefore, ATP concentrations are not subject to the effects of α-syn on mitochondrial function and ATP production. Thus, dopamine uptake is dependent on VMAT2 protein expression or transporter function (i.e., substrate recognition or transporter velocity). VMAT2 protein expression is unaffected by α-syn in our experiments as measured by ^{3}H-DTBZ binding and Western analyses (Figure 4.6). α-Syn has no effect on VMAT2 affinity for dopamine (K_M) with 5 minutes of uptake (Table 4.1). However, α-syn increases the velocity of TBZ-sensitive dopamine transport (Figure 2.5). The fold increase in

velocity of VMAT2 is similar to that seen by coexpression of the CAPS 1 and 2 proteins (Brunk et al., 2009). Additionally, α-syn is localized to the intravesicular lumen of synaptic vesicles (Lee et al., 2005). Previous studies have shown that $G_{o2}\alpha$ and $G_i\alpha$ interaction with VMAT2 via the first intraluminal loop inhibits VMAT2 activity in monoamine preloaded vesicles (Brunk et al., 2006). While CAPS may be involved, the mechanism underlying this regulation is unknown. Perhaps α-syn plays a role in mediating this effect as both CAPS and α-syn proteins are known to play a role in SNARE assembly (Burre et al., 2010; Daily et al., 2010; James et al., 2010; James et al., 2009).

We show here both a functional and physical interaction between VMAT2 and α-syn. These data demonstrate that α-syn plays a role in optimizing VMAT2 activity supporting the hypothesis that α-syn is a critical regulator of dopamine homeostasis. Interestingly, mutant A53T α-syn behaves similarly to WT α-syn in our experiment. There is no evidence of aggregation by α-syn staining (Figure 4.4) nor by thioflavin-S staining (data not shown) nor any evidence of overt cell toxicity in our experiments.

Potential Role for α-Syn in C-Terminal-Mediated Trafficking of VMAT2 to Vesicles.

α-Syn is a soluble cytosolic protein and can transiently associate with synaptic vesicles (Maroteaux et al., 1988). VMAT2 localizes to both SSVs and LDCVs in the presynaptic axon terminal or tubulovesicular structures in the dendrites and cell body (Nirenberg et al., 1995) while α-syn also interacts with both LDCVs and SSVs in neurons (Berg et al., 2000). These findings are consistent with our observations in both striatal fractionation studies and immunofluorescent staining in cultured neurons (Figure 4.2 and 4.3). We show that α-syn interacts with VMAT2's C-terminus which plays a critical role in trafficking (Figure 4.7). The C-terminus is a critical regulator of VMAT2 and mutations in the region can completely alter or prevent VMAT2 localization to mature SSVs and LDCVs (Krantz et al., 1997; Waites et al., 2001; Yao et al., 2004). Previous studies from cell cultures have implicated α-syn in regulation of the secretory

pathway (Thayanidhi et al., 2010) and suggested a role as a chaperone through promotion of SNARE assembly (Burre et al., 2010; Chandra et al., 2005).   Thus, α-syn could additionally function as a chaperone and aid in trafficking VMAT2 to both SSVs and LDCVs.   Alternatively, the ability of α-syn to increase VMAT2 activity may occur indirectly by relieving the inhibitory effect that HSP70 chaperone protein exerts on VMAT2 (Hinault et al., 2010; Requena et al., 2009).

Evidence Supporting α-Syn Direct Interaction with VMAT2

Despite previous yeast two-hybrid assay data, coimmunoprecipitation experiments were unable to confirm this interaction.   While α-syn did on occasion appear to coimmunoprecipitate with VMAT2, this effect was not consistently reproducible and control experiments suggested that α-syn protein detected in VMAT2 pull-downs is possibly due to nonspecific binding of α-syn to IgGs and/or Protein A/G agarose beads or due to insufficient washing of beads prior to elution.

Other potential technical problems addressed include epitope competition. The "best" antibody for VMAT2 immunoprecipitation is raised against the C-terminus of VMAT2 where the proposed α-syn interaction exists according to yeast two-hybrid data.   Therefore, it is hypothesized that this antibody may only immunoprecipitate a pool of VMAT2 that is not bound to α-syn because of antibody/α-syn competition for C-terminal binding. Another antibody raised against the vesicular luminal loop of VMAT2 is also used for coimmunoprecitptation experiments; however, immunoprecipitation of VMAT2 with this antibody appears weaker and this antibody does not work for western applications requiring visualization of VMAT2 with the C-terminal epitope antibody.   At the time of these experiments, new lot numbers of the C-terminal antibody did not work for westerns.

To combat VMAT2 antibody issues, coimmunoprecipitations are also performed with N-terminal epitope-tagged VMAT2 using epitope tag-specific antibody for VMAT2. In addition,

salt concentrations in the immunoprecipitation buffer are varied to favor weaker interactions, including using the assay buffer used for uptake experiments. None of these experiments yield clear results. Stably expressing VMAT2 cells transiently transfected with higher amounts of α-syn are also used for immunoprecipitation experiments in order to assure maximal VMAT2 immunoprecipitation; however, these experiments also do not yield evidence of a direct interaction. Since a clear effect is not achieved by traditional methods, crosslinking studies are performed to detect any transient or weak interactions. However, these experiments are limited to non-sulfhydryl crosslinking because α-syn does not contain any cysteine residues and do not yield evidence of a physical interaction. Nonetheless, a functional interaction exists between VMAT2 and α-syn. CAPS proteins also appear to affect VMAT2 independently of a physical interaction with a very similar functional upregulation of VMAT2 activity (40-60% increase in V_{MAX}) as seen in the present study with α-syn (Brunk et al., 2009).

There are several strengths and weaknesses associated with study. Cellular models are useful to study the effect of one protein on another because it is much easier to isolate and control variables that might affect the outcome of experiments. For instance, by performing these experiments on lysates containing vesicles we were able to control for the known effects of α-syn on plasmalemmal monoamine transporters. Since α-syn has been shown to affect the activity of these proteins, uptake in intact cells is extremely difficult to interpret. However, one caveat of ectopic protein expression is that they are not always appropriate to determine the physiological function of proteins. This is particularly the case when the protein's function and toxicity is so tightly linked to its expression.

While the ability to inhibit VMAT2 activity is easily achieved via multiple small molecules and other proteins, the ability to enhance VMAT2 is not easily achieved. Genetic studies have shown that women carrying gain-of-function promoter haplotypes in VMAT2 have a reduced risk of Parkinson's disease suggesting that VMAT2 is protective against Parkinson's

disease (Glatt et al., 2006). Consistent with this hypothesis, increasing VMAT2 activity protects dopamine neurons from both L-DOPA and methamphetamine toxicity through an unknown mechanism (Guillot et al., 2008b; Mosharov et al., 2009). Mechanisms that increase VMAT2 activity offer exciting potential for the development of neuroprotective drugs and deserve further investigation.

A Model for α-Syn and VMAT2 Role in Dopamine Homeostasis.

Together these data support the hypothesis that α-syn plays a critical role in dopamine neuron pathophysiology. Based on our data and others, we are proposing a model for the effect of α-syn on the dopaminergic system. We propose that α-syn responds to a signal that recognizes an elevated cytosolic dopamine level, possibly through α-syn known ability to interact with oxidized dopamine species, as a cellular rheostat. α-Syn decreases TH and AADC activities to reduce cytosolic dopamine levels. α-Syn also increases VMAT2 activity, which sequesters cytosolic dopamine into vesicles where it is more protected from oxidation. This is an attractive model; however, much debate exists surrounding conflicting reports that α-syn both increases and decreases TH, DAT, and VMAT2 activities (Alerte et al., 2008; Cao et al., 2010; Guo et al., 2008; Lee et al., 2001; Lou et al., 2010; Marrachelli et al., 2010; Moszczynska et al., 2007; Nemani et al., 2010; Peng et al., 2005; Perez et al., 2002; Tehranian et al., 2006; Wersinger and Sidhu, 2003; Wersinger et al., 2004; Wersinger et al., 2003a). These differences are most likely the result of experiments performed under different conditions, including α-syn expression levels as suggested in (Perez et al., 2002). Cumulatively, these data support the notion that overexpression of α-syn leads to a loss of soluble, functional α-syn (Perez and Hastings, 2004). However, some studies in α-syn knockout mice do not support a loss of function role of α-syn in dopamine neuron death because loss of α-syn does not alter cytosolic dopamine levels (Mosharov et al., 2006). The effect of α-syn loss of function on dopamine levels are only revealed in aged α-syn knockout mice (Al-Wandi et al., 2010). It may be the case that protein redundancy of other

synuclein proteins in dopamine neurons have a remarkable ability to cope with loss of α-syn function over a short period of time, but over time this disruption of α-syn regulation of dopamine homeostasis leads to dopamine loss. This may play some role in toxicity. Regardless, α-syn (over)expression appears to be the critical for toxicity associated with dopamine neurons.

It is widely believed that α-syn-induced pathology in Parkinson's disease is a byproduct of gain-of function toxicity. However, as α-syn becomes insoluble and aggregates, it may no longer be able to perform its normal cellular duties. Ultimately, decreased functional α-syn and increased dysfunctional α-syn could result in a sustained increase in cytosolic dopamine levels, which would be more susceptible to oxidation. Since oxidized dopamine stabilizes α-syn protofibrils, this could essentially generate a positive feedback loop that would increase α-syn insolubility in the cell and perpetuate α-syn protofibril-induced toxicity in dopaminergic neurons (Asanuma et al., 2003; Bisaglia et al., 2010b; Conway et al., 2001; Follmer et al., 2007; Mazzulli et al., 2007; Mazzulli et al., 2006; Norris et al., 2005; Rochet et al., 2004). α-Syn oligomers form protofibril pores or disrupt membrane bilayers that cause leakage of synaptic vesicles (van Rooijen et al., 2010a; van Rooijen et al., 2010b; Volles and Lansbury, 2002; Volles et al., 2001). Therefore, if α-syn is overexpressed or harbors mutations that increase α-syn insolubility, dopamine storage can be reduced by decreased VMAT2 activity and/or vesicular leakage. Consistent with this hypothesis, overexpression of α-syn by either lentivirus or stable transformation of dopaminergic cells increases cytosolic dopamine, impairs vesicular pH gradients, decreases vesicular dopamine, and decreases dopamine release (Guo et al., 2008; Larsen et al., 2006; Lotharius et al., 2002; Mosharov et al., 2006). These early pathological effects of α-syn dysfunction and impaired dopamine homeostasis are attributed to events that prelude cell death (Cappai et al., 2005; Leong et al., 2009; Mosharov et al., 2009). Thus a combination of loss of function and toxic gain of functional may be responsible for the dopamine neurons demise.

However, some experts in the field suggest that vesicular leakage of dopamine is normal and perhaps even physiologically critical (Eisenhofer et al., 2004b). If this is true, then one might anticipate some regulated form of vesicular leakage to occur. Furthermore, the mechanism by which dopamine would pass across the vesicular membrane into the cytosol is unclear. Reversal of VMAT2 may occur as it does with amphetamine. Passive diffusion of dopamine across the vesicular membrane would be inefficient, but presumably concentration –dependent. Alternatively, pores formed in the vesicular membrane by other proteins may mediate this process. Since studies have shown that α-syn can form pores under laboratory conditions that are kinetically stabilized by dopamine-quinones, it may be possible for this to occur *in vivo* (Conway et al., 2000; Conway et al., 2001; Volles and Lansbury, 2002; Volles et al., 2001). Additionally, α-syn monomers can also permeabilize vesicles *in vitro* when Ca^{2+} levels are low by a detergent-like mechanism (Volles and Lansbury, 2002). Perhaps α-syn regulates vesicular leakage as a part of normal physiology whereby low levels of expression signal increased uptake of dopamine while greater expression promotes vesicle leakage. If α-syn does form pores under physiological conditions, pathophysiological conditions may be a result of unregulated, excessive vesicular leakage caused from pathological levels of oligomeric α-syn. Supporting the idea that α-syn undergoes both regulated and unregulated modification is the discovery that dopamine-quinones modify α-syn by both covalent and non-covalent binding (Bisaglia et al., 2010b). This is an attractive hypothesis that will require much more attention to test.

Can α-Syn Affect VMAT2 Function in the Pancreas?

Additionally, α-syn is expressed in the pancreas. A recent report shows that α-syn is localized to insulin-secreting granules of beta cells and interacts with the K^+-ATP channel that regulates K+ efflux into the beta cell and insulin-containing secretory vesicles (Geng et al., 2010). α-syn knockout mice also have increased insulin release from isolated islets under hypoglycemic and euglycemic conditions. This demonstrates that both α-syn and VMAT2 play a role in

regulating beta cell function in addition to neuronal function. Based on our model, one would anticipate that loss of α-syn from beta cells may decrease VMAT2 activity leading to increased insulin release if α-syn were exerting its regulatory effects through increasing VMAT2 activity and dopamine release. However, α-syn's effects on TH and other beta cell proteins most likely play a role. Future studies investigating dopamine levels, VMAT2 activity, and K^+ currents in α-syn knockout mice may help illuminate a novel signaling mechanism for the regulation of insulin release. Together these data demonstrate an important role for VMAT2 in the regulation of glucose homeostasis.

Final Thoughts

PCBs Are Environmental Toxicants that Impair Dopamine Homeostasis in Multiple Tissues with Implications for Both Neurological and Neuroendocrine Disorders

Here, I have presented evidence that VMAT2 function is regulated by α-syn, a critical protein in Parkinson's disease pathogenesis and that VMAT2 is expressed in monoaminergic tissues of the brain and pancreas. Loss of VMAT2 expression affects monoaminergic homeostasis in both of these organs. Dissecting the relative contribution of brain versus pancreatic or neuronal versus beta cell VMAT2 expression to the regulation of glucose homeostasis is difficult, and contributions of both organ systems most likely play a role in physiological regulation by VMAT2. However, these studies highlight the possibility that this largely considered neuronal protein may have critical functions outside of the neuron. I provide evidence for the first time that VMAT2 protein loss in the pancreas can lead to dramatically reduced catecholamine levels.

I have also provided direct evidence for the first time that PCBs can in fact alter glucose homeostasis in an animal leading to changes that are known to predispose individuals to develop diabetes. Since PCBs inhibit VMAT2 and loss of VMAT2 also affects glucose homeostasis, these studies highlight the novel contribution of VMAT2 and monoamines in glucose homeostasis (Figures 5.1, 5.2, and 5.3). These data also beg the question "are Parkinson's disease patients with increased PCB serum levels at a higher risk of diabetes than those patients with low levels of PCB and vice versa?" "If so, how does dopamine replacement therapy affect their glucose status?" Together this body of work proves to be an important addition towards understanding the complex interaction between toxicant exposures, neurochemistry, and disease.

Figure 5.1: PCBs and Monoaminergic Dysfunction as Related to Parkinson's Disease and Diabetes Mellitus. This model proposes that PCBs act via monoaminergic (VMAT2) dysfunction to promote Parkinson's disease and diabetes mellitus pathology. Additionally, α-syn may affect this model via monoaminergic dysfunction (VMAT2) to partially explaining the role of α-syn in Parkinson's disease while proposing a new role for VMAT2 in glucose homeostasis (diabetes mellitus). This model may in part explain the proposed association between Parkinson's disease and diabetes mellitus comorbidity.
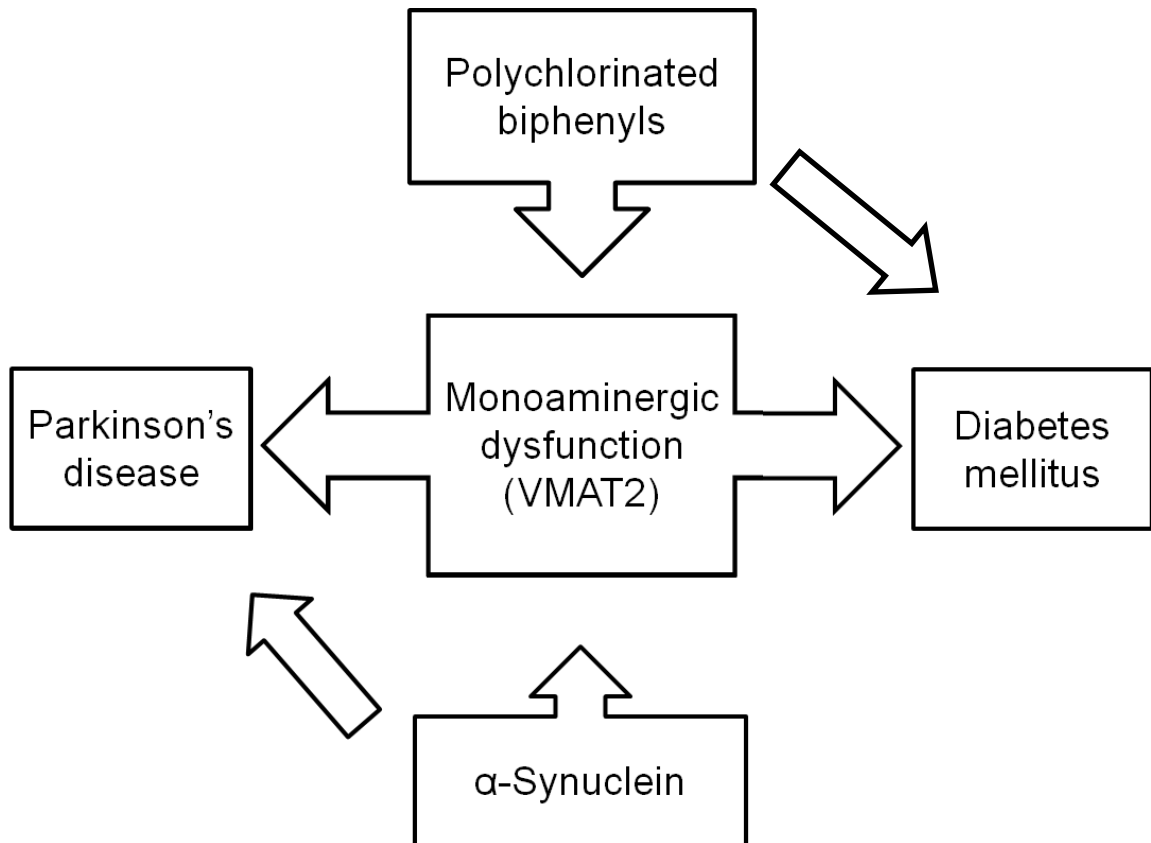
Figure 5.2: Proposed Mechanism of PCB-mediated Effects on Glucose Homeostasis. Since beta cells corelease dopamine with insulin upon glucose stimulation, local action of dopamine on dopamine receptors can act as feedback inhibition of insulin release. PCBs inhibit VMAT2 in isolated vesicles and reduce dopamine levels in the pancreas leading to increased glucose-stimulated insulin release. However, PCBs have been shown to act directly on adipocytes to affect insulin sensitivity. AhR and estrogen sensitive effects combined with dopaminergic effects lead to impaired glucose tolerance.

Increased Insulin Release
Estrogenic/AhR Effects
Increased Insulin
Resistance in
Females

Tyrosine

L-DOPA

Dopamine

Beta Cell

VMAT2

Monoamine
Receptors

Insulin

PCB

Ca^{2+} channel

Ca^{2+}

GLUT-2

Glucose

PCB

Adipocyte
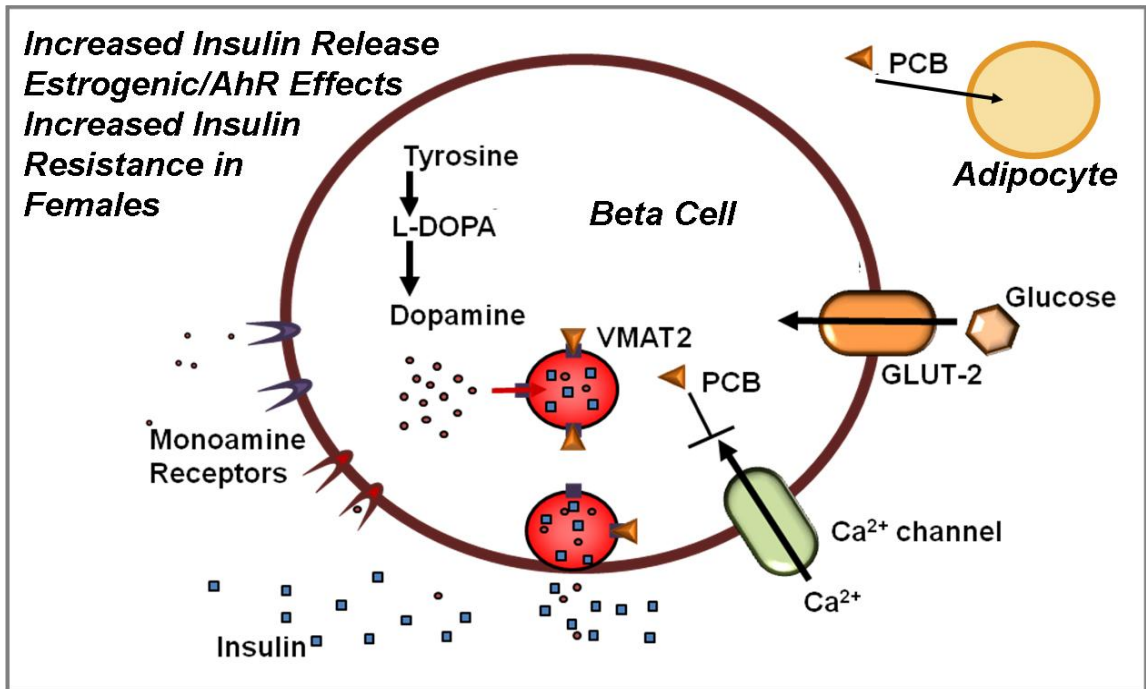
Figure 5.3: Proposed Mecanism of VMAT2 Inhibiton-Mediated Effects on Glucose Homeostasis. Since beta cells corelease dopamine with insulin upon glucose stimulation, local action of dopamine on dopamine receptors can act as feedback inhibition of insulin release. VMAT2 inhibition reduces dopamine levels in the pancreas leading to increased glucose-stimulated insulin release.

Increased Insulin Release
Decreased Blood Glucose

Beta Cell

Tyrosine

L-DOPA

Dopamine

Glucose

GLUT-2

Monoamine
Receptors

VMAT2

Ca²⁺ channel

Insulin

Ca²⁺
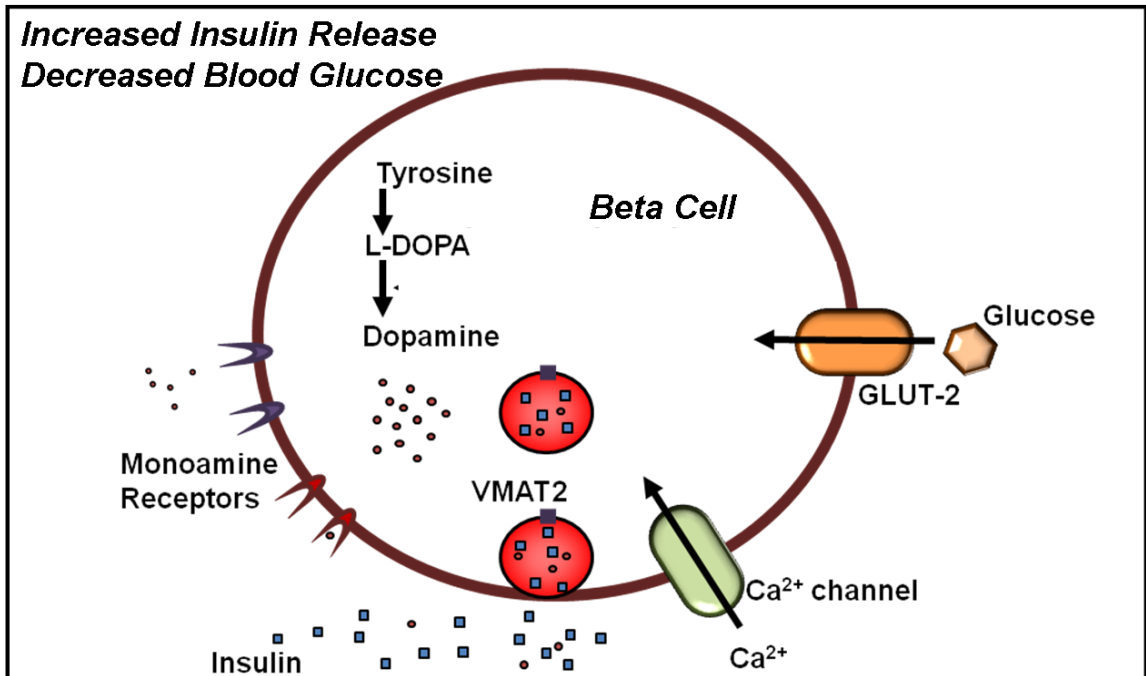
Appendix

Vitamin D Depletion Does Not Exacerbate MPTP-Induced Dopamine Neuron Damage in Mice

Abstract

Recent clinical evidence supports a link between vitamin D insufficiency (serum 25-hydroxyvitamin D (25(OH)D) levels <30 ng/mL) and Parkinson's disease. To investigate the effect of vitamin D depletion on neuronal susceptibility to toxic insult, we induced a state of vitamin D insufficiency in mice and then challenged them with the dopaminergic neurotoxin 1-methyl-4-phenyl-1,2,3,6-tetrahydropyridine (MPTP). We found there was no significant difference between control and vitamin D-deficient animals in striatal dopamine levels or dopamine transporter and tyrosine hydroxylase expression after lesioning with MPTP. Additionally, we found no difference in nigral tyrosine hydroxylase expression. While other studies have indicated that increasing vitamin D levels may provide a protective effect against neurotoxic insult, these data suggest that depleting serum vitamin D has no effect on the vulnerability of nigral dopaminergic neurons to lesion in this model system of parkinsonism and raise the question of whether vitamin D insufficiency is causal or simply a byproduct of disease state and its role in neuroprotection.

Introduction

Parkinson's disease is a progressive, neurodegenerative disease affecting approximately 1% of individuals over the age of 65 (Hindle, 2010). Several studies have suggested a role of vitamin D deficiency in the pathogenesis of Parkinson's disease (Knekt et al., 2010). Recently, we have shown that vitamin D insufficiency is present at diagnosis of Parkinson's disease in the DATATOP cohort (Evatt et al., 2011). Also, we demonstrate that patients with Parkinson's disease were more likely to have vitamin D insufficiency than either healthy age-matched controls or patients with another neurodegenerative disease (Alzheimer's disease) (Evatt et al., 2008). Additionally, certain vitamin D receptor polymorphisms are risk factors for Parkinson's disease (Butler et al., 2011; Kim et al., 2005). Vitamin D concentrations tend to be lower in patients with more advanced disease, suggesting that as patients' mobility declines so do vitamin D levels or vice versa (Sato et al., 1997; Sato et al., 2005). However, whether vitamin D deficiency is causal or merely correlative remains poorly understood.

While it is well known that Vitamin D plays a critical role in the maintenance of bone health by optimizing calcium homeostasis, vitamin D may also play a role in the homeostasis of the neuronal populations affected in Parkinson's disease. Vitamin D receptors and 1-alpha hydroxylase enzyme (activating enzyme for vitamin D hormone) are expressed throughout the human brain, but are particularly enriched in the large (possibly dopaminergic) neurons of the substantia nigra (Eyles et al., 2005). Together these findings have led to speculation that vitamin D deficiency may leave nigrostriatal neurons more vulnerable to insult (Evatt, 2010; Newmark and Newmark, 2007). Indeed, several lines of evidence from animal and cell culture studies have supported this hypothesis, including the finding that pre-treatment with vitamin D protects dopaminergic neurons from 6-hydroxydopamine and N-methyl-4-phenylpyridinium (MPP+) toxicity (Shinpo et al., 2000; Wang et al., 2001). The goal of this study was to determine if

vitamin D deficiency would similarly render mice more vulnerable to insult by the dopaminergic neurotoxin 1-methyl-4-phenyl-1,2,3,6-tetrahydropyridine (MPTP).

Materials and Methods

Animals and behavioral testing

All animal procedures were conducted in accordance with the National Institutes of Health *Guide for Care and Use of Laboratory Animals* and were approved by Emory University Institutional Animal Care and Use Committee for these specific experiments. Retired breeder male C57Bl/6J mice were purchased from Jackson Laboratory. VMAT2 WT and LO mice have been previously described (Caudle et al., 2007; Mooslehner et al., 2001). Mice were individually housed on a 12 hour light: 12 hour dark cycle with ultraviolet-free bulbs and were given food and water *ad libitum*. Mice were randomly assigned to either the control or depleted group. Control mice were fed vitamin D control rodent chow (Harlan Teklad Catalog # TD.89124) while depleted mice were fed vitamin D depleted rodent chow (Harlan Teklad Catalog # TD.89123). Under these conditions, the only source of vitamin D for laboratory mice is via the diet. A diagram of the study design can be found in the supplementary materials. (Figure A.1.)

Mice received daily subcutaneous injections at the nape of the neck of either phosphate-buffered saline (PBS) or 15mg/kg of 1-methyl-4-phenyl-1,2,3,6-tetrahydropyridine (MPTP-HCl salt Sigma-Aldrich, St. Louis, MO) in PBS for 4 days. Mice were allowed to recover for 7 days after the last MPTP dose. Mice were sacrificed by either live decapitation for tissue collections or anesthetized by isofluorane and transcardially perfused with PBS followed by 4% paraformaldehyde in PBS (PFA).

Motor Behavioral Assessment by Forepaw Stride Length

To determine if vitamin D depletion affects motor behavior, forepaw stride length was measured. Individually housed mice were allowed to acclimate to their home cage for a minimum of three days prior to assays. Each mouse was transferred briefly to a novel cage. The home cage was turned on its' side at the end of a 2 inch wide by 14 inch long track with white paper lining the bottom. The mice were briefly suspended by the tail over a tray of nontoxic, black ink so the mice could ink their forepaws. The mice were then place at the beginning of the track opposite their home cage. The mice were allowed to walk to their home cage. Stride length was only measured as a minimum of 4 uninterrupted strides. If the mouse paused during the procedure, the mouse was not allowed to reach its' home cage and was put back in the novel cage to repeat the procedure. If a mouse failed to complete the task again, it was excluded from the behavioral assessment. Stride lengths were scored as the distance between forepaw pad to forepaw pad. The average of at least 4 strides was taken for each mouse.

When vitamin D depletion was confirmed, mice were trained daily on the task for 5 days. On the 6th day, forepaw stride lengths were collected for pretreatment baseline measures. Mice then received daily subcutaneous injections of either Phosphate Buffered Saline (PBS) or 15mg/kg of 1-methyl-4-phenyl-1,2,3,6-tetrahydropyridine (MPTP-HCl salt used from Sigma) in PBS for 4 days. Mice were allowed to recover for 7 days. On the 6th day of recovery, mice received an additional day of reinforcement training on the forepaw stride length task. On the 7th day, forepaw stride length measures were taken.

Vitamin D Determination

C57Bl/6J mice were subjected to the control or vitamin D-deficient diet for 6 weeks prior to MPTP challenge. Before MPTP challenge, blood was collected into a BD Microtainer® Serum Separation Tube from the lateral tail vein without restraint. Blood was held on ice for 10 minutes and then centrifuged at 10,000 x g. Serum 25(OH)D levels were assayed by 25(OH)D

Direct EIA kit (Immunodiagnostic Systems, Fountain Hills, AZ) per manufacturer's protocol to confirm depletion. Alternatively, tail vein blood was collected from VMAT2 WT and LO mice for 25(OH)D measures.

Western analyses of striatal dopaminergic markers

Tissues were analyzed by Western blotting technique as previously (Caudle et al., 2007; Miller et al., 1997). Unilateral striatum was homogenized with a tissue tearer (Biospec Products, Inc.) in a homogenization buffer of 0.32 M sucrose, 5 mM HEPES pH 7.4 with 1X protease inhibitor cocktail (Sigma Aldrich). Homogenates were centrifuged at 1200 x g for 5 minutes at 4°C. The post-nuclear lysate was collected and centrifuged at 20,000 x g for 45 minutes at 4°C. The resulting synaptosomal pellet was resuspended in 100 µl of homogenization buffer. Protein concentrations were determined by BCA protein assay (Thermo Scientific.) 20 µg of protein lysates was electrophoresed on a NuPAGE 10% Bis-Tris Gel (Invitrogen) and then transferred to a 0.2µm PVDF membrane (Invitrogen). Blots were blocked in 8% instant milk powder solution (Carnation) for 1 hour at 18-22°C. Primary antibodies (rabbit polyclonal anti-TH and rat polyclonal anti-DAT, Chemicon, Temecula, CA and mouse anti-tubulin, Sigma-Aldrich, St. Louis, MO) were incubated with blots at 4°C for 12-18 hours. Upon several washes, a HRP-conjugated secondary antibody (Sigma) was incubated with the blots for 1 hour at 18-22°C. Blots were washed and then developed with the Super Signal Dura substrate system (Thermo Scientific.) Blots were then imaged immediately using a Fluorchem Imaging system (Alpha Innotech). Densitometric analyses were performed using the accompanying software.

HPLC Analyses of MPP$^+$, Dopamine and Metabolite Levels

An Agilent 1100 Series Capillary HPLC system coupled with an ESA Coulochem III electrochemical detector was used for separation and quantification of dopamine, 3,4-dihydroxyphenylacetic acid (DOPAC) and homovanillic acid (HVA). Briefly, the striatal region

of each mouse was weighed and homogenized using a sucrose media (0.32 M sucrose, 10 mM Tris base, 0.5 mM EDTA) at 10% w/v. A 100 µL aliquot was taken and proteins were precipitated by addition of 5 µL perchloric acid. Samples were then spun at 10,000 x g for 3 minutes to pellet precipitated proteins. 10 µL of each sample solution was injected and separated using a Thermo Scientific C18 Aquasil column (2.1 x 150 mm, 100 Å). Mobile phase consisted of 50 mM citric acid, 1.8 mM sodium heptane sulfonate, 0.2% trifluoroacetic acid (v/v),pH 3.0 (A) and acetonitrile (B). Gradient conditions were as follows: 3% B at 0 min, 3% B at 8 min, 18% B at 19 min, 3% B at 20 min and 3 % B at 35 min using a flow rate of 250 µL/min. dopamine, DOPAC and HVA were detected using electrodes set at potentials of -150 and +300 mV. Calibration curves were generated using standards (i.e., dopamine and HVA) and utilized to convert peak area to concentration units.

MPP+ levels were measured similarly as described previously (Richardson et al., 2006; Richardson et al., 2008). Briefly, upon depletion mice were given a single dose of MPTP (20mg/kg, s.c.) and sacrificed 90 minutes later for striatal dissection as described above. Bilateral striata were used for detection. MPP+ iodide, acetonitrile ($\geq$ 99.9% HPLC grade), sodium trichloroacetate (TCA, 97.0%) and potassium phosphate monobasic (($\geq$ 99.0%) were purchased from Sigma Aldrich (St. Louis, MO). For analysis of MPP$^+$ levels, striata were sonicated (Branson S-250A with a double stepped microtip; Danbury, CT) in 5 volumes of 5% TCA and centrifuged for 10 min at 14,000 g. MPP$^+$ levels were determined by analysis of supernatant using an Agilent Model 1200 HPLC equipped diode array detector operated at a wavelength of 290 nm. Separation was achieved on a reverse phase Altima C18 column (5 um, L=150mm, ID=4.6 mm, Catalog No. 88052; Alltech Associates Inc., Deerfield, IL) with a mobile phase consisting of 89% 50 mM KH_2PO_4 and 11% acetonitrile. MPP$^+$ was identified by comparison of retention time with known standards and concentrations were calculated from a 6-point standard curve of known concentrations of MPP$^+$. Protein concentrations were determined by Bradford Assay.

Immunohistochemistry of striatal and nigral dopaminergic markers

Perfused brains were kept at 4°C for 12 hours in 4% PFA. Brains were then transferred to 30% sucrose and stored at 4°C. Brains were sliced at 40 μm (Microm HM450). Sections were transferred to Tris-buffered saline and stored at 4°C until use. Immunohistochemical staining was performed. Briefly, thin sections were washed six times in 1X TBS to remove all traces of PFA. Thin sections were incubated with a rat monoclonal anti-dopamine transporter (DAT) (1:750; Chemicon), or a rabbit polyclonal anti-tyrosine hydroxylase (TH) antibody (1:2000; Chemicon) overnight at 4°C and then incubated in a biotinylated-goat ant-rat or goat anti-rabbit secondary antibody (Jackson Immunoresearch) for 1 hour at room temperature. Visualization was performed using 0.03% 3,3'-diaminobenzidine (Sigma Aldrich, St Louis, MO) at room temperature.

Statistical Analyses

All statistical analyses were performed using Graph Pad Prism 5.0. Student t-tests were performed for initial two group comparisons with significant values reported as $p < 0.05$. Two-way AVOVA analyses were performed on all multi-group comparisons with Bonferroni post-hoc tests to determine significant interactions. Significant values are reported as $p < 0.05$.

Results

Short Term Vitamin D depletion had no effect on body mass or behavior of the mice

Since a laboratory animal's sole source of vitamin D is dietary, mice were merely transferred from standard rodent chow (Purina) to a vitamin D deficient diet to deplete serum 25(OH)D levels. There was no difference between starting body mass in the control and Vitamin D depletion groups prior to changing their chow (mean body mass ± SEM- control chow group- 30.44 ± 0.741 grams; depletion chow group- 30.60 ± 0.754 grams) (Figure A.2A). While both groups of mice gained body mass on the new chow formulation, no differences were observed

between control-fed and vitamin D depletion chow-fed groups at the time of depletion (mean body mass $\pm$ SEM- control chow group- 34.72 $\pm$ 1.1 grams; depletion chow group- 33.37 $\pm$ 1.1 grams) (Figure A.2B). After 6 weeks of depleted chow, serum 25(OH)D levels were depleted by nearly 80% (Figure A.3A). Vitamin D control chow-fed and depletion chow-fed mice had a mean $\pm$ SEM 25(OH)D serum level of 43.9 $\pm$ 0.7 ng/ml and 7.17 $\pm$ 0.4 ng/ml, respectively (n= 6; p<0.0001). Additionally, vitamin D depletion had no effect on forepaw stride length Mean stride lengths (Control Group- 6.28 $\pm$ 0.16 cm; Vitamin D Depletion Group- 6.14 $\pm$ 0.22 cm) (Figure A3.B). Thus, 6 weeks of vitamin D depletion had no overt effect on the mice's health.

Vitamin D depletion did not further exacerbate the effects of MPTP in mice

After depletion was confirmed, the mice were treated with MPTP (4 x 15 mg/kg) to produce a mild lesion resulting in approximately 50-60% reduction of striatal dopamine. This dose was chosen so that exacerbation or protection could be detected in the vitamin D-depleted animals. MPTP lesion was confirmed by measuring changes in dopamine, dopamine metabolites, and markers of dopamine neuron. Striatal dopamine (Figure A4.A) was significantly reduced by 60% in MPTP-lesioned animals as compared to saline-treated animals (Control/Saline- 25.546 $\pm$ 3.6 pmol/mg of protein, Control/MPTP- 10.523 $\pm$ 1.2 pmol/mg of protein, Depleted/Saline- 32.735 $\pm$ 1.4 pmol/mg of protein, Depleted/MPTP- 13.369 $\pm$ 5.0 pmol/mg of protein; n=4). While vitamin D depleted animals trended towards having higher dopamine, there was no significant difference in striatal dopamine levels observed between Vitamin D control chow- fed and depleted chow fed animals with or without MPTP lesion.

MPTP treatment did not significantly affect forepaw stride length measured at the end of the study (Control Saline Group- 6.46 $\pm$ 0.26 cm; Control MPTP Group- 6.47 $\pm$ 0.26 cm; Vitamin D Depletion Saline Group- 7.02 $\pm$ 0.29 cm; Vitamin D Depletion MPTP Group- 5.97 $\pm$ 0.25 cm;

n=7-9.) (Figure A.4B). Interestingly, the difference within the vitamin D depletion groups is significant (*, p<0.05).

A significant 46% and 49% reduction in striatal tyrosine hydroxylase and dopamine transporter protein levels were observed with MPTP lesion, respectively (Figures A.5); however, vitamin D depletion did not exacerbate the total loss of terminal markers in this paradigm. Additionally, immunohistochemical analyses revealed a dramatic reduction in both of the striatal TH (Figure A.6A) and DAT levels (data not shown) and the nigral TH levels (Figure A.6B) of MPTP lesioned animals that were not further exacerbated by Vitamin D depletion. Further studies in a separate cohort of mice confirmed that MPTP metabolism as measured by MPP+ levels is not altered by vitamin D depletion (Figure A.7).

We also determined whether dopaminergic neuron damage affected Vitamin D serum levels. 25(OH)D serum levels were not affected in animals with MPTP lesion within ten days of lesion (Figure A.8). In addition, lifelong deficiency in dopamine levels has no effect on 25(OH)D levels (Figure A.9). There are no differences in serum 25(OH)D levels in VMAT2 WT and LO mice in young or old mice. Interestingly, older mice had significantly higher serum 25(OH)D levels than younger mice (***, p<0.0001).

Discussion

Until recently the role that vitamin D plays in the pathogenesis of disease (with exception to bone and tooth health) has been understudied and underappreciated. Because epidemiological data have suggested a link between vitamin D status and Parkinson's disease, we sought to investigate the effects of vitamin D depletion in a mouse model of parkinsonism. We found that while we are able to effectively deplete mice of serum vitamin D and lesion animals with MPTP, there was no relationship between vitamin D serum levels and the magnitude of MPTP injury. We found no significant difference between MPTP lesioned animals regardless of vitamin D

status as measured by striatal and nigral dopamine neuronal markers, striatal dopamine, and gait analysis.

MPTP is a reliable toxicant used to selectively lesion dopamine neurons and is the only toxicant model available for animal studies that also undoubtedly causes a parkinsonian syndrome in humans (Ballard et al., 1985). The MPTP dosing paradigm used in this study is designed to cause a moderate loss of dopamine and terminal markers that does not induce behavioral deficits, i.e. stride length. Therefore, any effect of vitamin D on MPTP susceptibility should be revealed. However, there are some limitations to this study. First, while the MPTP mouse is the most common animal model of Parkinson's disease, it is limited by several factors including peripheral and central metabolism of MPTP to MPP+, expression of DAT on the surface of target cells, and the inability to reproduce the non-motor and progressive symptoms of the disease. We did not detect any effect of vitamin D depletion on MPTP metabolism or DAT levels under our experimental conditions. It is possible that the dosage of MPTP used in this study was simply too great and masked any beneficial effects of vitamin D; however, a previous unpublished pilot study from our laboratory using a milder 4 x 10 mg/kg MPTP dosing paradigm also revealed no effects of vitamin D depletion on MPTP toxicity (data not shown). Perhaps other models of Parkinson's disease (such as a transgenic A53T α-synuclein mouse may yield different results (Chesselet, 2008). However, chronic dopamine depletion as seen in VMAT2 LO mice did not affect serum 25(OH)D levels (Figure A.9). This suggests that dopamine status does not influence vitamin D status. Certainly in human populations, vitamin D status can become and remain low over a lifetime. Therefore, our short term (six week) depletion which could be considered equivalent to the course of only a few years in a human may have not reproduced any changes that take place in neurons under chronic deficiency states. Additionally, this study was performed in male mice only. In the experimental autoimmune encephalomyelitis model of multiple sclerosis, vitamin D supplementation was shown to protect in females, but not in males (Spach

and Hayes, 2005). This suggests that there may be some relationship between vitamin D, gender, and toxicity that would not be addressed in our model.

In humans, midlife vitamin D insufficiency is associated with higher Parkinson's disease risk while higher serum levels are associated with reduced risk of Parkinson's disease (Knekt et al., 2010). Whether these effects are causal or correlative remain unknown, but it has been proposed that vitamin D plays a protective role in the health of the neurons affected in Parkinson's disease and that lower serum levels of vitamin D predispose these neurons to damage. Indeed, pretreatment of rat mesencephalic cultures with 1,25-dihydroxyvitamin D (the active form of the hormone) confers resistance of dopaminergic neurons to MPP^+ (the active form of the toxin) (Shinpo et al., 2000). More recently, it was shown that administration of 1,25-dihydroxyvitamin D partially restored TH expression in the nigra of 6-hydroxydopamine lesioned rats (Sanchez et al., 2009). Vitamin D could be protective by several distinct mechanisms, including stimulating the action of growth factors, acting as an antioxidant, or increasing glutathione production (Eyles et al., 2009; Lin et al., 2005; Shinpo et al., 2000). Interestingly, we did not find the inverse that short term 25(OH)D depletion (for eight weeks) made dopaminergic nigral neurons more susceptible to insult by MPTP. Still, additional studies are warranted to explore the role of vitamin D deficiency on the long term health of dopaminergic neurons.

Vitamin D deficiency during development has profound effects on brain volume, cell proliferation, and cortical thickness in rats (Eyles et al., 2009). Additionally, drug-induced hyperlocomotion, increased striatal DAT, and decreased dopamine turnover are seen in rats developmentally deficient in vitamin D (Kesby et al., 2006; Kesby et al., 2010). This suggests that early deficiency can cause permanent changes to the dopaminergic pathways that may persist into adulthood (Tekes et al., 2009b) and future generations (Tekes et al., 2009a).

Conclusions

Our data suggest that short term vitamin D depletion does not render dopamine neurons more susceptible to the neurotoxin, MPTP as we initially hypothesized. Rather, we propose that as demonstrated in previous studies vitamin D acts as a neuroprotectant and that supplementation of vitamin D, when deficient, may help spare further neuronal loss in patients or perhaps protect more sensitive populations against insult. Further studies are warranted to explore whether long-standing deficiency of vitamin D or gestational vitamin D depletion have a role in the pathophysiology of Parkinson's disease.

Figure A.1: Diagram of Experimental Procedure. On day 1, mice were weighed and randomly assigned to either the control chow or vitamin D depletion chow groups. Mice were weighed weekly to check for changes in body mass. After six weeks, 25-hydroxyvitamin D depletion was confirmed by ELISA assay. Then, mice were trained to learn the forepaw stride length task from days 44-48. On day 49, baseline behavior was measured. On day 50, MPTP injections began. Mice received a daily injection of either PBS or 15 mg/kg MPTP for 4 days. The mice were allowed to recover for 7 days. On day 60, post-MPTP behavior was measured prior to sacrificing the mice.

**Mice begin
depleted chow**

**Mice
depleted**

**MPTP
lesion**

**Sacrifice
mice**

Training

25- hydroxyvitamin D serum levels

Day 1

35

50-53

60
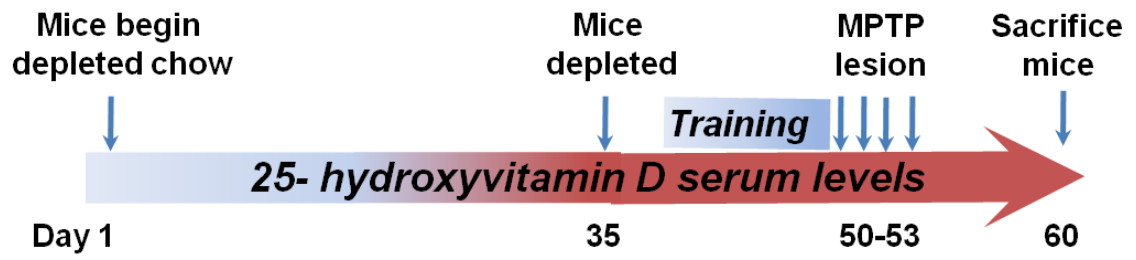
Figure A.2: Vitamin D Depletion Has No Effect on Body Mass. Male retired breeder C57Bl/6J mice were randomly assigned to either the control or depletion group. Control mice were fed vitamin D control rodent chow while depletion mice were fed vitamin D depleted rodent chow. A) Predepletion body mass of mice. There is no difference between Control and Depletion groups prior to switching the rodent chows. B) Body mass after 6 weeks on chow. There is no difference between Control and vitamin D depleted groups after vitamin D depletion; however, both groups gained body mass after being switched to the new chow.

A
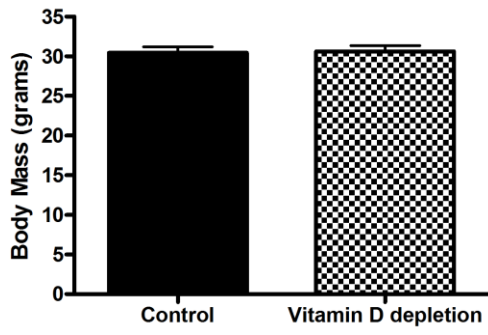
B
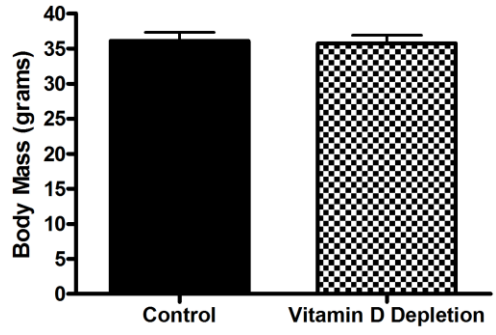
Figure A.3: Short Term Vitamin D Depletion Has No Observable Effect on Mouse Behavior. A) Serum 25(OH)D levels after 6 weeks on either control or vitamin D depletion rodent chow. Results are presented as absolute mean values (ng/ml) $\pm$ SEM for eight animals per group (***$p<0.0001$.) B) Pre-MPTP lesion stride length measures.

A

B
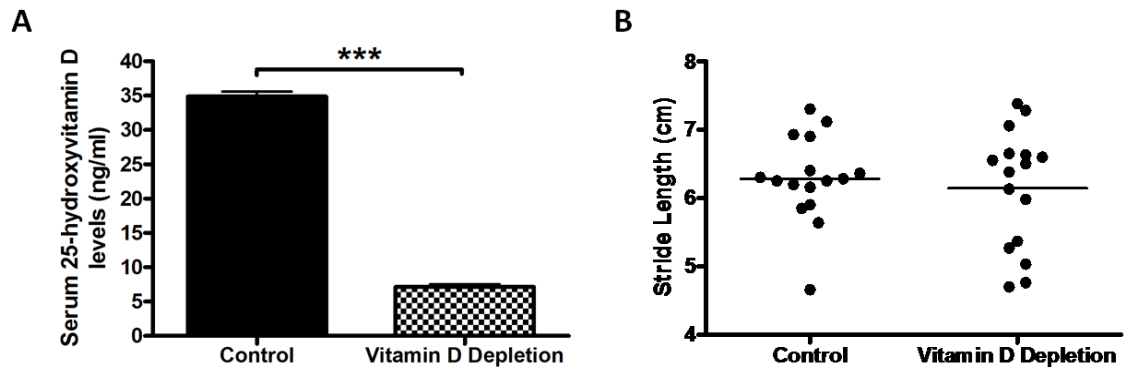
Figure A.4: Behavioral and Neurochemical Effects of Vitamin D Depletion on MPTP susceptibility in mice. A) HPLC analysis of striatal dopamine levels in mice lesioned with MPTP after vitamin D depletion. Results are presented as raw values (pmol/mg protein ± SEM; n=4, ***$p<0.001$). B) Post-lesion stride length was measured. There was no significant difference control and vitamin D depletion group animals with or without MPTP lesion. Interestingly, the difference within the Vitamin D Depletion groups is significant (*, $p<0.05$) with an increase in forepaw stride length in Vitamin D Depleted not treated with MPTP over control animals.

A
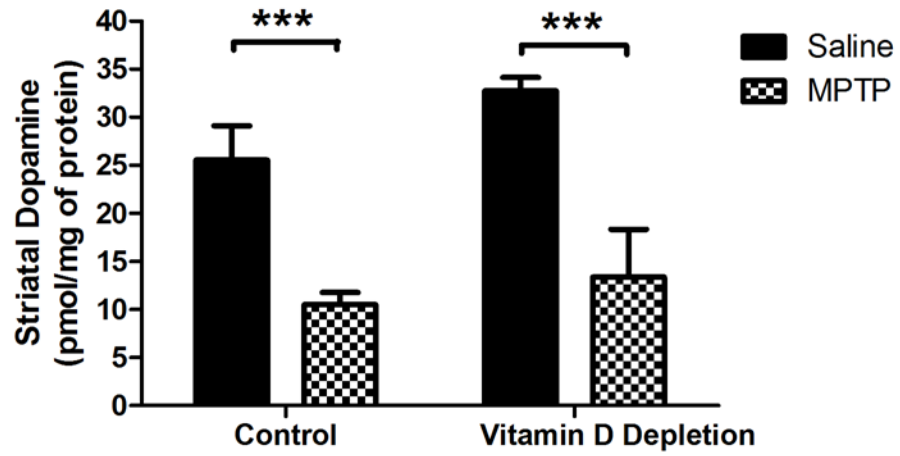
B
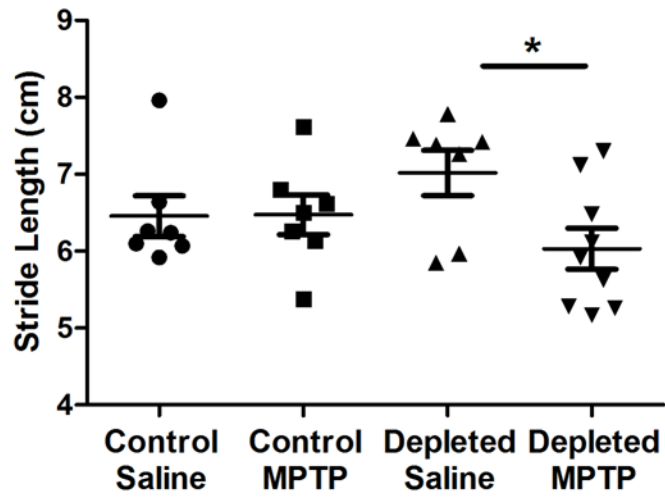
Figure A.5: Effects of Vitamin D Depletion on TH and DAT Expression in MPTP-Lesioned Mice. A) Western analyses of striatal TH and DAT levels after MPTP lesion in vitamin D depletion mice. A representative blot is shown. β-tubulin is shown as a loading control. B,C) Densitometric analyses of striatal TH and DAT are shown (Relative values $\pm$ SEM; n=4, ***p<0.001), respectively.
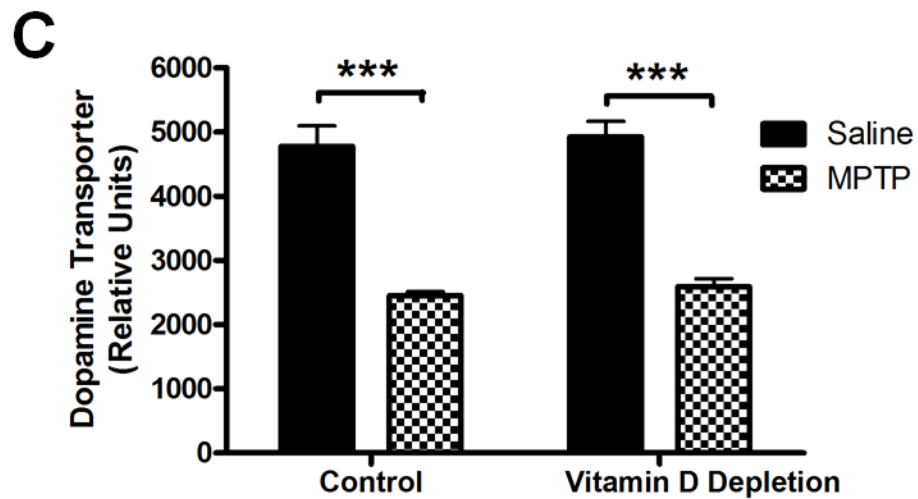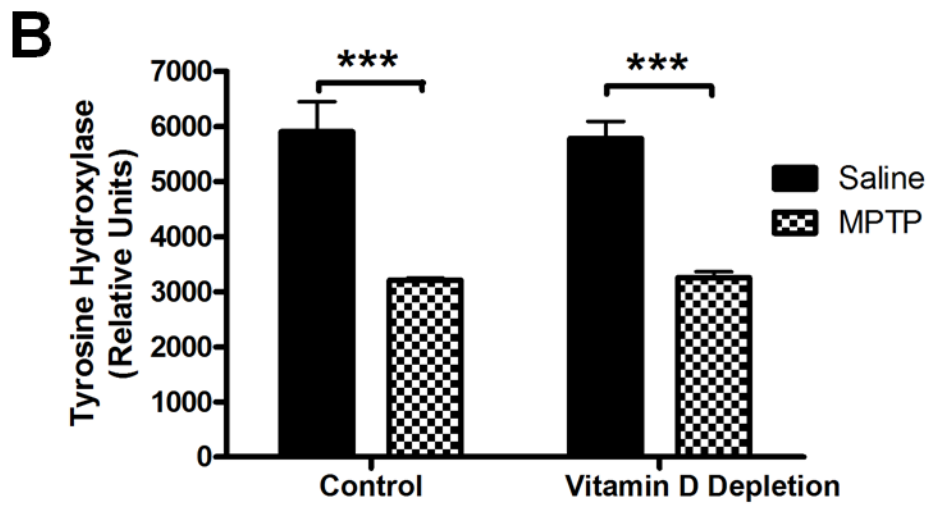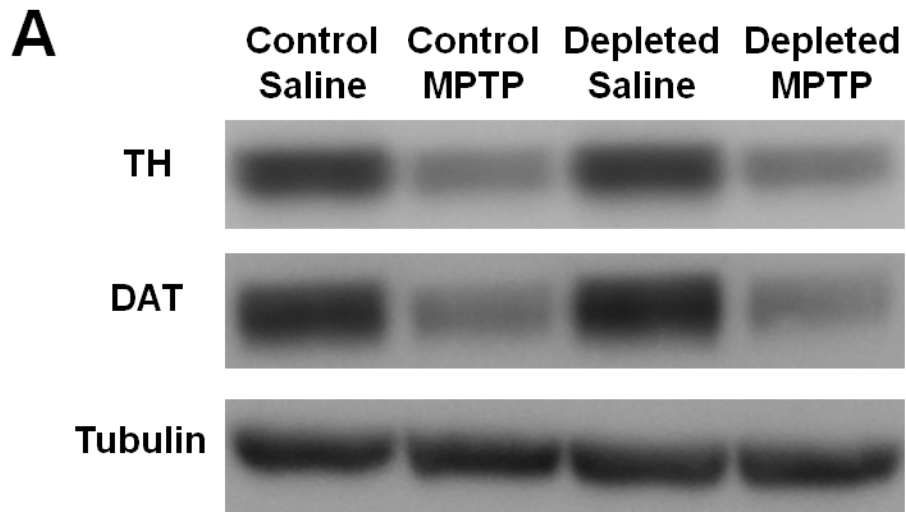
Figure A.6: **Vitamin D Depletion Does Not the Exacerbate Loss of Tyrosine Hydroxylase Staining in the Striatum and Nigra after MPTP Lesion.** A) Representative TH staining of the striatum. B) Representative TH staining of the nigra.
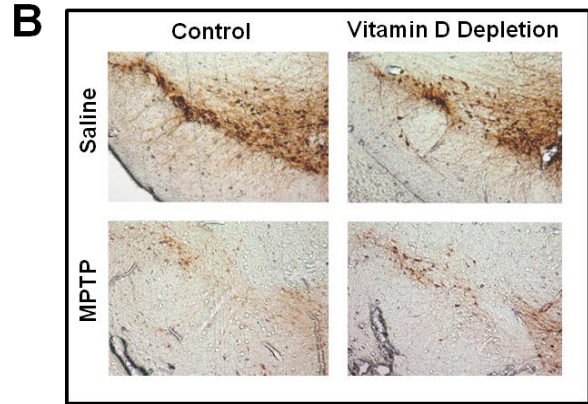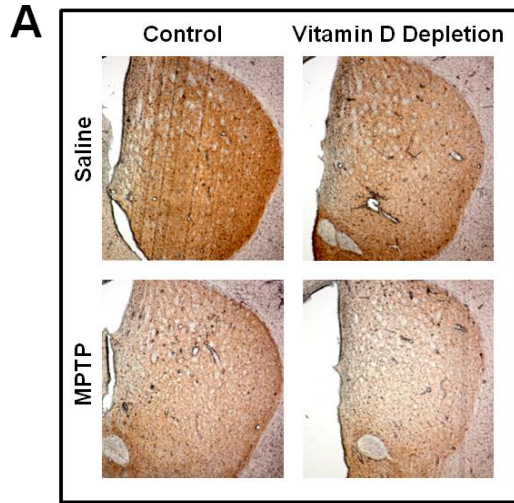
Figure A.7: MPP+ Levels Are Not Altered by Vitamin D Depletion. Mice were fed vitamin depleted chow for 50 days and given a single dose of MPTP (20 mg/kg). MPP+ levels were measured by HPLC.
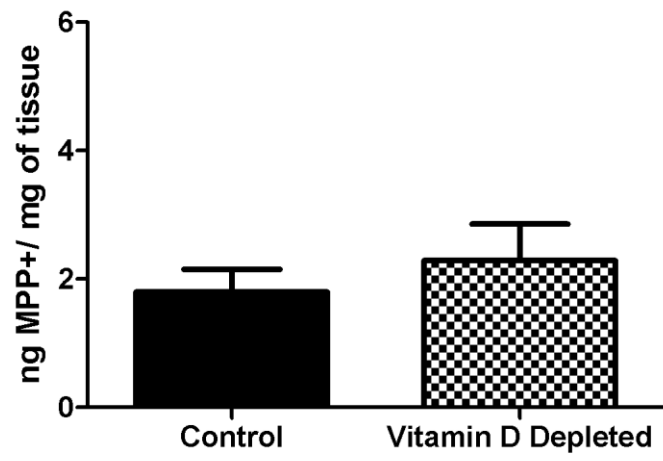
Figure A.8: MPTP Lesioning Does Not Affect Serum 25-hydroxyvitamin D Levels. After MPTP lesion, serum 25-hydroxyvitamin D levels were measured to determine if MPTP lesion had any effect (Control/Saline Group- 40.40 ± 1.1 ng/ml; Control/MPTP Group- 40.60 ± 1.1 ng/ml; Vitamin D Depletion/Saline Group- 6.60 ± 0.7 ng/ml; Vitamin D Depletion/MPTP Group- 5.91 ± 1.4 ng/ml; n=4 (***, $p<0.0001$). There is no effect observed one week after lesioning; however, the effect of MPTP lesion on mice that are lesioned and then allowed to age is unknown. Further research is necessary to determine the effect of MPTP on long term vitamin D status.
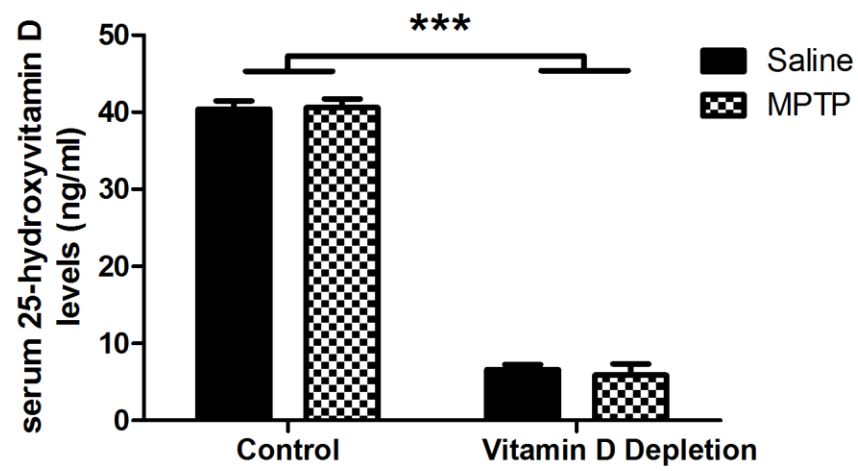
Figure A.9: Serum 25-hydroxyvitamin D Levels Are Not Changed in VMAT2 LO Mice. Serum 25-hydroxyvitamin D levels were measured in both young and old VMAT2 WT and LO mice to determine loss of dopamine has any effect on vitamin D serum levels No differences were observed between WT and LO mice; however, older mice have higher serum 25-hydroxyvitamin D levels than young mice (***, p<0.0001).
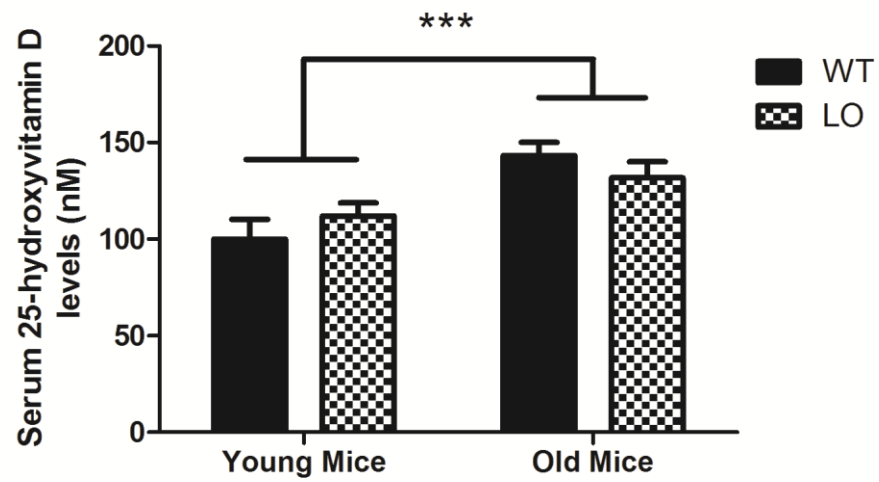
References

Abeliovich A., Schmitz Y., Farinas I., Choi-Lundberg D., Ho W.H., Castillo P.E., Shinsky N., Verdugo J.M., Armanini M., Ryan A., Hynes M., Phillips H., Sulzer D., Rosenthal A. (2000) Mice lacking alpha-synuclein display functional deficits in the nigrostriatal dopamine system. Neuron 25:239-52. DOI: S0896-6273(00)80886-7 [pii].

Adler M.W. (1964) Enhanced Depressant Effect of Tetrabenazine after Repeated Administration. Psychopharmacologia 5:393-6.

Ahren B., Taborsky G.J., Jr. (1988) Effects of pancreatic noradrenaline infusion on basal and stimulated islet hormone secretion in the dog. Acta Physiol Scand 132:143-50.

Ahren B., Ericson L.E., Lundquist I., Loren I., Sundler F. (1981) Adrenergic innervation of pancreatic islets and modulation of insulin secretion by the sympatho-adrenal system. Cell Tissue Res 216:15-30.

Al-Wandi A., Ninkina N., Millership S., Williamson S.J., Jones P.A., Buchman V.L. (2010) Absence of alpha-synuclein affects dopamine metabolism and synaptic markers in the striatum of aging mice. Neurobiol Aging 31:796-804. DOI: S0197-4580(08)00397-7 [pii] 10.1016/j.neurobiolaging.2008.11.001.

Alerte T.N., Akinfolarin A.A., Friedrich E.E., Mader S.A., Hong C.S., Perez R.G. (2008) Alpha-synuclein aggregation alters tyrosine hydroxylase phosphorylation and immunoreactivity: lessons from viral transduction of knockout mice. Neurosci Lett 435:24-9. DOI: S0304-3940(08)00173-0 [pii] 10.1016/j.neulet.2008.02.014.

Alvarez C., Vitalis T., Fon E.A., Hanoun N., Hamon M., Seif I., Edwards R., Gaspar P., Cases O. (2002) Effects of genetic depletion of monoamines on somatosensory cortical development. Neuroscience 115:753-64.

Andreassen O.A., Dedeoglu A., Stanojevic V., Hughes D.B., Browne S.E., Leech C.A., Ferrante R.J., Habener J.F., Beal M.F., Thomas M.K. (2002) Huntington's disease of the endocrine

pancreas: insulin deficiency and diabetes mellitus due to impaired insulin gene expression. Neurobiol Dis 11:410-24. DOI: S0969996102905620 [pii].

Anlauf M., Eissele R., Schafer M.K., Eiden L.E., Arnold R., Pauser U., Kloppel G., Weihe E. (2003) Expression of the two isoforms of the vesicular monoamine transporter (VMAT1 and VMAT2) in the endocrine pancreas and pancreatic endocrine tumors. J Histochem Cytochem 51:1027-40.

Arneric S.P., Chow S.A., Long J.P., Fischer L.J. (1984) Dopamine analog-induced hyperglycemia in rats: involvement of the adrenal medulla and the endocrine pancreas. J Pharmacol Exp Ther 228:551-9.

Arsenescu V., Arsenescu R.I., King V., Swanson H., Cassis L.A. (2008) Polychlorinated biphenyl-77 induces adipocyte differentiation and proinflammatory adipokines and promotes obesity and atherosclerosis. Environ Health Perspect 116:761-8. DOI: 10.1289/ehp.10554.

Arzuaga X., Ren N., Stromberg A., Black E.P., Arsenescu V., Cassis L.A., Majkova Z., Toborek M., Hennig B. (2009) Induction of gene pattern changes associated with dysfunctional lipid metabolism induced by dietary fat and exposure to a persistent organic pollutant. Toxicol Lett 189:96-101. DOI: S0378-4274(09)00255-0 [pii]

10.1016/j.toxlet.2009.05.008.

Asanuma M., Miyazaki I., Ogawa N. (2003) Dopamine- or L-DOPA-induced neurotoxicity: the role of dopamine quinone formation and tyrosinase in a model of Parkinson's disease. Neurotox Res 5:165-76.

Ballard P.A., Tetrud J.W., Langston J.W. (1985) Permanent human parkinsonism due to 1-methyl-4-phenyl-1,2,3,6-tetrahydropyridine (MPTP): seven cases. Neurology 35:949-56.

Barbeau A., Giguere R., Hardy J. (1961) [Clinical experience with tolbutamide in Parkinson's disease]. Union Med Can 90:147-51.

Bargsten G. (2004) Cytological and immunocytochemical characterization of the insulin secreting insulinoma cell line RINm5F. Arch Histol Cytol 67:79-94.

Becker C., Brobert G.P., Johansson S., Jick S.S., Meier C.R. (2008) Diabetes in patients with idiopathic Parkinson's disease. Diabetes Care 31:1808-12. DOI: dc08-0479 [pii]

10.2337/dc08-0479.

Bemis J.C., Seegal R.F. (2004) PCB-induced inhibition of the vesicular monoamine transporter predicts reductions in synaptosomal dopamine content. Toxicol Sci 80:288-95. DOI: 10.1093/toxsci/kfh153

kfh153 [pii].

Bemis J.C., Nazarenko D.A., Gasiewicz T.A. (2005) Coplanar polychlorinated biphenyls activate the aryl hydrocarbon receptor in developing tissues of two TCDD-responsive lacZ mouse lines. Toxicol Sci 87:529-36. DOI: kfi260 [pii]

10.1093/toxsci/kfi260.

Benedict C., Hallschmid M., Hatke A., Schultes B., Fehm H.L., Born J., Kern W. (2004) Intranasal insulin improves memory in humans. Psychoneuroendocrinology 29:1326-34. DOI: 10.1016/j.psyneuen.2004.04.003

S0306453004000526 [pii].

Benedict C., Hallschmid M., Schmitz K., Schultes B., Ratter F., Fehm H.L., Born J., Kern W. (2007) Intranasal insulin improves memory in humans: superiority of insulin aspart. Neuropsychopharmacology 32:239-43. DOI: 1301193 [pii]

10.1038/sj.npp.1301193.

Berg E.A., Johnson R.J., Leeman S.E., Boyd N., Kimerer L., Fine R.E. (2000) Isolation and characterization of substance P-containing dense core vesicles from rabbit optic nerve and termini. J Neurosci Res 62:830-9.

Berglund E.D., Li C.Y., Poffenberger G., Ayala J.E., Fueger P.T., Willis S.E., Jewell M.M., Powers A.C., Wasserman D.H. (2008) Glucose metabolism in vivo in four commonly used inbred mouse strains. Diabetes 57:1790-9. DOI: db07-1615 [pii]

10.2337/db07-1615.

Bielefeldt K., Reis H.E. (1989) [Autonomic neuropathy in diabetes mellitus, chronic renal failure and liver cirrhosis]. Med Klin (Munich) 84:72-6.

Billett E.E. (2004) Monoamine oxidase (MAO) in human peripheral tissues. Neurotoxicology 25:139-48. DOI: S0161-813X(03)00094-9 [pii]

10.1016/S0161-813X(03)00094-9.

Bisaglia M., Mammi S., Bubacco L. (2007) Kinetic and structural analysis of the early oxidation products of dopamine: analysis of the interactions with alpha-synuclein. J Biol Chem 282:15597-605.

Bisaglia M., Greggio E., Maric D., Miller D.W., Cookson M.R., Bubacco L. (2010a) Alpha-synuclein overexpression increases dopamine toxicity in BE2-M17 cells. BMC Neurosci 11:41. DOI: 1471-2202-11-41 [pii]

10.1186/1471-2202-11-41.

Bisaglia M., Tosatto L., Munari F., Tessari I., de Laureto P.P., Mammi S., Bubacco L. (2010b) Dopamine quinones interact with alpha-synuclein to form unstructured adducts. Biochem Biophys Res Commun 394:424-8. DOI: S0006-291X(10)00482-1 [pii]

10.1016/j.bbrc.2010.03.044.

Blackmore C.G., Varro A., Dimaline R., Bishop L., Gallacher D.V., Dockray G.J. (2001) Measurement of secretory vesicle pH reveals intravesicular alkalinization by vesicular monoamine transporter type 2 resulting in inhibition of prohormone cleavage. J Physiol 531:605-17.

Blomqvist M.E., Silburn P.A., Buchanan D.D., Andreasen N., Blennow K., Pedersen N.L., Brookes A.J., Mellick G.D., Prince J.A. (2004) Sequence variation in the proximity of

IDE may impact age at onset of both Parkinson disease and Alzheimer disease. Neurogenetics 5:115-9. DOI: 10.1007/s10048-004-0173-4.

Bohnen N.I., Albin R.L., Koeppe R.A., Wernette K.A., Kilbourn M.R., Minoshima S., Frey K.A. (2006) Positron emission tomography of monoaminergic vesicular binding in aging and Parkinson disease. J Cereb Blood Flow Metab 26:1198-212.

Boller F., Mizutani T., Roessmann U., Gambetti P. (1980) Parkinson disease, dementia, and Alzheimer disease: clinicopathological correlations. Ann Neurol 7:329-35. DOI: 10.1002/ana.410070408.

Bolte S., Cordelieres F.P. (2006) A guided tour into subcellular colocalization analysis in light microscopy. J Microsc 224:213-32. DOI: JMI1706 [pii]

10.1111/j.1365-2818.2006.01706.x.

Borelli M.I., Gagliardino J.J. (2001) Possible modulatory effect of endogenous islet catecholamines on insulin secretion. BMC Endocr Disord 1:1.

Boyd A.E., 3rd, Lebovitz H.E., Feldman J.M. (1971) Endocrine function and glucose metabolism in patients with Parkinson's disease and their alternation by L-Dopa. J Clin Endocrinol Metab 33:829-37.

Braak E., Sandmann-Keil D., Rub U., Gai W.P., de Vos R.A., Steur E.N., Arai K., Braak H. (2001) alpha-synuclein immunopositive Parkinson's disease-related inclusion bodies in lower brain stem nuclei. Acta Neuropathol (Berl) 101:195-201.

Brooks D.J., Frey K.A., Marek K.L., Oakes D., Paty D., Prentice R., Shults C.W., Stoessl A.J. (2003) Assessment of neuroimaging techniques as biomarkers of the progression of Parkinson's disease. Exp Neurol 184 Suppl 1:S68-79.

Brown D.F., Dababo M.A., Bigio E.H., Risser R.C., Eagan K.P., Hladik C.L., White C.L., 3rd. (1998) Neuropathologic evidence that the Lewy body variant of Alzheimer disease represents coexistence of Alzheimer disease and idiopathic Parkinson disease. J Neuropathol Exp Neurol 57:39-46.

Brunk I., Blex C., Speidel D., Brose N., Ahnert-Hilger G. (2009) Ca2+-dependent activator proteins of secretion promote vesicular monoamine uptake. J Biol Chem 284:1050-6. DOI: M805328200 [pii]

10.1074/jbc.M805328200.

Brunk I., Blex C., Rachakonda S., Holtje M., Winter S., Pahner I., Walther D.J., Ahnert-Hilger G. (2006) The first luminal domain of vesicular monoamine transporters mediates G-protein-dependent regulation of transmitter uptake. J Biol Chem 281:33373-85.

Burr I.M., Jackson A., Culbert S., Sharp R., Felts P., Olson W. (1974) Glucose intolerance and impaired insulin release following 6-hydroxydopamine administration to intact rats. Endocrinology 94:1072-6.

Burre J., Sharma M., Tsetsenis T., Buchman V., Etherton M.R., Sudhof T.C. (2010) Alpha-synuclein promotes SNARE-complex assembly in vivo and in vitro. Science 329:1663-7. DOI: science.1195227 [pii]

10.1126/science.1195227.

Butler M.W., Burt A., Edwards T.L., Zuchner S., Scott W.K., Martin E.R., Vance J.M., Wang L. (2011) Vitamin D receptor gene as a candidate gene for Parkinson disease. Ann Hum Genet 75:201-10. DOI: 10.1111/j.1469-1809.2010.00631.x.

Cao P., Yuan Y., Pehek E.A., Moise A.R., Huang Y., Palczewski K., Feng Z. (2010) Alpha-synuclein disrupted dopamine homeostasis leads to dopaminergic neuron degeneration in Caenorhabditis elegans. PLoS One 5:e9312. DOI: 10.1371/journal.pone.0009312.

Cappai R., Leck S.L., Tew D.J., Williamson N.A., Smith D.P., Galatis D., Sharples R.A., Curtain C.C., Ali F.E., Cherny R.A., Culvenor J.G., Bottomley S.P., Masters C.L., Barnham K.J., Hill A.F. (2005) Dopamine promotes alpha-synuclein aggregation into SDS-resistant soluble oligomers via a distinct folding pathway. FASEB J 19:1377-9. DOI: 04-3437fje [pii]

10.1096/fj.04-3437fje.

Cartier E.A., Parra L.A., Baust T.B., Quiroz M., Salazar G., Faundez V., Egana L., Torres G.E. (2010) A biochemical and functional protein complex involving dopamine synthesis and transport into synaptic vesicles. J Biol Chem 285:1957-66. DOI: M109.054510 [pii]

10.1074/jbc.M109.054510.

Caudle W.M., Richardson J.R., Delea K.C., Guillot T.S., Wang M., Pennell K.D., Miller G.W. (2006) Polychlorinated biphenyl-induced reduction of dopamine transporter expression as a precursor to Parkinson's disease-associated dopamine toxicity. Toxicol Sci 92:490-9. DOI: kfl018 [pii]

10.1093/toxsci/kfl018.

Caudle W.M., Richardson J.R., Wang M.Z., Taylor T.N., Guillot T.S., McCormack A.L., Colebrooke R.E., Di Monte D.A., Emson P.C., Miller G.W. (2007) Reduced vesicular storage of dopamine causes progressive nigrostriatal neurodegeneration. J Neurosci 27:8138-48.

Cegrell L. (1968) [Insulin biosynthesis, storage and secretion. 12. Biogenic mono-amines in the endocrine pancreas of guinea pigs]. Lakartidningen 65:3616-7.

Champy M.F., Selloum M., Zeitler V., Caradec C., Jung B., Rousseau S., Pouilly L., Sorg T., Auwerx J. (2008) Genetic background determines metabolic phenotypes in the mouse. Mamm Genome 19:318-31. DOI: 10.1007/s00335-008-9107-z.

Chandra S., Chen X., Rizo J., Jahn R., Sudhof T.C. (2003) A broken alpha -helix in folded alpha -Synuclein. J Biol Chem 278:15313-8.

Chandra S., Gallardo G., Fernandez-Chacon R., Schluter O.M., Sudhof T.C. (2005) Alpha-synuclein cooperates with CSPalpha in preventing neurodegeneration. Cell 123:383-96. DOI: S0092-8674(05)01022-6 [pii]

10.1016/j.cell.2005.09.028.

Chauhan K.R., Kodavanti P.R., McKinney J.D. (2000) Assessing the role of ortho-substitution on polychlorinated biphenyl binding to transthyretin, a thyroxine transport protein. Toxicol Appl Pharmacol 162:10-21. DOI: 10.1006/taap.1999.8826

S0041-008X(99)98826-9 [pii].

Chen C.X., Huang S.Y., Zhang L., Liu Y.J. (2005) Synaptophysin enhances the neuroprotection of VMAT2 in MPP+-induced toxicity in MN9D cells. Neurobiol Dis 19:419-26.

Chesselet M.F. (2008) In vivo alpha-synuclein overexpression in rodents: a useful model of Parkinson's disease? Exp Neurol 209:22-7. DOI: S0014-4886(07)00307-X [pii]

10.1016/j.expneurol.2007.08.006.

Chou S.M., Miike T., Payne W.M., Davis G.J. (1979) Neuropathology of "spinning syndrome" induced by prenatal intoxication with a PCB in mice. Ann N Y Acad Sci 320:373-95.

Chu I., Villeneuve D.C., Yagminas A., Lecavalier P., Hakansson H., Ahlborg U.G., Valli V.E., Kennedy S.W., Bergman A., Seegal R.F., et al. (1995) Toxicity of PCB 77 (3,3',4,4'-tetrachlorobiphenyl) and PCB 118 (2,3',4,4'5-pentachlorobiphenyl) in the rat following subchronic dietary exposure. Fundam Appl Toxicol 26:282-92. DOI: S0272059085710998 [pii].

Chu I., Villeneuve D.C., Yagminas A., Lecavalier P., Poon R., Feeley M., Kennedy S.W., Seegal R.F., Hakansson H., Ahlborg U.G., Valli V.E., Bergman A. (1996) Toxicity of 2,2',4,4',5,5'-hexachlorobiphenyl in rats: effects following 90-day oral exposure. J Appl Toxicol 16:121-8. DOI: 10.1002/(SICI)1099-1263(199603)16:2<121::AID-JAT320>3.0.CO;2-G [pii]

10.1002/(SICI)1099-1263(199603)16:2<121::AID-JAT320>3.0.CO;2-G.

Chua C.E., Tang B.L. (2006) alpha-synuclein and Parkinson's disease: the first roadblock. J Cell Mol Med 10:837-46. DOI: 010.004.04 [pii].

Colebrooke R.E., Chan P.M., Lynch P.J., Mooslehner K., Emson P.C. (2007) Differential gene expression in the striatum of mice with very low expression of the vesicular monoamine transporter type 2 gene. Brain Res 1152:10-6.

Colebrooke R.E., Humby T., Lynch P.J., McGowan D.P., Xia J., Emson P.C. (2006) Age-related decline in striatal dopamine content and motor performance occurs in the absence of nigral cell loss in a genetic mouse model of Parkinson's disease. Eur J Neurosci 24:2622-30.

Conway K.A., Harper J.D., Lansbury P.T., Jr. (2000) Fibrils formed in vitro from alpha-synuclein and two mutant forms linked to Parkinson's disease are typical amyloid. Biochemistry 39:2552-63. DOI: bi991447r [pii].

Conway K.A., Rochet J.C., Bieganski R.M., Lansbury P.T., Jr. (2001) Kinetic stabilization of the alpha-synuclein protofibril by a dopamine-alpha-synuclein adduct. Science 294:1346-9.

Corrigan F.M., Murray L., Wyatt C.L., Shore R.F. (1998) Diorthosubstituted polychlorinated biphenyls in caudate nucleus in Parkinson's disease. Exp Neurol 150:339-42. DOI: S0014-4886(98)96776-0 [pii]

10.1006/exnr.1998.6776.

Corrigan F.M., Wienburg C.L., Shore R.F., Daniel S.E., Mann D. (2000) Organochlorine insecticides in substantia nigra in Parkinson's disease. J Toxicol Environ Health A 59:229-34.

Costes S.V., Daelemans D., Cho E.H., Dobbin Z., Pavlakis G., Lockett S. (2004) Automatic and quantitative measurement of protein-protein colocalization in live cells. Biophys J 86:3993-4003. DOI: 10.1529/biophysj.103.038422

S0006-3495(04)74439-2 [pii].

Cruz-Muros I., Afonso-Oramas D., Abreu P., Rodriguez M., Gonzalez M.C., Gonzalez-Hernandez T. (2007) Deglycosylation and subcellular redistribution of VMAT2 in the mesostriatal system during normal aging. Neurobiol Aging.

Daily N.J., Boswell K.L., James D.J., Martin T.F. (2010) Novel interactions of CAPS (Ca2+-dependent activator protein for secretion) with the three neuronal SNARE proteins required for vesicle fusion. J Biol Chem 285:35320-9. DOI: M110.145169 [pii]

10.1074/jbc.M110.145169.

Davidson W.S., Jonas A., Clayton D.F., George J.M. (1998) Stabilization of alpha-synuclein secondary structure upon binding to synthetic membranes. J Biol Chem 273:9443-9.

Dawson T.M., Ko H.S., Dawson V.L. (2010) Genetic animal models of Parkinson's disease. Neuron 66:646-61. DOI: S0896-6273(10)00327-2 [pii]

10.1016/j.neuron.2010.04.034.

De Giorgio R., Su D., Peter D., Edwards R.H., Brecha N.C., Sternini C. (1996) Vesicular monoamine transporter 2 expression in enteric neurons and enterochromaffin-like cells of the rat. Neurosci Lett 217:77-80.

de Leeuw van Weenen J.E., Parlevliet E.T., Maechler P., Havekes L.M., Romijn J.A., Ouwens D.M., Pijl H., Guigas B. (2010) The dopamine receptor D2 agonist bromocriptine inhibits glucose-stimulated insulin secretion by direct activation of the alpha2-adrenergic receptors in beta cells. Biochem Pharmacol 79:1827-36. DOI: S0006-2952(10)00067-5 [pii]

10.1016/j.bcp.2010.01.029.

Driver J.A., Smith A., Buring J.E., Gaziano J.M., Kurth T., Logroscino G. (2008) Prospective cohort study of type 2 diabetes and the risk of Parkinson's disease. Diabetes Care 31:2003-5. DOI: dc08-0688 [pii]

10.2337/dc08-0688.

Dunning B.E., Ahren B., Veith R.C., Taborsky G.J., Jr. (1988) Nonadrenergic sympathetic neural influences on basal pancreatic hormone secretion. Am J Physiol 255:E785-92.

Eiden L.E., Giraud P., Affolter H.U., Herbert E., Hotchkiss A.J. (1984) Alternative modes of enkephalin biosynthesis regulation by reserpine and cyclic AMP in cultured chromaffin cells. Proc Natl Acad Sci U S A 81:3949-53.

Eisenhofer G., Kopin I.J., Goldstein D.S. (2004a) Catecholamine metabolism: a contemporary view with implications for physiology and medicine. Pharmacol Rev 56:331-49. DOI: 10.1124/pr.56.3.1

56/3/331 [pii].

Eisenhofer G., Kopin I.J., Goldstein D.S. (2004b) Leaky catecholamine stores: undue waste or a stress response coping mechanism? Ann N Y Acad Sci 1018:224-30. DOI: 10.1196/annals.1296.027

1018/1/224 [pii].

Elbaz A., Clavel J., Rathouz P.J., Moisan F., Galanaud J.P., Delemotte B., Alperovitch A., Tzourio C. (2009) Professional exposure to pesticides and Parkinson disease. Ann Neurol 66:494-504. DOI: 10.1002/ana.21717.

Eliezer D., Kutluay E., Bussell R., Jr., Browne G. (2001) Conformational properties of alpha-synuclein in its free and lipid-associated states. J Mol Biol 307:1061-73.

Erickson J.D., Schafer M.K., Bonner T.I., Eiden L.E., Weihe E. (1996) Distinct pharmacological properties and distribution in neurons and endocrine cells of two isoforms of the human vesicular monoamine transporter. Proc Natl Acad Sci U S A 93:5166-71.

Ericson L.E., Hakanson R., Lundquist I. (1977) Accumulation of dopamine in mouse pancreatic B-cells following injection of L-DOPA. Localization to secretory granules and inhibition of insulin secretion. Diabetologia 13:117-24.

Eriksson O., Jahan M., Johnstrom P., Korsgren O., Sundin A., Halldin C., Johansson L. (2010) In vivo and in vitro characterization of [18F]-FE-(+)-DTBZ as a tracer for beta-cell mass. Nucl Med Biol 37:357-63. DOI: S0969-8051(09)00294-7 [pii]

10.1016/j.nucmedbio.2009.12.004.

Evatt M.L. (2010) Beyond vitamin status: is there a role for vitamin d in Parkinson disease? Arch Neurol 67:795-7. DOI: 67/7/795 [pii]

10.1001/archneurol.2010.123.

Evatt M.L., Delong M.R., Khazai N., Rosen A., Triche S., Tangpricha V. (2008) Prevalence of vitamin d insufficiency in patients with Parkinson disease and Alzheimer disease. Arch Neurol 65:1348-52. DOI: 65/10/1348 [pii]

10.1001/archneur.65.10.1348.

Evatt M.L., Delong M.R., Kumari M., Auinger P., McDermott M.P., Tangpricha V. (2011) High Prevalence of Hypovitaminosis D Status in Patients With Early Parkinson Disease. Arch Neurol 68:314-319. DOI: 68/3/314 [pii]

10.1001/archneurol.2011.30.

Everett C.J., Frithsen I., Player M. (2011) Relationship of polychlorinated biphenyls with type 2 diabetes and hypertension. J Environ Monit 13:241-51. DOI: 10.1039/c0em00400f.

Eyles D.W., Smith S., Kinobe R., Hewison M., McGrath J.J. (2005) Distribution of the vitamin D receptor and 1 alpha-hydroxylase in human brain. J Chem Neuroanat 29:21-30. DOI: S0891-0618(04)00117-6 [pii]

10.1016/j.jchemneu.2004.08.006.

Eyles D.W., Feron F., Cui X., Kesby J.P., Harms L.H., Ko P., McGrath J.J., Burne T.H. (2009) Developmental vitamin D deficiency causes abnormal brain development. Psychoneuroendocrinology 34 Suppl 1:S247-57. DOI: S0306-4530(09)00143-7 [pii]

10.1016/j.psyneuen.2009.04.015.

Fagerholm V., Mikkola K.K., Ishizu T., Arponen E., Kauhanen S., Nagren K., Solin O., Nuutila P., Haaparanta M. (2010) Assessment of islet specificity of dihydrotetrabenazine radiotracer binding in rat pancreas and human pancreas. J Nucl Med 51:1439-46. DOI: jnumed.109.074492 [pii]

10.2967/jnumed.109.074492.

Feldman J.M., Boyd A.E., 3rd, Lebovitz H.E. (1971) Structural determinants of catecholamine action on in vitro insulin release. J Pharmacol Exp Ther 176:611-21.

Finn J.P., 3rd, Edwards R.H. (1997) Individual residues contribute to multiple differences in ligand recognition between vesicular monoamine transporters 1 and 2. J Biol Chem 272:16301-7.

Fischer L.J., Zhou H.R., Wagner M.A. (1996) Polychlorinated biphenyls release insulin from RINm5F cells. Life Sci 59:2041-9. DOI: S0024320596005577 [pii].

Fischer L.J., Wagner M.A., Madhukar B.V. (1999) Potential involvement of calcium, CaM kinase II, and MAP kinases in PCB-stimulated insulin release from RINm5F cells. Toxicol Appl Pharmacol 159:194-203. DOI: 10.1006/taap.1999.8728

S0041-008X(99)98728-8 [pii].

Fischer L.J., Seegal R.F., Ganey P.E., Pessah I.N., Kodavanti P.R. (1998) Symposium overview: toxicity of non-coplanar PCBs. Toxicol Sci 41:49-61. DOI: S1096-6080(97)92386-6 [pii]

10.1006/toxs.1997.2386.

Fishbein L. (1974) Mutagens and potential mutagens in the biosphere. I. DDT and its metabolites, polychlorinated biphenyls, chlorodioxins, polycyclic aromatic hydrocarbons, haloethers. Sci Total Environ 2:305-40.

Fleming L., Mann J.B., Bean J., Briggle T., Sanchez-Ramos J.R. (1994) Parkinson's disease and brain levels of organochlorine pesticides. Ann Neurol 36:100-3. DOI: 10.1002/ana.410360119.

Follmer C., Romao L., Einsiedler C.M., Porto T.C., Lara F.A., Moncores M., Weissmuller G., Lashuel H.A., Lansbury P., Neto V.M., Silva J.L., Foguel D. (2007) Dopamine affects the stability, hydration, and packing of protofibrils and fibrils of the wild type and variants of alpha-synuclein. Biochemistry 46:472-82.

Fon E.A., Pothos E.N., Sun B.C., Killeen N., Sulzer D., Edwards R.H. (1997) Vesicular transport regulates monoamine storage and release but is not essential for amphetamine action. Neuron 19:1271-83.

Fonnum F., Mariussen E. (2009) Mechanisms involved in the neurotoxic effects of environmental toxicants such as polychlorinated biphenyls and brominated flame retardants. J Neurochem 111:1327-47. DOI: JNC6427 [pii]

10.1111/j.1471-4159.2009.06427.x.

Freeby M., Goland R., Ichise M., Maffei A., Leibel R., Harris P. (2008) VMAT2 quantitation by PET as a biomarker for beta-cell mass in health and disease. Diabetes Obes Metab 10 Suppl 4:98-108. DOI: DOM943 [pii]

10.1111/j.1463-1326.2008.00943.x.

Freis E.D. (1954) Mental depression in hypertensive patients treated for long periods with large doses of reserpine. N Engl J Med 251:1006-8. DOI: 10.1056/NEJM195412162512504.

Freis E.D., Ari R. (1954) Clinical and experimental effects of reserpine in patients with essential hypertension. Ann N Y Acad Sci 59:45-53.

Frey K.A., Koeppe R.A., Kilbourn M.R. (2001) Imaging the vesicular monoamine transporter. Adv Neurol 86:237-47.

Frey K.A., Koeppe R.A., Kilbourn M.R., Vander Borght T.M., Albin R.L., Gilman S., Kuhl D.E. (1996) Presynaptic monoaminergic vesicles in Parkinson's disease and normal aging. Ann Neurol 40:873-84.

Fumagalli F., Gainetdinov R.R., Wang Y.M., Valenzano K.J., Miller G.W., Caron M.G. (1999) Increased methamphetamine neurotoxicity in heterozygous vesicular monoamine transporter 2 knock-out mice. J Neurosci 19:2424-31.

Gagliardino J.J., Iturriza F.C., Hernandez R.E., Zieher L.M. (1970) Effect of catecholamines precursors on insulin secretion. Endocrinology 87:823-5.

Gainetdinov R.R., Fumagalli F., Wang Y.M., Jones S.R., Levey A.I., Miller G.W., Caron M.G. (1998) Increased MPTP neurotoxicity in vesicular monoamine transporter 2 heterozygote knockout mice. J Neurochem 70:1973-8.

Garcia-Tornadu I., Ornstein A.M., Chamson-Reig A., Wheeler M.B., Hill D.J., Arany E., Rubinstein M., Becu-Villalobos D. (2010) Disruption of the dopamine d2 receptor impairs insulin secretion and causes glucose intolerance. Endocrinology 151:1441-50. DOI: en.2009-0996 [pii]

10.1210/en.2009-0996.

Gaziano J.M., Cincotta A.H., O'Connor C.M., Ezrokhi M., Rutty D., Ma Z.J., Scranton R.E. (2010) Randomized clinical trial of quick-release bromocriptine among patients with type 2 diabetes on overall safety and cardiovascular outcomes. Diabetes Care 33:1503-8. DOI: dc09-2009 [pii]

10.2337/dc09-2009.

Geng X., Lou H., Wang J., Li L., Swanson A.L., Sun M., Beers Stolz D., Watkins S.K., Perez R.G., Drain P. (2010) {alpha}-Synuclein Binds the KATP Channel at Insulin Secretory Granules and Inhibits Insulin Secretion. Am J Physiol Endocrinol Metab. DOI: ajpendo.00262.2010 [pii]

10.1152/ajpendo.00262.2010.

Giachetti A., Hollenbeck R.A., Shore P.A. (1974) Localization and binding of reserpine in the membrane of adrenomedullary amine storage granules. Naunyn Schmiedebergs Arch Pharmacol 283:263-75.

Glatt C.E., Wahner A.D., White D.J., Ruiz-Linares A., Ritz B. (2006) Gain-of-function haplotypes in the vesicular monoamine transporter promoter are protective for Parkinson disease in women. Hum Mol Genet 15:299-305.

Goland R., Freeby M., Parsey R., Saisho Y., Kumar D., Simpson N., Hirsch J., Prince M., Maffei A., Mann J.J., Butler P.C., Van Heertum R., Leibel R.L., Ichise M., Harris P.E. (2009)

11C-dihydrotetrabenazine PET of the pancreas in subjects with long-standing type 1 diabetes and in healthy controls. J Nucl Med 50:382-9. DOI: jnumed.108.054866 [pii]

10.2967/jnumed.108.054866.

Goldstein D.S. (2010) Catecholamines 101. Clin Auton Res 20:331-52. DOI: 10.1007/s10286-010-0065-7.

Greenamyre J.T., Hastings T.G. (2004) Biomedicine. Parkinson's--divergent causes, convergent mechanisms. Science 304:1120-2.

Grundy S.M., Benjamin I.J., Burke G.L., Chait A., Eckel R.H., Howard B.V., Mitch W., Smith S.C., Jr., Sowers J.R. (1999) Diabetes and cardiovascular disease: a statement for healthcare professionals from the American Heart Association. Circulation 100:1134-46.

Guay D.R. (2010) Tetrabenazine, a monoamine-depleting drug used in the treatment of hyperkinetic movement disorders. Am J Geriatr Pharmacother 8:331-73. DOI: S1543-5946(10)00070-X [pii]

10.1016/j.amjopharm.2010.08.006.

Guillot T.S., Shepherd K.R., Richardson J.R., Wang M.Z., Li Y., Emson P.C., Miller G.W. (2008a) Reduced vesicular storage of dopamine exacerbates methamphetamine-induced neurodegeneration and astrogliosis. J Neurochem 106:2205-17. DOI: JNC5568 [pii]

10.1111/j.1471-4159.2008.05568.x.

Guillot T.S., Richardson J.R., Wang M.Z., Li Y.J., Taylor T.N., Ciliax B.J., Zachrisson O., Mercer A., Miller G.W. (2008b) PACAP38 increases vesicular monoamine transporter 2 (VMAT2) expression and attenuates methamphetamine toxicity. Neuropeptides 42:423-34. DOI: S0143-4179(08)00051-6 [pii]

10.1016/j.npep.2008.04.003.

Guo J.T., Chen A.Q., Kong Q., Zhu H., Ma C.M., Qin C. (2008) Inhibition of vesicular monoamine transporter-2 activity in alpha-synuclein stably transfected SH-SY5Y cells. Cell Mol Neurobiol 28:35-47. DOI: 10.1007/s10571-007-9227-0.

Hajri T., Tao H., Wattacheril J., Marks-Shulman P., Abumrad N.N. (2011) Regulation of adiponectin production by insulin: interactions with tumor necrosis factor-{alpha} and interleukin-6. Am J Physiol Endocrinol Metab 300:E350-60. DOI: ajpendo.00307.2010 [pii]

10.1152/ajpendo.00307.2010.

Hall F.S., Sora I., Uhl G.R. (2003) Sex-dependent modulation of ethanol consumption in vesicular monoamine transporter 2 (VMAT2) and dopamine transporter (DAT) knockout mice. Neuropsychopharmacology 28:620-8.

Hampshire J., Moraru E., Altszuler N. (1978) On the mechanism of hyperglycemia and stimulation of growth hormone secretion by L-dopa. Pharmacology 17:138-48.

Han W., Li C. (2010) Linking type 2 diabetes and Alzheimer's disease. Proc Natl Acad Sci U S A 107:6557-8. DOI: 1002555107 [pii]

10.1073/pnas.1002555107.

Harrington K.A., Augood S.J., Kingsbury A.E., Foster O.J., Emson P.C. (1996) Dopamine transporter (Dat) and synaptic vesicle amine transporter (VMAT2) gene expression in the substantia nigra of control and Parkinson's disease. Brain Res Mol Brain Res 36:157-62.

Hasegawa T., Matsuzaki-Kobayashi M., Takeda A., Sugeno N., Kikuchi A., Furukawa K., Perry G., Smith M.A., Itoyama Y. (2006) Alpha-synuclein facilitates the toxicity of oxidized catechol metabolites: implications for selective neurodegeneration in Parkinson's disease. FEBS Lett 580:2147-52.

Hatcher J.M., Pennell K.D., Miller G.W. (2008a) Parkinson's disease and pesticides: a toxicological perspective. Trends Pharmacol Sci 29:322-9. DOI: S0165-6147(08)00082-5 [pii]

10.1016/j.tips.2008.03.007.

Hatcher J.M., Delea K.C., Richardson J.R., Pennell K.D., Miller G.W. (2008b) Disruption of dopamine transport by DDT and its metabolites. Neurotoxicology 29:682-90. DOI: S0161-813X(08)00051-X [pii]

10.1016/j.neuro.2008.04.010.

Heintz N., Zoghbi H. (1997) alpha-Synuclein--a link between Parkinson and Alzheimer diseases? Nat Genet 16:325-7. DOI: 10.1038/ng0897-325.

Hinault M.P., Cuendet A.F., Mattoo R.U., Mensi M., Dietler G., Lashuel H.A., Goloubinoff P. (2010) Stable alpha-synuclein oligomers strongly inhibit chaperone activity of the Hsp70 system by weak interactions with J-domain co-chaperones. J Biol Chem 285:38173-82. DOI: M110.127753 [pii]

10.1074/jbc.M110.127753.

Hindle J.V. (2010) Ageing, neurodegeneration and Parkinson's disease. Age Ageing 39:156-61. DOI: afp223 [pii]

10.1093/ageing/afp223.

Holtje M., von Jagow B., Pahner I., Lautenschlager M., Hortnagl H., Nurnberg B., Jahn R., Ahnert-Hilger G. (2000) The neuronal monoamine transporter VMAT2 is regulated by the trimeric GTPase Go(2). J Neurosci 20:2131-41.

Hoque A., Sigurdson A.J., Burau K.D., Humphrey H.E., Hess K.R., Sweeney A.M. (1998) Cancer among a Michigan cohort exposed to polybrominated biphenyls in 1973. Epidemiology 9:373-8. DOI: 00001648-199807000-00001 [pii].

Hu E., Liang P., Spiegelman B.M. (1996) AdipoQ is a novel adipose-specific gene dysregulated in obesity. J Biol Chem 271:10697-703.

Hu G., Jousilahti P., Bidel S., Antikainen R., Tuomilehto J. (2007) Type 2 diabetes and the risk of Parkinson's disease. Diabetes Care 30:842-7. DOI: dc06-2011 [pii]

10.2337/dc06-2011.

Huang C.Y., McLeod J.G., Holland R.T., Elliot C. (1976) Tetrabenazine in the treatment of Huntington's chorea. Med J Aust 1:583-4.

Hunt M.J., Morton A.J. (2005) Atypical diabetes associated with inclusion formation in the R6/2 mouse model of Huntington's disease is not improved by treatment with hypoglycaemic agents. Exp Brain Res 166:220-9. DOI: 10.1007/s00221-005-2357-z.

Ichise M., Harris P.E. (2010) Imaging of beta-cell mass and function. J Nucl Med 51:1001-4. DOI: jnumed.109.068999 [pii]

10.2967/jnumed.109.068999.

Inabnet W.B., Milone L., Harris P., Durak E., Freeby M.J., Ahmed L., Sebastian M., Lifante J.C., Bessler M., Korner J. (2010) The utility of [(11)C] dihydrotetrabenazine positron emission tomography scanning in assessing beta-cell performance after sleeve gastrectomy and duodenal-jejunal bypass. Surgery 147:303-9. DOI: S0039-6060(09)00501-7 [pii]

10.1016/j.surg.2009.08.005.

Iturriza F.C., Zieher L.M., Mainetti J.M. (1970) A fluorescent reaction for monoamines in an insulinoma. J Clin Endocrinol Metab 31:580-1.

Jaim-Etcheverry G., Zieher L.M. (1968) Electron microscopic cytochemistry of 5-hydroxytryptamine (5-HT) in the beta cells of guinea pig endocrine pancreas. Endocrinology 83:917-23.

James D.J., Khodthong C., Kowalchyk J.A., Martin T.F. (2010) Phosphatidylinositol 4,5-bisphosphate regulation of SNARE function in membrane fusion mediated by CAPS. Adv Enzyme Regul 50:62-70. DOI: S0065-2571(09)00069-7 [pii]

10.1016/j.advenzreg.2009.10.012.

James D.J., Kowalchyk J., Daily N., Petrie M., Martin T.F. (2009) CAPS drives trans-SNARE complex formation and membrane fusion through syntaxin interactions. Proc Natl Acad Sci U S A 106:17308-13. DOI: 0900755106 [pii]

10.1073/pnas.0900755106.

Jankovic J. (2008) Parkinson's disease: clinical features and diagnosis. J Neurol Neurosurg Psychiatry 79:368-76. DOI: 79/4/368 [pii]

10.1136/jnnp.2007.131045.

Jetton T.L., Liang Y., Cincotta A.H. (2001) Systemic treatment with sympatholytic dopamine agonists improves aberrant beta-cell hyperplasia and GLUT2, glucokinase, and insulin immunoreactive levels in ob/ob mice. Metabolism 50:1377-84. DOI: S0026-0495(01)05024-7 [pii]

10.1053/meta.2001.26741.

Jo E., McLaurin J., Yip C.M., St George-Hyslop P., Fraser P.E. (2000) alpha-Synuclein membrane interactions and lipid specificity. J Biol Chem 275:34328-34.

Jo E., Darabie A.A., Han K., Tandon A., Fraser P.E., McLaurin J. (2004) alpha-Synuclein-synaptosomal membrane interactions: implications for fibrillogenesis. Eur J Biochem 271:3180-9.

Josefsen K., Nielsen M.D., Jorgensen K.H., Bock T., Norremolle A., Sorensen S.A., Naver B., Hasholt L. (2008) Impaired glucose tolerance in the R6/1 transgenic mouse model of Huntington's disease. J Neuroendocrinol 20:165-72. DOI: JNE1629 [pii]

10.1111/j.1365-2826.2007.01629.x.

Kadowaki T., Yamauchi T., Kubota N., Hara K., Ueki K., Tobe K. (2006) Adiponectin and adiponectin receptors in insulin resistance, diabetes, and the metabolic syndrome. J Clin Invest 116:1784-92. DOI: 10.1172/JCI29126.

Kempster P.A., Hurwitz B., Lees A.J. (2007) A new look at James Parkinson's Essay on the Shaking Palsy. Neurology 69:482-5. DOI: 69/5/482 [pii]

10.1212/01.wnl.0000266639.50620.d1.

Kesby J.P., Burne T.H., McGrath J.J., Eyles D.W. (2006) Developmental vitamin D deficiency alters MK 801-induced hyperlocomotion in the adult rat: An animal model of schizophrenia. Biol Psychiatry 60:591-6. DOI: S0006-3223(06)00387-8 [pii]

10.1016/j.biopsych.2006.02.033.

Kesby J.P., Cui X., O'Loan J., McGrath J.J., Burne T.H., Eyles D.W. (2010) Developmental vitamin D deficiency alters dopamine-mediated behaviors and dopamine transporter function in adult female rats. Psychopharmacology (Berl) 208:159-68. DOI: 10.1007/s00213-009-1717-y.

Kietz S., Fischer B. (2003) Polychlorinated biphenyls affect gene expression in the rabbit preimplantation embryo. Mol Reprod Dev 64:251-60. DOI: 10.1002/mrd.10226.

Kilbourn M., Lee L., Vander Borght T., Jewett D., Frey K. (1995) Binding of alpha-dihydrotetrabenazine to the vesicular monoamine transporter is stereospecific. Eur J Pharmacol 278:249-52.

Kilbourn M.R. (2010) Rat pancreas uptake of [11C]dihydrotetrabenazine stereoisomers. Nucl Med Biol 37:869-71. DOI: S0969-8051(10)00305-7 [pii]

10.1016/j.nucmedbio.2010.06.001.

Kim H., Toyofuku Y., Lynn F.C., Chak E., Uchida T., Mizukami H., Fujitani Y., Kawamori R., Miyatsuka T., Kosaka Y., Yang K., Honig G., van der Hart M., Kishimoto N., Wang J., Yagihashi S., Tecott L.H., Watada H., German M.S. (2010) Serotonin regulates pancreatic beta cell mass during pregnancy. Nat Med 16:804-8. DOI: nm.2173 [pii]

10.1038/nm.2173.

Kim J.S., Kim Y.I., Song C., Yoon I., Park J.W., Choi Y.B., Kim H.T., Lee K.S. (2005) Association of vitamin D receptor gene polymorphism and Parkinson's disease in Koreans. J Korean Med Sci 20:495-8. DOI: 200506495 [pii].

Knekt P., Kilkkinen A., Rissanen H., Marniemi J., Saaksjarvi K., Heliovaara M. (2010) Serum vitamin D and the risk of Parkinson disease. Arch Neurol 67:808-11. DOI: 67/7/808 [pii]

10.1001/archneurol.2010.120.

Krantz D.E., Peter D., Liu Y., Edwards R.H. (1997) Phosphorylation of a vesicular monoamine transporter by casein kinase II. J Biol Chem 272:6752-9.

Krishnan S., Chi E.Y., Wood S.J., Kendrick B.S., Li C., Garzon-Rodriguez W., Wypych J., Randolph T.W., Narhi L.O., Biere A.L., Citron M., Carpenter J.F. (2003) Oxidative dimer formation is the critical rate-limiting step for Parkinson's disease alpha-synuclein fibrillogenesis. Biochemistry 42:829-37. DOI: 10.1021/bi026528t.

Kruger R., Kuhn W., Muller T., Woitalla D., Graeber M., Kosel S., Przuntek H., Epplen J.T., Schols L., Riess O. (1998) Ala30Pro mutation in the gene encoding alpha-synuclein in Parkinson's disease. Nat Genet 18:106-8.

Kruger R., Vieira-Saecker A.M., Kuhn W., Berg D., Muller T., Kuhnl N., Fuchs G.A., Storch A., Hungs M., Woitalla D., Przuntek H., Epplen J.T., Schols L., Riess O. (1999) Increased susceptibility to sporadic Parkinson's disease by a certain combined alpha-synuclein/apolipoprotein E genotype. Ann Neurol 45:611-7.

Kung H.F., Lieberman B.P., Zhuang Z.P., Oya S., Kung M.P., Choi S.R., Poessl K., Blankemeyer E., Hou C., Skovronsky D., Kilbourn M. (2008a) In vivo imaging of vesicular monoamine transporter 2 in pancreas using an (18)F epoxide derivative of tetrabenazine. Nucl Med Biol 35:825-37. DOI: S0969-8051(08)00179-0 [pii]

10.1016/j.nucmedbio.2008.08.004.

Kung M.P., Hou C., Lieberman B.P., Oya S., Ponde D.E., Blankemeyer E., Skovronsky D., Kilbourn M.R., Kung H.F. (2008b) In vivo imaging of beta-cell mass in rats using 18F-FP-(+)-DTBZ: a potential PET ligand for studying diabetes mellitus. J Nucl Med 49:1171-6. DOI: jnumed.108.051680 [pii]

10.2967/jnumed.108.051680.

Kurose T., Seino Y., Nishi S., Tsuji K., Taminato T., Tsuda K., Imura H. (1990) Mechanism of sympathetic neural regulation of insulin, somatostatin, and glucagon secretion. Am J Physiol 258:E220-7.

Kurose T., Tsuda K., Ishida H., Tsuji K., Okamoto Y., Tsuura Y., Kato S., Usami M., Imura H., Seino Y. (1992) Glucagon, insulin and somatostatin secretion in response to sympathetic neural activation in streptozotocin-induced diabetic rats. A study with the isolated perfused rat pancreas in vitro. Diabetologia 35:1035-41.

Kwak S.H., Cho Y.M., Moon M.K., Kim J.H., Park B.L., Cheong H.S., Shin H.D., Jang H.C., Kim S.Y., Lee H.K., Park K.S. (2008) Association of polymorphisms in the insulin-degrading enzyme gene with type 2 diabetes in the Korean population. Diabetes Res Clin Pract 79:284-90. DOI: S0168-8227(07)00431-7 [pii]

10.1016/j.diabres.2007.08.017.

Langston J.W., Ballard P.A., Jr. (1983) Parkinson's disease in a chemist working with 1-methyl-4-phenyl-1,2,5,6-tetrahydropyridine. N Engl J Med 309:310.

Langston J.W., Ballard P., Tetrud J.W., Irwin I. (1983) Chronic Parkinsonism in humans due to a product of meperidine-analog synthesis. Science 219:979-80.

Larsen K.E., Fon E.A., Hastings T.G., Edwards R.H., Sulzer D. (2002) Methamphetamine-induced degeneration of dopaminergic neurons involves autophagy and upregulation of dopamine synthesis. J Neurosci 22:8951-60.

Larsen K.E., Schmitz Y., Troyer M.D., Mosharov E., Dietrich P., Quazi A.Z., Savalle M., Nemani V., Chaudhry F.A., Edwards R.H., Stefanis L., Sulzer D. (2006) Alpha-synuclein overexpression in PC12 and chromaffin cells impairs catecholamine release by interfering with a late step in exocytosis. J Neurosci 26:11915-22.

Lebovitz H.E., Feldman J.M. (1973) Pancreatic biogenic amines and insulin secretion in health and disease. Fed Proc 32:1797-802.

Lee F.J., Liu F., Pristupa Z.B., Niznik H.B. (2001) Direct binding and functional coupling of alpha-synuclein to the dopamine transporters accelerate dopamine-induced apoptosis. FASEB J 15:916-26.

Lee H.J., Patel S., Lee S.J. (2005) Intravesicular localization and exocytosis of alpha-synuclein and its aggregates. J Neurosci 25:6016-24. DOI: 25/25/6016 [pii]

10.1523/JNEUROSCI.0692-05.2005.

Lehmensiek V., Tan E.M., Schwarz J., Storch A. (2002) Expression of mutant alpha-synucleins enhances dopamine transporter-mediated MPP+ toxicity in vitro. Neuroreport 13:1279-83.

Leong S.L., Cappai R., Barnham K.J., Pham C.L. (2009) Modulation of alpha-synuclein aggregation by dopamine: a review. Neurochem Res 34:1838-46. DOI: 10.1007/s11064-009-9986-8.

Leung K. (2004a) 2-Hydroxy-3-isobutyl-9-[11C]methoxy-10-methoxy-1,2,3,4,6,7,-hexahydro-11bH -bezo[alpha]-quinolizine. DOI: NBK23597 [bookaccession].

Leung K. (2004b) (+)-2-Hydroxy-3-isobutyl-9-(3-[18F]fluoropropoxy)-10-methoxy-1,2,3,4,6,7-hexahydro-11bH-benzo[a]quinolizine. DOI: NBK23463 [bookaccession].

Li S., Shin H.J., Ding E.L., van Dam R.M. (2009) Adiponectin levels and risk of type 2 diabetes: a systematic review and meta-analysis. JAMA 302:179-88. DOI: 302/2/179 [pii]

10.1001/jama.2009.976.

Liang Y., Lubkin M., Sheng H., Scislowski P.W., Cincotta A.H. (1998) Dopamine agonist treatment ameliorates hyperglycemia, hyperlipidemia, and the elevated basal insulin release from islets of ob/ob mice. Biochim Biophys Acta 1405:1-13.

Lin A.M., Chen K.B., Chao P.L. (2005) Antioxidative effect of vitamin D3 on zinc-induced oxidative stress in CNS. Ann N Y Acad Sci 1053:319-29. DOI: 1053/1/319 [pii]

10.1196/annals.1344.028.

Lin K.J., Weng Y.H., Wey S.P., Hsiao I.T., Lu C.S., Skovronsky D., Chang H.P., Kung M.P., Yen T.C. (2010) Whole-body biodistribution and radiation dosimetry of 18F-FP-(+)-DTBZ (18F-AV-133): a novel vesicular monoamine transporter 2 imaging agent. J Nucl Med 51:1480-5. DOI: jnumed.110.078196 [pii]

10.2967/jnumed.110.078196.

Lind P.M., Orberg J., Edlund U.B., Sjoblom L., Lind L. (2004) The dioxin-like pollutant PCB 126 (3,3',4,4',5-pentachlorobiphenyl) affects risk factors for cardiovascular disease in female rats. Toxicol Lett 150:293-9. DOI: 10.1016/j.toxlet.2004.02.008

S0378427404000669 [pii].

Lipman I.J., Boykin M.E., Flora R.E. (1974) Glucose intolerance in Parkinson's disease. J Chronic Dis 27:573-9.

Liu Y., Edwards R.H. (1997) The role of vesicular transport proteins in synaptic transmission and neural degeneration. Annu Rev Neurosci 20:125-56. DOI: 10.1146/annurev.neuro.20.1.125.

Liu Y., Peter D., Roghani A., Schuldiner S., Prive G.G., Eisenberg D., Brecha N., Edwards R.H. (1992) A cDNA that suppresses MPP+ toxicity encodes a vesicular amine transporter. Cell 70:539-51. DOI: 0092-8674(92)90425-C [pii].

Login I.S., Cronin M.J., MacLeod R.M. (1982) Tetrabenazine has properties of a dopamine receptor antagonist. Ann Neurol 12:257-62. DOI: 10.1002/ana.410120308.

Login I.S., Cronin M.J., Harcus C.T., MacLeod R.M. (1983) Neuroendocrine evidence that tetrabenazine is a dopamine antagonist. Proc Soc Exp Biol Med 172:225-31.

Lotharius J., Barg S., Wiekop P., Lundberg C., Raymon H.K., Brundin P. (2002) Effect of mutant alpha-synuclein on dopamine homeostasis in a new human mesencephalic cell line. J Biol Chem 277:38884-94.

Lou H., Montoya S.E., Alerte T.N., Wang J., Wu J., Peng X., Hong C.S., Friedrich E.E., Mader S.A., Pedersen C.J., Marcus B.S., McCormack A.L., Di Monte D.A., Daubner S.C., Perez

R.G. (2010) Serine 129 phosphorylation reduces the ability of alpha-synuclein to regulate tyrosine hydroxylase and protein phosphatase 2A in vitro and in vivo. J Biol Chem 285:17648-61. DOI: M110.100867 [pii]

10.1074/jbc.M110.100867.

Lundquist I. (1971) Insulin secretion. Its regulation by monoamines and acid amyloglucosidase. Acta Physiol Scand Suppl 372:1-47.

Lundquist I., Panagiotidis G., Stenstrom A. (1991) Effect of L-dopa administration on islet monoamine oxidase activity and glucose-induced insulin release in the mouse. Pancreas 6:522-7.

Lyng G.D., Seegal R.F. (2008) Polychlorinated biphenyl-induced oxidative stress in organotypic co-cultures: experimental dopamine depletion prevents reductions in GABA. Neurotoxicology 29:301-8. DOI: S0161-813X(07)00273-2 [pii]

10.1016/j.neuro.2007.12.002.

Mak S.K., McCormack A.L., Langston J.W., Kordower J.H., Di Monte D.A. (2009) Decreased alpha-synuclein expression in the aging mouse substantia nigra. Exp Neurol 220:359-65. DOI: S0014-4886(09)00408-7 [pii]

10.1016/j.expneurol.2009.09.021.

Mariussen E., Fonnum F. (2001) The effect of polychlorinated biphenyls on the high affinity uptake of the neurotransmitters, dopamine, serotonin, glutamate and GABA, into rat brain synaptosomes. Toxicology 159:11-21. DOI: S0300-483X(00)00374-7 [pii].

Mariussen E., Morch Andersen J., Fonnum F. (1999) The effect of polychlorinated biphenyls on the uptake of dopamine and other neurotransmitters into rat brain synaptic vesicles. Toxicol Appl Pharmacol 161:274-82. DOI: 10.1006/taap.1999.8806

S0041-008X(99)98806-3 [pii].

Mariussen E., Andersson P.L., Tysklind M., Fonnum F. (2001) Effect of polychlorinated biphenyls on the uptake of dopamine into rat brain synaptic vesicles: a structure-activity study. Toxicol Appl Pharmacol 175:176-83. DOI: 10.1006/taap.2001.9231

S0041-008X(01)99231-2 [pii].

Mariussen E., Myhre O., Reistad T., Fonnum F. (2002) The polychlorinated biphenyl mixture aroclor 1254 induces death of rat cerebellar granule cells: the involvement of the N-methyl-D-aspartate receptor and reactive oxygen species. Toxicol Appl Pharmacol 179:137-44. DOI: 10.1006/taap.2002.9353

S0041008X02993531 [pii].

Maroteaux L., Campanelli J.T., Scheller R.H. (1988) Synuclein: a neuron-specific protein localized to the nucleus and presynaptic nerve terminal. J Neurosci 8:2804-15.

Marrachelli V.G., Miranda F.J., Alabadi J.A., Milan M., Cano-Jaimez M., Kirstein M., Alborch E., Farinas I., Perez-Sanchez F. (2010) Perivascular nerve fiber alpha-synuclein regulates contractility of mouse aorta: a link to autonomic dysfunction in Parkinson's disease. Neurochem Int 56:991-8. DOI: S0197-0186(10)00145-2 [pii]

10.1016/j.neuint.2010.04.011.

Martinez-Vicente M., Talloczy Z., Kaushik S., Massey A.C., Mazzulli J., Mosharov E.V., Hodara R., Fredenburg R., Wu D.C., Follenzi A., Dauer W., Przedborski S., Ischiropoulos H., Lansbury P.T., Sulzer D., Cuervo A.M. (2008) Dopamine-modified alpha-synuclein blocks chaperone-mediated autophagy. J Clin Invest 118:777-88. DOI: 10.1172/JCI32806.

Maser R.E., Steenkiste A.R., Dorman J.S., Nielsen V.K., Bass E.B., Manjoo Q., Drash A.L., Becker D.J., Kuller L.H., Greene D.A., et al. (1989) Epidemiological correlates of diabetic neuropathy. Report from Pittsburgh Epidemiology of Diabetes Complications Study. Diabetes 38:1456-61.

Mazzulli J.R., Armakola M., Dumoulin M., Parastatidis I., Ischiropoulos H. (2007) Cellular oligomerization of alpha-synuclein is determined by the interaction of oxidized catechols with a C-terminal sequence. J Biol Chem 282:31621-30. DOI: M704737200 [pii] 10.1074/jbc.M704737200.

Mazzulli J.R., Mishizen A.J., Giasson B.I., Lynch D.R., Thomas S.A., Nakashima A., Nagatsu T., Ota A., Ischiropoulos H. (2006) Cytosolic catechols inhibit alpha-synuclein aggregation and facilitate the formation of intracellular soluble oligomeric intermediates. J Neurosci 26:10068-78. DOI: 26/39/10068 [pii] 10.1523/JNEUROSCI.0896-06.2006.

Mei Q., Mundinger T.O., Lernmark A., Taborsky G.J., Jr. (2002) Early, selective, and marked loss of sympathetic nerves from the islets of BioBreeder diabetic rats. Diabetes 51:2997-3002.

Merickel A., Edwards R.H. (1995) Transport of histamine by vesicular monoamine transporter-2. Neuropharmacology 34:1543-7.

Messier C., Teutenberg K. (2005) The role of insulin, insulin growth factor, and insulin-degrading enzyme in brain aging and Alzheimer's disease. Neural Plast 12:311-28. DOI: 10.1155/NP.2005.311.

Miller G.W., Kirby M.L., Levey A.I., Bloomquist J.R. (1999a) Heptachlor alters expression and function of dopamine transporters. Neurotoxicology 20:631-7.

Miller G.W., Staley J.K., Heilman C.J., Perez J.T., Mash D.C., Rye D.B., Levey A.I. (1997) Immunochemical analysis of dopamine transporter protein in Parkinson's disease. Ann Neurol 41:530-9. DOI: 10.1002/ana.410410417.

Miller G.W., Erickson J.D., Perez J.T., Penland S.N., Mash D.C., Rye D.B., Levey A.I. (1999b) Immunochemical analysis of vesicular monoamine transporter (VMAT2) protein in Parkinson's disease. Exp Neurol 156:138-48. DOI: S0014-4886(98)97008-X [pii] 10.1006/exnr.1998.7008.

Mills S.A., 3rd, Thal D.I., Barney J. (2007) A summary of the 209 PCB congener nomenclature. Chemosphere 68:1603-12. DOI: S0045-6535(07)00429-8 [pii]

10.1016/j.chemosphere.2007.03.052.

Mishizen-Eberz A.J., Guttmann R.P., Giasson B.I., Day G.A., 3rd, Hodara R., Ischiropoulos H., Lee V.M., Trojanowski J.Q., Lynch D.R. (2003) Distinct cleavage patterns of normal and pathologic forms of alpha-synuclein by calpain I in vitro. J Neurochem 86:836-47. DOI: 1878 [pii].

Miyake Y., Tanaka K., Fukushima W., Sasaki S., Kiyohara C., Tsuboi Y., Yamada T., Oeda T., Miki T., Kawamura N., Sakae N., Fukuyama H., Hirota Y., Nagai M. (2010) Case-control study of risk of Parkinson's disease in relation to hypertension, hypercholesterolemia, and diabetes in Japan. J Neurol Sci 293:82-6. DOI: S0022-510X(10)00105-X [pii]

10.1016/j.jns.2010.03.002.

Mochizuki A., Komatsuzaki Y., Shoji S. (2002) Association of Lewy bodies and glial cytoplasmic inclusions in the brain of Parkinson's disease. Acta Neuropathol (Berl) 104:534-7.

Mohlig M., Wegewitz U., Osterhoff M., Isken F., Ristow M., Pfeiffer A.F., Spranger J. (2002) Insulin decreases human adiponectin plasma levels. Horm Metab Res 34:655-8. DOI: 10.1055/s-2002-38248.

Moore M.C., Cherrington A.D., Wasserman D.H. (2003) Regulation of hepatic and peripheral glucose disposal. Best Pract Res Clin Endocrinol Metab 17:343-64. DOI: S1521690X03000368 [pii].

Mooslehner K.A., Chan P.M., Xu W., Liu L., Smadja C., Humby T., Allen N.D., Wilkinson L.S., Emson P.C. (2001) Mice with very low expression of the vesicular monoamine transporter 2 gene survive into adulthood: potential mouse model for parkinsonism. Mol Cell Biol 21:5321-31.

Morris J.K., Bomhoff G.L., Stanford J.A., Geiger P.C. (2010) Neurodegeneration in an animal model of Parkinson's disease is exacerbated by a high-fat diet. Am J Physiol Regul Integr Comp Physiol 299:R1082-90. DOI: ajpregu.00449.2010 [pii]

10.1152/ajpregu.00449.2010.

Morris J.K., Zhang H., Gupte A.A., Bomhoff G.L., Stanford J.A., Geiger P.C. (2008) Measures of striatal insulin resistance in a 6-hydroxydopamine model of Parkinson's disease. Brain Res 1240:185-95. DOI: S0006-8993(08)02161-6 [pii]

10.1016/j.brainres.2008.08.089.

Mosharov E.V., Larsen K.E., Kanter E., Phillips K.A., Wilson K., Schmitz Y., Krantz D.E., Kobayashi K., Edwards R.H., Sulzer D. (2009) Interplay between cytosolic dopamine, calcium, and alpha-synuclein causes selective death of substantia nigra neurons. Neuron 62:218-29. DOI: S0896-6273(09)00166-4 [pii]

10.1016/j.neuron.2009.01.033.

Mosharov E.V., Staal R.G., Bove J., Prou D., Hananiya A., Markov D., Poulsen N., Larsen K.E., Moore C.M., Troyer M.D., Edwards R.H., Przedborski S., Sulzer D. (2006) Alpha-synuclein overexpression increases cytosolic catecholamine concentration. J Neurosci 26:9304-11. DOI: 26/36/9304 [pii]

10.1523/JNEUROSCI.0519-06.2006.

Moszczynska A., Saleh J., Zhang H., Vukusic B., Lee F.J., Liu F. (2007) Parkin disrupts the alpha-synuclein/dopamine transporter interaction: consequences toward dopamine-induced toxicity. J Mol Neurosci 32:217-27. DOI: JMN:32:3:217 [pii].

Mullerova D., Kopecky J., Matejkova D., Muller L., Rosmus J., Racek J., Sefrna F., Opatrna S., Kuda O., Matejovic M. (2008) Negative association between plasma levels of adiponectin and polychlorinated biphenyl 153 in obese women under non-energy-restrictive regime. Int J Obes (Lond) 32:1875-8. DOI: ijo2008169 [pii]

10.1038/ijo.2008.169.

Munoz E., Oliva R., Obach V., Marti M.J., Pastor P., Ballesta F., Tolosa E. (1997) Identification of Spanish familial Parkinson's disease and screening for the Ala53Thr mutation of the alpha-synuclein gene in early onset patients. Neurosci Lett 235:57-60.

Nakadate T., Nakaki T., Muraki T., Kato R. (1980) Adrenergic regulation of blood glucose levels: possible involvement of postsynaptic alpha-2 type adrenergic receptors regulating insulin release. J Pharmacol Exp Ther 215:226-30.

Nakajo S., Tsukada K., Omata K., Nakamura Y., Nakaya K. (1993) A new brain-specific 14-kDa protein is a phosphoprotein. Its complete amino acid sequence and evidence for phosphorylation. Eur J Biochem 217:1057-63.

Nakaki T., Nakadate T., Kato R. (1980) Alpha 2-adrenoceptors modulating insulin release from isolated pancreatic islets. Naunyn Schmiedebergs Arch Pharmacol 313:151-3.

Narayan K.M., Boyle J.P., Thompson T.J., Sorensen S.W., Williamson D.F. (2003) Lifetime risk for diabetes mellitus in the United States. JAMA 290:1884-90. DOI: 10.1001/jama.290.14.1884
290/14/1884 [pii].

Narbonne J.F., Daubeze M., Gillet G. (1978a) [Effect of polychlorinated biphenyls in the rat: II.-- Preliminary report on metabolic alterations (author's transl)]. Toxicol Eur Res 1:153-8.

Narbonne J.F., Daubeze M., Gillet G. (1978b) [Effect of polychlorinated biphenyls in the rat. IV - Metabolic alterations and residual effects of DP6 dietary exposure (author's transl)]. Toxicol Eur Res 1:229-36.

Near J.A., Mahler H.R. (1983) Reserpine labels the catecholamine transporter in synaptic vesicles from bovine caudate nucleus. FEBS Lett 158:31-5. DOI: 0014-5793(83)80670-X [pii].

Nemani V.M., Lu W., Berge V., Nakamura K., Onoa B., Lee M.K., Chaudhry F.A., Nicoll R.A., Edwards R.H. (2010) Increased expression of alpha-synuclein reduces neurotransmitter release by inhibiting synaptic vesicle reclustering after endocytosis. Neuron 65:66-79. DOI: S0896-6273(09)01041-1 [pii]

10.1016/j.neuron.2009.12.023.

Neumann K.F., Rojo L., Navarrete L.P., Farias G., Reyes P., Maccioni R.B. (2008) Insulin resistance and Alzheimer's disease: molecular links & clinical implications. Curr Alzheimer Res 5:438-47.

Newmark H.L., Newmark J. (2007) Vitamin D and Parkinson's disease--a hypothesis. Mov Disord 22:461-8. DOI: 10.1002/mds.21317.

Nirenberg M.J., Liu Y., Peter D., Edwards R.H., Pickel V.M. (1995) The vesicular monoamine transporter 2 is present in small synaptic vesicles and preferentially localizes to large dense core vesicles in rat solitary tract nuclei. Proc Natl Acad Sci U S A 92:8773-7.

Norris E.H., Giasson B.I., Hodara R., Xu S., Trojanowski J.Q., Ischiropoulos H., Lee V.M. (2005) Reversible inhibition of alpha-synuclein fibrillization by dopaminochrome-mediated conformational alterations. J Biol Chem 280:21212-9.

Patel C.J., Bhattacharya J., Butte A.J. (2010) An Environment-Wide Association Study (EWAS) on type 2 diabetes mellitus. PLoS One 5:e10746. DOI: 10.1371/journal.pone.0010746.

Patel J., Mooslehner K.A., Chan P.M., Emson P.C., Stamford J.A. (2003) Presynaptic control of striatal dopamine neurotransmission in adult vesicular monoamine transporter 2 (VMAT2) mutant mice. J Neurochem 85:898-910.

Pearson S.J., Reynolds G.P. (1988) Depletion of monoamine transmitters by tetrabenazine in brain tissue in Huntington's disease. Neuropharmacology 27:717-9.

Pelletier C., Imbeault P., Tremblay A. (2003) Energy balance and pollution by organochlorines and polychlorinated biphenyls. Obes Rev 4:17-24.

Peng X., Tehranian R., Dietrich P., Stefanis L., Perez R.G. (2005) Alpha-synuclein activation of protein phosphatase 2A reduces tyrosine hydroxylase phosphorylation in dopaminergic cells. J Cell Sci 118:3523-30. DOI: jcs.02481 [pii]

10.1242/jcs.02481.

Perez R.G., Hastings T.G. (2004) Could a loss of alpha-synuclein function put dopaminergic neurons at risk? J Neurochem 89:1318-24.

Perez R.G., Waymire J.C., Lin E., Liu J.J., Guo F., Zigmond M.J. (2002) A role for alpha-synuclein in the regulation of dopamine biosynthesis. J Neurosci 22:3090-9. DOI: 20026307

22/8/3090 [pii].

Peter D., Liu Y., Sternini C., de Giorgio R., Brecha N., Edwards R.H. (1995) Differential expression of two vesicular monoamine transporters. J Neurosci 15:6179-88.

Peterhoff M., Sieg A., Brede M., Chao C.M., Hein L., Ullrich S. (2003) Inhibition of insulin secretion via distinct signaling pathways in alpha2-adrenoceptor knockout mice. Eur J Endocrinol 149:343-50.

Pimplikar S.W., Nixon R.A., Robakis N.K., Shen J., Tsai L.H. (2010) Amyloid-independent mechanisms in Alzheimer's disease pathogenesis. J Neurosci 30:14946-54. DOI: 30/45/14946 [pii]

10.1523/JNEUROSCI.4305-10.2010.

Pocar P., Klonisch T., Brandsch C., Eder K., Frohlich C., Hoang-Vu C., Hombach-Klonisch S. (2006) AhR-agonist-induced transcriptional changes of genes involved in thyroid function in primary porcine thyrocytes. Toxicol Sci 89:408-14. DOI: kfj042 [pii]

10.1093/toxsci/kfj042.

Polymeropoulos M.H., Lavedan C., Leroy E., Ide S.E., Dehejia A., Dutra A., Pike B., Root H., Rubenstein J., Boyer R., Stenroos E.S., Chandrasekharappa S., Athanassiadou A., Papapetropoulos T., Johnson W.G., Lazzarini A.M., Duvoisin R.C., Di Iorio G., Golbe L.I., Nussbaum R.L. (1997) Mutation in the alpha-synuclein gene identified in families with Parkinson's disease. Science 276:2045-7.

Poon L.H., Kang G.A., Lee A.J. (2010) Role of tetrabenazine for Huntington's disease-associated chorea. Ann Pharmacother 44:1080-9. DOI: aph.1M582 [pii]

10.1345/aph.1M582.

Pothos E.N., Larsen K.E., Krantz D.E., Liu Y., Haycock J.W., Setlik W., Gershon M.D., Edwards R.H., Sulzer D. (2000) Synaptic vesicle transporter expression regulates vesicle phenotype and quantal size. J Neurosci 20:7297-306.

Prevention C.f.D.C.a. (2009) Fourth National Report on Human Exposure to Environmental Chemicals.

Prevention C.f.D.C.a. (2011) National diabetes fact sheet: national estimates and general information on diabetes and prediabetes in

the United States, 2011.

Quickel K.E., Jr., Feldman J.M., Lebovitz H.E. (1971) Inhibition of insulin secretion by serotonin and dopamine: species variation. Endocrinology 89:1295-302.

Raffo A., Hancock K., Polito T., Xie Y., Andan G., Witkowski P., Hardy M., Barba P., Ferrara C., Maffei A., Freeby M., Goland R., Leibel R.L., Sweet I.R., Harris P.E. (2008) Role of vesicular monoamine transporter type 2 in rodent insulin secretion and glucose metabolism revealed by its specific antagonist tetrabenazine. J Endocrinol 198:41-9. DOI: JOE-07-0632 [pii]

10.1677/JOE-07-0632.

Reger M.A., Watson G.S., Green P.S., Wilkinson C.W., Baker L.D., Cholerton B., Fishel M.A., Plymate S.R., Breitner J.C., DeGroodt W., Mehta P., Craft S. (2008) Intranasal insulin improves cognition and modulates beta-amyloid in early AD. Neurology 70:440-8. DOI: 01.WNL.0000265401.62434.36 [pii]

10.1212/01.WNL.0000265401.62434.36.

Requena D.F., Parra L.A., Baust T.B., Quiroz M., Leak R.K., Garcia-Olivares J., Torres G.E. (2009) The molecular chaperone Hsc70 interacts with the vesicular monoamine transporter-2. J Neurochem 110:581-94. DOI: JNC6135 [pii]

10.1111/j.1471-4159.2009.06135.x.

Richardson J.R., Miller G.W. (2004) Acute exposure to aroclor 1016 or 1260 differentially affects dopamine transporter and vesicular monoamine transporter 2 levels. Toxicol Lett 148:29-40.

Richardson J.R., Caudle W.M., Wang M., Dean E.D., Pennell K.D., Miller G.W. (2006) Developmental exposure to the pesticide dieldrin alters the dopamine system and increases neurotoxicity in an animal model of Parkinson's disease. Faseb J 20:1695-7.

Richardson J.R., Caudle W.M., Wang M.Z., Dean E.D., Pennell K.D., Miller G.W. (2008) Developmental heptachlor exposure increases susceptibility of dopamine neurons to N-methyl-4-phenyl-1,2,3,6-tetrahydropyridine (MPTP)in a gender-specific manner. Neurotoxicology 29:855-63. DOI: S0161-813X(08)00101-0 [pii]

10.1016/j.neuro.2008.05.007.

Richardson J.R., Shalat S.L., Buckley B., Winnik B., O'Suilleabhain P., Diaz-Arrastia R., Reisch J., German D.C. (2009) Elevated serum pesticide levels and risk of Parkinson disease. Arch Neurol 66:870-5. DOI: 66/7/870 [pii]

10.1001/archneurol.2009.89.

Riederer P., Bartl J., Laux G., Grunblatt E. (2011) Diabetes type II: a risk factor for depression-Parkinson-Alzheimer? Neurotox Res 19:253-65. DOI: 10.1007/s12640-010-9203-1.

Ritter R., Scheringer M., MacLeod M., Moeckel C., Jones K.C., Hungerbuhler K. (2011) Intrinsic human elimination half-lives of polychlorinated biphenyls derived from the temporal evolution of cross-sectional biomonitoring data from the United Kingdom. Environ Health Perspect 119:225-31. DOI: 10.1289/ehp.1002211.

Rochet J.C., Outeiro T.F., Conway K.A., Ding T.T., Volles M.J., Lashuel H.A., Bieganski R.M., Lindquist S.L., Lansbury P.T. (2004) Interactions among alpha-synuclein, dopamine, and biomembranes: some clues for understanding neurodegeneration in Parkinson's disease. J Mol Neurosci 23:23-34.

Rosengren A.H., Jokubka R., Tojjar D., Granhall C., Hansson O., Li D.Q., Nagaraj V., Reinbothe T.M., Tuncel J., Eliasson L., Groop L., Rorsman P., Salehi A., Lyssenko V., Luthman H., Renstrom E. (2010) Overexpression of alpha2A-adrenergic receptors contributes to type 2 diabetes. Science 327:217-20. DOI: science.1176827 [pii]

10.1126/science.1176827.

Rubi B., Ljubicic S., Pournourmohammadi S., Carobbio S., Armanet M., Bartley C., Maechler P. (2005) Dopamine D2-like receptors are expressed in pancreatic beta cells and mediate inhibition of insulin secretion. J Biol Chem 280:36824-32. DOI: M505560200 [pii]

10.1074/jbc.M505560200.

Rudovich N., Pivovarova O., Fisher E., Fischer-Rosinsky A., Spranger J., Mohlig M., Schulze M.B., Boeing H., Pfeiffer A.F. (2009) Polymorphisms within insulin-degrading enzyme (IDE) gene determine insulin metabolism and risk of type 2 diabetes. J Mol Med 87:1145-51. DOI: 10.1007/s00109-009-0540-6.

Ruzzin J., Petersen R., Meugnier E., Madsen L., Lock E.J., Lillefosse H., Ma T., Pesenti S., Sonne S.B., Marstrand T.T., Malde M.K., Du Z.Y., Chavey C., Fajas L., Lundebye A.K., Brand C.L., Vidal H., Kristiansen K., Froyland L. (2010) Persistent organic pollutant exposure leads to insulin resistance syndrome. Environ Health Perspect 118:465-71. DOI: 10.1289/ehp.0901321.

Sabbagh M.N., Adler C.H., Lahti T.J., Connor D.J., Vedders L., Peterson L.K., Caviness J.N., Shill H.A., Sue L.I., Ziabreva I., Perry E., Ballard C.G., Aarsland D., Walker D.G., Beach T.G. (2009) Parkinson disease with dementia: comparing patients with and without Alzheimer pathology. Alzheimer Dis Assoc Disord 23:295-7. DOI: 10.1097/WAD.0b013e31819c5ef4

00002093-200907000-00019 [pii].

Sable H.J., Eubig P.A., Powers B.E., Wang V.C., Schantz S.L. (2009) Developmental exposure to PCBs and/or MeHg: effects on a differential reinforcement of low rates (DRL) operant

task before and after amphetamine drug challenge. Neurotoxicol Teratol 31:149-58. DOI: S0892-0362(09)00008-7 [pii]

10.1016/j.ntt.2008.12.006.

Sable H.J., Monaikul S., Poon E., Eubig P.A., Schantz S.L. (2010) Discriminative stimulus effects of cocaine and amphetamine in rats following developmental exposure to polychlorinated biphenyls (PCBs). Neurotoxicol Teratol. DOI: S0892-0362(10)00172-8 [pii]

10.1016/j.ntt.2010.10.003.

Saisho Y., Harris P.E., Butler A.E., Galasso R., Gurlo T., Rizza R.A., Butler P.C. (2008) Relationship between pancreatic vesicular monoamine transporter 2 (VMAT2) and insulin expression in human pancreas. J Mol Histol 39:543-51. DOI: 10.1007/s10735-008-9195-9.

Sala G., Brighina L., Saracchi E., Fermi S., Riva C., Carrozza V., Pirovano M., Ferrarese C. (2010) Vesicular monoamine transporter 2 mRNA levels are reduced in platelets from patients with Parkinson's disease. J Neural Transm 117:1093-8. DOI: 10.1007/s00702-010-0446-z.

Sanchez B., Relova J.L., Gallego R., Ben-Batalla I., Perez-Fernandez R. (2009) 1,25-Dihydroxyvitamin D3 administration to 6-hydroxydopamine-lesioned rats increases glial cell line-derived neurotrophic factor and partially restores tyrosine hydroxylase expression in substantia nigra and striatum. J Neurosci Res 87:723-32. DOI: 10.1002/jnr.21878.

Sandoval D.A., Obici S., Seeley R.J. (2009) Targeting the CNS to treat type 2 diabetes. Nat Rev Drug Discov 8:386-98. DOI: nrd2874 [pii]

10.1038/nrd2874.

Sandyk R. (1993) The relationship between diabetes mellitus and Parkinson's disease. Int J Neurosci 69:125-30.

Sato Y., Kikuyama M., Oizumi K. (1997) High prevalence of vitamin D deficiency and reduced bone mass in Parkinson's disease. Neurology 49:1273-8.

Sato Y., Honda Y., Iwamoto J., Kanoko T., Satoh K. (2005) Abnormal bone and calcium metabolism in immobilized Parkinson's disease patients. Mov Disord 20:1598-603. DOI: 10.1002/mds.20658.

Savelieva K.V., Caudle W.M., Miller G.W. (2006) Altered ethanol-associated behaviors in vesicular monoamine transporter heterozygote knockout mice. Alcohol 40:87-94.

Savontaus E., Fagerholm V., Rahkonen O., Scheinin M. (2008) Reduced blood glucose levels, increased insulin levels and improved glucose tolerance in alpha2A-adrenoceptor knockout mice. Eur J Pharmacol 578:359-64. DOI: S0014-2999(07)01042-4 [pii] 10.1016/j.ejphar.2007.09.015.

Schraenen A., Lemaire K., de Faudeur G., Hendrickx N., Granvik M., Van Lommel L., Mallet J., Vodjdani G., Gilon P., Binart N., in't Veld P., Schuit F. (2010) Placental lactogens induce serotonin biosynthesis in a subset of mouse beta cells during pregnancy. Diabetologia 53:2589-99. DOI: 10.1007/s00125-010-1913-7.

Schulz-Schaeffer W.J. (2010) The synaptic pathology of alpha-synuclein aggregation in dementia with Lewy bodies, Parkinson's disease and Parkinson's disease dementia. Acta Neuropathol 120:131-43. DOI: 10.1007/s00401-010-0711-0.

Seegal R.F., Brosch K.O., Bush B. (1986) Polychlorinated biphenyls produce regional alterations of dopamine metabolism in rat brain. Toxicol Lett 30:197-202. DOI: 0378-4274(86)90103-7 [pii].

Seegal R.F., Bush B., Shain W. (1990) Lightly chlorinated ortho-substituted PCB congeners decrease dopamine in nonhuman primate brain and in tissue culture. Toxicol Appl Pharmacol 106:136-44.

Seegal R.F., Bush B., Brosch K.O. (1991) Sub-chronic exposure of the adult rat to Aroclor 1254 yields regionally-specific changes in central dopaminergic function. Neurotoxicology 12:55-65.

Seegal R.F., Okoniewski R.J., Brosch K.O., Bemis J.C. (2002) Polychlorinated biphenyls alter extraneuronal but not tissue dopamine concentrations in adult rat striatum: an in vivo microdialysis study. Environ Health Perspect 110:1113-7. DOI: sc271_5_1835 [pii].

Seegal R.F., Marek K.L., Seibyl J.P., Jennings D.L., Molho E.S., Higgins D.S., Factor S.A., Fitzgerald E.F., Hills E.A., Korrick S.A., Wolff M.S., Haase R.F., Todd A.C., Parsons P., McCaffrey R.J. (2010) Occupational exposure to PCBs reduces striatal dopamine transporter densities only in women: a beta-CIT imaging study. Neurobiol Dis 38:219-25. DOI: S0969-9961(10)00011-2 [pii]

10.1016/j.nbd.2010.01.009.

Shain W., Bush B., Seegal R. (1991) Neurotoxicity of polychlorinated biphenyls: structure-activity relationship of individual congeners. Toxicol Appl Pharmacol 111:33-42.

Shinpo K., Kikuchi S., Sasaki H., Moriwaka F., Tashiro K. (2000) Effect of 1,25-dihydroxyvitamin D(3) on cultured mesencephalic dopaminergic neurons to the combined toxicity caused by L-buthionine sulfoximine and 1-methyl-4-phenylpyridine. J Neurosci Res 62:374-82. DOI: 10.1002/1097-4547(20001101)62:3<374::AID-JNR7>3.0.CO;2-7 [pii].

Simon K.C., Chen H., Schwarzschild M., Ascherio A. (2007) Hypertension, hypercholesterolemia, diabetes, and risk of Parkinson disease. Neurology 69:1688-95. DOI: 01.wnl.0000271883.45010.8a [pii]

10.1212/01.wnl.0000271883.45010.8a.

Simpson N.R., Souza F., Witkowski P., Maffei A., Raffo A., Herron A., Kilbourn M., Jurewicz A., Herold K., Liu E., Hardy M.A., Van Heertum R., Harris P.E. (2006) Visualizing

pancreatic beta-cell mass with [11C]DTBZ. Nucl Med Biol 33:855-64. DOI: S0969-8051(06)00129-6 [pii]

10.1016/j.nucmedbio.2006.07.002.

Snead A.N., Santos M.S., Seal R.P., Miyakawa M., Edwards R.H., Scanlan T.S. (2007) Thyronamines inhibit plasma membrane and vesicular monoamine transport. ACS Chem Biol 2:390-8. DOI: 10.1021/cb700057b.

Song J., Xu Y., Hu X., Choi B., Tong Q. (2010) Brain expression of Cre recombinase driven by pancreas-specific promoters. Genesis 48:628-34. DOI: 10.1002/dvg.20672.

Souza F., Simpson N., Raffo A., Saxena C., Maffei A., Hardy M., Kilbourn M., Goland R., Leibel R., Mann J.J., Van Heertum R., Harris P.E. (2006) Longitudinal noninvasive PET-based beta cell mass estimates in a spontaneous diabetes rat model. J Clin Invest 116:1506-13. DOI: 10.1172/JCI27645.

Spach K.M., Hayes C.E. (2005) Vitamin D3 confers protection from autoimmune encephalomyelitis only in female mice. J Immunol 175:4119-26. DOI: 175/6/4119 [pii].

Spillantini M.G., Crowther R.A., Jakes R., Hasegawa M., Goedert M. (1998) alpha-Synuclein in filamentous inclusions of Lewy bodies from Parkinson's disease and dementia with lewy bodies. Proc Natl Acad Sci U S A 95:6469-73.

Steen E., Terry B.M., Rivera E.J., Cannon J.L., Neely T.R., Tavares R., Xu X.J., Wands J.R., de la Monte S.M. (2005) Impaired insulin and insulin-like growth factor expression and signaling mechanisms in Alzheimer's disease--is this type 3 diabetes? J Alzheimers Dis 7:63-80.

Stockhorst U., de Fries D., Steingrueber H.J., Scherbaum W.A. (2004) Insulin and the CNS: effects on food intake, memory, and endocrine parameters and the role of intranasal insulin administration in humans. Physiol Behav 83:47-54. DOI: S0031-9384(04)00348-8 [pii]

10.1016/j.physbeh.2004.07.022.

Takahashi N., Miner L.L., Sora I., Ujike H., Revay R.S., Kostic V., Jackson-Lewis V., Przedborski S., Uhl G.R. (1997) VMAT2 knockout mice: heterozygotes display reduced amphetamine-conditioned reward, enhanced amphetamine locomotion, and enhanced MPTP toxicity. Proc Natl Acad Sci U S A 94:9938-43.

Takayanagi M., Watanabe T. (1996) Immunocytochemical colocalizations of insulin, aromatic L-amino acid decarboxylase, dopamine beta-hydroxylase, S-100 protein and chromogranin A in B-cells of the chicken endocrine pancreas. Tissue Cell 28:17-24. DOI: S0040-8166(96)80040-1 [pii].

Taylor T.N., Caudle W.M., Shepherd K.R., Noorian A., Jackson C.R., Iuvone P.M., Weinshenker D., Greene J.G., Miller G.W. (2009) Nonmotor symptoms of Parkinson's disease revealed in an animal model with reduced monoamine storage capacity. J Neurosci 29:8103-13. DOI: 29/25/8103 [pii]

10.1523/JNEUROSCI.1495-09.2009.

Tehranian R., Montoya S.E., Van Laar A.D., Hastings T.G., Perez R.G. (2006) Alpha-synuclein inhibits aromatic amino acid decarboxylase activity in dopaminergic cells. J Neurochem 99:1188-96. DOI: JNC4146 [pii]

10.1111/j.1471-4159.2006.04146.x.

Tekes K., Gyenge M., Hantos M., Csaba G. (2009a) Transgenerational hormonal imprinting caused by vitamin A and vitamin D treatment of newborn rats. Alterations in the biogenic amine contents of the adult brain. Brain Dev 31:666-70. DOI: S0387-7604(08)00253-2 [pii]

10.1016/j.braindev.2008.10.007.

Tekes K., Gyenge M., Folyovich A., Csaba G. (2009b) Influence of neonatal vitamin A or vitamin D treatment on the concentration of biogenic amines and their metabolites in the adult rat brain. Horm Metab Res 41:277-80. DOI: 10.1055/s-0028-1103287.

Thayanidhi N., Helm J.R., Nycz D.C., Bentley M., Liang Y., Hay J.C. (2010) Alpha-synuclein delays endoplasmic reticulum (ER)-to-Golgi transport in mammalian cells by antagonizing ER/Golgi SNAREs. Mol Biol Cell 21:1850-63. DOI: E09-09-0801 [pii] 10.1091/mbc.E09-09-0801.

Tjalve H. (1971) Catechol- and indolamines in some endocrine cell systems. An autoradiographical, histochemical and radioimmunological study. Acta Physiol Scand Suppl 360:1-122.

Toll L., Howard B.D. (1978) Role of Mg2+-ATPase and a pH gradient in the storage of catecholamines in synaptic vesicles. Biochemistry 17:2517-23.

Toll L., Gundersen C.B., Jr., Howard B.D. (1977) Energy utilization in the uptake of catecholamines by synaptic vesicles and adrenal chromaffin granules. Brain Res 136:59-66. DOI: 0006-8993(77)90131-7 [pii].

Tolosa E., Marti M.J., Valldeoriola F., Molinuevo J.L. (1998) History of levodopa and dopamine agonists in Parkinson's disease treatment. Neurology 50:S2-10; discussion S44-8.

Travis E.R., Wang Y.M., Michael D.J., Caron M.G., Wightman R.M. (2000) Differential quantal release of histamine and 5-hydroxytryptamine from mast cells of vesicular monoamine transporter 2 knockout mice. Proc Natl Acad Sci U S A 97:162-7.

Tsao H.H., Lin K.J., Juang J.H., Skovronsky D.M., Yen T.C., Wey S.P., Kung M.P. (2010) Binding characteristics of 9-fluoropropyl-(+)-dihydrotetrabenzazine (AV-133) to the vesicular monoamine transporter type 2 in rats. Nucl Med Biol 37:413-9. DOI: S0969-8051(10)00004-1 [pii] 10.1016/j.nucmedbio.2010.01.002.

Tuttle K.R., Marker J.C., Dalsky G.P., Schwartz N.S., Shah S.D., Clutter W.E., Holloszy J.O., Cryer P.E. (1988) Glucagon, not insulin, may play a secondary role in defense against hypoglycemia during exercise. Am J Physiol 254:E713-9.

van Rooijen B.D., Claessens M.M., Subramaniam V. (2010a) Membrane Permeabilization by Oligomeric alpha-Synuclein: In Search of the Mechanism. PLoS One 5:e14292. DOI: 10.1371/journal.pone.0014292.

van Rooijen B.D., Claessens M.M., Subramaniam V. (2010b) Membrane interactions of oligomeric alpha-synuclein: potential role in Parkinson's disease. Curr Protein Pept Sci 11:334-42. DOI: CPPS-52 [pii].

Vander Borght T.M., Kilbourn M.R., Koeppe R.A., DaSilva J.N., Carey J.E., Kuhl D.E., Frey K.A. (1995) In vivo imaging of the brain vesicular monoamine transporter. J Nucl Med 36:2252-60.

Vasiliu O., Cameron L., Gardiner J., Deguire P., Karmaus W. (2006) Polybrominated biphenyls, polychlorinated biphenyls, body weight, and incidence of adult-onset diabetes mellitus. Epidemiology 17:352-9. DOI: 10.1097/01.ede.0000220553.84350.c5.

Veluthakal R., Harris P. (2010) In vivo beta-cell imaging with VMAT 2 ligands--current state-of-the-art and future perspective. Curr Pharm Des 16:1568-81. DOI: BSP/CPD/E-Pub/00024 [pii].

Vepsalainen S., Parkinson M., Helisalmi S., Mannermaa A., Soininen H., Tanzi R.E., Bertram L., Hiltunen M. (2007) Insulin-degrading enzyme is genetically associated with Alzheimer's disease in the Finnish population. J Med Genet 44:606-8. DOI: jmg.2006.048470 [pii] 10.1136/jmg.2006.048470.

Vokonas P.S., Kannel W.B. (1996) Diabetes mellitus and coronary heart disease in the elderly. Clin Geriatr Med 12:69-78.

Volles M.J., Lansbury P.T., Jr. (2002) Vesicle permeabilization by protofibrillar alpha-synuclein is sensitive to Parkinson's disease-linked mutations and occurs by a pore-like mechanism. Biochemistry 41:4595-602. DOI: bi0121353 [pii].

Volles M.J., Lansbury P.T., Jr. (2003) Zeroing in on the pathogenic form of alpha-synuclein and its mechanism of neurotoxicity in Parkinson's disease. Biochemistry 42:7871-8.

Volles M.J., Lee S.J., Rochet J.C., Shtilerman M.D., Ding T.T., Kessler J.C., Lansbury P.T., Jr. (2001) Vesicle permeabilization by protofibrillar alpha-synuclein: implications for the pathogenesis and treatment of Parkinson's disease. Biochemistry 40:7812-9. DOI: bi0102398 [pii].

Voronina S., Henry J., Vaillant C., Dockray G.J., Varro A. (1997) Amine precursor uptake and decarboxylation: significance for processing of the rat gastrin precursor. J Physiol 501 (Pt 2):363-74.

Waites C.L., Mehta A., Tan P.K., Thomas G., Edwards R.H., Krantz D.E. (2001) An acidic motif retains vesicular monoamine transporter 2 on large dense core vesicles. J Cell Biol 152:1159-68.

Wakabayashi K., Tanji K., Mori F., Takahashi H. (2007) The Lewy body in Parkinson's disease: molecules implicated in the formation and degradation of alpha-synuclein aggregates. Neuropathology 27:494-506.

Wang J.Y., Wu J.N., Cherng T.L., Hoffer B.J., Chen H.H., Borlongan C.V., Wang Y. (2001) Vitamin D(3) attenuates 6-hydroxydopamine-induced neurotoxicity in rats. Brain Res 904:67-75. DOI: S0006-8993(01)02450-7 [pii].

Wang S., Tulina N., Carlin D.L., Rulifson E.J. (2007) The origin of islet-like cells in Drosophila identifies parallels to the vertebrate endocrine axis. Proc Natl Acad Sci U S A 104:19873-8. DOI: 0707465104 [pii]

10.1073/pnas.0707465104.

Wang Y.M., Gainetdinov R.R., Fumagalli F., Xu F., Jones S.R., Bock C.B., Miller G.W., Wightman R.M., Caron M.G. (1997) Knockout of the vesicular monoamine transporter 2 gene results in neonatal death and supersensitivity to cocaine and amphetamine. Neuron 19:1285-96.

Watanabe T., Nagatsu I. (1991) Immunohistochemical colocalization of insulin, aromatic L-amino acid decarboxylase and dopamine beta-hydroxylase in islet B cells of chicken pancreas. Cell Tissue Res 263:131-6.

Watson G.S., Craft S. (2003) The role of insulin resistance in the pathogenesis of Alzheimer's disease: implications for treatment. CNS Drugs 17:27-45. DOI: 170103 [pii].

Weisskopf M.G., Knekt P., O'Reilly E.J., Lyytinen J., Reunanen A., Laden F., Altshul L., Ascherio A. (2010) Persistent organochlorine pesticides in serum and risk of Parkinson disease. Neurology 74:1055-61. DOI: 74/13/1055 [pii]

10.1212/WNL.0b013e3181d76a93.

Wersinger C., Sidhu A. (2003) Attenuation of dopamine transporter activity by alpha-synuclein. Neurosci Lett 340:189-92. DOI: S0304394003000971 [pii].

Wersinger C., Sidhu A. (2005) Disruption of the interaction of alpha-synuclein with microtubules enhances cell surface recruitment of the dopamine transporter. Biochemistry 44:13612-24.

Wersinger C., Vernier P., Sidhu A. (2004) Trypsin disrupts the trafficking of the human dopamine transporter by alpha-synuclein and its A30P mutant. Biochemistry 43:1242-53.

Wersinger C., Jeannotte A., Sidhu A. (2006a) Attenuation of the norepinephrine transporter activity and trafficking via interactions with alpha-synuclein. Eur J Neurosci 24:3141-52.

Wersinger C., Rusnak M., Sidhu A. (2006b) Modulation of the trafficking of the human serotonin transporter by human alpha-synuclein. Eur J Neurosci 24:55-64.

Wersinger C., Prou D., Vernier P., Sidhu A. (2003a) Modulation of dopamine transporter function by alpha-synuclein is altered by impairment of cell adhesion and by induction of oxidative stress. FASEB J 17:2151-3. DOI: 10.1096/fj.03-0152fje

03-0152fje [pii].

Wersinger C., Prou D., Vernier P., Niznik H.B., Sidhu A. (2003b) Mutations in the lipid-binding domain of alpha-synuclein confer overlapping, yet distinct, functional properties in the regulation of dopamine transporter activity. Mol Cell Neurosci 24:91-105.

Wilson J.P., Downs R.W., Jr., Feldman J.M., Lebovitz H.E. (1974) Beta cell monoamines: further evidence for their role in modulating insulin secretion. Am J Physiol 227:305-12.

Wimalasena K. (2010) Vesicular monoamine transporters: Structure-function, pharmacology, and medicinal chemistry. Med Res Rev. DOI: 10.1002/med.20187.

Wolff M.S., Anderson H.A. (1999) Correspondence re: J. M. Schildkraut et al., Environmental contaminants and body fat distribution. Cancer Epidemiol. Biomark. Prev., 8: 179-183, 1999. Cancer Epidemiol Biomarkers Prev 8:951-2.

Wolkersdorfer M., Laslop A., Lazure C., Fischer-Colbrie R., Winkler H. (1996) Processing of chromogranins in chromaffin cell culture: effects of reserpine and alpha-methyl-p-tyrosine. Biochem J 316 (Pt 3):953-8.

Wongseree W., Assawamakin A., Piroonratana T., Sinsomros S., Limwongse C., Chaiyaratana N. (2009) Detecting purely epistatic multi-locus interactions by an omnibus permutation test on ensembles of two-locus analyses. BMC Bioinformatics 10:294. DOI: 1471-2105-10-294 [pii]

10.1186/1471-2105-10-294.

Wood S.J., Wypych J., Steavenson S., Louis J.C., Citron M., Biere A.L. (1999) alpha-synuclein fibrillogenesis is nucleation-dependent. Implications for the pathogenesis of Parkinson's disease. J Biol Chem 274:19509-12.

Wooten G.F., Currie L.J., Bovbjerg V.E., Lee J.K., Patrie J. (2004) Are men at greater risk for Parkinson's disease than women? J Neurol Neurosurg Psychiatry 75:637-9.

Wu F., Khan S., Wu Q., Barhoumi R., Burghardt R., Safe S. (2008) Ligand structure-dependent activation of estrogen receptor alpha/Sp by estrogens and xenoestrogens. J Steroid Biochem Mol Biol 110:104-15. DOI: S0960-0760(08)00039-3 [pii]

10.1016/j.jsbmb.2008.02.008.

Xu J., Kao S.Y., Lee F.J., Song W., Jin L.W., Yankner B.A. (2002) Dopamine-dependent neurotoxicity of alpha-synuclein: a mechanism for selective neurodegeneration in Parkinson disease. Nat Med 8:600-6.

Yamauchi T., Kamon J., Waki H., Terauchi Y., Kubota N., Hara K., Mori Y., Ide T., Murakami K., Tsuboyama-Kasaoka N., Ezaki O., Akanuma Y., Gavrilova O., Vinson C., Reitman M.L., Kagechika H., Shudo K., Yoda M., Nakano Y., Tobe K., Nagai R., Kimura S., Tomita M., Froguel P., Kadowaki T. (2001) The fat-derived hormone adiponectin reverses insulin resistance associated with both lipoatrophy and obesity. Nat Med 7:941-6. DOI: 10.1038/90984

90984 [pii].

Yao J., Erickson J.D., Hersh L.B. (2004) Protein kinase A affects trafficking of the vesicular monoamine transporters in PC12 cells. Traffic 5:1006-16.

Yao Z., Wei X., Wu X., Katz J.L., Kopajtic T., Greig N.H., Sun H. (2011) Preparation and evaluation of tetrabenazine enantiomers and all eight stereoisomers of dihydrotetrabenazine as VMAT2 inhibitors. Eur J Med Chem 46:1841-8. DOI: S0223-5234(11)00157-7 [pii]

10.1016/j.ejmech.2011.02.046.

Yavich L., Jakala P., Tanila H. (2006) Abnormal compartmentalization of norepinephrine in mouse dentate gyrus in alpha-synuclein knockout and A30P transgenic mice. J Neurochem 99:724-32.

Yavich L., Tanila H., Vepsalainen S., Jakala P. (2004) Role of alpha-synuclein in presynaptic dopamine recruitment. J Neurosci 24:11165-70.

Yavich L., Oksman M., Tanila H., Kerokoski P., Hiltunen M., van Groen T., Puolivali J., Mannisto P.T., Garcia-Horsman A., MacDonald E., Beyreuther K., Hartmann T., Jakala P. (2005) Locomotor activity and evoked dopamine release are reduced in mice

overexpressing A30P-mutated human alpha-synuclein. Neurobiol Dis 20:303-13. DOI: S0969-9961(05)00085-9 [pii]

10.1016/j.nbd.2005.03.010.

Yelin R., Schuldiner S. (1995) The pharmacological profile of the vesicular monoamine transporter resembles that of multidrug transporters. FEBS Lett 377:201-7. DOI: 0014-5793(95)01346-6 [pii].

Yi E., Smith T.G., Baker R.C., Love J.A. (2004) Catecholamines and 5-hydroxytryptamine in tissues of the rabbit exocrine pancreas. Pancreas 29:218-24. DOI: 00006676-200410000-00007 [pii].

Zarranz J.J., Alegre J., Gomez-Esteban J.C., Lezcano E., Ros R., Ampuero I., Vidal L., Hoenicka J., Rodriguez O., Atares B., Llorens V., Gomez Tortosa E., del Ser T., Munoz D.G., de Yebenes J.G. (2004) The new mutation, E46K, of alpha-synuclein causes Parkinson and Lewy body dementia. Ann Neurol 55:164-73.

Zern R.T., Bird J.L., Feldman J.M. (1980) Effect of increased pancreatic islet norepinephrine, dopamine and serotonin concentration on insulin secretion in the golden hamster. Diabetologia 18:341-6.